Developmental Trajectories of Motor Networks in Health and Tourette Syndrome:

Insights from Multimodal Neuroimaging

Doctoral thesis

for

the award of the doctoral degree

of the Faculty of Mathematics and Natural Sciences

of the University of Cologne

submitted by

Julia Schmidgen

Reviewers:

Prof. Dr. Stephan Bender

Prof. Dr. Martin Nawrot

Contents

Abstract

Maturation of motor control represents a key aspect of brain development, characterized by a complex reorganization of cortical and subcortical networks that enable increasingly refined motor abilities. Deviations from these maturational trajectories are closely linked to the onset of various neurodevelopmental disorders. Within this framework, the present dissertation investigates the neural dynamics underlying motor control in typical development and identifies alterations of developmental patterns associated with Tourette syndrome (TS). Using a multimodal approach, including electroencephalography (EEG) with high temporal resolution, transcranial magnetic stimulation (TMS), and functional magnetic resonance imaging (fMRI) with high spatial resolution, this work provides a comprehensive insight into the organization and function of motor networks from early childhood through adolescence. To study processes related to motor preparation, sensorimotor integration, and the coordination of voluntary movement, participants performed cued motor tasks.

Healthy development was characterized by a progressive improvement in motor performance, reflected in reduced reaction times and error rates. At the neural level, both EEG and fMRI provided converging evidence for the ongoing maturation of motor networks throughout childhood and adolescence. Motor preparation was associated with an age-related increase in supplementary motor area (SMA) recruitment, paralleled by a shift in the influence of the SMA on the ipsilateral primary motor cortex (M1) from inhibitory to excitatory. These results indicate a transition toward more proactive motor control strategies. Additionally, the inhibitory influence of the intraparietal sulcus (IPS) on SMA was associated with better motor performance, suggesting that maturing frontoparietal interactions play a regulatory role in refining motor output. Cortical activity related to preparatory motor control shifted from stronger ipsilateral to increasing contralateral motor area excitation, aligning with more efficient hemispheric specialization. Furthermore, fMRI revealed a linear increase in left parietal activity, particularly within visuomotor integration regions. Finally, TMS-EEG measurements demonstrated an age-related reduction in the N100 component, a marker of $GABA_B$-related cortical inhibition, indicating refinement of inhibitory processes as the motor system matures.

Children and adolescents with TS revealed comparable or even enhanced motor performance in cued tasks, despite showing deficits in blink suppression. Neurophysiological analyses

revealed reduced theta-band connectivity and decreased network efficiency following informative cues, suggesting disrupted sensorimotor integration and perception-action binding. This reduction may reflect a compensatory attempt to minimize premature or involuntary motor output. During movement preparation and execution, data indicated a reorganization of motor networks, including increased connectivity within SMA and premotor regions. These adaptations occurred alongside overactivation of ipsilateral M1 and S1, with activation levels positively correlated with task accuracy, suggesting recruitment of additional motor resources to support performance. Further analysis revealed increased interhemispheric communication between left and right IPS, and a shift from inhibitory to excitatory influence of the IPS on premotor cortex (PMC). This may contribute to motor system hyperexcitability and atypical perception-action binding observed in TS. Finally, TS was characterized by reduced modulatory capacity of cortical inhibition during both motor preparation and execution, suggesting diminished flexibility in motor network regulation.

These findings demonstrate that typical motor development is driven by increasing specialization and integration of frontoparietal and sensorimotor networks, supporting more efficient and lateralized motor function. In contrast, TS is marked by altered anticipatory processes and reduced inhibitory flexibility, counterbalanced by compensatory recruitment of alternative motor and sensory networks to maintain performance. This multimodal framework provides valuable insights into developmental mechanisms and highlights the dynamic interaction between dysfunction and adaptation in TS, offering direction for future therapeutic strategies.

Zusammenfassung

Die Fähigkeit zur gezielten Steuerung von Bewegungen entwickelt sich im Laufe der Kindheit und Jugend und spiegelt zentrale Reifungsprozesse des Gehirns wider. Neuronale Prozesse, die der Entwicklung der motorischen Kontrolle zugrunde liegen, bieten wichtige Einblicke in gesunde Entwicklungsverläufe sowie in die Mechanismen neuroentwicklungsbedingter Störungen. Basierend auf diesen Grundlagen untersucht die vorliegende Dissertation die funktionellen Entwicklung neuronaler Netzwerke im Laufe der Kindheit und Jugend und vergleicht diese mit den Veränderungen, die bei Kindern und Jugendlichen mit Tourette-Syndrom (TS) auftreten. Mithilfe verschiedener multimodalen Messungen, einschließlich hochauflösendem Elektroenzephalogramm (EEG), transkranieller Magnetstimulation (TMS) sowie funktioneller Magnetresonanztomografie (fMRI) wurden motorische Netzwerke im Rahmen von Aufgaben zur motorischen Vorbereitung, sensomotorischen Integration und Bewegungskoordination untersucht.

Bei gesunden Kindern und Jugendlichen zeigten sich mit zunehmendem Alter verbesserte motorische Leistungen, die mit einer stärkeren Rekrutierung des supplementär-motorischen Areals (SMA), begleitet von einer Verschiebung des Einflusses der SMA auf den ipsilateralen Motorkortex (M1) von hemmend zu erregend, einherging. Diese Ergebnisse deuten auf ein zunehmende Bedeutung der SMA für die Planung, Initiierung und Koordination komplexer Bewegungsabläufe im Rahmen der motorischen Entwicklung hin. Zudem zeigte sich eine lineare Zunahme der Aktivität im linken Parietallappen, insbesondere in Regionen der visumotorischen Integration sowie eine Verschiebung von einer Inhibition der ipsilateralen motorischen Areale hin zu einer verstärkten Aktivierung der kontralateralen Motorregionen. Dies deutet auf effizientere Spezialisierung der Hemispären hin. TMS-EEG-Daten zeigten eine altersabhängige Abnahme der N100-Komponente, die $GABA_B$-vermittelte Inhbiton wiedespieglt und auf eine Reifung inhibitorischer kortikaler Mechanismen hindeutet.

Kinder und Jugendliche mit TS zeigten, trotz intakter oder sogar verbesserter motorischer Reaktion, eine Beeinträchtigung der motorischen Inhibition in der Blinzelunterdrückung. Neuronal zeigten sich reduzierte Theta-Konnektivität und eingeschränkte Netzwerk-Effizienz nach Warn-Stimuli, die Information über die Bewegungsseite gaben. Dies lässt auf eine gestörte sensomotorische Integration schließen, möglicherweise könnte es sich jedoch auch um einen kompensatorischen Mechanismus zur Vermeidung verfrühter motorischer Reaktionen handeln.

Während der Bewegungsvorbereitung und -ausführung zeigten sich eine Reorganisation motorischer Netzwerke und eine verstärkte Aktivität in ipsilateralen motorischen- und somatosensorischen Arealen, die positiv mit der motorischen Performance korrelierte. Zusammen mit einer verstärkte interhemisphärische Kommunikation zwischen linken und rechten intraparietalen Sulci, lässt sich auf die Nutzung zusätzlicher Hirnareale als kompensatorischer Mechanismus zur Erhaltung der motorischen Kontrolle schließen. Die Verschiebung des Einflusses von IPS auf den Prämotorkortex von hemmend zu erregend, könnte auf eine Hyperexzitabilität motorischer Netzwerke und eine veränderte Wahrnehmungs-Handlungs-Kopplung hinweisen. Zudem wiesen TS-Patienten eine verminderte Modulationsfähigkeit der N100-Komponenete auf, was auf Defizite der dynamischen inhibitorischen Kontolle hindeutet.

Diese Ergebnisse unterstreichen die Bedeutung der Netzwerkorganisation und Plastizität für die motorische Entwicklung und zeigen, dass bei TS kompensatorische Anpassungen helfen können, Leistungsdefizite auszugleichen. Die Erkenntnisse bieten neue Ansatzpunkte für gezielte Interventionen bei neuroentwicklungsbedingten Störungen wie dem Tourette-Syndrom.

Abbreviations

ACC	Anterior cingulate cortex
ADHD	Attention deficit hyperactivity disorder
AEP	Auditory evoked potential
BOLD	Blood oxygenation level dependent
CNV	Contingent negative variation
CSD	Current source density
CSTC	Cortico-striatal-thalamo-cortical circuit
DCM	dynamic causal modelling
DLPFC	Dorsolateral prefrontal cortex
EEG	Electroencephalogram
$\mathbf{E_{glob}}$	Global efficiency
EHI	Edinburgh Handedness Inventory
ERD	Event-related desynchronization
ERP	Event-related potential
ERS	Event-related synchronization
FDR	False discovery rate
fMRI	functional magnetic resonance imaging

GABA	γ-aminobutyric acid
HC	Healthy controls
ICA	Independent component analysis
iCNV	initial or early CNV
IPL	Inferior parietal lobule
IPS	Intraparietal sulcus
IQR	Interquartile range
lCNV	late CNV
LICI	Long-interval intracortical inhibition
LORETA	Low Resolution Brain Electromagnetic Tomography
LRP	Lateralized readiness potential
M	Mean
M1	Primary motor cortex
Mdn	Median
MEP	Motor evoked potential
MSO	Maximum stimulator output
PFC	Prefrontal cortex
PINV	Post-imperative negative variation

PMA/PMC	Premotor area/premotor cortex
POC	Parieto-Occipital cortex
PPC	Posterior parietal cortex
RMT	Resting motor threshold
ROI	Region of interest
(r)PLV	(relative) Phase locking value
RT	Reaction-time
S1	Primary somatosensory cortex
SD	Standard deviation
SMA	Supplementary motor area
SPL	superior parietal lobule
SSLOFO	Current Standardized shrinking LORETA-FOCUSS
TEP	TMS evoked potential
TMS	Transcranial magnetic stimulation
TS/TP	Tourette syndrome/Tourette syndrome patients
VMC	Visuomotor coordination
WM	Working memory
YGTSS	Yale Global Tic Severity Scale

1 Introduction

1.1 General Background

Understanding the neural mechanisms underlying healthy brain development and neurodevelopmental disorders is a central goal in neuroscience (van Duijvenvoorde et al., 2022). During childhood and adolescence, the human brain undergoes complex structural and functional changes that support the development of cognitive, emotional, and behavioral abilities. These developmental processes are driven by dynamic changes in brain connectivity, both at the functional and structural levels (Fornito & Harrison, 2012; Lim et al., 2020; López-Vicente et al., 2021; Pollmann et al., 2024). The refinement of motor control is a fundamental aspect within these maturational trajectories. It allows children to interact effectively with the environment, improving goal-directed behavior, enhancing flexibility in responses to external stimuli, and the development of increasingly complex cognitive and social skills that are essential for daily life (Hao et al., 2024; Munakata & Michaelson, 2021; Pfurtscheller et al., 2003; Shi & Feng, 2022). As motor control matures, it supports the improvement of both gross and fine motor abilities, the coordination of complex movement patterns, and the effective integration of sensory feedback to optimize and refine motor performance.

These processes are driven by the progressive development of motor regions, including the primary motor cortex (M1), premotor cortex (PMC), supplementary motor areas (SMA), cerebellum, and basal ganglia, and their interactions with frontal, parietal, and sensorimotor networks (see Figure 1; (Kandel et al., 2000)). The M1 plays a central role in voluntary motor control by generating the corticospinal output that directly activates skeletal muscles (Bhattacharjee et al., 2021; Rizzolatti et al., 1998). While it heavily relies on input from other brain regions, M1 functions as a key component within complex sensorimotor networks that integrate and coordinate motor commands (Hatsopoulos & Suminski, 2011; Knudsen et al., 2025). The PMC and SMA are crucial for the involvement of higher-level aspects of movement planning, selection, and sequencing, and interact extensively with M1, frontal, and parietal areas to coordinate complex motor behaviors (de la Peña et al., 2020; Goldberg, 1985; Nachev et al., 2007; Ohbayashi, 2021). Integrating proprioceptive, vestibular, and visual inputs, mediated by parietal and occipital regions, enables the brain to build internal models of body position and movement. The parietal cortex combines multisensory information for spatial awareness, visuo-motor integration, and movement planning, while occipital areas process

visual cues essential for guiding actions (Iacoboni, 2006; Pennartz et al., 2023). The development of frontal regions, especially the prefrontal cortex, plays a central role in higher-order aspects of motor control. The prefrontal cortex is not only essential for the planning of complex movements, but also for executive functions such as working memory, attention, error prediction, and inhibitory control (Brass & Von Cramon, 2002; Ebbesen et al., 2018; Krämer et al., 2013; Krigolson & Holroyd, 2007).

The cerebellum and basal ganglia represent key subcortical structures that are extensively connected to multiple cortical areas (Bostan & Strick, 2010; Caligiore et al., 2017; Groenewegen, 2003). The nuclei are crucial for the integration of widespread cortical activity to enable coordinated motor and cognitive control. Disruptions within these circuits are suggested to underlie the development of various neurological and neurodevelopmental disorders (Caligiore et al., 2017; Hall et al., 2025; Middleton & Strick, 2000; Peters et al., 2016).

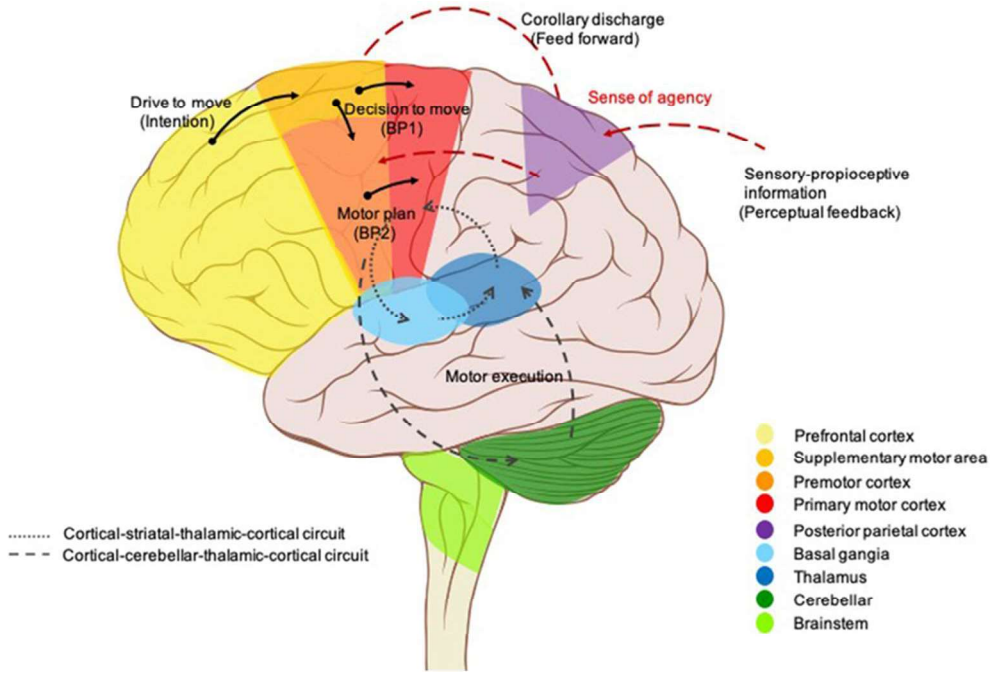

Figure 1. Brain circuits of voluntary movements. Voluntary actions are initiated in the prefrontal cortex and limbic areas, programmed by supplementary motor regions, and executed via the motor cortex with modulation from the basal ganglia and cerebellum. (Figure reproduced from Virameteekul and Bhidayasiri (2022), *Frontiers in Neurology*, CC BY 4.0).

1.2 Maturation of Motor Control

Given the extensive anatomical and functional interconnections between these regions, motor control maturation depends on the precise integration and dynamic coordination of multiple distributed functional brain networks. This complexity requires a highly coordinated developmental network reorganization between cortical and subcortical structures. The reorganization is characterized by a transition from widespread, diffuse connectivity toward more functionally specialized and efficient neural networks. Mathematical models of neuronal connectivity in the developing brain indicate that small-world network organization, characterized by high clustering and short path lengths, becomes increasingly prevalent with age. (Biane et al., 2015; Diedrichsen & Kornysheva, 2015; Hartwigsen & Volz, 2021). This architecture enables efficient information transfer by increasing localized processing within a sub-network as well as fast communication across distant brain regions. These restructuring processes are driven by several key neurobiological mechanisms. (1) Myelination increases the speed of signal transmission along axons, thereby enhancing the coordination between distant brain regions. (2) Synaptic pruning eliminates redundant or weak synaptic connections, improving neural circuits and signal-to-noise ratios. (3) Experience-dependent plasticity further refines motor networks, as repeated practice and environmental interaction reinforce the most efficient and task-relevant pathways (Bloom et al., 2022; Faust et al., 2021; Sowell et al., 2004; Valizadeh & Madadi Asl, 2023).

Building on fundamental aspects of motor control development, higher-order motor areas become increasingly specialized and integrated, supporting the progression from simple to more complex motor behaviors. The SMA, in particular, emerges as a crucial area in this process. Neuroimaging studies have shown age-related cortical thinning within regions overlapping with the SMA, indicating maturation and increased functional specialization (Sowell et al., 2004; Tamnes et al., 2010). In parallel, SMA activation has been shown to increase with both age and task complexity (Mall et al., 2005; Turesky et al., 2018). This developmental trajectory is further supported by electrophysiological findings, with increasing SMA involvement reflected in the amplitude and distribution of slow cortical potentials, such as the Bereitschaftspotential (BP) and contingent negative variation (CNV), which serve as markers of motor preparation. The BP precedes voluntary movements, reflecting motor preparation (Gehring & Coles, 1994; Schurger et al., 2021; Wen et al., 2018), whereas the CNV emerges in response to warning cues during reaction-time tasks, reflecting anticipatory

attention and motor readiness. Both markers provide valuable insights into the maturation of motor planning processes and were shown to exhibit immature cortical activation patterns in young children. This immaturity was reflected by reduced SMA engagement as well as reduced contralateral activation of motor areas (Bender et al., 2005; Bender et al., 2002; Pangelinan et al., 2013; Wakim et al., 2023).

The development of motor control is not limited to motor regions but also relies on the maturation of parietal, fronto-parietal, and prefrontal networks. The parietal cortex becomes more specialized in integrating sensory information into motor commands and in supporting error correction, contributing to the refinement of complex motor skills. Furthermore, neuroimaging studies have shown that during maturation, the fronto-parietal network undergoes an increasing integration and directed functional connectivity within this network, supporting the development of more flexible and adaptive motor control (Li et al., 2019; Wendelken et al., 2017). Besides more efficient information integration and refined motor output, the development of motor control critically involves the growing capacity to inhibit inappropriate or unwanted movements. This increasing inhibitory control is related to a linear increase in activation in frontal, temporal, parietal, and occipital areas (Bunge et al., 2002; Cope et al., 2020), supported by a progressive specialization of fronto-striato-thalamic and fronto-cerebellar circuits (Rubia et al., 2007). The maturation of these neural pathways enhances the efficiency of communication between cortical and subcortical regions, thereby supporting the development of precise and complex motor control.

1.3 Tourette Syndrome

Given the complexity of brain maturation, deviations in developmental trajectories can lead to the emergence of neurodevelopmental conditions, such as tic disorders or Tourette syndrome (TS), caused by alterations in network organization. TS is a childhood-onset neuropsychiatric disorder specified by multiple chronic motor and at least one vocal tic that lasts for more than one year. Tics can appear simple or complex and typically occur in bouts of varying frequency and intensity. Simple tics involve only a few muscle groups and can be described as brief, repetitive movements or vocalizations, such as eye blinking, nose twitching, throat clearing, or sniffing. In contrast, complex tics are defined by coordinated patterns of movements involving multiple muscles, such as jumping, head shaking, shouting, imitating gestures, or repeating words and phrases. The presence of tics typically fluctuates over time and can be highly

influenced by factors such as stress, excitement, concentration, and fatigue (Jafari et al., 2022; Johnson et al., 2023).

The severity of TS follows a consistent time course. Tics typically emerge as simple motor tics in early childhood during preschool or early school-age years. Tic frequency and intensity usually increase throughout development, reaching peak severity between the ages of 10 and 12 years (Bloch & Leckman, 2009). For most TS patients, tic symptoms begin to decrease during late adolescence and continue to diminish into young adulthood with a significant reduction or complete remission of symptoms (Erenberg et al., 1987; Leckman et al., 1998).

Tics are typically preceded by a so-called premonitory urge, a distinct, uncomfortable sensation that is temporarily relieved after ticcing. Notably, the awareness and reporting of premonitory urges emerge around the ages of eight to ten years and increase with age (Woods et al., 2005). Younger children often do not recognize or report sensations prior to their tics, suggesting that the development of premonitory urges is linked to age and cognitive maturation. Most individuals with TS are able to temporarily suppress their tics. However, prolonged suppression of tics is typically associated with a subsequent increase in tic frequency and/or intensity.

Tics are associated with reduced self-esteem, increased psychosocial stress, and can significantly impair quality of life (Ludolph et al., 2012). Furthermore, TS is highly associated with comorbid disorders, such as attention-deficit-hyperactivity disorder (ADHD), obsessive-compulsive disorder (OCD), and poor impulse control (Leckman et al., 2001; Robertson, 2000). These overlapping symptoms often complicate diagnosis and treatment, highlighting the need for further research.

1.4 Pathophysiology of Tourette Syndrome

Many neuroimaging studies were conducted to determine the pathophysiological abnormalities of TS. Although the precise neurobiological mechanisms underlying TS are not completely understood, most studies have suggested disruptions within cortico-striato-thalamo-cortical (CSTC) circuits. These dysregulated interactions between the cortex, the basal ganglia, and the thalamus are thought to contribute to impaired inhibitory control and increased cortical hyperexcitability (Franzkowiak et al., 2012; Jackson et al., 2015; Rae et al., 2022).

Disruptions within the CSTC circuits are closely associated with neurotransmitter imbalances in TS, particularly involving abnormal dopamine signaling, which has been strongly implicated in the pathophysiology of the disorder (Buse et al., 2013; Maia & Conceição, 2018; Palminteri et al., 2011; Singer et al., 1982). Hyperactivity of the dopaminergic system, especially within the striatum, is believed to underlie the emergence of tics by disrupting the normal balance between excitation and inhibition in motor pathways. Furthermore, alterations in the inhibitory γ-aminobutyric acid (GABA) transmission have also been observed in TS (Clarke et al., 2012; Ramamoorthi & Lin, 2011). Reduced GABAergic signaling is thought to be a primary cause of the disinhibition of motor pathways, potentially leading to the involuntary release of movements observed in TS. In addition to dopaminergic and GABAergic dysfunction, recent research has increasingly focused on glutamate dysregulation in TS pathophysiology, reflecting a broader shift toward understanding the role of excitatory-inhibitory imbalances (Kanaan et al., 2017; Mahone et al., 2018; Singer et al., 2010). However, neurotransmitter dysfunction does not fully explain the complexity of TS. Besides these chemical alterations, differences in structural and functional connectivity, atypical maturational trajectories of sensorimotor networks, and compensatory neural mechanisms also play important roles in the pathophysiology of TS.

Earlier neuroimaging studies largely focused on structural and functional alterations within the CSTC network. Structural MRI studies, in particular, have consistently reported atypical anatomical features of the basal ganglia in individuals with TS. Notably, several studies have found reduced volumes of basal ganglia nuclei, most prominently in the caudate nucleus (Peterson et al., 1993; Peterson et al., 2003; Singer et al., 1993). More recent studies and meta-analyses indicated a more complex pattern involving the decrease as well as the increase in grey matter volume in different brain regions (Greene et al., 2017; Yang et al., 2025). Sowell et al. (2008) reported a reduced cortical thickness in the frontal and parietal lobes. Notably, thinning in sensorimotor areas was associated with tic severity, indicating its significance for mechanisms underlying TS.

Functional neuroimaging studies have revealed widespread tic-related alterations within sensorimotor, default mode, and frontoparietal networks, as well as dynamic fluctuations in network organization over time. Hyperactivation in subcortical regions is often accompanied by deviant functional connectivity with cortical areas such as the SMA, M1, and anterior cingulate cortex (ACC). Tic execution, in particular, has been primarily associated with M1

hyperactivity, which is thought to result from increased functional interactions between M1 and the SMA (Franzkowiak et al., 2012; Tübing et al., 2018). Given its pronounced involvement in both tic generation and motor planning, the SMA has been considered a central contributer to the pathophysiology of TS; (1) the SMA shows increased activity in the seconds before tic onset (Bloch et al., 2006; Hampson et al., 2009), (2) it has been associated with the experience of premonitory urges (Kwon et al., 2011; Le et al., 2013), and (3) SMA activity levels have been positively correlated with tic frequency (Mantovani et al., 2007; Wu et al., 2014). Supporting this, tics often occur without a preceding BP, further suggesting that tics emerge from altered, potentially non-volitional motor pathways. While these findings underscore the hyperactive role of the SMA in tic generation, more recent large-scale meta-analyses assume a more complex involvement. A multimodal meta-analysis by Yang et al. (2025) identified significant hypoactivation in the left SMA, alongside overactivation in the right superior frontal and temporal gyri. These findings suggest that the TS-related functional alterations may be more complex and context-dependent or may reflect differences across study populations, methodologies, or study designs.

In line with this broader perspective, recent findings revealed altered sensorimotor integration and increased perception-action binding to underlie tic generation (Friedrich et al., 2021; Kleimaker et al., 2020; Petruo et al., 2019). In typical development, voluntary motor control is highly regulated by sensory feedback, enabling flexible and accurate motor output. This sensorimotor integration is suggested to be disrupted in TS, contributing to the involuntary occurrence of tics. Differences in connectivity between sensory and motor regions, such as the somatosensory cortices, SMA, and M1, may reduce the ability to integrate internal and external information. This can lead to an increased binding between perception and action, thereby raising the probability that a sensory input will trigger a motor output (Friedrich et al., 2021; Petruo et al., 2019).

Over the past few years, our understanding of TS has developed from a disorder primarily affecting motor regions and the CSTC circuit to a more extended network-level disorder, characterized by widespread alterations across multiple connected neural systems. These findings underscore the complexity of disrupted mechanisms underlying TS, suggesting that a deeper understanding of tic generation and motor control deficits requires investigating the dynamic relationships within these brain networks.

1.5 Methodological Backgrounds

To investigate developmental trajectories of motor control and these complex network alterations in TS, this work used advanced neurophysiological methods to capture both spatial and temporal aspects of brain activity. The maturation of neuronal network dynamics and deviations from typical developmental trajectories can be effectively assessed using a range of neuroimaging and electrophysiological techniques.

1.5.1 Electroencephalographie

A major part of this dissertation relies on Electroencephalographie (EEG) based investigations, using complementary techniques to capture different aspects of neural dynamics. EEG is a non-invasive, widely used, and highly valuable method for investigating neuronal activity. It measures intrinsic electrical activity through electrodes placed on the scalp. The recorded neural signal represents postsynaptic potentials generated by pyramidal neurons in the neocortex and allocortex, with their synchronous activity producing measurable scalp potentials (Amzica & Lopes da Silva, 2017; Kirschstein & Köhling, 2009; Tudor et al., 2005). EEG can measure brain activity changes on the millisecond scale. To ensure consistency across studies, EEG electrodes are attached to an elastic cap and positioned over the scalp according to the 10-20 System, a standardized protocol for electrode placement. EEG cap alignment relies on the nasion (nasal bridge), inion (occipital protuberance), and preauricular points (anterior to the ear tragus), used as anatomical landmarks. In this work, a variety of advanced analysis techniques were applied to the EEG data to capture the complexity of brain dynamics underlying motor control and its development.

1.5.2 EEG Analysis Techniques

Event-related potentials

One key advantage of EEG is its high temporal resolution, which enables the precise analysis of rapid changes in brain activity. This property is particularly beneficial for studying event-related potentials (ERPs), facilitating the detailed examination of neural responses to external stimuli. These small, time-locked voltage changes reflect the sum of synchronized neuronal firing induced by sensory, motor, or cognitive events (Sur & Sinha, 2009). The amplitude of an EEG signal depends on the number of synchronously active neurons, where larger

populations firing in synchrony generate stronger electrical fields detectable at the scalp (Niedermeyer & da Silva, 2005).

The CNV is an established ERP component representing anticipatory attention and motor preparation induced between a warning (S1) and a commonly behaviorally relevant imperative stimulus (S2) (Kononowicz & Penney, 2016; Walter et al., 1964). This slow, cortical surface-negative potential reflects primarily the recruitment of fronto-central neuronal populations, however, multiple brain areas contribute to the global CNV signal. The CNV can be subdivided into two main components: the early or initial CNV (iCNV) and the late CNV (lCNV) (Weerts & Lang, 1973). Whereas the iCNV is modulated by stimulus properties (Rohrbaugh et al., 1976), including modality, intensity, and interstimulus intervals (Van Rijn et al., 2011), the lCNV precedes the imperative stimulus and serves as a neurophysiological marker of motor planning and preparation for the upcoming response. Neuroimaging studies identified the SMA as well as M1 as the main generators for the late phase (Gomez et al., 2003)

The CNV has been widely used in developmental neurophysiological research to investigate age-related changes in motor preparation and cognitive control, as well as to identify deviations in clinical populations (Bender et al., 2005; Jonkman, 2006; Nagai et al., 2004; Segalowitz et al., 2010). In this work, the CNV paradigm was employed to assess distinct states and mechanisms of movement preparation, offering a reliable electrophysiological marker to track developmental trajectories and identify TS-related alterations.

Frequency Decomposition

Beyond ERPs, further insights into developmental and disorder-related brain dynamics can be gained by examining the EEG signal in the frequency domain. EEG signals exhibit rhythmic activity across different frequencies, commonly categorized into frequency bands ranging from slow delta (0.5 - 4 Hz) to fast gamma (>30 Hz). Frequency decomposition allows the breakdown of the electrical signal into the separated frequency bands, enabling the precise investigation of neural dynamics associated with different cognitive and physiological states. In this work, I focused the EEG analyses on the mu (8–13 Hz) and theta (4–8 Hz) frequency bands. The mu rhythm is less commonly analyzed than the widely known alpha rhythm, which typically ranges from 8 to 12 Hz. It is strongly related to motor functions, as its amplitude decreases during motor planning and execution, as well as during the imagination or

observation of movements (Hari & Salmelin, 1997; Mitiureva et al., 2023; Pineda, 2005; Volpe et al., 2011). While alpha rhythm is most prominent over the occipital cortex during relaxed wakefulness, the mu-rhythm is restricted to the sensorimotor cortex and requires active motor engagement, typically induced by a motor task paradigm (Jenson et al., 2020; Pineda, 2005; Urgen et al., 2013). Its amplitude decreases, known as event-related desynchronization (ERD), indicates that sensorimotor regions are becoming actively engaged, with neuronal populations transitioning from a resting, synchronized state to an active state that supports dynamic processing of motor-related information (Pfurtscheller & Lopes da Silva, 1999). In addition to the mu rhythm, the theta band was analyzed due to its established role in cognitive control, sensorimotor integration, and preparatory motor processes (Böttcher et al., 2023; Cruikshank et al., 2012; Tan et al., 2024). Particularly due to its crucial role in perception-action binding, theta activity was especially useful for investigating atypical motor network dynamics in TS.

Source Localization (LORETA)

While EEG provides an excellent temporal resolution, it shows only poor spatial resolution. The EEG signal is composed of a mixture of electrical activities from various neuronal populations, making it challenging to accurately localize the sources of brain activity. This so-called EEG inverse problem refers to the fact that different configurations of active intracranial sources can generate the same electrical field distribution on the scalp (Baillet, 2022). To address this problem, neuronal generators of the recorded activity can be estimated by computational source localization techniques, such as low-resolution brain electromagnetic tomography (LORETA), introduced in 1994 (Pascual-Marqui et al., 1994). LORETA uses a standardized three-shell (scalp, skull, brain) spherical head model registered to the MNI brain atlas (Talairach, 1988) with fixed grid points (voxel) for each source (Dattola et al., 2020). The model assumes that neighboring neurons are more likely to fire synchronously, resulting in spatially smooth electrical fields. The mathematical approach of LORETA minimizes the Laplacian of the current density distribution, enforcing solutions where activity varies gradually across adjacent brain regions. This approach addresses the inverse problem by prioritizing source configurations that reflect realistic patterns of neural activation. However, this increases the risk of oversimplifying the underlying source generators. The integration of high-density EEG data and individual MRI-derived head models significantly refines spatial details and enables a more accurate source estimation (Michel & Brunet, 2019; Song et al.,

2015; Wang et al., 2011). The Standardized Shrinking LORETA-FOCUSS (SSLOFO) is an improved mathematical algorithm that improves the model performance of source estimation. It combines sLORETA, an advanced LORETA approach that integrates normalization by the standard error, with FOCUSS (FOCal Underdetermined System Solver), an algorithm that employs the re-weighted minimum norm to emphasize regions with high current density and reduce noise (Liu et al., 2005). Overall, the use of SSLOFO increased the spatial interpretability of the EEG findings, allowing for more precise insights into the cortical regions involved in motor and cognitive processes.

Phase Locking Value and Graph Theory-Based Network Analysis

Besides analyzing local activation, phase-locking values (PLVs) were calculated to examine functional connectivity within motor networks. PLV measures how consistently the phases of oscillatory signals from different brain regions are aligned, ranging from 0 (no consistent phase relationship) to 1 (complete phase synchronization) (Aydore et al., 2013; Schmidt et al., 2014). This approach allows us to assess the coordination between different cortical areas and networks at specific frequencies, providing insight into the organization of complex neural processes. PLVs in the theta band were computed to assess TS-related disruptions in sensorimotor integration, perception-action binding, and movement preparation.

Furthermore, we applied graph theory to characterize the organization and efficiency of these functional networks. Graph theory provides a mathematical framework for modeling the brain as a network of interconnected nodes (brain regions) and edges (structural or functional connections) (Bassett & Sporns, 2017; Bullmore & Sporns, 2009; Rubinov & Sporns, 2010). By applying graph-based metrics to EEG-derived connectivity data, it is possible to quantify properties such as network efficiency, clustering, and integration, offering a systems-level perspective on how brain regions interact during motor and cognitive tasks (Ismail & Karwowski, 2020; Yan et al., 2024). We mainly focused on network efficiency to determine whether potential deviations in connectivity reflect dysfunctional processing or compensatory adaptations in TS motor networks.

1.5.3 Transcranial Magnetic Stimulation

To complement EEG-based measures of functional connectivity and preparatory activity, this study also incorporates transcranial magnetic stimulation (TMS) combined with EEG. TMS is

a non-invasive neuromodulatory technique that uses magnetic pulses to directly acts on the cortical electrophysiological activity (Ilmoniemi & Kičić, 2010). An electromagnetic coil generates pulsed magnetic fields that penetrate the skull and induce small electric currents in the brain. These currents are powerful enough to depolarize cell membranes in the targeted area. Due to the depolarization, voltage-gated ion channels open and action potentials are triggered (Hallett, 2007; Kobayashi & Pascual-Leone, 2003; Lefaucheur, 2019). TMS-induced changes of neuronal activity can be directly displayed in the EEG recordings, known as TMS-evoked potentials (TEPs).

In the EEG signal, the N100 component, a negative deflection occurring approximately 100 ms after stimulation, is one of the most robust TMS-evoked potentials (Bender et al., 2005; Du et al., 2018; Kaarre et al., 2018). The N100 is thought to reflect $GABA_B$-mediated inhibitory neurotransmission and serves as a robust index of cortical inhibition in both health and disease (Kaarre et al., 2018; Premoli et al., 2014). The N100 was shown to be highly sensitive to age (Bender et al., 2005; Määttä et al., 2017; Noda et al., 2017; Oberman & Benussi, 2024) and neurodevelopmental disorders (Bruckmann et al., 2012; Finisguerra et al., 2019; Jannati et al., 2022). TMS can directly assess cortical excitability and inhibitory processes, providing valuable insights into the neurophysiological mechanisms underlying motor control. This is particularly valuable in TS, where altered inhibitory control is a crucial aspect, and the N100 may provide a sensitive neurophysiological marker for the identification of individual differences in motor inhibition and network dysfunction.

1.5.4 Functional Magnetic Resonance Imaging

In addition to electrophysiological measures, functional magnetic resonance imaging (fMRI) was analyzed to investigate the spatial organization of motor network activity and connectivity patterns, providing complementary insights into the neural activity underlying motor control and compensatory mechanisms in TS. While advanced source localization techniques like SSLOFO refine EEG's spatial precision, their accuracy remains constrained by the volume conduction problem and limited anatomical specificity. Structural and functional MRI provide high-resolution anatomy data using blood-oxygen-level-dependent (BOLD) signals that reflect neuronal activity dynamics. fMRI measures haemodynamic changes after enhanced neural activity (Ogawa et al., 1990; Smith, 2004). However, since these vascular responses evolve

over several seconds, the resulting signal is inherently delayed and temporally blurred relative to the underlying neural events, leading to poor temporal resolution.

While fMRI-based functional connectivity captures statistical correlations between brain regions, it is limited in its ability to assess the causal mechanisms by which a neuronal system directly influences another (Friston et al., 2003). A possible method to quantify this so-called effective connectivity, which underlies functional connectivity, is dynamic causal modeling (DCM) (Friston et al., 2003; Marreiros et al., 2010). The DCM framework models causal interactions by considering the brain as a dynamic input-output system, allowing for the estimation of directionality and strength of influence between brain regions over time. Unlike functional connectivity, which is based on undirected correlations, DCM incorporates temporal dependencies and generative models to infer how activity in one area drives changes in another, thereby providing a more mechanistic understanding of neural integration and network dynamics (Friston, 2011; Saetia et al., 2020). DCM was used to compare how causal interactions between motor and cognitive control regions are reconstructed during healthy development and how these connectivity patterns are altered in children and adolescents with TS.

1.6 Hypothesis

I hypothesize that healthy neurodevelopment is characterized by a progressive, non-linear shift in the control of complex motor functions, with the frontal cortex gaining an increasingly dominant role in the planning, regulation, and inhibition of motor actions. This development is revealed by brain networks becoming increasingly integrated, specialized, and efficient, alongside increased hemispheric specialization that refines motor and cognitive functions.

In children and adolescents with TS, this typical maturation of motor control networks is altered. Specifically, I expect to observe differences and delays in the development of motor-related brain areas, with reduced or atypical engagement of frontal control regions. As a result, patients may rely more heavily on compensatory strategies within motor circuits to regulate motor output.

The aims of these studies are (1) to characterize the developmental trajectory of motor network organization in healthy children and adolescents, (2) to identify TS specific network alterations in brain dynamics that could serve as potential targets for clinical intervention, (3) to investigate

how atypical patterns of neural activity and connectivity in TS are related to deficits in motor control, perception-action binding, and inhibitory processes, distinguishing maladaptive dysfunction from possible compensatory mechanisms, and (4) to evaluate the usability of EEG-derived measures as sensitive biomarkers for both typical development and clinical deviations, supporting their use in future intervention studies.

1.7 Significance of Manuscripts

The first publication establishes the normative framework for motor network maturation across childhood and adolescence. Using high-density EEG and a directional contingent negative variation (CNV) paradigm, this study systematically investigates age-related changes in attention allocation, motor preparation, and movement evaluation in a sample of healthy children and adolescents. By establishing key electrophysiological markers and developmental trends, this work provides essential indicators for identifying deviations in clinical populations.

The second work builds directly on the healthy framework by investigating how developmental processes are altered in TS. Through EEG-based network analyses in the theta band, it explores potential differences in network connectivity and integration in children and adolescents with TS, with a particular focus on sensorimotor integration and the processing of external stimuli. This study is central for understanding how atypical development may manifest at the network level and how these adaptations might help maintain motor performance.

The third article extends this approach by employing fMRI-based connectivity modeling to investigate both healthy development and TS-related deviations, with an increased spatial precision. This work specifically examines how the directionality and strength of interactions between key brain regions evolve with age in typical development and how these patterns are altered in TS. By comparing effective connectivity profiles between groups, the study aims to identify both disruptions and compensatory adaptations within the motor system, providing a mechanistic understanding of how atypical development manifests at the network level.

The forth publication used the strengths of combined TMS-EEG to directly asses motor network excitability and inhibition in both healthy development and TS. By combining single-pulse TMS over M1 with EEG recordings, the study analyses how inhibitory responses are dynamically modulated during changes of external stimulation as well as during different

movement states (preparation, execution). By integrating these approaches, the work provides novel insights into the temporal dynamics and context-dependency of inhibitory deficits in TS.

By combining high-resolution EEG, advanced analytical methods, TMS/EEG, and fMRI across both healthy development and TS-related alterations, this dissertation provides a comprehensive view of motor network maturation as a dynamic and context-dependent process. These insights not only increase our understanding of motor system development in health and disease, but also provide a more comprehensive basis for future research that could lead to more effective therapies for neurodevelopmental conditions such as TS.

2 Study 1: Developmental Changes in Motor Preparation

From preparation to post-processing: Insights into evoked and induced cortical activity during pre-cued motor reactions in children and adolescents

Julia Schmidgen , Theresa Heinen, Kerstin Konrad , Stephan Bender

This article has been published in *Neuroimage*. 2024 Aug 15;297:120735.

doi: 10.1016/j.neuroimage.2024.120735.

This study advances our understanding of how motor networks mature during childhood and adolescence by taking advantage of the high temporal resolution of EEG to capture the rapid and dynamic changes in neural processes underlying motor control across development. The key strengths of this work were the simultaneous analysis of event-related potentials (ERPs), mu-rhythm (de)synchronization, and source localization that enabled a detailed analysis of temporal dynamics across the different stages of movement planning, execution, and evaluation.

The results reveal distinct developmental trajectories in both behavioral performance and neural activation patterns, showing growing involvement of higher-order control regions, increased hemispheric specialization, and the neural basis of proactive, efficient motor control.

The identification of robust electrophysiological markers and developmental trajectories enables the identification of atypical patterns in motor network development

2.1 Contribution

I contributed to the design of the study and was responsible for the acquisition and preprocessing of data, statistical analysis, and visualization of results. I interpreted the findings, drafted the manuscript, prepared the figures and tables, and revised the work based on feedback. I coordinated the research process and ensured the scientific integrity and clarity of the paper.

NeuroImage 297 (2024) 120735

Contents lists available at ScienceDirect

NeuroImage

journal homepage: www.elsevier.com/locate/ynimg

From preparation to post-processing: Insights into evoked and induced cortical activity during pre-cued motor reactions in children and adolescents

Julia Schmidgen [a,*], Theresa Heinen [b,c], Kerstin Konrad [b,c], Stephan Bender [a]

[a] Department of Child and Adolescent Psychiatry, University of Cologne, University Hospital Cologne, Germany
[b] Section Child Neuropsychology, Department of Child and Adolescent Psychiatry, Psychosomatics and Psychotherapy, RWTH, University Hospital, Aachen, Germany
[c] JARA-BRAIN Institute II, Molecular Neuroscience and Neuroimaging, Forschungszentrum Jülich GmbH and RWTH Aachen University, Germany

ARTICLE INFO

Keywords:
Brain development
Motor preparation
Contingent negative variation
Event-related-potentials
Event-related desynchronization

ABSTRACT

Introduction: The motor system undergoes significant development throughout childhood and adolescence. The contingent negative variation (CNV), a brain response reflecting preparation for upcoming actions, offers valuable insights into these changes. However, previous CNV studies of motor preparation have primarily focused on adults, leaving a gap in our understanding of how cortical activity related to motor planning and execution matures in children and adolescents.

Methods: The study addresses this gap by investigating the maturation of motor preparation, pre-activation, and post-processing in 46 healthy, right-handed children and adolescents aged 5–16 years. To overcome the resolution limitations of previous studies, we combined 64-electrode high-density Electroencephalography (EEG) and advanced analysis techniques, such as event-related potentials (ERPs), mu-rhythm desynchronization as well as source localization approaches. The combined analyses provided an in-depth understanding of cortical activity during motor control.

Results: Our data showed that children exhibited prolonged reaction times, increased errors, and a distinct pattern of cortical activation compared to adolescents. The findings suggest that the supplementary motor area (SMA) plays a progressively stronger role in motor planning and response evaluation as children age. Additionally, we observe a decrease in sensory processing and post-movement activity with development, potentially reflecting increased efficiency. Interestingly, adolescent subjects, unlike young adults in previous studies, did not yet show contralateral activation of motor areas during the motor preparation phase (late CNV).

Conclusion: The progressive increase in SMA activation and distinct cortical activation patterns in younger participants suggest immature motor areas. These immature regions might be a primary cause underlying the age-related increase in motor action control efficiency. Additionally, the study demonstrates a prolonged maturation of cortical motor areas, extending well into early adulthood, challenging the assumption that motor control is fully developed by late adolescence. This research, extending fundamental knowledge of motor control development, offers valuable insights that lay the foundation for understanding and treating motor control difficulties.

Abbreviations

ACC	anterior cingulate cortex
CNV	contingent negative variation
CSD	current source density
EEG	electroencephalogram
EHI	edinburgh handedness inventory
ERD	event-related desynchronization
ERP	event-related potential
ERS	event-related synchronization
ICA	independent component analysis
iCNV	initial or early CNV
lCNV	late CNV

(continued on next column)
(continued)
(continued on next page)

* Corresponding author.
E-mail address: Julia.schmidgen@uk-koeln.de (J. Schmidgen).

https://doi.org/10.1016/j.neuroimage.2024.120735
Received 7 February 2024; Received in revised form 2 May 2024; Accepted 11 July 2024
Available online 14 July 2024

(continued)

LORETA	low-resolution brain electromagnetic tomography
LRP	lateralized readiness potential
M1	primary motor cortex
MRP	motor evoked potential
PINV	post-imperative negative variation
SMA	supplementary motor area
SSLOFO	current standardized shrinking LORETA-FOCUSS

1. Introduction

Cortical development in childhood and adolescence underlies complex restructuring processes characterized by extensive anatomical (Huttenlocher, 1979; Shaw et al., 2008) as well as functional changes in the cerebral cortex (Thatcher, 1992). Gaining proficient motor skills stands as a key cornerstone in human development; however, there is limited understanding regarding the relationship between brain development and the acquisition of motor abilities.

The motor system engages in various processes when preparing for movement. This includes the selection of the involved muscles, determining the required contraction force, and arranging the temporal sequence of movements. Changes in brain activity prior to a movement reflect neural processes associated with movement preparation and execution (Deecke et al., 1969). Thereby, it was shown that the supplementary motor area (SMA) plays a crucial role in planning and coordinating voluntary movements (Roland et al., 1980; Tanji, 2001) and that SMA activity has a modulatory effect on the output of the primary motor cortex (M1) (Côté et al., 2020).

The maturation of functional activity related to motor network preactivation can be studied by analyzing age-dependent changes of event-related potentials (ERPs) before the execution of a movement. The negative potential arising between a warning stimulus (S1) and a behaviorally relevant imperative stimulus (S2) is described as contingent negative variation (CNV) and is associated with processes of movement preparation and attention allocation (Rockstroh, 1982; Walter et al., 1964). The imperative stimulus follows the warning stimulus in fixed time intervals and requires a fast motor response. To efficiently process the imperative stimulus, the neuronal network responsible for initiating the chosen response movement must be pre-activated. Since the CNV is based on a predictable, external cue, it allows to temporally disentangle early response selection and preparation processes, i.e., the recruitment and selection processes of the specific neuronal networks required for a fast response (Gomez et al., 2003).

The CNV consists of an early low, negative component that typically follows the warning stimulus with a latency of 550 to 750 ms and a more pronounced negative late component that precedes the behaviorally relevant imperative stimulus. The early CNV (abbreviated as iCNV; initial CNV; "O-wave") is suggested to reflect an orienting response (Rockstroh, 1982) and to originate from the SMA and the anterior cingulate cortex (ACC) (Cui et al., 2000; Gomez et al., 2001). The late CNV (abbreviated as lCNV; E-wave) is associated with preparatory processes and stimulus anticipation (Rohrbaugh et al., 1976) observed as pre-activation of the contralateral motor areas. Furthermore, the CNV contains a post-movement potential known as post-imperative negative variation (PINV). This slow negative potential can be studied to evaluate processes related to motor performance evaluation (Klein et al., 1996). Previously, the PINV was interpreted as a potential measure of uncertainty regarding the accuracy of motor performance (Werner et al., 2011). While PINV has been extensively studied in various contexts, including neurological and psychiatric conditions, there has been relatively limited research specifically focused on PINV maturation in healthy subjects.

The CNV has been extensively analyzed to study pathophysiological differences between control subjects and subjects with various neurological and mental disorders. However, healthy maturation related to preparatory brain activity remains largely unexplored in terms of its underlying developmental mechanisms. Electrophysiological studies comparing late CNV potentials of children and adolescents showed increasing negativity over pre- and primary motor areas (Bender et al., 2005; 2002; Gomez et al., 2003). The results were interpreted as immaturity of the frontal cortex. However, it remains unclear if absent or low pre-movement negativity in young children directly reflects activity states of the underlying cortical areas and to what extent the supplementary motor area contributes to early response selection, especially in young children.

EEG research of the early CNV component revealed more contradictory results. It was shown that the early CNV exhibits modality-specific characteristics. Specifically, it shows higher amplitudes in response to auditory warning stimuli (S1) compared to visual warning stimuli. Concerning the maturation of early CNV studies focusing on auditory CNV paradigms have reported decreasing amplitudes over frontal electrodes during childhood and adolescence (Bender et al., 2005), whereas investigations involving visual CNV paradigms have indicated rising frontal early CNV amplitudes within the same age range (Jonkman et al., 2003). These findings suggest that S1 post-processing exhibits a modality-specific contribution to the early CNV, showing stimulus-dependent developmental differences. Simultaneously, an S1-modality independent component results in increasing fronto-central amplitudes during response selection processes (Jonkman, 2006; Jonkman et al., 2003).

Besides electrophysiological ERP data, changes in brain oscillatory activity of different frequency bands can be analyzed to study task-related power changes. Changes within the alpha band are typically observed in motor-related brain areas during processes of motor planning (Pfurtscheller and Lopes da Silva, 1999). The analysis of alpha power enables the modulation of more widespread cortical dynamics and provides complementary information to the analysis of evoked potentials (Claudio Babiloni et al., 1999). A relative increase of frequencies related to the alpha rhythm, commonly assessed in a range of 8 to 12 Hz, refers to alpha band event-related-synchronization (ERS) and is suggested to reflect active processes of inhibition (Jensen and Mazaheri, 2010; Klimesch et al., 2007). Alpha band event-related-desynchronization (ERD) is related to a decrease in oscillatory activity and an increased activity of underlying brain areas (Niedermeyer, 1997). Even though analysis of the alpha rhythm provides additional insights into maturational processes, CNV-induced oscillatory changes have been studied rarely in the context of healthy brain development.

While ERPs and power changes provide valuable information about the timing and general location of brain activity, they lack the spatial resolution to pinpoint the exact source of the electrical signals. To gain a deeper understanding of how underlying neuronal networks contribute to cortical activation, source localization can be applied (Eom, 2023). By incorporating anatomical information about the brain with the EEG recordings, source localization allows to estimate the activity of specific brain regions underlying the recorded changes and to analyze developmental changes in recruited brain areas more precisely.

The primary aim of this study was to investigate maturational changes in attention allocation, motor program pre-activation, and performance evaluation. Each quantifier (CNV, PINV, alpha ERS/ERD) offers unique insights into different aspects of motor control development. While CNV reflects preparatory processes and attention allocation, PINV provides information on motor performance evaluation, and alpha band oscillations offer insights into cortical inhibition and activation patterns in cortico-thalamic loops. Integrating these quantifiers allows for a comprehensive understanding of the maturation of motor-related brain activity during childhood and adolescence.

We hypothesize that both iCNV and lCNV amplitudes will increase with age, reflecting enhanced neural efficiency and maturity of preparatory processes. It is assumed that the lCNV will exhibit stronger pre-activation of contralateral motor areas with age, indicating pre-

activation of cortical areas required for a fast response. We expect the PINV to show an age-related reduction in its magnitude, indicating a developmental tendency for children to exhibit greater uncertainty about the correctness of their performance. Since inhibitory control was shown to increase during childhood (Macdonald et al., 2014), we hypothesize an increase in alpha power desynchronization, reflecting improved (inhibitory) motor control and more efficient neural communication during movement preparation.

These hypotheses will be tested through the analysis of high-density EEG data and movement performances collected from children and adolescents aged 5 to 16 years, using a CNV paradigm. To enhance response selection processes in comparison to other developmental studies, we chose a directional warning stimulus S1 (arrow pointing to the right or left side) that indicated the movement side required for the motor response to the imperative stimulus S2. To prevent overlaps with the cortical activity of auditory post-processing, we used visual stimuli. By employing a multimodal approach that integrates complementary analyses of cortical activation patterns, oscillatory dynamics, and underlying neural sources, we aim to achieve a deeper understanding of the developmental processes that shape motor skill acquisition and motor control in children and adolescents.

2. Material and methods

2.1. Subjects

A total of 46 typically developing subjects in the age range of 5- to 16-years were recruited. For details regarding demographic characteristics, see Table 1. All participants had no history of motor impairments or any neuropsychiatric condition. A diagnostic interview was used for all subjects to assess and exclude neuropsychiatric disorders (Kinder-DIPS; Adornetto et al. (2008)). The study included only right-handed participants (Edinburgh Handedness Inventory, Oldfield (1971)) who had an IQ score of at least 70 (WISC V; Wechsler, D. (2017)). Participants with an individual or a family history of epilepsy, severe or acute psychiatric diseases, and neurological or non-correctable visual impairments were excluded from the study. Subjects were not permitted to take any psychoactive or antipsychotic drugs affecting the central nervous system. Two participants had to be excluded from the analysis due to high artifact levels.

The experiments were performed in accordance with the Declaration of Helsinki. In an age-adjusted information letter as well as in a personal briefing, participants and parents were informed about the procedure of the measurements and the possibility of terminating participation at any time without giving reasons. Before participation, participants and their parents signed written informed consent.

2.2. Experimental procedure

The software package *Presentation* (Version 10.3, Neurobehavioral Systems Inc., Albany, CA) was used to generate a task-related program with alternating visual stimuli displayed on a monitor at a distance of 90 cm from subjects. To prevent any distractions, the light was dimmed, and the noise level was reduced to the highest possible minimum. To minimize distracting eye movements, a fixation cross was displayed in between visual stimuli. Subjects sat in a comfortable position on a skid-proof chair, reducing muscle activity as much as possible to prevent interfering contractions.

Table 1
Sample characteristics.

Age Group (Years)	N	Mean age (± SD)
5–8	12 (5 m, 7 f)	7.27 (± 1.14)
9–12	17 (7 m, 10 f)	10.68 (± 1.34)
13–16	15 (7 m, 8 f)	14.72 (± 1.13)

2.3. Behavioral CNV task paradigm

Subjects performed a visual CNV (Fig. 1) task with 50 trials, respectively for each response side. The warning stimulus (S1) was presented as a black arrow on a white background pointing to the left or right side. The imperative stimulus (S2) was presented as a colored sheriff on a white background. Both stimuli were displayed for 150 ms, interstimulus intervals were set to 3.05 s, and pseudorandomized intertrial intervals varied from 3 to 6 s. The warning stimulus indicated the side of the required button press, whereby arrows were presented in a pseudorandomized order. Subjects were instructed to respond to the imperative stimulus S2 as fast as possible by pressing either the right or left button on a German standard keyboard (ctrl for left button press, enter on the numeric keypad for right button press) with the left or right thumb.

2.4. Electroencephalography

EEG was recorded using a 64-channel BrainAmp system (Brain-Products, Munich, Germany) and Brain Vision Recorder software (BrainProducts). Elastic EEG caps with direct current sintered Ag/AgCl disc electrodes (BrainProducts) were selected based on head sizes. Electrodes were named based on their location on the scalp, consistent with the international 10–20 system, electrode impedances were kept below 5 kΩ. Additionally, EOG electrodes were positioned under the left and right eye and on the nasion. The sampling rate was set to 5000 Hz, electrode CZ was used as a recording reference.

2.5. Electromyography

Surface EMG (compound muscle action potential) was recorded using self-adhesive silver-silver chloride electrodes in a belly tendon montage respectively for the left and right hand. To record thumb movement, active electrodes were placed on the adductor pollicis muscle, reference electrodes were attached to the exterior proximal phalanx of the thumb. The ground electrode was placed on the inner forearm. The EMG was recorded using the bipolar BrainAmp ExG amplifier (Brain Products, Munich, Germany), which was synchronized with the EEG recordings.

2.6. Signal preprocessing

EEG and EMG data were processed using the BrainVision Analyzer2 software (BrainProducts, Munich, Germany). To reduce large file sizes, data were downsampled to 500 Hz. For ERP analysis, EEG data were re-referenced to an average reference. For the analysis of current source density and alpha ERD, signals were transformed to reference-free data (for details, see section 2.7.4 for CSD and 2.7.6 for alpha ERD). For the analysis of the CNV characteristics, EEG data were segmented into epochs of 7.5 s (from 800 ms before warning stimulus S1 to 3000 ms after imperative stimulus S2), respectively for left and right button press conditions. Only trials with a correct response within the time window of 100 to 1500 ms following S2 were included in further analysis. Muscle artifacts were rejected by visual inspection, and independent component analysis (ICA) was used to remove artifacts evoked by eye movement (Mennes et al., 2010). Baseline correction was set from 500 to 0 ms preceding the warning stimulus (S1), and signals were filtered digitally (50 Hz notch filter). To prevent slow drift effects from affecting EEG data, a linear DC detrend was applied. Visual inspection before and after DC detrending confirmed that there was no systematic effect on the EEG data, preserving the overall shape and characteristics of the signal. Averages were calculated, respectively for each experimental condition and parameter.

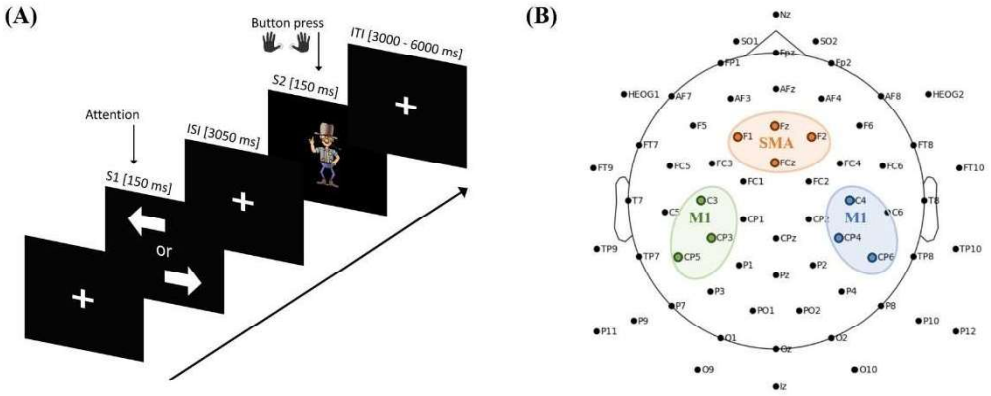

Fig. 1. Experimental design **(A)** Contingent negative variation (CNV) task paradigm with a directional warning stimulus S1 and a behaviourally relevant imperative stimulus S2. **(B)** Electrode locations with regions of interest and specific electrodes used for data analysis marked in orange (SMA), green (M1 right), and blue (M1 left). Sensor locations were plotted by using MNE-Python (Gramfort et al., 2013).

2.7. Analysis of parameters

2.7.1. Behavioral data

Reaction times were calculated as the mean time between the presentation of S2 and the button press of correct response trials. Error rates were calculated, based on the recorded 100 trails, as the sum of no or false alarms (button press between S1 and S2) and incorrect button presses in response to S2 (button press on wrong movement side).

2.7.2. Conceptual design: parameters, time windows, and scalp-locations

To gain a deep insight into the development of motor control, changes of evoked potentials (ERPs) and alpha power changes (ERD) were investigated. The analyses were performed separately for each CNV component, after confirming the well-known interaction between the CNV components and scalp areas, which indicates different topographies for the components. Moreover, to investigate generators of cortical activity during early motor-preparation (iCNV) source localization approaches (CSD and SSLOFO) were applied.

The following time windows were used for the analysis of the different components, respectively for left and right response conditions: iCNV was defined as the mean value of a 200 ms time window around the maximum negative amplitude at mid-frontocentral electrodes (Fz, FCz′, FC1′, FC2′) between 550 and 1400 ms following S1 (Bender et al., 2002; Böcker et al., 1990; Kropp et al., 1999). Data inspection and iCNV latency analysis revealed a pronounced, continuous latency shift of the early component, especially in younger subjects (see Fig. 3A). Consequently, the iCNV peak detection time window was extended from 550 - 750 to 550 - 1400 ms after S1 to prevent the shadowing of maturational differences in iCNV amplitudes. The lCNV component was calculated as the mean voltage of the interval of 200 ms preceding the imperative stimulus S2 (Böcker et al., 1990). The PINV was defined as the mean value of a 200 ms time window around the maximum negative amplitude between 500 and 1500 ms following the imperative stimulus (S2).

Electrodes Cz, FCz′, FC1′, FC2′ were used to analyze midfrontocentral activity (Cui et al., 2000; Gerloff et al., 1998), electrodes C4, CP4′CP6′, respectively C3, CP3′, CP5′were used to analyze motor activity over centro-parietal areas related to the right and left primary motor cortex (Gerloff et al., 1998). Fig. 1B shows an overview of the sensor distribution and electrodes used for data analysis.

2.7.3. Event-related potentials (ERP)

To investigate age-related CNV characteristics, ERPs were investigated, respectively for each component. For the analysis of the evoked cortical activity, topographical distribution, CNV waveforms, and amplitudes were analyzed. To analyze potential differences in the timing of motor preparation and post-processing, iCNV and PINV latencies of the amplitudes were investigated.

2.7.4. Current source density (CSD) analysis

To enhance spatial resolution (Nunez et al., 1994) and identify locations of current sources involved in iCNV generation, we used CSD analysis. This approach is particularly valuable because previous studies investigating developmental differences in early motor preparation using ERPs have yielded inconsistent findings. Given the potential for modality-specific and modality-independent components to contribute to iCNV activity observed in ERP analysis, CSD analysis offers a more precise tool for identifying the true underlying neural sources.

For CSD estimation, EEG signals were transformed into reference-free data, since it enables the estimation of current source generators without relying on a specific reference electrode, thereby minimizing potential biases and artifacts associated with reference choices (Tenke and Kayser, 2005). CSD analysis relies on the relative differences in voltage between neighboring electrodes. The spherical spline interpolation method was applied before surface Laplacian based on the EEG voltage distribution was used. CSD data is indicated as $\mu V/m^2$. The topographical distribution of cortical activity over mid-front areas (Cz, FCz′, FC1′, FC2′), which is likely to originate from the SMA (Pfurtscheller et al., 2003), was analyzed.

2.7.5. Current standardized shrinking loreta-focuss (SSLOFO)

In addition to CSD analysis, the inverse SSLOFO (standardized shrinking LORETA-FOCUSS) algorithm was used to enhance the precision of cortical source reconstruction (Liu et al., 2005) during iCNV. The algorithm combines multiple techniques to improve source localization abilities. Initially, a low-resolution sLORETA image is calculated. To improve spatial resolution, the re-weighted minimum norm of FOCUSS is applied. "Standardization" technique is used to enhance the ability of localization, as in sLORETA. Further insights into the specifics of the SSLOFO algorithm, along with comprehensive performance comparisons against other prevalent algorithms, can be found in Liu et al. (2005).

2.7.6. Alpha event-related desynchronization (alpha-ERD)

We analyzed alpha band desynchronization to study movement-related changes of cortical oscillations in the frequency range of 8 to 12 Hz. EEG studies in infants have indicated that lower frequency ranges (6–8 Hz, theta rhythm) can be considered comparable to the mu-rhythm observed in adults (Cochin et al., 2001). However, there is no clear

evidence that theta rhythm in infants and mu-rhythm in adults represent equal processes. Furthermore, Berchicci et al. (2011) observed that a shift of "central alpha" activity was most pronounced in the first years of life and reached a frequency of 9 Hz at the age of 4 years. Since our subject sample started at the age of 5 years and to ensure comparability between young children and adolescent subjects, we analyzed common alpha band ERD of 8 to 12 Hz.

Alpha ERD was calculated based on reference-free (current source density) EEG data to minimize the impact of reference-related artifacts on ERD calculations. Moreover, CSD estimation enhances the spatial resolution of EEG data by estimating the underlying neural sources directly, without relying on scalp electrodes. This can provide more precise localization of alpha oscillatory activity and define brain regions involved in power changes more precisely.

The same time windows, trials, and electrodes as in ERP analysis were used for the analysis of alpha ERD, respectively for the iCNV, lCNV, and PINV components. The signal was bandpass filtered in the frequency range of 8 to 12 Hz, subsequently squared, and averaged across segments (Pfurtscheller and Da Silva, 1999). ERD output data was normalized, i.e., baseline corrected and rescaled relative to the mean value within the reference interval of 1000 ms before the onset of the imperative stimulus S1. ERD magnitude at each electrode was expressed as percentage changes of the instantaneous power.

2.7.6.1. Analysis of alpha ERD lateralization during lCNV. Data of alpha ERD during late motor preparation (lCNV), suggested a robust pattern of lateralization across age groups, albeit with shifts of the cortical activity. The analysis of the lateralized portion of the alpha-ERD was included to investigate the overall timing and strength of cortical changes during motor preparation across the age groups, unbiased by the specific cortical regions engaged.

The calculation is known from the double subtraction method of the lateralized readiness potential (LRP, see de Jong et al. (1988)). The method involves subtracting the average ERP/alpha ERD of ipsilateral electrodes (e.g., left centro-parietal area for left response condition and right centro-parietal area for right response condition) from the average ERP of contralateral electrodes (e.g., right centro-parietal area for left response condition and left centro-parietal area for right response condition). Subsequently, the mean of the differences obtained was calculated.

2.8. Statistical analysis

2.8.1. Analysis of age-groups

Statistical analysis was performed using IBM SPSS Statistics 28 software (IBM Corp.; Version 28). To examine maturational changes, data were divided into age groups (5- to 8-year-olds ($n = 12$), 9- to 12-year-olds ($n = 17$) and 13- to 16-year-olds ($n = 15$)). This approach enhances the capabilities to investigate and illustrate *interactions* between age-dependent development and other factors, such as scalp area, especially when data underlies non-linear maturational trajectories. Repeated measurement analysis of variance (ANOVA) with these three age groups was performed since it effectively captures interactions between variables, a capability that linear regression lacks. Dividing the participants into equally sized age groups enables a systematic examination of development across various stages, allowing us to assess effects that are not strictly linear. Expanding the age ranges for each group would likely reduce the resolution of developmental effects, particularly considering the significant differences observed between 5 and 8-year-olds and older children. Meanwhile, increasing the number of age groups would have resulted in smaller sample sizes per group, compromising the statistical power of the analysis.

Repeated measurement analysis of variance (ANOVA) with the within-subject factors movement side (right, left) and scalp area (mid-frontocentral, right and left centro-parietal) and the between-subject factors age group (5- to 8-year-olds, 9- to 12-year-olds and 13- to 16-year-olds) and gender (male, female) were applied to investigate ERP latencies for iCNV and PINV as well as ERP and alpha-ERD amplitudes for iCNV, lCNV and PINV. The between-subject factor gender exhibited no significant effect or trend toward significance in the data and is consequently not further discussed. This suggests that, overall, gender might not be a major influencing factor. However, it's important to acknowledge the limitations of the analysis due to the small sample size for males in each age group. The possibility of interaction effects between gender and age group cannot be entirely ruled out, even though the results remain consistent in our data when the gender factor is excluded.

Pairwise comparisons of estimated marginal means, including Šídák correction for multiple testing, were integrated into the linear mixed model to test for significant differences across the different age groups and scalp areas. For ANOVA testing and pairwise comparisons of the estimated marginal mean, values of $p < .05$ were considered statistically significant.

Multiple *t*-tests were used to identify areas with activity that significantly differed from the baseline. To address the issue of multiple comparisons, an alpha correction (Bonferroni correction) related to the tested scalp regions was applied. Due to variations in the number of multiple comparisons across observed parameters, corresponding statistically significant p-values are reported directly with each parameter.

2.8.2. Regression analysis

To verify that the group cut-offs did not introduce artificial effects, scatterplots, and regression analyses were examined for differences across different age groups and scalp areas, identified by ANOVA. Furthermore, regression analyses were used to investigate the relationship between mid-frontocentral activity and task performance.

Due to developmental trajectories showing curvilinear age effects on certain dependent variables (i.e., more pronounced changes in younger children) (Fietzek et al., 2000; Klein, 2001), regression analysis was performed either as linear regression using age as a predictor ($y = a + b *$ age; y = predicted original data; a = constant; b = regression coefficient) or as non-linear regression using age-1 as predictor (regression equation $y = a + b * \text{age}^{-1}$). An exploratory analysis of the scatterplots was used to determine if data showed a linear relationship between age and a dependent variable, i.e., a constant development of the variable throughout the examined age range of 5 to 16 years, or a non-linear influence of the factor age on the dependent variables, i.e., more pronounced development in younger (or older) subjects. The most suitable regression model (predictors age or age^{-1}) was chosen based on data examination respectively for each variable.

3. Results

3.1. Behavioural task performance (reaction time)

Behavioral task performance across age groups was investigated by analyzing error rates and reaction times. The ANOVA analysis on the dependent variable total response error rate, with the between-subject factors of age group and gender revealed significant differences between the age groups ($F(2, 38) = 5.75$, $p = .007$). Post-hoc Tukey-HSD comparisons indicated that the oldest age group of 13- to 16-year-olds (3.93 ± 3.33) performed significantly better than the youngest age group of 5- to 8-year-olds (13.75 ± 11.01, $p = .009$). The middle age group of 9- to 12-year-olds (10.76 ± 8.25, $p = .056$) exhibited only a trend toward increased errors compared to the oldest age group and no significant differences compared to the youngest age group. The most frequent error observed was a button press during the intertrial interval, occurring between the warning stimulus S1 and the imperative stimulus S2. Only trials with a correct response to S2 were included in further analysis.

Regarding reaction times, ANOVA analysis with age group and

gender as between-subject factors showed a trend toward differences among the age groups ($F(2, 38) = 2.96$, $p = .064$). Tukey-HSD posthoc comparisons indicated that the youngest age group (443.02 ± 117.42 ms) showed slower reactions compared to the middle (342.03 ± 112.91 ms, $p = .046$) and a trend compared to the oldest age group (369.83 ± 114.12 ms, $p = .05$).

3.2. Early orienting response and motor preparation (initial contingent negative variation)

3.2.1. Latency of iCNV component

The initial component of the CNV potentials was used to investigate developmental changes during childhood and adolescence related to early movement preparatory processes.

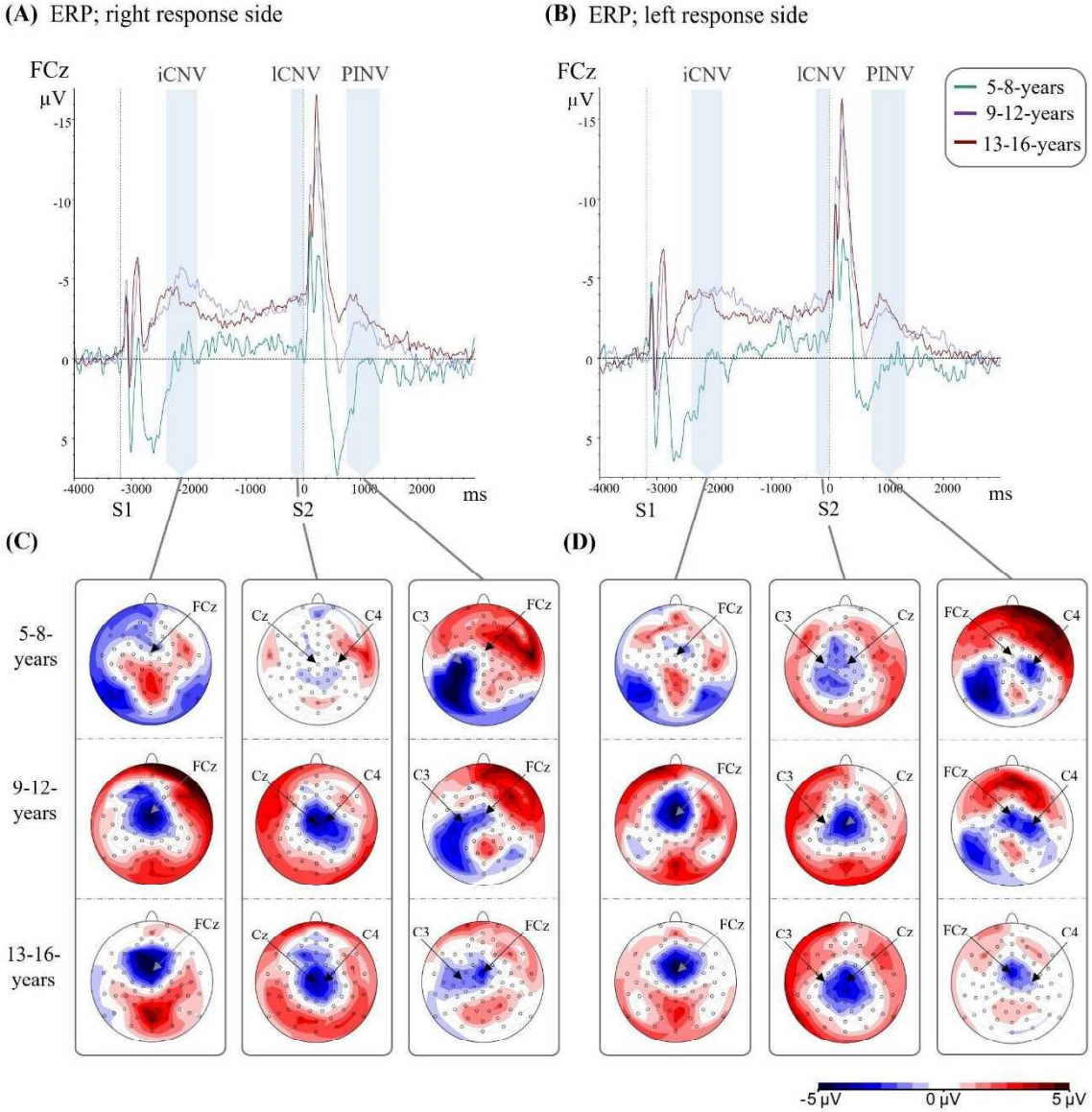

Fig. 2. Grand average CNV waveforms and topographic voltage maps, separately displayed for each age group to demonstrate maturational differences. **(A)** CNV course of the right and **(B)** left response condition at FCz (right), respectively for 5- to 8-year-old subjects (green line), 9- to 13-year-old subjects (purple line), and 13- to 16-year-old subjects (red line). The first vertical dashed line indicates the presentation of the warning stimulus S1 (directional arrow), and the second vertical dashed line indicates the presentation of the imperative stimulus S2. Time windows for iCNV, lCNV, and PINV are highlighted in light blue. Please note that voltage scales are presented upside down with negative values going upward. See for more detailed amplitude values supplementary material, Table 1. **(C)** Voltage maps of each CNV component for the right and **(D)** left response condition, displayed as the average of 5- to 8-year-old (top), 9- to 12-year-old (middle) and 13- to 16-year-old subjects (bottom). Maps are scaled from −5 µV (blue) to +5 µV (red). Older subjects showed increasing negativity of mid-frontocentral areas in each component. Most pronounced differences were observed between the age group of 5- to 8-year-old and 9-to 12-year-old subjects.

The repeated measures ANOVA revealed a significant effect of the factor age on iCNV latencies ($F(2, 38) = 4.84$, $p = .013$). The delayed onset of early mid-frontocentral negativity in younger subjects is illustrated in Figs. 2A, 2B, and 3A. For mean latencies with standard deviations, see supplementary material, Table 2.

3.2.2. ERP amplitudes of iCNV component

The CNV topography of evoked cortical activity showed significant age-related developmental changes, most pronounced between the age range of 5- to 12-years. Fig. 2 illustrates the stimulus-locked ERP waveforms for each group (for mean amplitudes with standard deviations see supplementary material, Table 1).

Comparing the evoked amplitudes of the early CNV component, the repeated measures ANOVA showed a highly significant interaction between scalp areas and age group ($F(4, 76) = 6.76$, $p < 0.001$).

Pairwise comparisons of estimated marginal means indicated significant differences in the activation of the mid-frontocentral area between the youngest age group of 5- to 8-year-olds (0.16 ± 2.78 μV) and the two older age groups of 9- to 12-year-olds (-3.66 ± 3.09 μV; $p < 0.001$) and 13- to 16-year-olds (-2.78 ± 2.03 μV; $p = 0.01$). Mid-frontocentral negativity of the youngest age group was shown not to differ significantly from baseline (see supplementary material, Table 1). In addition, no significant differences were observed when comparing the two older age groups. Centro-parietal scalp areas were found to exhibit no significant age effect during early movement planning.

To investigate the correlation between the early increasing mid-frontocentral activity and improved task performance, regression analyses were performed. The data showed a trend towards a curvilinear dependence between the mid-frontocentral activity and reaction time (RT^{-1}: $R^2 = 0.115$, F (1, 42) = 5.48, $p = .024$), however there was no significant correlation between mid-frontocentral activity and the performed errors (error rate: $R^2 = 0.104$, F (1, 42) = 4.88, $p = .033$; significant at $\alpha < 0.0125$).

3.2.3. Alpha-event-related desynchronization during the iCNV component

Analysis of the alpha band event-related desynchronization (ERD) was conducted to investigate developmental differences of mu rhythm attenuation related to motor behavior planning and whether children aged 5- to 8 years showed early motor preparation, even when significant frontal ERP activity was not observed. Repeated measurement ANOVA revealed a main effect for the factor age group ($F(2, 38) = 5.82$, $p = 0.006$).

Pairwise comparison of estimated marginal means demonstrated an increase of alpha ERD with increasing age, as indicated by significant amplitude differences, observed between the youngest age group of 5- to 8-year-olds (-19.41 ± 4.4 μV) and the oldest age group of 13- to 16-years-olds ($- 38.35 \pm 3.89$ μV; $p = 0.008$) as well as between the middle age group of 9- to 12-year-olds ($- 24.72 \pm 3.81$ μV) and the oldest age group ($p = .049$).

In addition, there was a main effect of the scalp area ($F(2, 76) = 45.87$, $p < 0.001$) which was qualified by an interaction between the movement side and scalp area ($F(2, 76) = 25.84$, $p < 0.001$). Alpha-ERD over contra- and ipsilateral centro-parietal areas but not over mid-frontocentral areas were shown to be highly significant for all age groups, as well as to be more pronounced over the contralateral hemisphere of the movement side (see Table 2). A pairwise comparison of estimated marginal means indicated that centro-parietal areas (right: $- 32.17 \pm 2.77$ μV; left: $- 32.32 \pm 2.48$ μV) showed significantly more desynchronization than the mid-frontocentral area ($- 17.98 \pm 2.33$ μV, $p < 0.001$). Moreover, the movement side had a highly significant effect on alpha ERD over centro-parietal areas of both hemispheres (right, $p < 0.001$, left: $p < 0.001$), showing distinct lateralization to the contralateral movement side (see Fig. 4C to 4F and supplementary material, Table 3). Thus, already 5- to 8-year-old children showed contralaterally lateralized alpha-ERD during early CNV (i.e., a selection of the required response side).

3.2.4. Current source density (CSD) of iCNV component

The qualitatively distinct pattern observed during iCNV in young subjects could also be evoked by strong, overlapping P300 activity masking the anticipated activity that was shown in older subjects. To investigate activity over mid-frontocentral areas in younger subjects more precisely and to reduce the influence of overlapping P300 activity, we conducted a Current Source Density (CSD) analysis.

To assess age effects, we conducted a repeated measures ANOVA, which indicated an interaction between scalp area and age group ($F(4, 76) = 3.13$, $p = 0.019$), suggesting age-related topographical maturation. Pairwise comparison of estimated marginal means revealed age-related activity differences over the centro-parietal scalp areas between the youngest (right: -29.48 ± 9.12 μV; left: -23.72 ± 9.96 μV) and the oldest age group (right: $4.09 + 8.06$ μV, $p = 0.026$; left: $10.0+ 8.8$ μV, $p = 0.045$), showing decreasing negativity over left and right centroparietal areas with age. However, CSD map topographies indicated that the topographic maximum related to these current sinks was over occipitotemporal areas, so we did not interpret this activation any further concerning motor processes.

More importantly, the mid-frontocentral area exhibited no significant differences between the age groups. Further examination of CSD map topographies (Fig. 3C, 3D) revealed that even children in the age range of 5- to 8 years exhibited a small current sink over mid-frontocentral areas (-10.92 ± 32.9 μV) which was however not significant ($t(11) = - 1.15$, $p = .27$). Fig. 3B and 3C illustrate that in younger subjects the positivity of the P3-complex and occipitotemporal negativity over visual cortical areas dominated the CSD maps. Conversely, in older subjects, mid-frontocentral negativity became more prominent.

3.2.5. Source analysis (SSLOFO) of iCNV component

SSLOFO analysis, an inverse algorithm to precisely reconstruct underlying sources, was applied to identify closely spaced cortical generators of the mid-frontocentral activity during iCNV of young subjects. Consistent with the findings from CSD analysis (overlapping P3-complex, occipitotemporal current sinks), SSLOFO analysis confirmed the presence of a prominent posterior source in young subjects during early movement planning. However, source analysis indicated that in young subjects aged 5 years, the supplementary motor area is likely to contribute, at least partly, to early negativity observed over mid-frontocentral areas (Figs. 3D and 3E).

3.3. Late motor preparation (late contingent negative variation)

3.3.1. ERP amplitudes of lCNV component

To investigate maturational processes related to direct motor preparation, we focused on the late component of the CNV paradigm. The lCNV topography showed pronounced differences between the age groups (see Fig. 2C and 2D and supplementary material, Table 1). Children aged 5 to 8 years displayed more widespread low ipsilateral negativity, most pronounced over centroparietal areas. In contrast, older subjects (9- to 16-year-olds) exhibited a more centrally localized negativity over mid-frontocentral and central areas, with decreasing activity over ipsilateral centro-parietal areas with age.

The repeated measurement ANOVA revealed significant interactions between scalp area and movement side ($F(2, 76) = 3.59$, $p = 0.034$) and between scalp area and age group ($F(4, 76) = 3.63$, $p = 0.009$). A pairwise comparison of estimated marginal means showed that the movement side had a significant effect on the left centroparietal scalp area (right-hand movements: $- 0.36 \pm 0.32$ μV; left-hand movements: $- 1.48 \pm 0.3$ μV, $p = 0.017$), with more pronounced ipsilateral negativity observed for the left movement side. The right centroparietal scalp area was observed not to be significantly influenced by the movement side.

Furthermore, significant amplitude differences over the mid-frontocentral area were observed between the youngest age group of 5- to 8-year-olds (-0.74 ± 0.73 μV) and the middle age group of 9- to 12-year-olds (-3.51 ± 0.58 μV; $p = .02$). There was also a trend towards

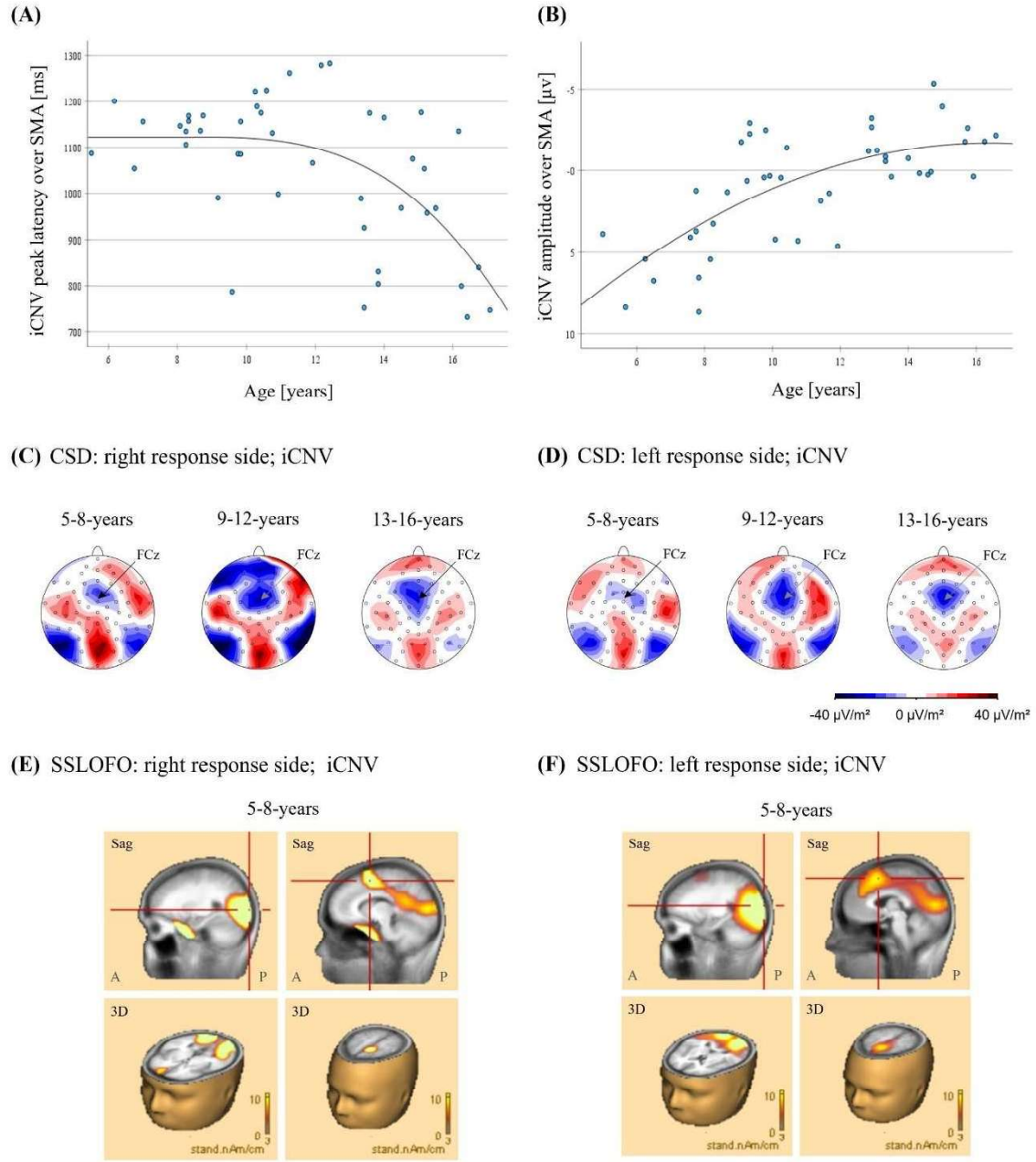

Fig. 3. Developmental characteristics of the early CNV (iCNV) component. **(A)** Scatterplots of iCNV mean peak latencies and **(B)** amplitudes. Data points represent mean amplitudes for both response conditions and each subject over the mid-frontocentral area (Cz, FCz, FC1′, FC2′). The grey lines show the corresponding fitting of a curvilinear regression model (age^{-1}), since age-related differences were more pronounced in younger subjects. **(C)** Average current source density (CSD) maps of the iCNV component for 5- to 8-year-old (left), 9- to 12-year-old (middle), and 13- to 16-year-old subjects (right), displayed for the right and **(D)** left response condition. CSD maps are scaled from −40 µV/cm^2 (blue) to +40 µV/cm^2 (red). **(E)** Image of current standardized shrinking LORETA-FOCUSS (SSLOFO) algorithm, calculated for right and **(F)** left response condition during iCNV. Images are displayed for 5- to 8-year-old subjects, to identify especially mid-frontocentral current sources in young subjects. Images showed a pronounced posterior (left images) as well as a mid-frontocentral cortical source (right images), related to the supplementary motor area. A: anterior side of the brain; P: posterior side of the brain; Sag: Sagittal plane.

Table 2
Mean Alpha-ERD amplitude values [%] ± standard deviation for each CNV component. Significances ($p \leq 0.017$) or trends towards significance ($p < .33$) are indicated for the respective values.

Alpha-ERD of CNV Component	Age Group	SMA [%]	M1 right [%]	M1 left [%]
iCNV right response condition	5- to 8-year-old	−6.27 ± 16.54	−16.24 ± 23.57 $t(-2.38)$; $p=.03$	−29.32 ± 22.05 $t(-4.61)$; $p < .001$
	9- to 12-year-old	−12.51 ± 12.79 $t(-4.03)$; $p < .001$	−23.99 ± 18.08 $t(-5.47)$; $p < .001$	−34.27 ± 16.6 $t(-8.51)$; $p < .001$
	13- to 16-year-old	−33.06 ± 21.39 $t(-5.78)$; $p < .001$	−35.79 ± 25.53 $t(-5.25)$; $p < .001$	−51.99 ± 19.55 $t(-9.95)$; $p < .001$
iCNV left response condition	5- to 8-year-old	−13.48 ± 18.88 $t(-2.47)$; $p = .03$	−34.59 ± 14.83 $t(-8.08)$; $p < .001$	−22.21 ± 16.84 $t(-4.57)$; $p < .001$
	9- to 12-year-old	−17.14 ± 12.39 $t(-5.71)$; $p < .001$	−37.33 ± 15.8 $t(-9.74)$; $p < .001$	−28.02 ± 15.27 $t(-7.57)$; $p < .001$
	13- to 16-year-old	−29.34 ± 19.5 $t(-5.63)$; $p < .001$	−46.64 ± 22.08 $t(-7.9)$; $p < .001$	−32.74 ± 21.71 $t(-5.64)$; $p < .001$
lCNV right response condition	5- to 8-year-old	9.22 ± 22.49	12.94 ± 22.65 $t(1.98)$; $p = .05$	−0.88± 20.88
	9- to 12-year-old	12.94 ± 20.23 $t(2.64)$; $p = .02$	24.51 ± 36.32 $t(2.78)$; $p = .01$	−9.23 ± 20.49 $t(-1.86)$; $p = .08$
	13- to 16-year-old	−4.44 ± 22.27	11.21 ± 33.57	−17.94 ± 23.53 $t(-2.85)$; $p = .01$
lCNV left response condition	5- to 8-year-old	6.91 ± 20.56	−5.44 ± 15.65	23.05 ± 22.12 $t(3.61)$; $p = .004$
	9- to 12-year-old	5.39 ± 17.78	−6.27 ± 16.57	14.44 ± 29.22 $t(2.04)$; $p = .06$
	13- to 16-year-old	−0.78 ± 17.74	−16.39 ± 21.64 $t(-2.84)$; $p = .01$	1.87 ± 28.42
PINV right response condition	5- to 8-year-old	−14.18 ± 17.43 $t(-2.82)$; $p = .01$	−28.78 ± 19.72 $t(-5.06)$; $p < .001$	−33.39 ± 21.89 $t(-5.28)$; $p < .001$
	9- to 12-year-old	−24.46 ± 16.12 $t(-6.25)$; $p < .001$	−35.88 ± 19.22 $t(-7.7)$; $p < .001$	−42.68 ± 20.93 $t(-8.41)$; $p < .001$
	13- to 16-year-old	−38.86 ± 25.46 $t(-5.71)$; $p < .001$	−46.71 ± 25.26 $t(-6.92)$; $p < .001$	−53.19 ± 23.43 $t(-8.35)$; $p < .001$
PINV left response condition	5- to 8-year-old	−18.07 ± 20.89 $t(-2.98)$; $p = .01$	−37.56 ± 19.86 $t(-6.55)$; $p < .001$	−23.38 ± 25.36 $t(-3.19)$; $p = .009$
	9- to 12-year-old	−24.37 ± 18.82 $t(-5.34)$; $p < .001$	−42.45 ± 20.31 $t(-8.61)$; $p < .001$	−43.86 ± 19.72 $t(-9.17)$; $p < .001$
	13- to 16-year-old	−39.88 ± 22.26 $t(-6.7)$; $p < .001$	−54.66 ± 24.5 $t(-8.35)$; $p < .001$	−48.49 ± 27.31 $t(-6.64)$; $p < .001$

more midfronto-central negativity for the oldest age group of 13- to 16-year-olds (- 3.04 ± 0.64 μV; $p = .067$) compared to 5- to 8-year-olds. Centro-parietal areas of both the contralateral and ipsilateral hemispheres did not show significant maturational changes.

3.3.2. Alpha-Event-related desynchronization of lCNV component

To investigate oscillatory modulation related to movement preparation and cortical pre-activation before a movement, we analyzed alpha ERD during lCNV.

Repeated measurement ANOVA showed a significant interaction between the movement side and scalp area ($F(2, 76) = 25.59$, $p < 0.001$). A pairwise comparison of the estimated marginal means revealed that alpha ERD over centroparietal areas was highly influenced by the movement side ($p < 0.001$).

Despite pronounced maturational differences of alpha power changes displayed in the related maps and data (Fig. 4A and 4B, Table 2), ANOVA analysis showed a trend towards differences between the age groups ($F(2, 38) = 2.84$, $p = 0.071$). To investigate the data in more detail, we performed a regression analysis over centroparietal motor areas. Regression analysis confirmed a strong trend towards a developmental trajectory with decreasing alpha band synchronization over ipsilateral motor areas and increasing desynchronization over contralateral motor areas (Age; ipsilaterally decreasing synchronization: $R^2 = 0.109$, $F(1, 42) = 5.16$, $p = .028$; contralaterally increasing desynchronization: $R^2 = 0.08$, $F(1, 42) = 3.77$, $p = .059$; significant for $\alpha < 0.025$) (for details see supplementary material, Fig. 1).

Interestingly, an analysis of the lateralization of alpha-ERD further illustrated that a constant degree of lateralization was maintained during development (Fig. 4C to 4D). Topographic distribution of the lateralized alpha-ERD during lCNV (Fig. 4E and 4F), as well as lateralized alpha-ERD amplitude analysis ($F(2, 38) = 0.014$, $p = .99$), confirmed no significant lateralization differences between the analyzed age groups, despite apparent differences in the contra- and ipsilateral induced alpha power (see Fig. 4A, 4B for the time course and topography of lateralized activation).

3.4. Response postprocessing and evaluation (post imperative negative variation, PINV)

3.4.1. Latency of PINV component

To investigate maturational changes in response evaluation processes, we analyzed cortical activity related to motor post-processing (PINV) within a CNV paradigm. Repeated measurement ANOVA showed a significant interaction between the movement side, the scalp area, and the age group ($F(3.86, 73.3) = 2.75$, $p = .036$).

A pairwise comparison of estimated marginal means indicated that, for the right movement side, negativity over the right ipsilateral hemisphere arose with an increased latency in the oldest age group (1171.18 ± 59.59 ms), compared to the youngest (897.47 ± 67.42 ms, $p = 0.013$) and the middle age group (865.71 ± 58.43 ms, $p = 0.002$). For the left-hand movement, no significant latency differences were observed.

3.4.2. ERP amplitudes of PINV

PINV topography varied strongly between the age groups (see Fig. 2). Younger subjects displayed maximum negativity over centro-parietal areas, while in older subjects pronounced negativity was shifted towards more mid-frontocentral areas. The repeated measurement ANOVA indicated a statistically significant interaction between scalp area and age group ($F(4, 76) = 4.12$, $p = 0.004$) and between the movement side and scalp area ($F(2, 76) = 8.9$, $p < 0.001$).

A pairwise comparison of estimated marginal means showed that the movement side had a significant effect on the right ($p = 0.009$) and left centro-parietal scalp area ($p = 0.001$), with more pronounced negativity observed over the contralateral hemisphere.

Maturational influences were found over the left centro-parietal scalp area, with a trend towards amplitude differences between the

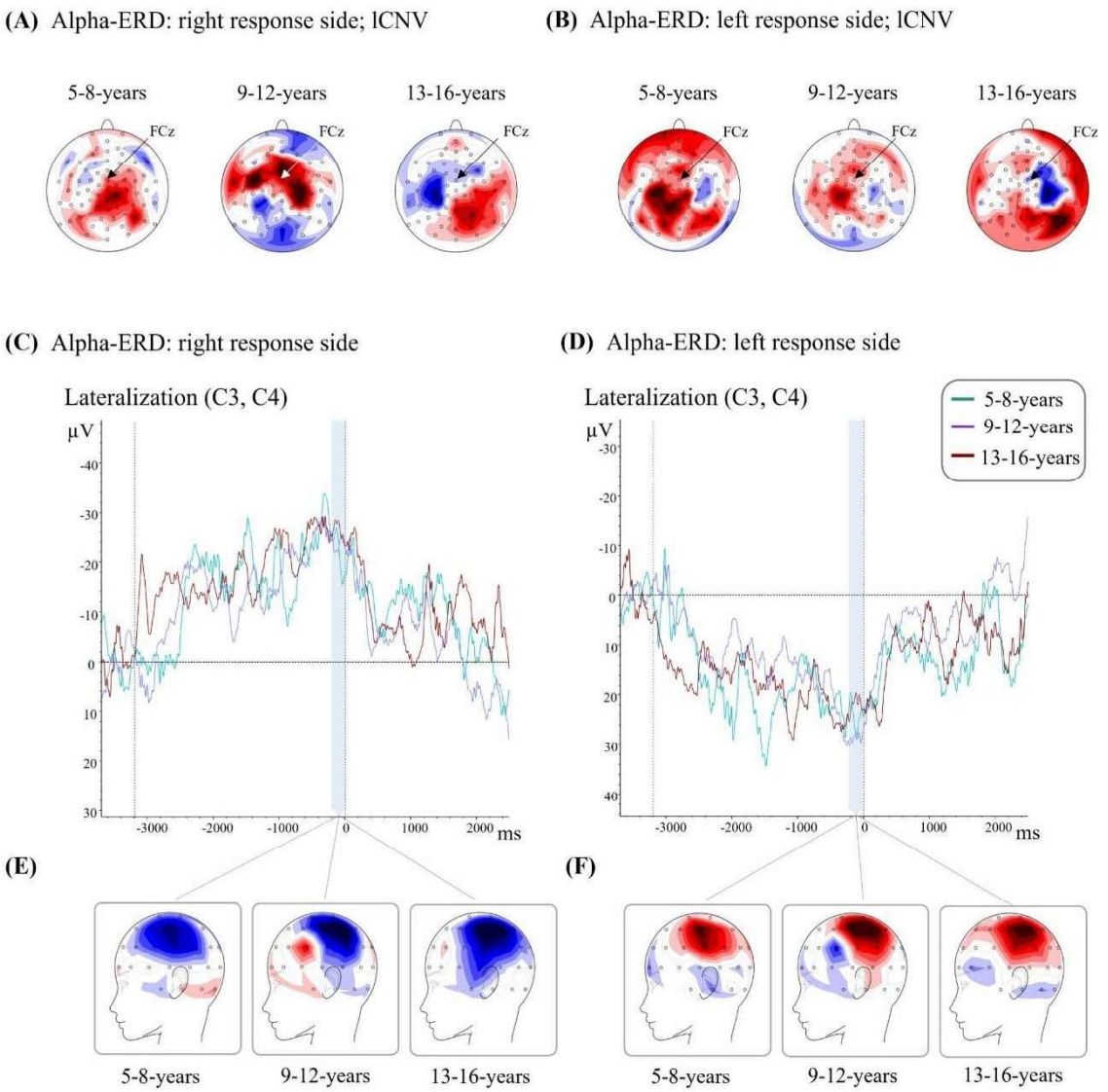

Fig. 4. Developmental characteristics of the late CNV (lCNV) component. (A) Isopotential line maps of alpha event-related desynchronization (ERD) during lCNV, shown for right and (B) left response conditions. Maps are displayed separately for the average alpha ERD of 5- to 8-year-old (left), 9- to 12-year-old (middle), and 13- to 16-year-old subjects (right). A decrease in alpha power (ERD) is indicated in blue, increase in alpha power (event-related synchronization; ERS) is indicated in red. Scaling ranges from −30 % to +30 % in relation to baseline values. Ipsilateral positivity over centro-parietal areas decreased with age, whereas contralateral negativity increased. (C) Lateralization (LRP) waveforms for the right and (D) left response condition, presented as average for 5- to 8-year-old subjects (green line), 9- to 13-year-old subjects (purple line), and 13- to 16-year-old subjects (red line). (E) LRP voltage maps of the contralateral hemisphere for the right response condition, (F) respectively for the ipsilateral hemisphere of the left response condition for 5- to 8-year-old (left), 9- to 12-year-old (middle) and 13- to 16-year-old subjects (right). Alpha-ERD showed an age-constant strong lateralization to the contralateral movement side during lCNV.

youngest (- 3.56 ± 0.77 µV) and the oldest age group (- 1.03 ± 0.68 µV; p = .054), showing decreasing PINV amplitude over the left-centroparietal area with age. Furthermore, negativity shifted from centro-parietal scalp areas in young subjects to mid-frontocentral areas in older subjects (see supplementary material, Table 1).

3.4.3. Alpha-Event-related desynchronization of PINV component

To study maturational changes of alpha band oscillation related to response evaluation, we analyzed alpha-ERD during PINV. Desynchronization of alpha power was present for all age groups over mid-frontocentral as well as over centro-parietal areas, and most pronounced in older subjects (Table 2).

ANOVA analysis showed an interaction between the movement side and scalp area ($F(2, 76) = 9.23$, $p < 0.001$). A pairwise comparison of the estimated marginal means indicated that alpha desynchronization was more pronounced over contralateral centro-parietal scalp areas, especially for the right hemisphere ($p < .001$).

Furthermore, there was a main effect of age group ($F(2, 38) = 5$, $p =$

0.012) as well as a trend towards an interaction between the scalp area and the age group ($F(4, 76) = 2.23$, $p = 0.074$). In total, alpha desynchronization was less pronounced in younger subjects aged 5- to 8-years (- 24.71 ± 5.33 %) than in older subjects aged 13- to −16 years (- 46.61± 4.72 %; $p = .012$). Regarding maturational differences of the separated scalp areas, negativity over mid-frontocentral areas was more pronounced in the oldest age group (- 39.0± 4.6 %), compared to the youngest (- 15.05± 5.21 %; $p = .004$) and the middle age group (- 21.51 ± 4.51 %; $p = .03$).

4. Discussion

Brain maturational processes and underlying neuronal mechanisms involved in the transition from an immature child brain to a fully developed adult brain are complex and difficult to identify. Our data provide evidence of pronounced cerebral maturation related to attention allocation, motor preparation, and movement evaluation during childhood and adolescence. The study compared behavioral task performance and cortical activation evoked and induced by a contingent negative variation (CNV) paradigm with a directional warning cue. We collected EEG data of subjects aged 5- to 16- years using a 64-equidistant electrode array.

Our data showed that enhanced SMA activity plays a critical role in increasing the efficiency of motor behavior during cortical maturation. Besides poorer task performance, young subjects displayed qualitatively different cortical activation patterns compared to older subjects. Previous CNV studies in children and adolescents have yielded inconsistent findings, potentially due to limitations in methodology. By employing a visual task paradigm and advanced analysis techniques, we were able to investigate CNV components more precisely and reveal a maturational increase in mid-frontocentral activity attributed to the SMA during different stages of motor control.

Our findings suggest a developmental shift towards proactive motor control. Alpha power exhibited a trend toward transitioning from ipsilateral synchronization (inhibition; deactivation) to contralateral desynchronization (disinhibition; pre-activation) within motor areas during late motor preparation (lCNV). In contrast to other studies (Bender et al., 2005; Flores et al., 2009), our findings demonstrate that motor development extends beyond adolescence. Compared to adults, adolescents still showed distinct cortical activation patterns, lacking the expected contralateral motor area activation during preparation. This suggests a more gradual maturation process.

Age-related reductions in PINV negativity over contralateral motor areas, coupled with increased SMA negativity, suggest reduced movement uncertainty with development (Thiemann, 2010; Bender et al., 2006).

4.1. Behavioral performance

Reaction times as well as performed errors improved with age, as typically observed in other studies (Bender et al., 2005; Bucsuházy and Semela, 2017; Kiselev et al., 2009). Motor improvement was characterized by shorter reaction times and reduced false alarms or wrong responses in older subjects. These results suggest that younger subjects exhibited more premature response reactions compared to older subjects. The observed developmental differences had an influence on the processing speed as well as on the ability to restrain motor behavior. Improved action control developed curvilinearly in the age range of 5 to 16 years, with the most pronounced maturation in the youngest age group of 5- to 8-year-old children.

4.2. Maturation of orienting response (early contingent negative variation)

The early or initial CNV component (iCNV) is associated with orienting processes as a response to a warning stimulus in a CNV paradigm (Weerts and Lang, 1973). According to Birbaumer et al. (1990), the iCNV reflects prefrontal activation that regulates the activation of more posterior motor areas necessary for movement execution.

The early component was investigated to study the impact of cerebral maturation on the orienting response to an informative external stimulus, including attentional processes and motor program selection. ERP analysis revealed immature iCNV topographies until late childhood and early adolescence. Electrophysiological data showed a pronounced maturation characterized by increasing early mid-frontocentral negativity through the investigated age range (see Figs. 2 and 3B–3D). In agreement with other studies using data from a reduced number of electrodes, young children showed only minor frontal negativity during orienting response (Jonkman et al., 2003; Segalowitz and Davies, 2004), i.e., activation of cortical areas related to the supplementary motor area (SMA) and anterior cingulate cortex (ACC) (Flores et al., 2009; Jonkman et al., 2003). The early frontal negativity stabilized during post-pubertal adolescence, reaching a strength of activation comparable to adult subjects (Tian et al., 2019; Weisz et al., 2002). Furthermore, we observed a consistent shift in iCNV latencies, with mid-frontocentral areas being recruited earlier in older subjects, suggesting faster processing of the warning stimulus (see Fig. 3A).

Besides small frontal negativity, young children showed enhanced processing of the directional warning cue over posterior-temporal and occipital areas related to visual cortices (Bender et al., 2010; Hecht et al., 2016) that caused partial masking of small SMA activity in the ERP analysis. Van Leeuwen et al. (1998) observed similar early topographies and found posterior sources for this so-called CNV/P3 complex. It is likely that other studies reporting contradictory decreasing mid-frontocentral negativity during iCNV with age (Bender et al., 2004), as well as reduced iCNV latencies in younger children (Flores et al., 2009), observed rather frontocentral negativity that was dependent on extended stimulus processing related to a posterior source than true frontal iCNV negativity associated with SMA activity. Enhanced activity reflected in a more pronounced CNV/P3 complex could be explained by an increased effort to process relevant task information. The orienting reaction is thus dominated by sensory post-processing and resource allocation in young children, while more frontal activation with decreasing latencies becomes a dominant part in adolescent subjects.

Since young children reacted with more spontaneous motor responses and showed an increased error rate, posterior networks recruited during movement preparation seem less efficient in attention regulation and action control. Precipitated movements might be caused by inefficient motor inhibition or by reduced efficiency of attention allocation due to an increased effort in target selection processes. The observed maturational shift is consistent with described strategy changes from a posterior, stimulus-driven orienting network in young children to an anterior, top-down attention network in adolescent subjects (Padilla et al., 2014; Smith et al., 2011).

Cortical source analysis of iCNV data using sSLOFO confirmed that the mid-frontocentral negativity is likely to originate from the supplementary motor area (SMA; see Figs. 3E and 3F). It was suggested that the SMA recruits and sustains networks activated during subsequent preparatory processes related to the lCNV (Gomez et al., 2003). In other studies, it was shown that the iCNV arises from the SMA and ACC and that the cortical areas were simultaneously coactivated (Gomez et al., 2003; Lee et al., 1999). Lee et al. (1999) observed that subregions of the SMA were recruited with different temporal profiles and that early stages of motor processing were associated with the activation of anterior SMA parts related to the pre-SMA. The pre-SMA is characterized by extensive pre-frontal connectivity (Luppino et al., 1993) and thought to be involved, inter alia, in maintaining working memory (Pollmann and Yves von Cramon, 2000) as well as motor program selection and movement intention (Lau et al., 2004). Nachev et al. (2007) performed a movement study on a patient with a rare lesion involving the pre-SMA and reported increased reaction times as well as inhibitory deficits. Other studies confirmed that the SMA mediates motor inhibition (Chen

et al., 2010; Toma et al., 1999). These results suggest that pre-SMA exhibits a critical role in action control and indicate that pre-SMA immaturity might be a primary cause for less efficient movement performances in young children. However, it is not possible to exclude an indirect correlation between task performance and SMA activation due to parallel age effects. Therefore, the direct functional relevance of the increased SMA activation in improving movement performance cannot be investigated based on the observed data.

Brain oscillatory activity was analyzed to gain insight into maturational changes of movement-related power modulation. Mu-rhythm desynchronization is observed for cortical areas involved in processes of movement preparation, planning, and execution (Leocani et al., 1997; Pfurtscheller and Lopes da Silva, 1999). During cognitive processing or attention allocation processes, alpha power is reduced and facilitates resources to be allocated to task-relevant processing. Cortical regions that are related to task-irrelevant and potentially disruptive processes exhibit mu-rhythm synchronization, i.e. inhibition of underlying areas (Klimesch et al., 2007). The results showed lateralized mu-rhythm desynchronization over contralateral centro-parietal areas during iCNV for all age groups (see Table 2). This suggests that contralateral motor areas were activated during early processes of movement side selection shortly after the presentation of the informative warning cue. Given that the early motor preparation in young children was already characterized by a lateralized activation of contralateral motor regions, it suggests that also young children exhibit motor-related preparatory processes. Moreover, the results confirm that motor program selection corresponds to the early stages of motor preparation, as reflected by contralateral motor area activation.

Compared to evoked cortical potentials, mu-rhythm desynchronization reflects more general sensorimotor network pre-activation (C. Babiloni et al., 1999; Defebvre et al., 1994). In contrast to evoked potentials, differences in early mu rhythm desynchronization over mid-frontocentral areas were most pronounced between the middle (9- to 12-year-olds) and the oldest age group (13- to 16-year-olds), which suggests a delayed development of preparatory alpha band power in relation to evoked cortical activity.

4.3. Maturation of motor cortical pre-activation (late contingent negative variation)

The late component of a CNV has been suggested to represent sensory and motor pre-activation of resources needed for effective task-specific performance (Gaillard, 1978). Midfronto-central negativity increased with age during response preparation (lCNV; see Fig. 2). Previous results confirm the continuous development of preparatory movement networks and maturation of the motor system into young adulthood (Bender et al., 2002; Jonkman, 2006; Killikelly and Szucs, 2013; Thillay et al., 2015). Significant lCNV activity indicates that adolescent subjects used proactive control strategies to perform more efficient task-related movements.

The late CNV component typically exhibits prominent negativity over the contralateral hemispheres, as reported in various studies (Dirnberger et al., 2003; van der Lubbe et al., 2000; Wauschkuhn et al., 1997). However, our findings deviate from developmental research using simpler CNV paradigms (Bender et al., 2005). In our study, adolescent subjects showed only transient contralateral negativity during early motor preparation, potentially reflecting early motor program selection. Notably, the late contralateral activity over premotor and primary motor areas, commonly observed in adolescents and young adults (Bender et al., 2005; Flores et al., 2009), was absent in our adolescent group. This qualitative difference in activation patterns between our adolescent subjects (up to 16 years old) and those typically observed in adults (Gomez et al., 2003) suggests an ongoing developmental process in cortical areas related to preparatory activity.

The characteristic and complexity of a CNV paradigm significantly influences the resulting waveforms, topographies, and amplitudes. Our paradigm presented a warning cue specifying the required movement side, unlike simpler paradigms that lack such informative cues or varying movement sides. This additional complexity likely demanded higher levels of executive motor control during preparatory processes. Consequently, the development of sustained lateralized negativity over contralateral central areas might be delayed compared to studies using simpler paradigms. These findings suggest that effective motor preparation for complex movements and pronounced pre-activation of effector-specific motor areas (Dirnberger et al., 2003) matures later, potentially extending into late adolescence or young adulthood.

Consistent with previous research (Nagai et al., 2004), our topographic analysis in adolescents showed that the SMA is also involved in late movement preparation. Notably, the data showed a shift in activation from frontal to more central negativity during preparatory CNV stages, as shown in Fig. 2. This suggests a dynamic engagement of SMA across different phases of motor preparation. Early pre-processing (iCNV) might rely more on the pre-SMA, given its established role in motor program planning (Lee et al., 1999). Conversely, the observed shift towards central negativity during late motor pre-activation (lCNV) potentially reflects increased involvement of the more caudal SMA (SMAc) and premotor areas, which have direct connections to the primary motor cortex (Luppino et al., 1993; Wang et al., 2005). This aligns with the notion that SMAc is crucial for movement initiation and execution (Lee et al., 1999).

Time-frequency analysis revealed that alpha-ERD (excitation) of the contralateral hemisphere linearly increased with age during late movement preparation and planning (lCNV), whereas alpha-ERS (inhibition) of the ipsilateral side decreased (see Fig. 4A and 4B). However, lateralization analysis of the alpha power band showed no differences in lateralization strength between young children and adolescent subjects, as shown in Fig. 4C to 4F. Since synchronized activity is related to deactivation of corresponding brain areas (Lopes da Silva, 2006; Pfurtscheller, 2001), the results suggest that processes related to alpha band oscillation of motor networks were shifted from inhibition of ipsilateral motor-related brain areas to pre-activation of contralateral motor-related areas. These findings sustain the hypothesis of a maturational shift from reactive to proactive motor control (Chevalier et al., 2014). Furthermore, age-consistent alpha-band lateralization showed that small SMA activity observed for young subjects was not evoked due to low motor preparation or a lack of motivation but due to qualitatively different preparatory processes.

4.4. Maturation of movement processing (post imperative negative variation)

The PINV is associated with movement evaluation processes and is suggested to represent uncertainty in task performance (Bender et al., 2006; Klein et al., 1996). Reliance of the PINV on response execution was confirmed due to its correlation with response execution timing rather than the timing of external stimuli (Bender et al., 2004). EEG studies showed enhanced PINV amplitudes in children and adult subjects when they had to perform non-controllable tasks (Kathmann et al., 1990; Yordanova et al., 1997).

ERP data showed a developmental shift from pronounced negativity over contralateral central areas to negativity over more frontocentral areas during performance evaluation (see Fig. 2). The PINV did not depend on preparatory CNV components since topographical distribution differed significantly, as shown in previous studies (Bender et al., 2004; 2005). Since the performance of younger subjects was associated with a lack of control, high PINV amplitudes might reflect the controllability of task-related movements. Moreover, the results suggest that young children were more likely to be uncertain about their response performance, reflected in an increased compensatory effort and enhanced evaluation processes. Future studies should address the question of whether increased motor post-processing supports motor learning in children.

As observed for evoked potentials, alpha band desynchronization increased with age over mid-frontocentral areas during response evaluation (see Table 2). These results indicate that mid-frontocentral areas associated with SMA activity are increasingly recruited with age during movement post-processing and motor maturation. ERP data, similar to observations of preparatory mu rhythm desynchronization, reveal the most prominent maturational shifts in PINV topographies for younger and middle-aged groups, whereas alpha-ERD was characterized by pronounced developmental differences between the middle and the oldest age groups. This pattern strengthens the suggestion of a protracted maturation of alpha-band oscillations, extending into late adolescence or early adulthood.

4.5. Limitations

Based on the presented results, it is not possible to identify physiological mechanisms that underlie the observed changes in cortical activity and alpha band oscillation. It is likely that the observed maturation depends, inter alia, on developmental changes in functional connectivity that induce altered network dynamics (Brookes et al., 2018). Future studies should include multi-modal comparisons (fMRI) and connectivity analyses to investigate brain development more precisely. Moreover, studies of developmental changes should include an analysis of longitudinal examinations and not be based exclusively on cross-sectional data. The investigation of cortical maturation on an individual, intra-subject level allows the generation of more reliable and accurate information.

5. Conclusion

Our data revealed pronounced maturational differences in cortical movement preparation and post-processing between child and adolescent subjects. Behavioral results indicated less efficient action preprocessing and a lack of inhibitory control, likely attributed to incomplete frontal lobe maturity in children. Activation of mid-frontocentral areas related to the supplementary motor area during movement preparation and evaluation became increasingly prominent with age. Alpha band power indicated developmental progress from inhibiting ipsilateral motor areas in young children to enhanced pre-activation of contralateral motor areas in adolescents. Based on our data, evoked cortical activation is likely to develop earlier than alpha-band oscillatory activity. The reported results support the hypothesis of a developmental shift from a reactive to a proactive control and indicate immaturity in supplementary-, pre-, and primary motor areas until late adolescence or early adulthood.

Funding

This work was funded by the Deutsche Forschungsgemeinschaft (DFG, German Research Foundation); Project-ID 431,549,029 – SFB 1451.

Ethics approval statement

This study was conducted in accordance with the local legislation and institutional requirements. The research protocol was reviewed and approved by the Ethics Committee of the University of Cologne and the Ethics Committee of the University of Aachen.

CRediT authorship contribution statement

Julia Schmidgen: Writing – original draft, Visualization, Validation, Methodology, Investigation, Formal analysis, Data curation, Conceptualization. **Theresa Heinen:** Writing – review & editing, Conceptualization. **Kerstin Konrad:** Writing – review & editing, Project administration, Funding acquisition, Conceptualization. **Stephan Bender:** Writing – review & editing, Supervision, Project administration, Methodology, Funding acquisition, Formal analysis, Conceptualization.

Declaration of competing interest

The authors declare that the research was conducted in the absence of any commercial or financial relationships that could be construed as a potential conflict of interest.

Data availability

Data will be made available on request.

Acknowledgements

We thank all our participants as well as Elena Borovik, Sally Kufall, and Amelie Busch for their assistance in data acquisition.

Supplementary materials

Supplementary material associated with this article can be found, in the online version, at doi:10.1016/j.neuroimage.2024.120735.

References

Adornetto, C., In-Albon, T., Schneider, S., 2008. Diagnostik im kindes-und jugendalter anhand strukturierter interviews: anwendung und durchführung des kinder-DIPS. Klin. Diagn. Eval. 1 (4), 363–377.

Babiloni, C., Carducci, F., Cincotti, F., Rossini, P.M., Neuper, C., Pfurtscheller, G., Babiloni, F., 1999. Human movement-related potentials vs desynchronization of EEG alpha rhythm: a high-resolution EEG study. Neuroimage 10 (6), 658–665.

Bender, S., Becker, D., Oelkers-Ax, R., Weisbrod, M., 2006. Cortical motor areas are activated early in a characteristic sequence during post-movement processing. Neuroimage 32 (1), 333–351. https://doi.org/10.1016/j.neuroimage.2006.03.009.

Bender, S., Behringer, S., Freitag, C.M., Resch, F., Weisbrod, M., 2010. Transmodal comparison of auditory, motor, and visual post-processing with and without intentional short-term memory maintenance. Clin. Neurophysiol. 121 (12), 2044–2064.

Bender, S., Oelkers-Ax, R., Resch, F., Weisbrod, M., 2004. Motor processing after movement execution as revealed by evoked and induced activity. Cogn. Brain Res. 21 (1), 49–58.

Bender, S., Weisbrod, M., Bornfleth, H., Resch, F., Oelkers-Ax, R., 2005. How do children prepare to react? Imaging maturation of motor preparation and stimulus anticipation by late contingent negative variation. Neuroimage 27 (4), 737–752. https://doi.org/10.1016/j.neuroimage.2005.05.020.

Bender, S., Weisbrod, M., Just, U., Pfuller, U., Parzer, P., Resch, F., Oelkers-Ax, R., 2002. Lack of age-dependent development of the contingent negative variation (CNV) in migraine children? Cephalalgia 22 (2), 132–136. https://doi.org/10.1046/j.1468-2982.2002.00334.x.

Berchicci, M., Zhang, T., Romero, L., Peters, A., Annett, R., Teuscher, U., Bertollo, M., Okada, Y., Stephen, J., Comani, S., 2011. Development of mu rhythm in infants and preschool children. Dev. Neurosci. 33 (2), 130–143. https://doi.org/10.1159/000329095.

Birbaumer, N., Elbert, T., Canavan, A.G., Rockstroh, B., 1990. Slow potentials of the cerebral cortex and behavior. Physiol. Rev. 70 (1), 1–41.

Brookes, M.J., Groom, M.J., Liuzzi, L., Hill, R.M., Smith, H.J., Briley, P.M., Hall, E.L., Hunt, B.A., Gascoyne, L.E., Taylor, M.J., 2018. Altered temporal stability in dynamic neural networks underlies connectivity changes in neurodevelopment. Neuroimage 174, 563–575.

Bucsuházy, K., Semela, M., 2017. Case study: reaction time of children according to age. Procedia Eng. 187, 408–413.

Chen, X., Scangos, K.W., Stuphorn, V., 2010. Supplementary motor area exerts proactive and reactive control of arm movements. J. Neurosci. 30 (44), 14657–14675.

Chevalier, N., James, T.D., Wiebe, S.A., Nelson, J.M., Espy, K.A., 2014. Contribution of reactive and proactive control to children's working memory performance: insight from item recall durations in response sequence planning. Dev. Psychol. 50 (7), 1999–2008. https://doi.org/10.1037/a0036644.

Cochin, S., Barthelemy, C., Roux, S., Martineau, J., 2001. Electroencephalographic activity during perception of motion in childhood. Eur. J. Neurosci. 13 (9), 1791–1796. https://doi.org/10.1046/j.0953-816x.2001.01544.x.

Côté, S.L., Elgbeili, G., Quessy, S., Dancause, N., 2020. Modulatory effects of the supplementary motor area on primary motor cortex outputs. J. Neurophysiol. 123 (1), 407–419.

Cui, R., Egkher, A., Huter, D., Lang, W., Lindinger, G., Deecke, L., 2000. High resolution spatiotemporal analysis of the contingent negative variation in simple or complex motor tasks and a non-motor task. Clin. Neurophysiol. 111 (10), 1847–1859.

de Jong, R., Wierda, M., Mulder, G., Mulder, L.J., 1988. Use of partial stimulus information in response processing. J. Exp. Psychol. 14 (4), 682. : Human perception and performance.

Deecke, L., Scheid, P., Kornhuber, H.H., 1969. Distribution of readiness potential, pre-motion positivity, and motor potential of the human cerebral cortex preceding voluntary finger movements. Exp. Brain Res. 7 (2), 158–168. https://doi.org/10.1007/BF00235441.

Defebvre, L., Bourriez, J.L., Dujardin, K., Derambure, P., Destee, A., Guieu, J.D., 1994. Spatiotemporal study of bereitschaftspotential and event-related desynchronization during voluntary movement in Parkinson's disease. Brain Topogr. 6 (3), 237–244. https://doi.org/10.1007/BF01187715.

Dirnberger, G., Greiner, K., Duregger, C., Endl, W., Lindinger, G., Lang, W., 2003. The effects of alteration of effector and side of movement on the contingent negative variation. Clin. Neurophysiol. 114 (11), 2018–2028. https://doi.org/10.1016/s1388-2457(03)00197-4.

Eom, T.H., 2023. Electroencephalography source localization. Clin. Exp. Pediatr. 66 (5), 201.

Fietzek, U., Heinen, F., Berweck, S., Maute, S., Hufschmidt, A., Schulte-Mönting, J., Lücking, C., Korinthenberg, R., 2000. Development of the corticospinal system and hand motor function: central conduction times and motor performance tests. Dev. Med. Child Neurol. 42 (4), 220–227.

Flores, A.B., Digiacomo, M.R., Meneres, S., Trigo, E., Gomez, C.M., 2009. Development of preparatory activity indexed by the contingent negative variation in children. Brain Cogn. 71 (2), 129–140. https://doi.org/10.1016/j.bandc.2009.04.011.

Gaillard, A.W.K., 1978. Slow Brain Potentials Preceding Task Performance TU Delft. Delft University of Technology.

Gerloff, C., Uenishi, N., Hallett, M., 1998. Cortical activation during fast repetitive finger movements in humans: dipole sources of steady-state movement-related cortical potentials. J. Clin. Neurophysiol. 15 (6), 502–513. https://doi.org/10.1097/00004691-199811000-00009.

Gomez, C.M., Delinte, A., Vaquero, E., Cardoso, M.J., Vazquez, M., Crommelinck, M., Roucoux, A., 2001. Current source density analysis of CNV during temporal gap paradigm. Brain Topogr. 13 (3), 149–159. https://doi.org/10.1023/a:1007816201345.

Gomez, C.M., Marco, J., Grau, C., 2003. Preparatory visuo-motor cortical network of the contingent negative variation estimated by current density. Neuroimage 20 (1), 216–224. https://doi.org/10.1016/s1053-8119(03)00295-7.

Gramfort, A., Luessi, M., Larson, E., Engemann, D., Strohmeier, D., Brodbeck, C., Goj, R., Jas, M., Brooks, T., Parkkonen, L., 2013. MEG and EEG data analysis with MNE-Python. Front. Neurosci. 7, 267. *Frontiers*.

Hecht, M., Thiemann, U., Freitag, C.M., Bender, S., 2016. Time-resolved neuroimaging of visual short term memory consolidation by post-perceptual attention shifts. Neuroimage 125, 964–977.

Huttenlocher, P.R., 1979. Synaptic density in human frontal cortex-developmental changes and effects of aging. Brain Res. 163 (2), 195–205.

Jensen, O., Mazaheri, A., 2010. Shaping functional architecture by oscillatory alpha activity: gating by inhibition. Front. Hum. Neurosci. 4, 186.

Jonkman, L.M., 2006. The development of preparation, conflict monitoring and inhibition from early childhood to young adulthood: a Go/Nogo ERP study. Brain Res. 1097 (1), 181–193. https://doi.org/10.1016/j.brainres.2006.04.064.

Jonkman, L.M., Lansbergen, M., Stauder, J.E., 2003. Developmental differences in behavioral and event-related brain responses associated with response preparation and inhibition in a go/nogo task. Psychophysiology 40 (5), 752–761. https://doi.org/10.1111/1469-8986.00075.

Kathmann, N., Jonitz, L., Engel, R.R., 1990. Cognitive determinants of the postimperative negative variation. Psychophysiology 27 (3), 256–263. https://doi.org/10.1111/j.1469-8986.1990.tb00380.x.

Killikelly, C., Szucs, D., 2013. Delayed development of proactive response preparation in adolescents: ERP and EMG evidence. Dev. Cogn. Neurosci. 3, 33–43. https://doi.org/10.1016/j.dcn.2012.08.002.

Kiselev, S., Espy, K.A., Sheffield, T., 2009. Age-related differences in reaction time task performance in young children. J. Exp. Child Psychol. 102 (2), 150–166.

Klein, C., 2001. Developmental functions for saccadic eye movement parameters derived from pro-and antisaccade tasks. Exp. Brain Res. 139, 1–17.

Klein, C., Rockstroh, B., Cohen, R., Berg, P., Dressel, M., 1996. The impact of performance uncertainty on the postimperative negative variation. Psychophysiology 33 (4), 426–433. https://doi.org/10.1111/j.1469-8986.1996.tb01068.x.

Klimesch, W., Sauseng, P., Hanslmayr, S., 2007. EEG alpha oscillations: the inhibition–timing hypothesis. Brain Res. Rev. 53 (1), 63–88.

Lau, H.C., Rogers, R.D., Haggard, P., Passingham, R.E., 2004. Attention to intention. Science 303 (5661), 1208–1210 (1979).

Lee, K.M., Chang, K.H., Roh, J.K., 1999. Subregions within the supplementary motor area activated at different stages of movement preparation and execution. Neuroimage 9 (1), 117–123.

Leocani, L., Toro, C., Manganotti, P., Zhuang, P., Hallett, M., 1997. Event-related coherence and event-related desynchronization/synchronization in the 10 Hz and 20 Hz EEG during self-paced movements. Electroencephalogr. Clin. Neurophysiol. 104 (3), 199–206. https://doi.org/10.1016/s0168-5597(96)96051-7.

Liu, H., Schimpf, P.H., Dong, G., Gao, X., Yang, F., Gao, S., 2005. Standardized shrinking LORETA-FOCUSS (SSLOFO): a new algorithm for spatio-temporal EEG source reconstruction. IEEE Trans. Biomed. Eng. 52 (10), 1681–1691. https://doi.org/10.1109/TBME.2005.855720.

Lopes da Silva, F.H., 2006. Event-related neural activities: what about phase? Prog. Brain Res. 159, 3–17. https://doi.org/10.1016/S0079-6123(06)59001-6.

Luppino, G., Matelli, M., Camarda, R., Rizzolatti, G., 1993. Corticocortical connections of area F3 (SMA-proper) and area F6 (pre-SMA) in the macaque monkey. J. Comp. Neurol. 338 (1), 114–140.

Macdonald, J.A., Beauchamp, M.H., Crigan, J.A., Anderson, P.J., 2014. Age-related differences in inhibitory control in the early school years. Child Neuropsychol. 20 (5), 509–526.

Mennes, M., Wouters, H., Vanrumste, B., Lagae, L., Stiers, P., 2010. Validation of ICA as a tool to remove eye movement artifacts from EEG/ERP. Psychophysiology 47 (6), 1142–1150.

Nachev, P., Wydell, H., O'Neill, K., Husain, M., Kennard, C., 2007. The role of the pre-supplementary motor area in the control of action. Neuroimage 36 (Suppl 2(3–3)), T155–T163. https://doi.org/10.1016/j.neuroimage.2007.03.034.

Niedermeyer, E., 1997. Alpha rhythms as physiological and abnormal phenomena. Int. J. Psychophysiol. 26 (1–3), 31–49.

Nunez, P.L., Silberstein, R.B., Cadusch, P.J., Wijesinghe, R.S., Westdorp, A.F., Srinivasan, R., 1994. A theoretical and experimental study of high resolution EEG based on surface Laplacians and cortical imaging. Electroencephalogr. Clin. Neurophysiol. 90 (1), 40–57.

Oldfield, R., 1971. Edinburgh handedness inventory. J. Abnorm. Psychol.

Padilla, M.L., Pfefferbaum, A., Sullivan, E.V., Baker, F.C., Colrain, I.M., 2014. Dissociation of preparatory attention and response monitoring maturation during adolescence. Clin. Neurophysiol. 125 (5), 962–970. https://doi.org/10.1016/j.clinph.2013.10.012.

Pfurtscheller, G., 2001. Functional brain imaging based on ERD/ERS. Vision Res. 41 (10–11), 1257–1260. https://doi.org/10.1016/s0042-6989(00)00235-2.

Pfurtscheller, G., Da Silva, F.L., 1999. Event-related EEG/MEG synchronization and desynchronization: basic principles. Clin. Neurophysiol. 110 (11), 1842–1857.

Pfurtscheller, G., Lopes da Silva, F.H., 1999. Event-related EEG/MEG synchronization and desynchronization: basic principles. Clin. Neurophysiol. 110 (11), 1842–1857. https://doi.org/10.1016/s1388-2457(99)00141-8.

Pfurtscheller, G., Woertz, M., Supp, G., Da Silva, F.L., 2003. Early onset of post-movement beta electroencephalogram synchronization in the supplementary motor area during self-paced finger movement in man. Neurosci. Lett. 339 (2), 111–114.

Pollmann, S., Yves von Cramon, D., 2000. Object working memory and visuospatial processing: functional neuroanatomy analyzed by event-related fMRI. Exp. Brain Res. 133, 12–22.

Rockstroh B. (1982). Slow brain potentials and behavior. *(No Title)*.

Rohrbaugh, J.W., Syndulko, K., Lindsley, D.B., 1976. Brain wave components of the contingent negative variation in humans. Science 191 (4231), 1055–1057. https://doi.org/10.1126/science.1251217 (1979).

Roland, P.E., Larsen, B., Lassen, N.A., Skinhøj, E., 1980. Supplementary motor area and other cortical areas in organization of voluntary movements in man. J. Neurophysiol. 43 (1), 118–136. https://doi.org/10.1152/jn.1980.43.1.118.

Segalowitz, S., Davies, P.L., 2004. Charting the maturation of the frontal lobe: an electrophysiological strategy. Brain Cogn. 55 (1), 116–133.

Shaw, P., Kabani, N.J., Lerch, J.P., Eckstrand, K., Lenroot, R., Gogtay, N., Greenstein, D., Clasen, L., Evans, A., Rapoport, J.L., Giedd, J.N., Wise, S.P., 2008. Neurodevelopmental trajectories of the human cerebral cortex. J. Neurosci. 28 (14), 3586–3594. https://doi.org/10.1523/JNEUROSCI.5309-07.2008.

Smith, A.B., Halari, R., Giampetro, V., Brammer, M., Rubia, K., 2011. Developmental effects of reward on sustained attention networks. Neuroimage 56 (3), 1693–1704.

Tanji, J., 2001. Sequential organization of multiple movements: involvement of cortical motor areas. Annu. Rev. Neurosci. 24 (1), 631–651.

Tenke, C.E., Kayser, J., 2005. Reference-free quantification of EEG spectra: combining current source density (CSD) and frequency principal components analysis (fPCA). Clin. Neurophysiol. 116 (12), 2826–2846.

Thatcher, R.W., 1992. Cyclic cortical reorganization during early childhood. Brain Cogn. 20 (1), 24–50.

Thillay, A., Roux, S., Gissot, V., Carteau-Martin, I., Knight, R.T., Bonnet-Brilhault, F., Bidet-Caulet, A., 2015. Sustained attention and prediction: distinct brain maturation trajectories during adolescence. Front. Hum. Neurosci. 9, 519. https://doi.org/10.3389/fnhum.2015.00519.

Tian, Q., Xu, S., Guo, Y., Li, J., Han, M., Ma, Y., Hou, X., Chen, J., Luo, D., Hong, Y., Nie, S., Liu, X., 2019. Contingent negative variation for the periodicity of migraine attacks without aura. JIN 18 (3), 269–276. https://doi.org/10.31083/j.jin.2019.03.193.

Toma, K., Honda, M., Hanakawa, T., Okada, T., Fukuyama, H., Ikeda, A., Nishizawa, S., Konishi, J., Shibasaki, H., 1999. Activities of the primary and supplementary motor areas increase in preparation and execution of voluntary muscle relaxation: an event-related fMRI study. J. Neurosci. 19 (9), 3527–3534.

van der Lubbe, R.H., Wauschkuhn, B., Wascher, E., Niehoff, T., Kompf, D., Verleger, R., 2000. Lateralized EEG components with direction information for the preparation of saccades versus finger movements. Exp. Brain Res. 132 (2), 163–178. https://doi.org/10.1007/s002219900328.

Van Leeuwen, T.H., Steinhausen, H.C., Overtoom, C.C., Pascual-Marqui, R.D., Van't Klooster, B., Rothenberger, A., Sergeant, J.A., Brandeis, D., 1998. The continuous performance test revisited with neuroelectric mapping: impaired orienting in children with attention deficits. Behav. Brain Res. 94 (1), 97–110.

Walter, W.G., Cooper, R., Aldridge, V.J., McCallum, W.C., Winter, A.L., 1964. Contingent negative variation : an electric sign of sensori-motor association and expectancy in the human brain. Nature 203 (4943), 380–384. https://doi.org/10.1038/203380a0.

Wauschkuhn, B., Wascher, E., Verleger, R., 1997. Lateralised cortical activity due to preparation of saccades and finger movements: a comparative study. Electroencephalogr. Clin. Neurophysiol. 102 (2), 114–124. https://doi.org/10.1016/s0921-884x(96)96585-6.

Weerts, T.C., Lang, P.J., 1973. The effects of eye fixation and stimulus and response location on the contingent negative variation (CNV). Biol. Psychol. 1 (1), 1–19. https://doi.org/10.1016/0301-0511(73)90010-0.
Weisz, N., Schandry, R., Jacobs, A.M., Mialet, J.P., Duschek, S., 2002. Early contingent negative variation of the EEG and attentional flexibility are reduced in hypotension. Int. J. Psychophysiol. 45 (3), 253–260. https://doi.org/10.1016/s0167-8760(02)00032-6.
Werner, J., Weisbrod, M., Resch, F., Roessner, V., Bender, S., 2011. Increased performance uncertainty in children with ADHD?-Elevated post-imperative negative variation (PINV) over the ventrolateral prefrontal cortex. Behav. Brain Funct. 7, 1–9.
Yordanova, J., Dumais-Huber, C., Rothenberger, A., Woerner, W., 1997. Frontocortical activity in children with comorbidity of tic disorder and attention-deficit hyperactivity disorder. Biol. Psychiatry 41 (5), 585–594. https://doi.org/10.1016/s0006-3223(96)00096-0.

3 Study 2: Altered Motor Connectivity in TS

Altered Network Connectivity and Global Efficiency in Tourette Syndrome: Insights into Sensorimotor Integration

Julia Schmidgen*; Theresa Valentine Heinen; Felix Schmitt; Kerstin Konrad; Stephan Bender

This work is under review at *NeuroImage: Clinical*, available as a preprint article at SSRN: https://ssrn.com/abstract=5205885 or http://dx.doi.org/10.2139/ssrn.5205885

This study extends the previous chapter by examining alterations in network connectivity and sensorimotor integration in children with Tourette syndrome (TS). While data were collected as part of the same overarching project, this analysis focuses on a distinct group of drug-naïve TS patients not included previously. Employing high-density EEG and the same CNV task, we assessed theta-band phase synchronization and global network efficiency in TS patients compared to age-matched healthy controls, utilizing graph theory to capture the complexity of neural networks.

Our findings reveal distinct changes in stimulus processing and network organization in TS, particularly during sensory integration and early motor preparation, while mechanisms of motor execution remain largely intact. By highlighting both impairments and potential compensatory adaptations, this study advances the conceptualization of TS as a disorder of network-level dysfunction. These results contribute to the broader aim of identifying neurophysiological markers and potential intervention targets for TS.

3.1 Contribution

I contributed to the design of the study and was responsible for the acquisition and preprocessing of data, statistical analysis, and visualization of results. I interpreted the findings, drafted the manuscript, prepared figures and tables, and revised the work based on feedback. I coordinated the research process and ensured the scientific integrity and clarity of the paper.

3.2 Abstract

This study investigates the role of theta connectivity in network mechanisms related to perception-action-binding, sensorimotor integration, and motor preparation in children with Tourette's Syndrome (TS). High-density EEG data were collected from 21 children with drug-

naïve TS and 21 age-matched healthy controls during a task combining an informative warning stimulus (S1) with a behaviorally relevant imperative stimulus (S2). Event-related phase synchronization and global efficiency were calculated to analyze stimulus processing and identify neural networks responsible for integrating sensory information with motor preparation processes. Results revealed widespread alterations in theta-band connectivity in TS, with patients exhibiting reduced connectivity and impaired network efficiency during S1 processing, including diminished DLPFC involvement. S2 processing revealed subtler group differences than S1, manifesting as shifts in network organization rather than overall loss in connectivity strength. Remarkably, global efficiency during S2 processing remained intact in the TS group. In both groups, higher global efficiency during S2 correlated with faster reaction times, highlighting a direct link between network efficiency and motor response speed. This suggests that, despite altered sensory processing during information integration of the warning stimulus, motor execution mechanisms remain preserved in TS. The reduced connectivity during S1 processing may represent a compensatory mechanism aimed at weakening perception-action binding, potentially preventing premature motor output and aiding in tic control. These findings support the view of TS as a network disorder extending beyond traditional cortico-striato-thalamo-cortical circuits and suggest potential targets for interventions to modulate network efficiency and compensatory mechanisms in TS.

3.3 Introduction

Motor control relies on a complex processing network including various brain structures and neural pathways. Disruption of these highly organized, dynamic networks can lead to movement disorders, such as Tic disorders or Tourette's syndrome (TS). TS is a complex neurodevelopmental childhood-onset disorder characterized by chronic motor and vocal tics. Tics are nonrhythmic, repetitive, involuntary movements or vocalizations occurring in bouts for a limited duration (Leckman et al., 2014). Tics can be simple or complex, ranging from sudden movements or sounds involving a limited number of muscle groups to coordinated action sequences. TS is diagnosed when multiple motor tics and at least one vocal tic have been present for a minimum of one year. The severity, frequency, and severity of tics fluctuate over time, often peaking in early adolescence and declining steadily for most individuals as they progress through adolescence (Ricketts et al., 2022). TS often comes along with various comorbidities such as attention deficit hyperactivity disorder (ADHD) and obsessive-

compulsive disorder, significantly impacting quality of life (Cravedi et al., 2017; Eapen et al., 2016; Kumar et al., 2016).

A key challenge in managing TS is the limited understanding of its pathophysiology, especially considering the complexity of the underlying mechanisms and the involvement of multiple brain regions (Albin, 2018; Yael et al., 2015). The pathophysiology of TS is thought to result from a complex interplay among different neural systems. Motor control deficits underlying tic generation have been closely linked to disruptions in the cortico-striato-thalamo-cortical circuits. Recent research has focused on the role of sensorimotor integration in TS, with emerging evidence indicating abnormalities in how sensory information is processed and integrated with motor output (Houghton et al., 2014). Individuals with TS frequently report premonitory urges and somatic hypersensitivity, suggesting potential impairments in sensorimotor integration. Furthermore, the concept of perception-action binding has gained increasing attention in TS research, with evidence suggesting that patients with TS exhibit an enhanced coupling between sensory stimuli and motor responses (Friedrich et al., 2021; Kleimaker et al., 2020).

Theta-band activity is strongly related to processes involving sensorimotor integration and perception-action binding (Beste et al., 2023; Cruikshank et al., 2012; Tomassini et al., 2017; Wendiggensen et al., 2023). Especially long-range theta connectivity is suggested to be a crucial factor for effective cognitive processing and coordination of task-dependent activity (Lisman & Jensen, 2013; Mizuhara et al., 2004; Von Stein & Sarnthein, 2000). Therefore, the investigation of theta-band connectivity related to stimulus-evoked network changes is of particular interest in the present study, as alterations in these networks may contribute to the abnormal sensorimotor integration and perception-action binding observed in TS.

Efficient coordination of brain activity requires intricate interactions between anatomically separated neural populations (Horwitz, 2003). Investigations of these interactions reveal complex networks underlying brain functions. Synchronization of anatomically separated neuronal populations is considered to play an important role in coordinating information and indicating enhanced functional connectivity (Buehlmann & Deco, 2010). Phase locking values (PLVs) provide a metric to quantify the degree of synchronization between neural oscillations across different brain areas and to investigate dynamic network communication (Lachaux et al., 1999). PLVs measure the consistency of phase differences between oscillatory signals

recorded from different brain regions. High PLVs (close to 1) suggest robust communication between neuronal populations, while low PLVs (close to 0) indicate weak or no functional interaction. To investigate task-related changes in network synchronization, relative PLVs (rPLVs) can be calculated to assess changes in phase locking relative to baseline synchronization. Only few studies examined theta connectivity in TS with preliminary findings pointing to altered network dynamics that vary by context. Takacs et al. (2024), using resting-state EEG, found that individuals with TS show increased adaptability in theta network architecture, potentially reflecting hyper-learning of sensorimotor patterns. In contrast, Loo et al. (2019) used a task-based EEG paradigm and observed reduced theta connectivity during voluntary movements, suggesting impaired task-specific coordination. Wang et al. (2025) described disrupted theta-related connectivity between the supplementary motor area (SMA) and basal ganglia circuits, supporting its role as a therapeutic target via rTMS.

The present study aims to investigate the role of theta connectivity in network mechanisms related to perception-action-binding, sensorimotor integration, and motor preparation. We calculated phase synchronization from high-density EEG data of children with TS and age-matched healthy controls. To achieve a more detailed analysis of stimulus processing, we employed a CNV task paradigm that combined an informative warning stimulus (S1, indicated by an arrow pointing to either the left or right) with a behaviorally relevant imperative stimulus (S2). This informative cue allowed participants to prepare a specific motor response in advance, thereby enabling the investigation of the neural networks responsible for integrating sensory information with motor preparation processes.

We hypothesize that (i) theta-band connectivity networks will be altered in children with TS; (ii) these alterations will be most pronounced during S1 stimulus processing, as this phase primarily involves sensorimotor integration and perception-action binding; and (iii) the strength of theta connectivity during the cue processing phase will predict subsequent task performance in both groups, reflecting the role of theta-band activity in cognitive processing and task-dependent coordination. Investigating the interactions among neural networks involved in sensory integration not only deepens our understanding of tic pathophysiology but also may guide the development of targeted therapeutic interventions and aid in identifying neurophysiological biomarkers for TS.

3.4 Material and Methods

3.4.1 Subjects

The study included 21 drug-naive TS patients and 21 healthy controls (CO) subjects aged 7 to 13 years. Tic patients were individually matched with healthy controls based on age and gender. The maximum age difference between any matched pair of tic patients and control subjects was 0.4 years. There were no gender differences between any matched pairs. This matching procedure ensured that both age- and gender-related differences were minimized between the two groups. One subject with TS had to be excluded from further analysis due to poor data quality (for details, see 2.6). To preserve the integrity of the matched-pair design, the corresponding CO subject was also removed from the analysis. Detailed sample characteristics are provided in Table 1. All subjects were right-handed, assessed by the Edinburgh Handedness Scale (Oldfield, 1971). To ensure diagnostic accuracy, we conducted the K-DIPS structured clinical interview with all parents and with adolescents aged 12 and older. This process confirmed the diagnoses in patients and verified the absence of neuropsychiatric conditions in healthy controls. Participants with (i) a full-scale IQ below 70 as measured by WISC-V, (ii) individuals with a history of epilepsy or other central nervous system (CNS) disorders, (iii) those born prematurely before 32 weeks gestation, (iv) individuals with uncorrectable visual impairments, (v) and those with current or previous use of psychoactive drugs were excluded. Furthermore, we did not include any tic patients with comorbid ADHD in our sample. This allows for analysis of theta-band connectivity networks in drug-naive patients and controls and their abnormalities specifically related to tics. All participants and their legal guardians provided informed written consent/assent in accordance with the Declaration of Helsinki. The local ethics committee reviewed and approved the study protocol.

Table 1. Sample Demographics

Sample Characteristics	TS (N = 20)	Control (N = 2ß)	Statistic	*p*
Age [M ± SD; range]	10.6 (± 1.8; 7.4 – 13.2) years	10.8 (± 1.7; 7.8 – 13.2)	t(38) = -0.35	.73
Male gender [n (%)]	16 (80)	16 (80)	X^2 (1) = .00	1.0
YGTSS total symptom score [M ± SD]	33.65 (± 13.21)			
Age at tic onset (M ± SD)	5.03 (± 1.66) years			
Duration of tics [years (M ± SD; range)]	5.41 (± 2.52)			
Comorbid ADHD [n (%)]	0			

Note. M = Mean; SD = Standard deviation, YGTSS = Yale Global Tic Severity Score, ADHD = Attention deficit hyperactivity disorder

3.4.2 Experimental Procedure

The software package *Presentation* (Version 10.3, Neurobehavioral Systems Inc., Albany, CA) was used to generate a task-related program with alternating visual stimuli displayed on a monitor at a distance of 90 cm from subjects. To prevent any distractions, the light was dimmed, and the noise level was reduced to the highest possible minimum. To minimize distracting eye movements, a fixation cross was displayed in between visual stimuli. Subjects

sat in a comfortable position on a skid-proof chair, reducing muscle activity as much as possible to prevent interfering contractions.

3.4.3 Behavioral CNV Task Paradigm

Participants completed a visual CNV task (Fig. 1) consisting of 50 trials per response side. The warning stimulus (S1) appeared as a black arrow on a white background, pointing either left or right. The imperative stimulus (S2) was depicted as a colored sheriff on a black background. Both stimuli were displayed for 150 ms, with a fixed interstimulus interval of 3.05 seconds. Intertrial intervals varied pseudorandomly between 3 and 6 seconds. The warning stimulus indicated the required response side, with arrows presented in a pseudorandomized order. Participants were instructed to respond as quickly as possible to the imperative stimulus (S2) by pressing the corresponding button - "Ctrl" for left and "Enter" on the numeric keypad for right - using their left or right thumb on a German standard keyboard.

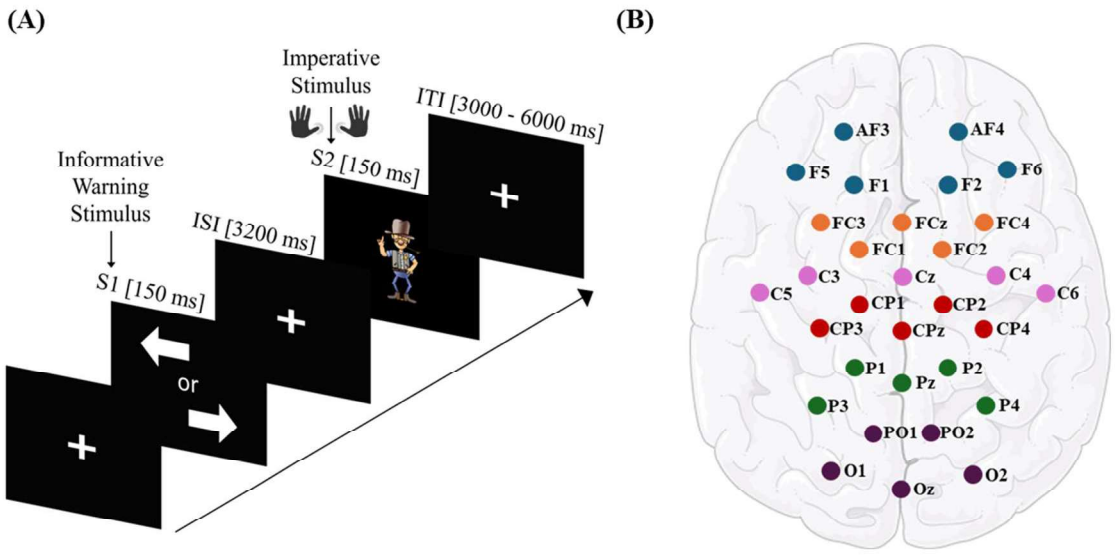

Figure 1. Experimental design **(A)** Contingent negative variation (CNV) task paradigm with a directional warning stimulus S1 and a behaviourally relevant imperative stimulus S2. **(B)** Electrode locations with regions of interest and specific electrodes used for data analysis marked in blue (DLPFC), orange (SMA/PMA), pink (M1), red (S1), green (PPC), and purple (POC). Sensor locations were plotted by using MNE-Python (Gramfort et al., 2013).

3.4.4 Electroencephalography

EEG was recorded using a 64-channel BrainAmp system (BrainProducts, Munich, Germany) and Brain Vision Recorder software (BrainProducts). Elastic EEG caps with direct current sintered Ag/AgCl disc electrodes (BrainProducts) were selected based on head sizes. Electrodes were named based on their location on the scalp, consistent with the international 10-20 system, electrode impedances were kept below 5 kΩ. Additionally, EOG electrodes were positioned under the left and right eyes and on the nasion. The sampling rate was set to 5000 Hz, electrode Cz was used as the online recording reference.

3.4.5 Electromyography

Surface EMG (compound muscle action potential) was recorded using self-adhesive silver-silver chloride electrodes in a belly tendon montage, respectively for the left and right hand. To record thumb movement, active electrodes were placed on the adductor pollicis muscle and reference electrodes were attached to the exterior proximal phalanx of the thumb. The ground electrode was placed on the inner forearm. The EMG was recorded using the bipolar BrainAmp ExG amplifier (Brain Products, Munich, Germany), which was synchronized with the EEG recordings.

3.4.6 Signal Preprocessing

The raw EEG data were preprocessed using MNE-Python (v0.22) within Python (v3.8.8). To reduce file size and computational load, data were downsampled to 200 Hz and digitally filtered using an FIR 50 Hz notch filter. The Cz online reference channel was reconstructed via spherical spline interpolation. EEG signals were then re-referenced to a common average reference and epoched around the imperative stimulus (S2) for both left and right button press conditions using MNE metadata. Epochs began 0.5 seconds before the warning stimulus (S1) for baseline computation and extended until 3 seconds after S2, capturing post-processing activity (total duration: 6.7 seconds, 1341 data points). Only trials in which participants responded correctly within 1.5 seconds following S2 were included in further analyses. To minimize the influence of slow drift effects on EEG data, a linear DC detrend was applied. Visual inspection before and after detrending confirmed that the overall signal shape and characteristics remained unaffected. For reproducibility, artifact rejection and trial exclusion were performed automatically using ‘Autoreject’, implemented in Python (Jas et al., 2017). This method employs cross-validation with a robust error metric to estimate rejection

thresholds, detecting and correcting outlier data segments for each sensor. Independent component analysis (ICA) was then conducted, and components associated with eye blinks, muscle activity (e.g., jaw clenching, swallowing), or other artifacts were automatically identified and removed using MNE-ICALabel. Finally, epoched and cleaned data were baseline-corrected using a reference window from 500 to 0 ms before the warning stimulus (S1).

After excluding trials with errors or strong artifacts (e.g., excessive movement), only participants with at least 35 valid trials per hand were included in further analysis. Based on these criteria, data from one participant with TS was removed. To preserve the matched-pair design, the corresponding CO participant was also excluded. This ensured that the study maintained its age- and gender-matched integrity throughout the analysis. Importantly, the number of valid trials did not differ between groups (TS: M = 83.05, SD = 9.76; CO: M = 82.45, SD = 11.18; $t(19) = 0.86$, $p = .399$, $d = 0.19$).

To minimize the effects of volume conduction, epoched data were transformed using current source density (CSD). Given the low spatial resolution of EEG, electrical signals from a single neural source can spread across multiple scalp electrodes (Nunez & Srinivasan, 2006). This diffusion can create the illusion of widespread synchronous or phase-locked activity, even when the signal originates from a single source. By applying Surface Laplacian spatial filtering, CSD enhances the localization of brain activity, effectively reducing the influence of distant sources (Tenke & Kayser, 2012).

3.4.7 Phase-Locking Connectivity Analysis

Epoched, cleaned, and reference-free data were transformed into the time-frequency domain using the Morlet wavelet transform. The analysis focused on the theta frequency range (4–7 Hz; 1 Hz increments) to capture oscillatory activity linked to attentional control, sensorimotor integration, and perception-action binding in children (Beste et al., 2023; Cruikshank et al., 2012; Tomassini et al., 2017; Wendiggensen et al., 2023). For subsequent phase-locking analysis, we used a modified version of the Dynamic Synchronization Toolbox (DST;(Rosjat & Daun, 2022)) implemented in MATLAB (v.R2022b, MathWorks, Natick, MA, USA).To ensure compatibility with the DST data structure, phase data arrays were reformatted. The final dataset was structured with dimensions corresponding to channels, time, trials, and frequencies and saved as a MATLAB matrix. The instantaneous Phase is defined as

$$PLV_{ij}(t) = \frac{1}{N}\left|\sum_{n=1}^{N} e^{-i(\varphi_i(t,n)-\varphi_j(t,n))}\right|$$

where $\varphi_i(t,n)$ and $\varphi_j(t,n)$ represent the instantaneous phases of signals i and j at time t in trial n with N for the total number of trials. Since our study focused on event-related phase-locking changes, PLVs were normalized relative to mean PLV baseline values [-3700, -3200] and denoted as "relative phase-locking values" (rPLV):

$$rPLV_{ij}(t) = \frac{PLV_{ij}(t) - \overline{PLV_{ij}}}{\overline{PLV_{ij}}}$$

Based on previous literature examining cue processing and perception-action binding, we focused our analysis on two critical time windows: [-3200, -2700] ms relative to the imperative stimulus for cue processing, and 500 ms following the imperative stimulus for initial motor preparation and response execution. These time windows were chosen to specifically capture stimulus-evoked sensorimotor, cognitive processing, and perception-action binding rather than classical CNV dynamics, which typically focus on activity between S1 and S2. While CNV studies often analyze early CNV (550–750 ms post-S1) or late CNV (response preparation just before S2), our approach prioritizes the neural mechanisms underlying stimulus processing and the initiation of motor responses. This distinction is crucial, as the study aims to investigate tic-related alterations in phase synchronization during cue and imperative stimulus processing, rather than sustained CNV activity (Morand-Beaulieu et al., 2015; Rothenberger & Kemmerling, 1982; van Woerkom et al., 1994).

3.4.8 Network of Interest (ROIs)

To investigate potential deficits in TS related to sensorimotor integration, visual processing, motor preparation, and control, we identified key brain regions for analysis. Given that different neural regions contribute to various aspects of these processes, multiple regions of interest (ROIs) were defined (Makeig et al., 2002). This approach enables a comprehensive examination of hierarchical processing, functional specialization, and network interactions during stimulus processing and sensorimotor integration. Table 2 provides an overview of the

selected brain areas, their associated functions, and corresponding electrode positions (see also Fig. 1B for graphical illustration).

Table 2. Regions of Interest

Brain areas	Involvement	Electrode position	References
Dorsolateral Prefrontal Cortex (DLPFC)	Cognitive control, attentional processing, motor preparation	F5, F1, AF3; AF4, F2, F6	(Fitzgerald et al., 2009; Kaneko et al., 2024)
SMA and Pre-motor Areas (SMA/PMA)	Action inhibition, motor control	FC4, FC2, FCZ, FC1, FC3	(Ahangama et al., 2023; Puzzo et al., 2010)
Primary Motor Cortex (M1)	Motor control of hand movement	C5, C1, Cz, C4, C6	(Jessy, 2009; Puzzo et al., 2010; Yuan et al., 2010)
Primary Somatosensory Cortex (S1)	sensorimotor integration and processing of sensory information	CP3, CP1, CPz, CP2, CP4	(Insausti-Delgado et al., 2021; Kim et al., 2021)
Posterior Parietal Cortex (PPC)	Sensorimotor integration, attention allocation	P3, P1, Pz, P2, P4	(Lin et al., 2015; SanMiguel et al., 2010)
Parieto-Occipital Cortex (POC)	Visual processing, integration of visual information	PO1, PO2, O1, Oz, O2	(Boutonnet et al., 2013; Pouryazdian & Erfanian, 2009)

3.4.9 Euclidean Distance

We calculated the time-resolved Euclidean distance, denoted as *d(t)*, to quantify differences between the functional connectivity networks of the TS and CO groups. Functional connectivity networks were constructed by averaging the within- and between-area connections for each group. The Euclidean distance *d(t)* was then computed using the group-averaged adjacency matrices, reshaped into vectors $A_{TS}(t)$ and $A_{CO}(t)$. The formula for *d(t)* is as follows:

$$d(t) = \|A_{TS}(t) - A_{CO}(t)\|_2$$

This measure quantifies the dynamic differences in functional connectivity between groups over time.

Furthermore, within-group variability was assessed by computing the variance of the Euclidean distance between each individual's connectivity pattern and their respective group mean. This analysis provides insight into the consistency of functional connectivity within each group and highlights potential heterogeneity in network organization.

3.4.10 Principal Component Analysis

We performed PCA on the functional connectivity networks of the TS and CO groups. Connectivity networks were constructed by averaging within- and between-region connections. The group average adjacency matrices were reshaped into vectors $A_{TS}(t)$ and $A_{CO}(t)$ and concatenated. Prior to PCA, the data was mean-centered and scaled to unit variance. The resulting eigenvectors were extracted and reshaped to the adjacency matrix.

3.4.11 Classification – Linear Discriminant Analysis

To assess distinction between TS and CO conditions based on functional connectivity patterns, we applied a machine learning classification approach. This analysis was not aimed at identifying TS biomarkers, as the data quality and sample size were insufficient. Instead, we explored whether group differences in connectivity were detectable and whether the data was separable within a given time window. We classified TS and CO conditions based on the functional connectivity networks within a given time window. Connectivity networks were constructed by averaging within- and between-region connections followed by temporal

averaging within the time windows of interest (500 ms post-S1 and S2, respectively). From the resulting symmetric 6×6 adjacency matrix, we extracted 21 independent features.

For classification, we performed 100-fold cross-validation, selecting a random test set of two subjects per fold. The remaining 38 subjects formed the training set, which was used for mean-centering and scaling the data to unit variance (Z-score), selecting the 10 most discriminative features based on the highest ANOVA F-values, and fitting the Linear Discriminant Analysis (LDA) classifier. Classification accuracies from the test sets were averaged across folds and reported. Due to the small dataset, we omitted a validation set and accepted data leakage while exploring hyperparameters (test set size, feature selection, and classifier choice). Consequently, reported accuracies are likely overestimated, and overfitting could not be controlled with a test set of only two samples.

As a control, we repeated the procedure with a surrogate dataset in which group labels were randomly shuffled in each fold, yielding chance-level performance (~50%).

3.4.12 Global Efficiency

Global efficiency (E_{glob}) was computed to assess the overall integration of the functional brain network using networkx library's built-in function nx.global_efficiency(G) in Python. The network was constructed based on rPLVs between electrode pairs. For each subject, functional connectivity matrices were extracted for the predefined time windows [-3200, -2700] and [0, 500], following the same approach as the rPLV analysis (see Section 2.7 for details). Time indices corresponding to each window were identified, and connectivity values were averaged across time points to obtain a representative adjacency matrix.

The resulting adjacency matrix was used to construct an undirected, weighted graph *G*, where nodes represented electrodes and edge weights reflected the functional connectivity strength between them. Global efficiency was then calculated using the following formula:

$$E_{glob} = \frac{1}{N(N-1)} \sum_{i \neq j}^{N} \frac{1}{L_{i,j}}$$

where N is the total number of nodes, and $L_{i,j}$ is the shortest path length between nodes i and j. Higher values of E_{glob} indicate more efficient information transfer across the network.

3.4.13 Statistical Analysis

Reaction times (RT) for left- and right-hand task conditions were averaged across trials for each participant to compare behavioral performance between groups. Trials with RTs exceeding 1500 ms after stimulus onset or occurring within 150 ms post-stimulus were excluded to eliminate anticipatory and excessively delayed responses. This criterion ensured that only valid, task-related reactions were included in the final analysis. Task accuracy was calculated as the percentage of correct responses, with anticipatory responses defined as button presses occurring between the warning stimulus (S1) and the imperative stimulus (S2). For behavioral data analysis, we employed the non-parametric Mann-Whitney U test due to the non-normal distribution of the data, as confirmed by Shapiro-Wilk tests ($p < 0.05$).

To identify regions with significant increases in phase locking within each group, we performed pointwise t-tests. Differences in rPLV and global efficiency between TS and CO subjects were assessed using non-parametric Mann-Whitney U tests, given the non-normal distribution of the data. Statistical tests were performed at a significance level of $p = .05$ (FDR corrected). For exploratory area-based analyses, we refrained from applying FDR correction due to the prohibitive number of comparisons arising from the high dimensionality of the data. This approach would have rendered significance thresholds overly conservative, obscuring biologically plausible effects. To validate our findings, we employed complementary multivariate approaches: PCA to identify dominant network configurations, Euclidean distance metrics to quantify global group separations, classifier accuracy to assess discriminative power, and global efficiency to evaluate network integration. These methods circumvented multiple-testing limitations by focusing on system-level dynamics rather than individual connections, providing converging evidence of robust group differences in network organization.

3.5 Results

3.5.1 Behavioral Task-Performance

Error rates and reaction times were analyzed to investigate behavioral task performance across TS and CO subjects. Between-group comparison showed no significant differences in motor performance regarding reaction times, anticipatory responses (errors in between stimuli), or general task accuracy (see Table 1).

Table 3. Task-performance parameters in TS and CO groups

Performance	TS subjects	CO subjects	Statistics	*P*
RT (left) [Mdn; IQR]	346.70; 97.57	326.10; 69.94	U = 224.00, Z = 0.65, r = 0.10	.53
RT (right) [Mdn; IQR]	329.40; 129.11	334.75; 67.44	U = 195.00, Z = -0.14, r = 0.02	.90
Anticipatory response [Mdn; IQR]	8.00; 9.50	7.00; 5.50	U = 219.50, Z = 0.53, r = 0.08	.61
Accuracy [Mdn; IQR]	89.50; 9.75	92.00; 4.5	U = 166.50, Z = -0.91, r = 0.14	.37

Note. RT = Reaction-time, Mdn = Median, IQR = Interquartile range.

3.5.2 Event-Related Strengthening of Phase-Based Connectivity

Prior to the analysis of group-related connectivity differences, rPLV data were examined for statistically significant connectivity patterns within the areas of interest. This approach aims to facilitate the definition of temporal windows exhibiting robust connectivity both within and between areas of interest.

For both groups, theta band phase locking showed a significant event-related increase, particularly in the time window of 0 to 500 ms following the warning and the imperative stimulus. Figure 2 illustrates time points and areas with an increase in phase locking for theta band frequency that were statistically significant for either left or right CNV motor tasks. For both groups, no significant connectivity was observed within the area of DLPFC. However, in contrast to tic subjects, control subjects showed significant phase locking between DLPFC and other ROIs. In all other areas, significant phase synchronization was observed both within and between regions in both groups. For posterior regions (PPC and POR), the increase in rPLV

was statistically most robust, indicating a stronger and more reliable connectivity pattern in these areas.

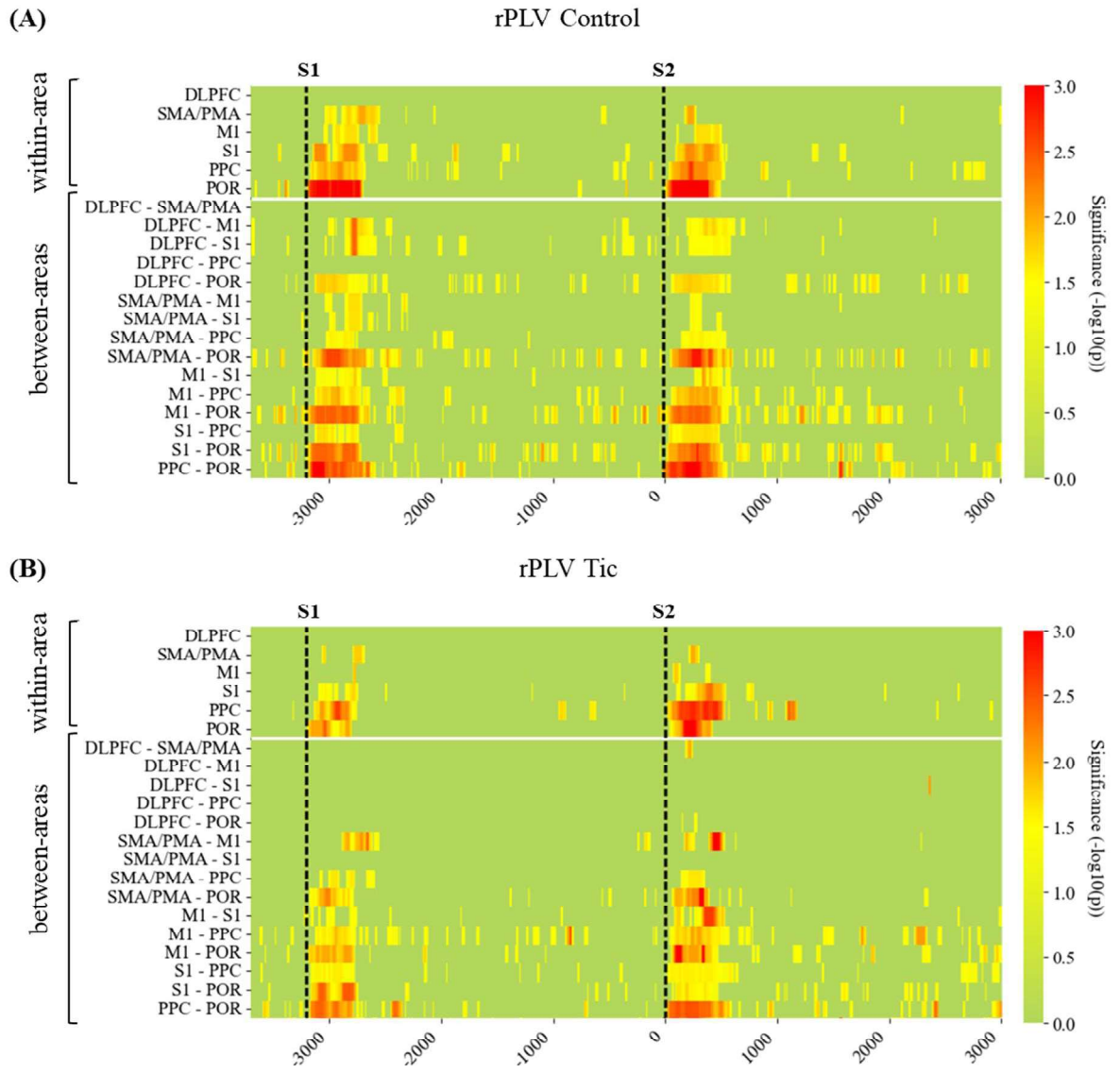

Figure 2. Event-related changes in theta phase locking. **(A)** Colormap representing statistical analysis of rPLV over time in CO and **(B)** TS subjects. Connectivity measures are cluster in within-area (upper part) and between-area connectivity (bottom part) of defined ROIs. Vertical dashed lines indicate stimulus presentation of warning and imperative stimulus. Connectivity significance is represented as $-\log_{10}(p)$, whereas higher values indicate more statistically reliable connectivity across subjects. *Note.* DLPFC = Dorsolateral prefrontal cortex; SMA/PMA = supplementary motor area/premotor area; M1 = primary motor cortex; S1 = primary somatosensory cortex; PPC = posterior parietal cortex; POR = parieto-occipital region.

Since event-related connectivity increase was most pronounced within 500 ms following stimulus presentation of S1 (warning cue) and S2 (imperative cue, motor response), we focused on those specific time windows to analyze group-related differences in stimulus processing, movement preparation, and motor output. Area-based connectivity showed no pronounced differences between left and right task conditions for both groups, therefore datasets were aggregated and used for the following analysis.

3.5.3 Differences in Phase Locking between Groups

To provide an initial overview of rPLV differences between TS and CO, connectivity matrices were plotted for the 0 - 500 ms time window following S1 and S2 (Figure 3A, B). These matrices represent group-averaged functional connectivity across all subjects within each group for all electrodes within ROIs. Visual inspection reveals distinct differences in overall connectivity patterns between TS and CO, with notable variations in the strength and distribution of functional connections, especially in the time window following S1. Average phase synchronization across all electrodes showed significantly reduced connectivity in TS subjects for S1 processing (Mdn = 0.22, IQR = 0.06; CO: Mdn = 0.30, IQR = 0.14; U = 98.000, Z = -2.76, p = 0.012, r = .44). Overall connectivity strengths within the time window of S2 processing did not show significant group differences (TS: Mdn = 0.31, IQR = 0.15; CO: Mdn = 0.36, IQR = 0.10; U = 165.000, Z = -0.95, p = .351, r = .15).

To validate differences in connectivity patterns, area-based analyses were conducted. Tic-related deviations in phase synchronization were examined by subdividing ROIs into within- and between-area connectivity. To capture dynamic changes, data were segmented into five 100-ms subintervals for S1 and S2 (Fig. 3C). Mann-Whitney U tests revealed significant between-group differences in event-related connectivity (for detailed statistics see Supplementary Material, Table 1). TS participants showed reduced phase synchronization within and between most brain areas after S1, with the strongest and most robust reductions in the POR area. While rPLV strengths in other regions also indicated tic-related reductions, within-area connectivity loss was less statistically consistent than the more pronounced between-area reductions across all ROIs.

Processing of S2 elicited less pronounced differences in synchronization between groups. Reductions in rPLV strength were mainly observed between the DLPFC and S1, as well as

between S1 and POR. Notably, TS participants showed a more pronounced increase in phase synchronization within the SMA/PMA (for detailed statistics see Supplementary Material, Table 2).

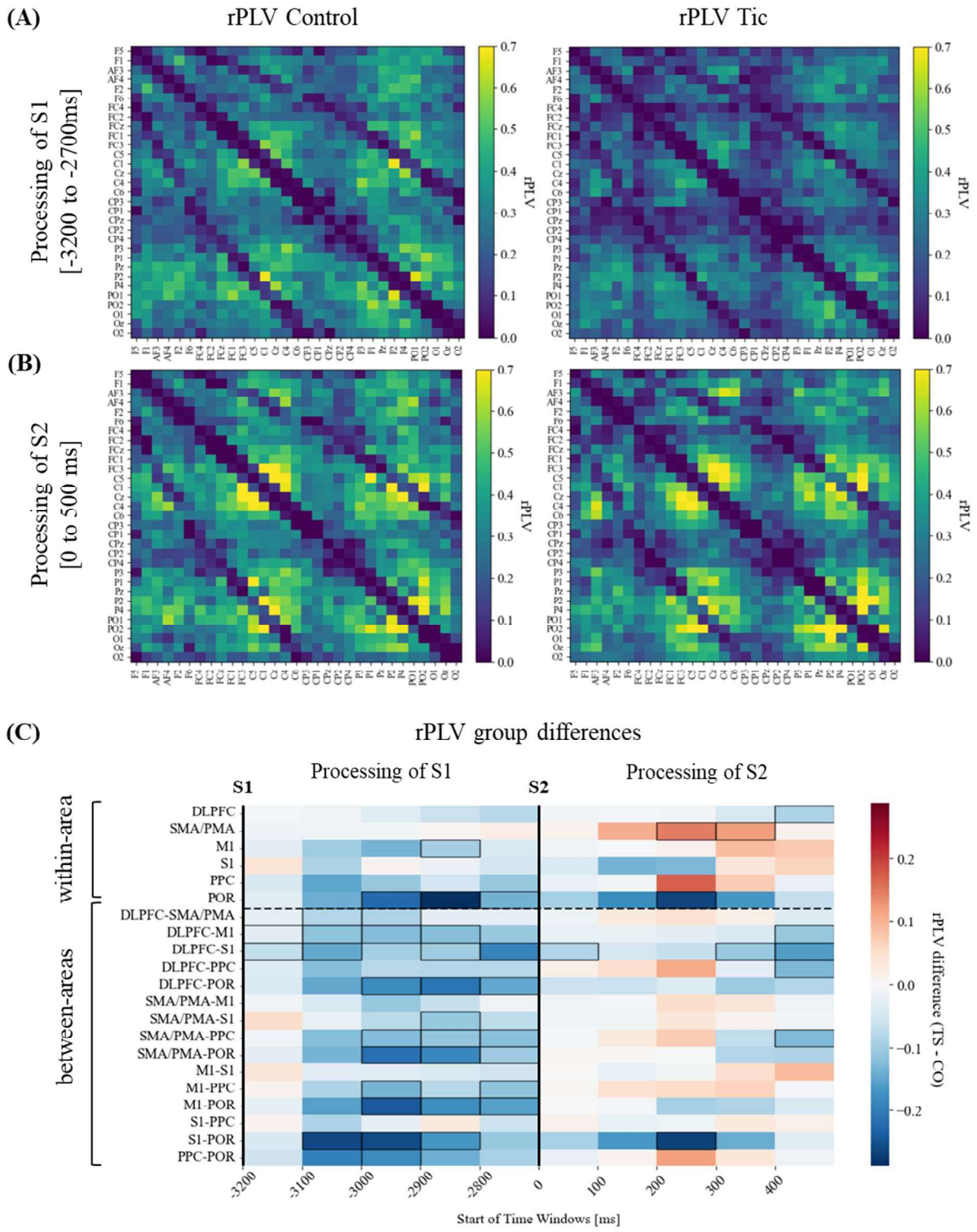

Figure 3. Average rPLV and differences between TS and CO across brain areas and time. **(A)** rPLC matrices of CO (right) and TS (left) subjects averaged across time windows of S1 processing, and **(B)** of S2 processing (respectively 0 to 500 ms after stimulus presentation). **(C)** Differences in event-related phase synchronization (rPLV) between TS and CO subjects. Data were calculated for 100 ms time windows, resulting in five time windows respectively after stimulus presentation of S1 (left) and S2 (right). rPLV connectivity was classified into

connections within each brain area (upper part) and connections between the predefined brain areas (lower part). Blue squares (negative values) indicate higher connectivity in CO, and red squares show increased connectivity in TS subjects. Time intervals and areas showing significant differences between TS and CO are framed in black. Please note, rPLV differences were not FDR-corrected due to the large number of areas and tests, making correction impractical. However, consistent patterns across multiple comparisons support the robustness of the findings. *Note.* DLPFC = dorsolateral prefrontal cortex; SMA/PMA = supplementary motor area/premotor area; M1 = primary motor cortex; S1 = primary somatosensory cortex; PPC = posterior parietal cortex; POR = parieto-occipital region.

3.5.4 Assessing Network Differences with PCA, Euclidean Distance and Classification

Leveraging PCA and Euclidean distance measures, we quantified global network disparities between groups, providing a dimensionality-reduced representation of connectivity changes associated with stimulus processing.

In the PCA analysis, Principal Component 1 (PC1) accounted for 30% of the variance in the dataset (Fig. 4A, B). The eigenvector matrix revealed that PC1 was associated with an increase in connectivity, as reflected by higher rPLVs in the original data. Notably, all other components accounted individually for less than 3% of the variance, highlighting that PC1 played a dominant role in explaining the patterns of connectivity in the datasets. Analysis of PC1 scores revealed distinct temporal patterns between groups (Fig. 4A). Following the warning stimulus (S1), CO subjects exhibited higher PC1 values compared to TS subjects, indicating a more pronounced increase in overall connectivity during S1 processing. However, after the imperative stimulus (S2), PC1 values converged between the groups, suggesting a reduction in the disparity of connectivity strengths.

Complementing the PCA findings, Euclidean distance analysis quantified the overall separation of neural states between groups. As expected, the most pronounced group differences were observed within 500 ms following both stimuli, with the largest separation occurring after S1 (for details see Fig 4C). This confirms that the critical divergences in network configuration between TS and CO groups are most evident in the immediate post-stimulus periods. While group separation strongly decreased during the inter-stimulus interval, a clear distinction remained after S2, albeit less pronounced than post-S1. Variance analysis revealed greater processing variance in the CO group after S1, while the TS group exhibited higher processing variance after S2 (Figure 4D).

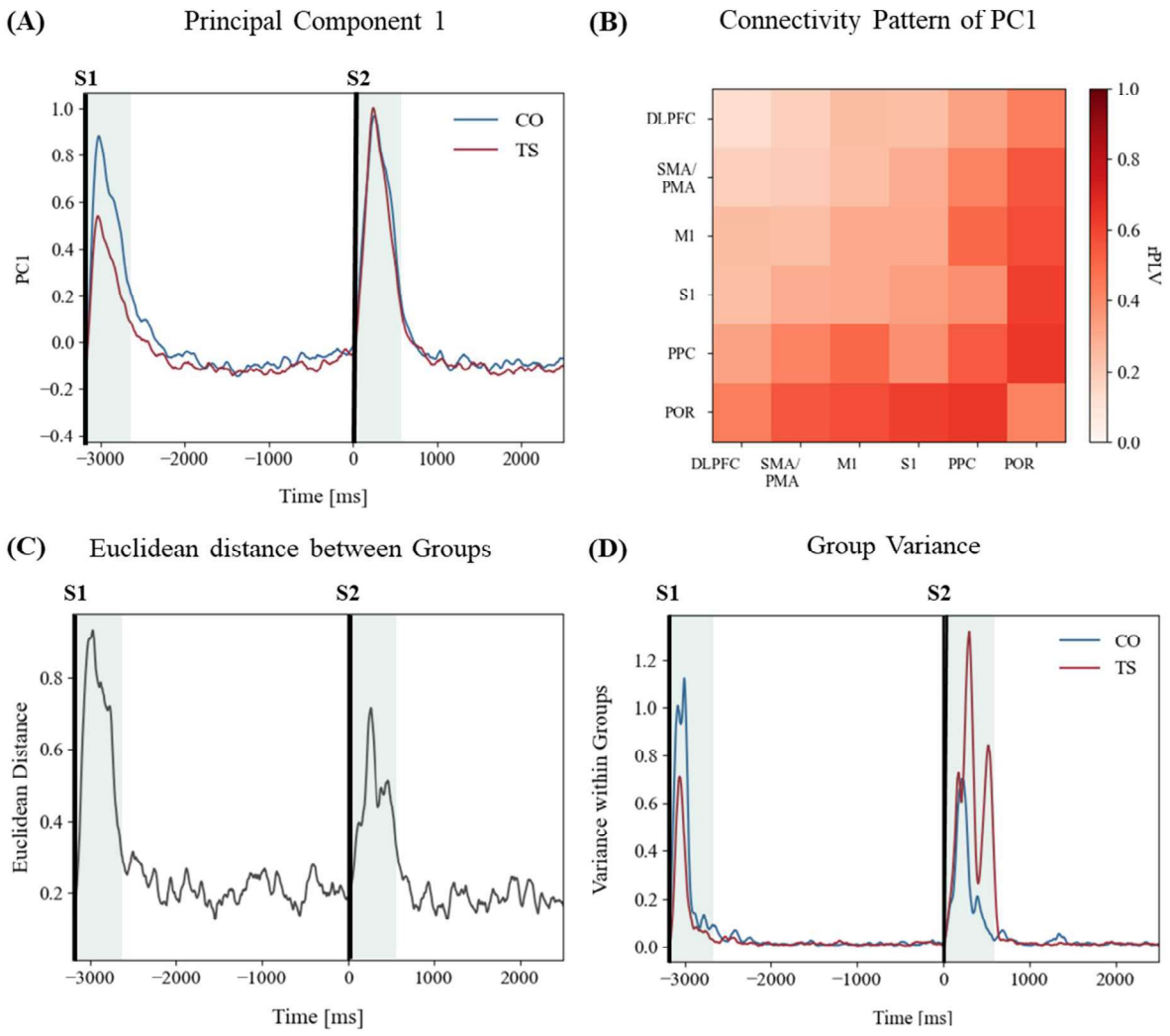

Figure 4. Network differences. (A) Time course of PC1 for TS (red) and CO (blue), with a pronounced increase within 500ms time windows after stimulus presentation. TS shows reduced PC1 values for the processing period of S1. **(B)** The connectivity pattern of PC1 shows an overall increase in phase synchronization, most pronounced for parietal areas. **(C)** Euclidean distance showed noticeable group separations after both S1 and S2, with the largest difference occurring after S1. **(D)** Variance within the group for TS (red) and CO (blue), with higher variance for CO after S1 and higher variance for TS after S2.

To assess the discriminative power of these network differences, we employed a classifier analysis. The classifier achieved an accuracy of 76.5% in the time window following S1, and 72.5% after S2. These results exceeded chance levels, as demonstrated by shuffled accuracy rates of 52.0% for S1 and 49.0% for S2. This classification performance further validates the presence of distinct network patterns between TS and CO groups during stimulus processing phases.

3.5.5 Global Efficiency Across Motor Performance

To determine whether connectivity differences - particularly the reduced connectivity observed in TS during S1 processing - affected network efficiency, we analyzed global efficiency following both S1 and S2 (Fig. 5A). Group comparison revealed significantly reduced efficiency during S1 processing in TS subjects (TS: Mdn = 0.46, IQR = 0.06; CO: Mdn = 0.56, IQR = 0.15; U = 77.000, Z = -3.33, p = .002, r = -.53). During processing of S2, groups showed comparable network efficiency (TS: Mdn = 0.59, IQR = 0.14; CO: Mdn = 0.6, IQR = 0.12; U = 168.000, Z = -0.87, p = .394, r = -.14).

Network efficiency following S2 correlated significantly with reaction time in both groups (TS: R^2 = .374, F(1, 18) = 10.77, p = .008; CO: R^2 = .467, F(1, 18) = 15.74, p = .003), indicating that higher efficiency was linked to faster responses (Fig. 5B). In contrast, efficiency during S1 processing showed no significant association with processing speed. Task accuracy and anticipatory errors showed no relationship with network efficiency in either group or time window.

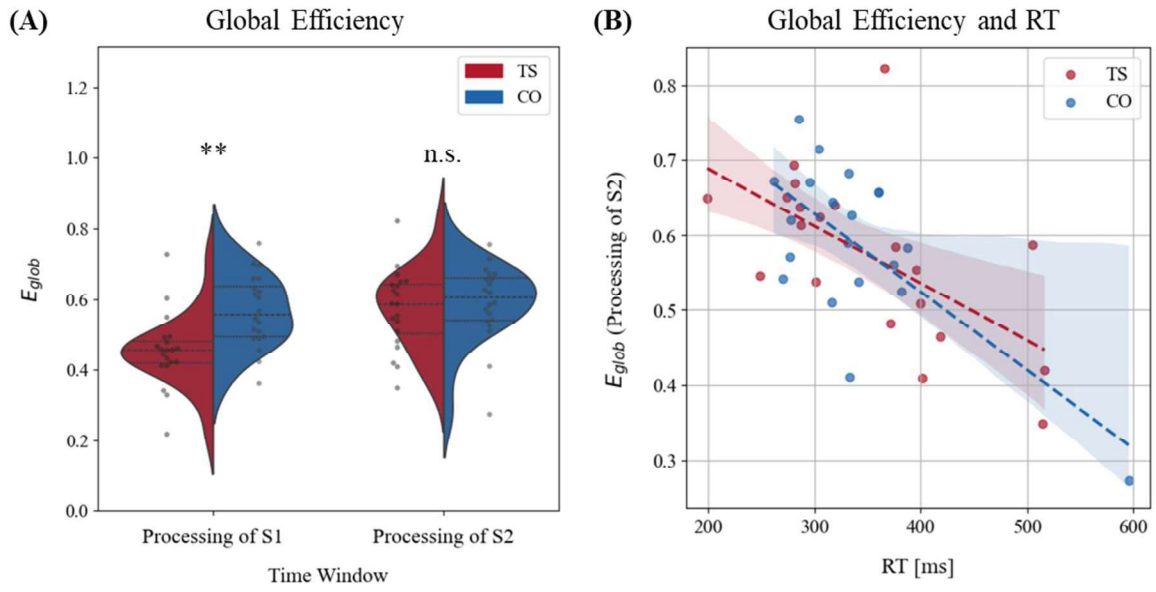

Figure 5. Global efficiency (A) Global Efficiency comparison between TS and CO for Processing of S1 and S2. Data are visualized using violin plots, with overlaid swarm plots to show individual subject data points. The statistical threshold (** $p \leq .01$) has been corrected for multiple comparisons using FDR. **(B)** Relationship between motor performance and Global

efficiency post S2. RT was significantly correlated with the Global efficiency of S2 processing (TS: $p = .008$; CO: $p = .004$; FDR corrected).

3.6 Discussion

This study examined functional connectivity during sensorimotor integration, motor preparation, and execution in children and adolescents with TS. Our findings revealed widespread alterations in theta-band connectivity across frontal, central, parietal, and occipital brain regions. The most pronounced differences emerged during the processing of the warning stimulus (S1), marked by a tic-related reduction in theta-band network synchronization. Distinct group differences were also observed during the processing of the imperative stimulus (S2), characterized by reorganized network patterns rather than diminished connectivity.

Both groups displayed the strongest phase coupling immediately after stimulus presentation, lasting for approximately 500 ms. The stimuli triggered a synchronized neural response across multiple brain regions, consistent with previous studies on visual-attentional processing in children (Santhana Gopalan et al., 2019; Zarka et al., 2021). During the first few hundred milliseconds, several key cognitive processes are engaged, including sensory processing, attentional allocation, information integration, motor preparation, resource distribution, and top-down modulation (Madl et al., 2011; Tan et al., 2024). These rapid and interconnected processes underscore the complex neural dynamics involved in stimulus processing and response preparation.

Neuronal networks arose across all examined brain regions. However, while healthy subjects exhibited modest connectivity between the DLPFC and other brain regions, subjects with TS showed nearly no significant integration of the DLPFC, highlighting distinct differences in network architecture between the groups. Previous studies showed an age-related increase of DLPFC activation (Achterberg et al., 2020), alongside a developmental increase of functional coupling to other brain regions involved in motor control (Steinbeis et al., 2014; Uddin et al., 2011). In line with our data, studies focusing on tic pathophysiology in children reported a reduced involvement of the frontal-parietal networks (Church et al., 2009; Fan et al., 2018). Fair et al. (2009) observed widespread differences in functional connectivity between frontoparietal control networks and suggested that reduced efficiency in TS is particularly pronounced between distant brain regions, suggesting a tic-related functional immaturity.

3.6.1 Processing of the Informative Warning Cue

Group differences in theta connectivity were most pronounced during the processing of the informative warning cue of our pre-cued reaction time task. The data suggest an extensive deviation in theta connectivity across all investigated brain regions. Besides a pronounced reduction in overall phase synchronization, subjects with TS showed a reduced network efficiency. This finding aligns with the growing understanding of TS as a network disorder rather than a condition affecting isolated brain regions. The reduced connectivity and network efficiency might reflect difficulties in efficiently allocating attentional resources during the preparatory phase. Furthermore, our analysis revealed reduced variability in network configurations (as measured by Euclidean distance) in TS subjects following S1. This decreased variability, coupled with reduced connectivity and network efficiency, suggests constrained neural flexibility during the preparatory phase. Notably, TS subjects achieved normal response execution efficiency during S2 processing, despite initial preparatory differences. They showed no impairment in motor performance regarding reaction times, accuracy, and especially anticipatory response (premature button press after presentation of warning stimulus). These findings are consistent with other studies reporting no tic-related deficits in task performance (Marsh et al., 2007; Schmidgen et al., 2023; Wylie et al., 2016). However, in contrast to our results, other research has demonstrated that individuals with TS exhibit impairments and reduced performance in visual processing, particularly in tasks requiring visuomotor integration (Brookshire et al., 1994; Schultz et al., 1998). The recruitment of parietal and frontal brain areas is essential for the dynamic process of visual feature integration (Castellano et al., 2014), involving top-down modulation from these regions. It cannot be ruled out that the CNV task paradigm may not be sensitive enough to detect subtle differences in performance that might be present in more complex or demanding tasks.

Adelhöfer et al. (2021) found increased neural noise levels (1/*f* noise) during sensorimotor processing in children and adults with Tourette Syndrome. Increased neural noise is associated with reduced synchronization of neuronal activity (Voytek et al., 2015). Higher noise levels during stimulus processing likely impair area synchronization and neuronal communication (González-Villar et al., 2017), suggesting TS-related alterations in neural dynamics. Sun et al. (2020) reported a stronger reduction of somatosensory evoked potentials 15 minutes after a rTMS protocol application (1Hz, 90% of the resting motor threshold) in TS patients. They suggested the motor-sensory cortex circuit to be responsible for the suppression of the sensory

system. This interpretation supports the view of TS as a sensorimotor disorder rather than solely a motor dysfunction. In an fMRI study by Atkinson-Clement et al. (2020), adult TS patients with intermittent explosive outbursts showed reduced connectivity within the sensory-motor cortico-basal ganglia network that was related to difficulties in sensorimotor integration, action selection, and decision-making. The findings align with our results, indicating reduced connectivity and network efficiency, particularly following the presentation of the informative S1 cue, which demanded greater sensory processing and motor preparation compared to S2 processing.

3.6.2 Perception-Action Binding

However, it is also plausible that these deviations represent a compensatory mechanism rather than a deficit, especially given that tic patients did not exhibit impaired motor performance. The reduced connectivity could reflect a compensatory reorganization aimed at weakening perception-action binding to prevent premature motor output. Research further suggests a compensatory downregulation in response to urges and heightened sensitivity to external stimuli (Friedrich et al., 2021).

Children with TS showed enhanced perceptual-motor sequence learning, likely due to strengthened connections between stimuli and motor responses (Shephard et al., 2019; Takács et al., 2018). This supports the idea that tic-related mechanisms may enhance habit formation (Delorme et al., 2016; Singer, 2016), indicating an increased tendency to form links between sensory cues and motor actions. The cognitive framework of the theory of event coding (TEC) explains how perception (stimulus) and action (response) are integrated within the brain (Hommel et al., 2001). The framework is based on the assumption that perception and action share a common representational format and that the binding information is stored in a binding "event file". This mechanism allows stimuli with shared features to trigger similar actions more efficiently, facilitating habit learning. Such associations influence subsequent stimulus processing and may contribute to automatic action triggering in TS (Kleimaker et al., 2020; Petruo et al., 2019). By weakening the perception-action binding, this neural adaptation may help TS patients prevent premature motor output and exert better control over their tics. This compensatory reorganization aligns with the observed enhanced perceptual-motor learning and increased habit formation in TS, suggesting a complex interplay between altered neural connectivity and behavioral adaptations in managing tic symptoms.

3.6.3 Phase Coupling following Imperative Stimulus

In contrast to S1 processing, the neural networks engaged during imperative stimulus (S2) processing showed more subtle group differences, characterized by shifts in network organization rather than changes in overall connectivity strength. Notably, children with TS demonstrated increased phase coupling both within and between several brain regions. Although the increase in synchronization of individual areas was largely not statistically significant, analyses of PCA and Euclidean distance revealed that global network dynamics differed significantly between groups. These multivariate approaches captured subtle yet consistent alterations in overall connectivity patterns, highlighting the importance of considering network-level changes in Tourette Syndrome that may not be apparent when examining individual connections in isolation. Interestingly, Euclidean distance analysis revealed a striking contrast in network variability for TS subjects across task phases. Following S1, variability was reduced, whereas after S2, TS subjects showed increased variability compared to controls. This heightened variability after the imperative stimulus suggests a potential "release" from the constrained neural states seen during the preparatory phase. Such a shift may indicate a transition from rigid control during preparation to more flexible, yet potentially less stable, network dynamics when responding rapidly. However, this compensatory mechanism may come at the cost of reduced neural flexibility, potentially limiting the ability to adapt to more complex or demanding tasks. Importantly, the processing networks of both groups achieved comparable efficiency. These results align with the idea that TS involves more complex alterations in preparatory and control processes rather than in basic motor execution mechanisms (Beste & Münchau, 2018; Mielke et al., 2021).

While the overall differences in imperative stimulus processing were less pronounced, a closer examination of specific brain regions revealed interesting patterns. Phase synchronization data suggest a significantly increased functional coupling within the SMA and premotor areas during late motor preparation and execution (200 to 400 ms post S2). Many studies suggested deviations within the SMA to be a crucial factor within tic-related pathophysiological mechanisms. Especially, it was shown that the SMA is actively involved in tic generation (Bloch et al., 2006; Hampson et al., 2009; Neuner et al., 2014). Applying 1 Hz inhibitory rTMS to the SMA resulted in reduced tic frequency, implying that excessive SMA activity is directly linked to tic manifestation (Le et al., 2013; Mantovani et al., 2007; Wu et al., 2014). Besides a tic-related overactivation of the SMA, research has revealed enhanced connectivity within

other areas related to SMA and premotor areas (Biswal et al., 1998; Fattapposta et al., 2005). These findings are consistent with our phase coupling data, underscoring the critical role of SMA hyperconnectivity in the pathophysiology of Tourette syndrome and its potential as a target for therapeutic interventions.

3.6.4 Global Efficiency and Task Performance

The efficiency of neural networks involved in processing S1 did not correlate with reaction times, suggesting that network efficiency during the preparatory phase may not directly influence motor response speed. In contrast, network efficiency following S2 showed a significant correlation with reaction times in both groups, indicating that greater global efficiency during imperative stimulus processing and response execution is directly linked to faster motor responses. These findings suggest that early preparatory processes may be less critical for determining motor performance than the efficiency of later stages of stimulus processing and action execution. Overall, the results underscore the importance of temporal dynamics in neural processing for predicting behavioral performance.

Global efficiency of brain networks, particularly within the motor system, has been linked to both motor performance and symptom severity in movement disorders, with higher efficiency generally associated with better performance and reduced motor symptoms (Li et al., 2022; Novaes et al., 2021; Xiao et al., 2016). The observed correlation between network efficiency and reaction time in both groups suggests that this relationship represents a fundamental aspect of motor control. This aligns with the notion that efficient information processing across brain networks is essential for rapid and accurate motor responses. Moreover, the preserved association between network efficiency and motor performance in TS subjects suggests that core motor control processes remain intact despite the presence of tics.

3.6.5 Limitations

While our study provides valuable insights into neural network efficiency and motor performance in Tourette Syndrome, several limitations should be considered when interpreting the results. (1) Our study included a relatively small sample size, which may have reduced statistical power, potentially obscuring subtle effects or relationships. (2) While EEG provides excellent temporal resolution, its spatial resolution is limited. Complementary neuroimaging techniques, such as fMRI, could provide additional spatial information about network

dynamics. (3) Our cross-sectional design provides a developmental snapshot, but longitudinal studies are essential to capture the dynamic changes in TS over time, particularly concerning symptom persistence or remission in adulthood. This would allow for a deeper understanding of developmental trajectories and compensatory mechanisms in TS.

3.7 Conclusion

TS patients exhibit reduced theta connectivity and network efficiency during the processing of the informative warning cue (S1), indicating disruptions in sensorimotor integration. The widespread deviations across all investigated brain regions suggest that network alterations in TS extend beyond the traditional cortico-striato-thalamo-cortical circuits, reflecting a more extensive reorganization of brain dynamics. Notably, the reduced connectivity during S1 processing may represent a compensatory mechanism aimed at weakening perception-action binding, potentially preventing premature motor output and aiding in tic control. During imperative stimulus (S2) processing, TS patients showed increased functional coupling within the SMA and premotor areas during late motor preparation and execution, aligning with prior research identifying these regions as central to tic generation and control. Importantly, TS patients demonstrated comparable network efficiency during S2 processing and preserved motor performance, supporting the view that basic motor execution mechanisms remain largely intact in TS. These findings underscore the complex neural network dysfunctions underlying TS, particularly in task-related processing and sensorimotor integration. Altered theta connectivity patterns may reflect compensatory adaptations or fundamental differences in how individuals with TS process and integrate sensory information.

3.8 Data and Code Availability

The code used for data analysis is available at https://github.com/JuliSchmidgen/rPLV-Connectivity-Analysis, to allow readers to review and revise the code. Due to ethical considerations, the data supporting the findings of this study are available upon reasonable request from the corresponding author. The data cannot be used with the code for reproduction of results until they are made available, which will be subject to ethical guidelines. Any requests for data access will be processed in accordance with the relevant procedures, including formal data-sharing agreements or approval from the appropriate ethics committee.

3.9 Funding

This work was funded by the Deutsche Forschungsgemeinschaft (DFG, German Research Foundation) – SFB 1451 – Project-ID 431549029.

3.10 References

Achterberg, M., van Duijvenvoorde, A. C. K., van, I. M. H., Bakermans-Kranenburg, M. J., & Crone, E. A. (2020). Longitudinal changes in DLPFC activation during childhood are related to decreased aggression following social rejection. *Proc Natl Acad Sci U S A*, *117*(15), 8602-8610. https://doi.org/10.1073/pnas.1915124117

Adelhöfer, N., Paulus, T., Mückschel, M., Bäumer, T., Bluschke, A., Takacs, A., Tóth-Fáber, E., Tárnok, Z., Roessner, V., & Weissbach, A. (2021). Increased scale-free and aperiodic neural activity during sensorimotor integration—a novel facet in Tourette syndrome. *Brain Communications*, *3*(4), fcab250.

Ahangama, T., Gurunayake, G., Yalpathwala, I., Wijayakulasooriya, J., Dassanayake, T., Harischandra, N., Kim, K., & Ranaweera, R. (2023). EEG-Based Frequency Domain Separation of Upward and Downward Movements of the Upper Limb. *medRxiv*, 2023.2012. 2011.23299840.

Albin, R. L. (2018). Tourette syndrome: a disorder of the social decision-making network. *Brain*, *141*(2), 332-347. https://doi.org/10.1093/brain/awx204

Atkinson-Clement, C., Sofia, F., Fernandez-Egea, E., de Liege, A., Beranger, B., Klein, Y., Deniau, E., Roze, E., Hartmann, A., & Worbe, Y. (2020). Structural and functional abnormalities within sensori-motor and limbic networks underpin intermittent explosive symptoms in Tourette disorder. *Journal of Psychiatric Research*, *125*, 1-6.

Beste, C., & Münchau, A. (2018). Tics and Tourette syndrome—surplus of actions rather than disorder? *Movement Disorders*, *33*(2), 238-242.

Beste, C., Münchau, A., & Frings, C. (2023). Towards a systematization of brain oscillatory activity in actions. *Communications Biology*, *6*(1), 137. https://doi.org/10.1038/s42003-023-04531-9

Biswal, B., Ulmer, J. L., Krippendorf, R. L., Harsch, H. H., Daniels, D. L., Hyde, J. S., & Haughton, V. M. (1998). Abnormal cerebral activation associated with a motor task in Tourette syndrome. *American Journal of Neuroradiology*, *19*(8), 1509-1512.

Bloch, M. H., Peterson, B. S., Scahill, L., Otka, J., Katsovich, L., Zhang, H., & Leckman, J. F. (2006). Adulthood outcome of tic and obsessive-compulsive symptom severity in children with Tourette syndrome. *Archives of pediatrics & adolescent medicine*, *160*(1), 65-69.

Boutonnet, B., Dering, B., Viñas-Guasch, N., & Thierry, G. (2013). Seeing objects through the language glass. *Journal of Cognitive Neuroscience*, *25*(10), 1702-1710.

Brookshire, B. L., Butler, I. J., Ewing-Cobbs, L., & Fletcher, J. M. (1994). Neuropsychological characteristics of children with Tourette syndrome: evidence for a nonverbal learning disability. *Journal of clinical and experimental neuropsychology*, *16*(2), 289-302.

Buehlmann, A., & Deco, G. (2010). Optimal information transfer in the cortex through synchronization. *PLoS computational biology*, *6*(9), e1000934.

Castellano, M., Plöchl, M., Vicente, R., & Pipa, G. (2014). Neuronal oscillations form parietal/frontal networks during contour integration. *Frontiers in integrative neuroscience*, *8*, 64.

Church, J. A., Fair, D. A., Dosenbach, N. U., Cohen, A. L., Miezin, F. M., Petersen, S. E., & Schlaggar, B. L. (2009). Control networks in paediatric Tourette syndrome show immature and anomalous patterns of functional connectivity. *Brain*, *132*(Pt 1), 225-238. https://doi.org/10.1093/brain/awn223

Cravedi, E., Deniau, E., Giannitelli, M., Xavier, J., Hartmann, A., & Cohen, D. (2017). Tourette syndrome and other neurodevelopmental disorders: a comprehensive review. *Child Adolesc Psychiatry Ment Health*, *11*, 59. https://doi.org/10.1186/s13034-017-0196-x

Cruikshank, L. C., Singhal, A., Hueppelsheuser, M., & Caplan, J. B. (2012). Theta oscillations reflect a putative neural mechanism for human sensorimotor integration. *Journal of neurophysiology*, *107*(1), 65-77.

Delorme, C., Salvador, A., Valabregue, R., Roze, E., Palminteri, S., Vidailhet, M., de Wit, S., Robbins, T., Hartmann, A., & Worbe, Y. (2016). Enhanced habit formation in Gilles de la Tourette syndrome. *Brain*, *139*(2), 605-615.

Eapen, V., Cavanna, A. E., & Robertson, M. M. (2016). Comorbidities, Social Impact, and Quality of Life in Tourette Syndrome. *Front Psychiatry*, *7*, 97. https://doi.org/10.3389/fpsyt.2016.00097

Fair, D. A., Cohen, A. L., Power, J. D., Dosenbach, N. U., Church, J. A., Miezin, F. M., Schlaggar, B. L., & Petersen, S. E. (2009). Functional brain networks develop from a "local to distributed" organization. *PLoS computational biology*, *5*(5), e1000381.

Fan, S., van den Heuvel, O. A., Cath, D. C., de Wit, S. J., Vriend, C., Veltman, D. J., & van der Werf, Y. D. (2018). Altered Functional Connectivity in Resting State Networks in Tourette's Disorder [Original Research]. *Frontiers in human neuroscience*, *12*. https://doi.org/10.3389/fnhum.2018.00363

Fattapposta, F., Restuccia, R., Colonnese, C., Labruna, L., Garreffa, G., & Bianco, F. (2005). Gilles de la Tourette syndrome and voluntary movement: a functional MRI study. *Psychiatry Research: Neuroimaging*, *138*(3), 269-272.

Fitzgerald, P. B., Maller, J. J., Hoy, K. E., Thomson, R., & Daskalakis, Z. J. (2009). Exploring the optimal site for the localization of dorsolateral prefrontal cortex in brain stimulation experiments. *Brain stimulation*, *2*(4), 234-237.

Friedrich, J., Spaleck, H., Schappert, R., Kleimaker, M., Verrel, J., Bäumer, T., Beste, C., & Münchau, A. (2021). Somatosensory perception–action binding in Tourette syndrome. *Scientific reports*, *11*(1), 13388. https://doi.org/10.1038/s41598-021-92761-4

González-Villar, A. J., Samartin-Veiga, N., Arias, M., & Carrillo-de-la-Peña, M. T. (2017). Increased neural noise and impaired brain synchronization in fibromyalgia patients during cognitive interference. *Scientific reports*, *7*(1), 5841.

Gramfort, A., Luessi, M., Larson, E., Engemann, D., Strohmeier, D., Brodbeck, C., Goj, R., Jas, M., Brooks, T., & Parkkonen, L. (2013). MEG and EEG data analysis with MNE-Python. Front. Neurosci. 7, 267. *Frontiers*.

Hampson, M., Tokoglu, F., King, R. A., Constable, R. T., & Leckman, J. F. (2009). Brain areas coactivating with motor cortex during chronic motor tics and intentional movements. *Biological psychiatry*, *65*(7), 594-599.

Hommel, B., Müsseler, J., Aschersleben, G., & Prinz, W. (2001). The theory of event coding (TEC): A framework for perception and action planning. *Behavioral and brain sciences*, *24*(5), 849-878.

Horwitz, B. (2003). The elusive concept of brain connectivity. *Neuroimage*, *19*(2), 466-470.

Houghton, D. C., Capriotti, M. R., Conelea, C. A., & Woods, D. W. (2014). Sensory Phenomena in Tourette Syndrome: Their Role in Symptom Formation and Treatment. *Curr Dev Disord Rep*, *1*(4), 245-251. https://doi.org/10.1007/s40474-014-0026-2

Insausti-Delgado, A., López-Larraz, E., Omedes, J., & Ramos-Murguialday, A. (2021). Intensity and dose of neuromuscular electrical stimulation influence sensorimotor cortical excitability. *Frontiers in Neuroscience*, *14*, 593360.

Jas, M., Engemann, D. A., Bekhti, Y., Raimondo, F., & Gramfort, A. (2017). Autoreject: Automated artifact rejection for MEG and EEG data. *Neuroimage*, *159*, 417-429.

Jessy, P. (2009). Analysis of eeg signals for eeg-based brain-computer interface. In.

Kaneko, N., Wada, M., Nakajima, S., Takano, M., Taniguchi, K., Honda, S., Mimura, M., & Noda, Y. (2024). Neuroplasticity of the left dorsolateral prefrontal cortex in patients with treatment-resistant depression as indexed with paired associative stimulation: a TMS–EEG study. *Cerebral Cortex*, *34*(2), bhad515.

Kim, B.-M., Lee, J., Choi, A. R., Chung, S. J., Park, M., Koo, J. W., Kang, U. G., & Choi, J.-S. (2021). Event-related brain response to visual cues in individuals with Internet gaming disorder: relevance to attentional bias and decision-making. *Translational Psychiatry*, *11*(1), 258.

Kleimaker, A., Kleimaker, M., Bäumer, T., Beste, C., & Münchau, A. (2020). Gilles de la Tourette syndrome—A disorder of action-perception integration. *Frontiers in Neurology*, *11*, 597898.

Kumar, A., Trescher, W., & Byler, D. (2016). Tourette Syndrome and Comorbid Neuropsychiatric Conditions. *Curr Dev Disord Rep*, *3*(4), 217-221. https://doi.org/10.1007/s40474-016-0099-1

Lachaux, J. P., Rodriguez, E., Martinerie, J., & Varela, F. J. (1999). Measuring phase synchrony in brain signals. *Human brain mapping*, *8*(4), 194-208.

Le, K., Liu, L., Sun, M., Hu, L., & Xiao, N. (2013). Transcranial magnetic stimulation at 1 Hertz improves clinical symptoms in children with Tourette syndrome for at least 6 months. *Journal of Clinical Neuroscience*, *20*(2), 257-262.

Leckman, J. F., King, R. A., & Bloch, M. H. (2014). Clinical Features of Tourette Syndrome and Tic Disorders. *J Obsessive Compuls Relat Disord*, *3*(4), 372-379. https://doi.org/10.1016/j.jocrd.2014.03.004

Li, X., Geng, J., Du, X., Si, H., & Wang, Z. (2022). Relationship between the practice of tai chi for more than 6 months with mental health and brain in university students: an exploratory study. *Frontiers in human neuroscience*, *16*, 912276.

Lin, H., Schulz, C., & Straube, T. (2015). Cognitive tasks during expectation affect the congruency ERP effects to facial expressions. *Frontiers in human neuroscience*, *9*, 596.

Lisman, J. E., & Jensen, O. (2013). The theta-gamma neural code. *Neuron*, *77*(6), 1002-1016.

Loo, S. K., Miyakoshi, M., Tung, K., Lloyd, E., Salgari, G., Dillon, A., Chang, S., Piacentini, J., & Makeig, S. (2019). Neural activation and connectivity during cued eye blinks in Chronic Tic Disorders. *NeuroImage: Clinical*, *24*, 101956.

Madl, T., Baars, B. J., & Franklin, S. (2011). The timing of the cognitive cycle. *PLoS One*, *6*(4), e14803. https://doi.org/10.1371/journal.pone.0014803

Makeig, S., Westerfield, M., Jung, T.-P., Enghoff, S., Townsend, J., Courchesne, E., & Sejnowski, T. J. (2002). Dynamic Brain Sources of Visual Evoked Responses. *Science*, *295*(5555), 690-694. https://doi.org/doi:10.1126/science.1066168

Mantovani, A., Leckman, J. F., Grantz, H., King, R. A., Sporn, A. L., & Lisanby, S. H. (2007). Repetitive transcranial magnetic stimulation of the supplementary motor area in the treatment of Tourette syndrome: report of two cases. *Clinical neurophysiology: official journal of the International Federation of Clinical Neurophysiology*, *118*(10), 2314-2315.

Marsh, R., Zhu, H., Wang, Z., Skudlarski, P., & Peterson, B. S. (2007). A developmental fMRI study of self-regulatory control in Tourette's syndrome. *American Journal of Psychiatry*, *164*(6), 955-966.

Mielke, E., Takacs, A., Kleimaker, M., Schappert, R., Conte, G., Onken, R., Künemund, T., Verrel, J., Bäumer, T., Beste, C., & Münchau, A. (2021). Tourette syndrome as a motor disorder revisited - Evidence from action coding. *Neuroimage Clin*, *30*, 102611. https://doi.org/10.1016/j.nicl.2021.102611

Mizuhara, H., Wang, L. Q., Kobayashi, K., & Yamaguchi, Y. (2004). A long-range cortical network emerging with theta oscillation in a mental task. *Neuroreport*, *15*(8), 1233-1238. https://doi.org/10.1097/01.wnr.0000126755.09715.b3

Morand-Beaulieu, S., O'Connor, K. P., Sauvé, G., Blanchet, P. J., & Lavoie, M. E. (2015). Cognitive-behavioral therapy induces sensorimotor and specific electrocortical changes in chronic tic and Tourette's disorder. *Neuropsychologia*, *79*, 310-321. https://doi.org/https://doi.org/10.1016/j.neuropsychologia.2015.05.024

Neuner, I., Werner, C. J., Arrubla, J., Stöcker, T., Ehlen, C., Wegener, H. P., Schneider, F., & Shah, N. J. (2014). Imaging the where and when of tic generation and resting state networks in adult Tourette patients [Original Research]. *Frontiers in human neuroscience*, *8*. https://doi.org/10.3389/fnhum.2014.00362

Novaes, N. P., Balardin, J. B., Hirata, F. C., Melo, L., Amaro Jr, E., Barbosa, E. R., Sato, J. R., & Cardoso, E. F. (2021). Global efficiency of the motor network is decreased in Parkinson's disease in comparison with essential tremor and healthy controls. *Brain and Behavior*, *11*(8), e02178.

Nunez, P. L., & Srinivasan, R. (2006). *Electric fields of the brain: the neurophysics of EEG*. Oxford University Press, USA.

Oldfield, R. (1971). Edinburgh handedness inventory. *Journal of Abnormal Psychology*.

Petruo, V., Bodmer, B., Brandt, V. C., Baumung, L., Roessner, V., Münchau, A., & Beste, C. (2019). Altered perception-action binding modulates inhibitory control in Gilles de la Tourette syndrome. *Journal of Child Psychology and Psychiatry*, *60*(9), 953-962.

Pouryazdian, S., & Erfanian, A. (2009). Detection of steady-state visual evoked potentials for brain-computer interfaces using PCA and high-order statistics. World Congress on Medical Physics and Biomedical Engineering, September 7-12, 2009, Munich, Germany: Vol. 25/9 Neuroengineering, Neural Systems, Rehabilitation and Prosthetics,

Puzzo, I., Cooper, N. R., Vetter, P., & Russo, R. (2010). EEG activation differences in the pre-motor cortex and supplementary motor area between normal individuals with high and low traits of autism. *Brain research*, *1342*, 104-110.

Ricketts, E. J., Woods, D. W., Espil, F. M., McGuire, J. F., Stiede, J. T., Schild, J., Yadegar, M., Bennett, S. M., Specht, M. W., Chang, S., Scahill, L., Wilhelm, S., Peterson, A. L., Walkup, J. T., & Piacentini, J. (2022). Childhood Predictors of Long-Term Tic Severity and Tic Impairment in Tourette's Disorder. *Behav Ther*, *53*(6), 1250-1264. https://doi.org/10.1016/j.beth.2022.07.002

Rosjat, N., & Daun, S. (2022). DST (Dynamic Synchronization Toolbox): a MATLAB implementation of the dynamic phase-locking pipeline from stimulus transformation into motor action: Dynamic graph analysis reveals a posterior-to-anterior shift in brain network communication of older subjects. *Journal of Open Research Software*, *10*(1).

Rothenberger, A., & Kemmerling, S. (1982). Bereitschaftspotential in children with multiple tics and Gilles de la Tourette syndrome. *Dev Neurol*, *6*, 257-270.

SanMiguel, I., Morgan, H. M., Klein, C., Linden, D., & Escera, C. (2010). On the functional significance of Novelty-P3: facilitation by unexpected novel sounds. *Biological Psychology*, *83*(2), 143-152.

Santhana Gopalan, P. R., Loberg, O., Hämäläinen, J. A., & Leppänen, P. H. (2019). Attentional processes in typically developing children as revealed using brain event-related potentials and their source localization in Attention Network Test. *Scientific reports*, *9*(1), 2940.

Schmidgen, J., Konrad, K., Roessner, V., & Bender, S. (2023). The external evocation and movement-related modulation of motor cortex inhibition in children and adolescents with Tourette syndrome–a TMS/EEG study. *Frontiers in Neuroscience*, *17*.

Schultz, R. T., Carter, A. S., Gladstone, M., Scahill, L., Leckman, J. F., Peterson, B. S., Zhang, H., Cohen, D. J., & Pauls, D. (1998). Visual–motor integration functioning in children with Tourette syndrome. *Neuropsychology*, *12*(1), 134.

Shephard, E., Groom, M. J., & Jackson, G. M. (2019). Implicit sequence learning in young people with Tourette syndrome with and without co-occurring attention-deficit/hyperactivity disorder. *Journal of Neuropsychology*, *13*(3), 529-549.

Singer, H. S. (2016). Habitual and goal-directed behaviours and Tourette syndrome. *Brain*, *139*(2), 312-316.

Steinbeis, N., Haushofer, J., Fehr, E., & Singer, T. (2014). Development of Behavioral Control and Associated vmPFC–DLPFC Connectivity Explains Children's Increased Resistance to Temptation in Intertemporal Choice. *Cerebral Cortex*, *26*(1), 32-42. https://doi.org/10.1093/cercor/bhu167

Sun, Y., Wei, H., Lin, Y., & Wang, Y. (2020). The suppressive effect of the motor system on the sensory system in patients with Tourette syndrome. *Frontiers in Neurology*, *11*, 855.

Takács, Á., Kobor, A., Chezan, J., Éltető, N., Tárnok, Z., Nemeth, D., Ullman, M. T., & Janacsek, K. (2018). Is procedural memory enhanced in Tourette syndrome? Evidence from a sequence learning task. *Cortex*, *100*, 84-94.

Takacs, A., Toth-Faber, E., Schubert, L., Tárnok, Z., Ghorbani, F., Trelenberg, M., Nemeth, D., Münchau, A., & Beste, C. (2024). Resting network architecture of theta oscillations reflects hyper-learning of sensorimotor information in Gilles de la Tourette syndrome. *Brain Communications*, *6*(2), fcae092.

Tan, E., Troller-Renfree, S. V., Morales, S., Buzzell, G. A., McSweeney, M., Antúnez, M., & Fox, N. A. (2024). Theta activity and cognitive functioning: Integrating evidence from resting-state and task-related developmental electroencephalography (EEG) research. *Dev Cogn Neurosci*, *67*, 101404. https://doi.org/10.1016/j.dcn.2024.101404

Tenke, C. E., & Kayser, J. (2012). Generator localization by current source density (CSD): implications of volume conduction and field closure at intracranial and scalp resolutions. *Clinical Neurophysiology*, *123*(12), 2328-2345.

Tomassini, A., Ambrogioni, L., Medendorp, W. P., & Maris, E. (2017). Theta oscillations locked to intended actions rhythmically modulate perception. *eLife*, *6*, e25618. https://doi.org/10.7554/eLife.25618

Uddin, L. Q., Supekar, K. S., Ryali, S., & Menon, V. (2011). Dynamic reconfiguration of structural and functional connectivity across core neurocognitive brain networks with development. *Journal of Neuroscience*, *31*(50), 18578-18589.

van Woerkom, T. C. A. M., Roos, R. A. C., & van Dijk, J. G. (1994). Altered attentional processing of background stimuli in Gilles de la Tourette syndrome: a study in auditory event-related potentials evoked in an oddball paradigm. *Acta Neurologica Scandinavica*, *90*(2), 116-123. https://doi.org/https://doi.org/10.1111/j.1600-0404.1994.tb02690.x

Von Stein, A., & Sarnthein, J. (2000). Different frequencies for different scales of cortical integration: from local gamma to long range alpha/theta synchronization. *International journal of psychophysiology*, *38*(3), 301-313.

Voytek, B., Kramer, M. A., Case, J., Lepage, K. Q., Tempesta, Z. R., Knight, R. T., & Gazzaley, A. (2015). Age-related changes in 1/f neural electrophysiological noise. *Journal of Neuroscience*, *35*(38), 13257-13265.

Wang, J., Yue, J., Wang, Y., Li, X. L., Deng, X. P., Lou, Y. T., Gao, L. Y., Chen, X. Q., Su, Q. Y., Zang, Y. F., & Feng, J. H. (2025). Function-Specific Localization in the Supplementary Motor Area: A Potential Effective Target for Tourette Syndrome. *CNS Neurosci Ther*, *31*(2), e70280. https://doi.org/10.1111/cns.70280

Wendiggensen, P., Prochnow, A., Pscherer, C., Münchau, A., Frings, C., & Beste, C. (2023). Interplay between alpha and theta band activity enables management of perception-action representations for goal-directed behavior. *Communications Biology*, *6*(1), 494. https://doi.org/10.1038/s42003-023-04878-z

Wu, S. W., Maloney, T., Gilbert, D. L., Dixon, S. G., Horn, P. S., Huddleston, D. A., Eaton, K., & Vannest, J. (2014). Functional MRI-navigated repetitive transcranial magnetic

stimulation over supplementary motor area in chronic tic disorders. *Brain stimulation*, *7*(2), 212-218.

Wylie, S. A., Claassen, D. O., Kanoff, K. E., van Wouwe, N. C., & van den Wildenberg, W. P. (2016). Stopping manual and vocal actions in Tourette's syndrome. *The Journal of Neuropsychiatry and Clinical Neurosciences*, *28*(4), 306-311.

Xiao, M., Ge, H., Khundrakpam, B. S., Xu, J., Bezgin, G., Leng, Y., Zhao, L., Tang, Y., Ge, X., & Jeon, S. (2016). Attention performance measured by attention network test is correlated with global and regional efficiency of structural brain networks. *Frontiers in Behavioral Neuroscience*, *10*, 194.

Yael, D., Vinner, E., & Bar-Gad, I. (2015). Pathophysiology of tic disorders. *Movement Disorders*, *30*(9), 1171-1178.

Yuan, H., Perdoni, C., & He, B. (2010). Relationship between speed and EEG activity during imagined and executed hand movements. *Journal of neural engineering*, *7*(2), 026001.

Zarka, D., Leroy, A., Cebolla, A. M., Cevallos, C., Palmero-Soler, E., & Cheron, G. (2021). Neural generators involved in visual cue processing in children with attention-deficit/hyperactivity disorder (ADHD). *European Journal of Neuroscience*, *53*(4), 1207-1224.

4 Study 3: fMRI Connectivity in TS and Controls

Motor Network Organisation in Healthy Development and Chronic Tic Disorders

Theresa Heinen*, **Julia Schmidgen**, Theresa Paul, Lukas Hensel, Gereon R. Fink, Lukas Volz, Christian Grefkes, Stephan Bender, Kerstin Konrad

This work is under review at *Brain Communications*

Building on the previous EEG-based findings, this study combines fMRI and DCM to examine effective connectivity patterns underlying both typical maturation and compensatory adaptations in TS. Using the advantage of high spatial resolution fMRI, this analysis directly compares the organization of functional brain networks in healthy children and those with TS, using data collected within the same overarching study to ensure methodological consistency. To accommodate the strengths of fMRI and address the limitations of the CNV paradigm for this modality, participants completed a simple reaction time task and an inhibition task, enabling the assessment of spatial distribution and interaction among motor and sensorimotor regions.

The results reveal that typically developing children exhibit progressive refinement of parietal and premotor connectivity, whereas children with TS engage alternative, compensatory pathways to maintain motor performance. By integrating hemodynamic measures with prior electrophysiological insights, this study provides a comprehensive view of both the temporal and spatial aspects of neural connectivity. This multimodal approach is crucial for capturing the complexity of motor network development and increasing the systems-level understanding of neurodevelopmental reorganization in TS.

4.1 Contribution

As the second author, I contributed to the design of the study, acquisition of data, interpretation of the results, and the critical revision of the manuscript.

4.2 Abstract

Tic Disorders (TD) are childhood-onset neurodevelopmental disorders characterised by sudden, repetitive motor and vocal tics, often with partial or complete remission by the time young adulthood is reached.

We here investigated motor control and compensatory neural processes in drug-naïve children and adolescents with chronic Motor Tic Disorder or Tourette Syndrome (TD) by examining motor network activity and connectivity compared to healthy controls. Using a reaction time (RT) task under varying cueing conditions, combined with functional magnetic resonance imaging (fMRI) and Dynamic Causal Modelling (DCM), we explored how TD-related motor networks adapt to support volitional movement control.

Participants with TD demonstrated enhanced task accuracy across internally and externally cued conditions despite deficits in sustained motor inhibition (blink suppression). Relative to controls, individuals with TD exhibited increased task-related activation in ipsilateral motor regions, particularly in the primary motor cortex, and somatosensory cortex, and enhanced interhemispheric connectivity between parietal sensory-motor hubs. Notably, while in typically developing participants, age-related increases in parietal lobe activation and modulatory connectivity between primary motor and premotor regions were linked to improved task accuracy, working memory, and visuomotor coordination, TD patients deviated from this normative developmental trajectory with distinct, atypical but neither delayed nor accelerated neural activation and connectivity patterns.

Our data suggest that TD involves compensatory neuroplastic adaptations that leverage additional sensorimotor resources to improve motor control but do not extend to motor inhibition processes. Moreover, the findings emphasise the intricate interplay between motor control and neural plasticity in TD, highlighting how compensatory mechanisms may serve as adaptive responses to motor challenges. These findings open avenues for therapeutic strategies that harness the brain's compensatory capacities to enhance motor control and facilitate TD management.

4.3 Introduction

Tic Disorders (TD) are childhood-onset movement disorders characterised by sudden, recurrent movements or vocalisations. These tics typically emerge during childhood, peaking between 9 and 11 years, with many children experiencing partial or complete remission as they approach early adulthood (Black et al., 2016; Cohen et al., 2013; Müller-Vahl, 2015). TD are considered to encompass a spectrum of interconnected conditions, including Tourette Syndrome (TS) and chronic Motor Tic Disorder, with TS generally regarded as the more severe

manifestation. However, both are recognised as expressions of a unified disease entity (Spencer et al., 1995; Tourette Association of America, 2017). While spontaneous remission of TD is common, the underlying mechanisms remain poorly understood (Cohen et al., 2013; Knight et al., 2012).

Recent research highlights the cortico-striatal-thalamo-cortical (CSTC) circuitry as a primary contributor to tic generation, proposing that disorganised network connectivity may result in disinhibition, leading to motor cortex hyperexcitability (Debes et al., 2017; Franzkowiak et al., 2012; Heise et al., 2010; Jackson et al., 2015; Mink, 2003; Rae & Critchley, 2022; Worbe et al., 2015). Two competing hypotheses have been put forward to explain tic discontinuation: (1) development of neuroplastic compensatory mechanisms in frontal and motor networks that adaptively enhance motor control over time (Jackson et al., 2011; Mueller et al., 2006; Plessen et al., 2009) and (2) delayed neurodevelopmental normalisation of CSTC circuits (Church et al., 2009; Pépés et al., 2016). Notably, these hypotheses imply distinct pathways and developmental trajectories for motor network organisation underlying motor control in TD, which remain to be explored.

Previous research reported inconclusive findings regarding voluntary motor control in TD. Studies in adults often revealed deficits in reflex inhibition and motor set selection or switching; (Channon et al., 2009; Dursun et al., 2000; Fan et al., 2018; Ganos et al., 2014; Georgiou et al., 1995; Rae et al., 2020; Rawji et al., 2020; Thomalla et al., 2014) (but see also references (Fan et al., 2018; Ganos et al., 2014; Rae et al., 2020; Rawji et al., 2020) for divergent findings). In contrast, research on paediatric patients typically found no significant deficits (Draper et al., 2014; Jackson et al., 2013; Jung et al., 2013; Jurgiel et al., 2021; Marsh et al., 2007; Openneer et al., 2021; Raz et al., 2009; Roessner et al., 2008; Schmidgen et al., 2023; Serrien et al., 2005) or even better motor performance (Jackson et al., 2007; Jung et al., 2015; Mueller et al., 2006). Further, neuroimaging studies stress divergent findings between children and adults with TD about brain structure, activation patterns, and connectivity (Gerard & Peterson, 2003; Nielsen et al., 2020; Pépés et al., 2016; Plessen et al., 2004).

Although voluntary motor performance of younger TD patients often resembles that of healthy controls, it remains unclear whether comparable behaviour results from similar physiological motor control or rather reflects successful neural adaptations in these TD patients. Notably, the distinction between compensatory and dysfunctional adaptations has significant clinical

implications. While compensatory mechanisms may support motor development, dysfunctional changes might perpetuate tics or impair broader motor control. Thus, clarifying these relationships is critical for understanding pathophysiological processes in TD and tailoring novel therapeutic interventions. For example, compensatory mechanisms that improve motor network development might be leveraged for therapeutic purposes, while identifying maladaptive processes could inform strategies to prevent long-term deficits. Of note, while adult TD patients often have a long-standing history of pharmacological treatments - including anti-dopaminergic drugs, central adrenergic inhibitors, SSRIs, or anti-epileptic medications - that can influence brain network development and organisation, paediatric drug-naïve patients offer a unique opportunity to examine 'natural' neural network adaptation. In children, compensatory processes appear to involve heightened activity in frontal motor control regions, such as the prefrontal cortex (PFC) and supplementary motor area (SMA), with additional recruitment of ipsilateral motor areas (Baym et al., 2008; Debes et al., 2017; Eichele & Plessen, 2013; Jackson et al., 2011; Marsh et al., 2007; Polyanska et al., 2017; Roessner et al., 2013; Roessner et al., 2012). These findings suggest that motor performance in paediatric TD is supported by active reorganisation of motor networks. However, whether these patterns reflect accelerated maturation or deviant development remains unclear (Church et al., 2009; Debes et al., 2015; Eichele et al., 2017; Greene et al., 2017; Makki et al., 2009; Marsh et al., 2007; Neuner et al., 2010; Nielsen et al., 2020; Pépés et al., 2016; Plessen et al., 2009; Plessen et al., 2004). Understanding how brain motor networks (re-)organise during typical development and comparing paediatric TD patients to age-matched healthy controls could provide a developmental framework essential for identifying TD-specific adaptations and clarifying the pathophysiological processes underlying TD.

The current study addresses the gaps mentioned above by investigating neural alterations in paediatric drug-naïve TD and their associations with motor control. We integrated findings from age-matched healthy controls and a large cohort of typically developing children to contextualise TD-specific patterns within normative development. Using functional MRI (fMRI) and Dynamic Causal Modelling (DCM), we examined neural activity and effective connectivity during reactive, goal-oriented movements assessed through a reaction time (RT) task. Behavioural measures of inhibitory control, evaluated using a blink-suppression paradigm, complemented the analyses.

We hypothesised that (i) motor performance in drug-naïve TD patients resembles or surpasses that of healthy controls, reflecting compensatory mechanisms; (ii) compensatory processes manifest as increased activation in motor regions and enhanced effective connectivity, particularly in frontal networks; and (iii) these neural patterns align with either normative developmental changes (accelerated maturation) or deviant adaptations specific to TD. Further elucidating these mechanisms may provide the foundation for targeted therapeutic approaches that harness beneficial compensatory changes and prevent maladaptive processes.

4.4 Materials and methods

4.4.1 Participants

The study involved 55 typically developing children and adolescents aged 5–17 years (M_{age} = 10.9, SD = 3.1, 46% male) and 21 never medicated patients aged 7–16 years (M_{age} = 10.2, SD = 2.3, 76% male), meeting DSM-V criteria for chronic Motor Tic Disorder (CTD; N = 2) or Tourette Syndrome (TS; N = 19). Table 1 provides an overview of the demographic and psychometric characteristics of the patient group and matched control sample included in the comparative behavioural analysis. Behavioural analyses of healthy subjects alone included sample sizes of N = 52 (task condition 'Internal') and N = 55 (task condition 'External'), while fMRI analyses excluded some patients ($N_{Internal}$ = 7; $N_{External}$ = 9) and controls ($N_{Internal}$ = 7; $N_{External}$ = 12) due to excessive head motion. Further exclusions for DCM analysis occurred due to insufficient voxel response in ipsilateral regions of interest ($N_{patients}$ = 2; $N_{controls}$ = 19). Developmental samples retained broad age coverage despite motion-related exclusions, which were more common in younger participants. Detailed sample sizes for each paradigm and analysis type are provided in Supplementary Table 1; age distributions across developmental samples are summarised in Supplementary Table 2. Group comparability between patients and matched controls was ensured for all analyses through statistical comparisons of demographic and psychometric variables across subsamples. Exclusion criteria were (i) full-scale IQ < 70 (ii) history of epilepsy or other central nervous system (CNS) disorders, (iii) significant premature birth (≤ 31 weeks), (iv) non-correctable visual impairments, (v) any contraindications to the MRI or (vi) current or previous use of psychoactive drugs (except for history of stimulant medication (n=1)). The Ethics Committee of the Medical Faculty, University Hospital Cologne approved the study, which adhered to the Declaration of Helsinki.

Participants and parents provided informed assent and consent, respectively, and subjects received financial compensation.

Table 1. *Demographic and psychometric characteristics of the patient and matched control sample*

Sample Characteristics	Controls (N = 20)	TS (N = 21)	Statistic	p
Age (M ± SD; range)	9.8 (± 2.3; 6 - 15)	10.2 (± 2.3; 7 - 16)	t (39) = .473	.639
Male gender [n (%)]	15 (75)	16 (76)	x^2 (1) = .008	.929
Right handedness [n (%)]	19 (95)	20 (95)	x^2 (1) = .001	.972
IQ (M ± SD)	110.8 (± 13.5)	108.1 (± 14.9)	t (39) = -.598	.553
Working memory Index (WMI) (M ± SD)	11.9 (± 2.6)	11.7 (± 3.2)	t (37) = -.185	.854
Processing speed Index (PSI) (M ± SD)	10.1 (± 1.9)	10.0 (± 3.0)	t (36) = -.070	.944
DIKJ total symptom score (M ± SD)	8.9 (± 4.8)	8.2 (± 5.5)	t (37) = -.481	.633
YGTSS total symptom score (M ± SD)		32 (± 14.0)		
Age at tic onset (M ± SD)		4.9 (± 1.8)		
Duration of tics [years (M ± SD; range)]		5.0 (± 2.5; 1-9)		
Tourette Syndrome [n (%)]		19 (90)		
Comorbid ADHD [n (%)]		5 (24)		

Note. Handedness as assessed by the Edinburgh Handedness Scale. General IQ based on Wechsler Intelligence Scale for Children - 5th Edition (WISC-V). Working memory, as assessed by Digit Span subtest (Scaled Scores/ or Raw scores). Processing speed (i.e., visuomotor coordination (VMC)), as assessed by Coding subtest (Scaled Scores/ or Raw scores). DIKJ = revised German version of Children's Depression Inventory (CDI). YGTSS = Yale Global Tic Severity Scale. M = Mean; SD = Standard deviation. Statistical comparisons of demographic and psychometric variables were conducted across all subsamples. No significant differences were found between groups in any of these characteristics.

4.4.2 Measures

A structured clinical interview (Kinder-DIPS) was conducted with all parents and adolescents (aged ≥ 12 years), ensuring diagnostic criteria in patients and the absence of any neuropsychiatric symptoms in healthy controls. The interview is widely used in German-speaking clinical research and shows high interrater reliability (k = 0.78–0.95, depending on diagnostic category) for DSM-V-based psychiatric disorders (Margraf et al., 2017; Schneider et al., 2018). Full-scale IQ was assessed using the German adaptation of the Wechsler Intelligence Scale for Children – Fifth Edition (WISC-V), which shows excellent internal consistency ($\alpha = 0.96$) and high convergent validity with other standard intelligence tests for children and adolescents (e.g., WPPSI-III: r = 0.89; KABC-II: r = 0.83). In addition to full-scale IQ, we extracted a Working Memory Index (Digit Span) and a Processing Speed Index (Coding), the latter reflecting visuomotor coordination (VMC) (Wechsler, 2017). Tic severity was assessed using the Yale Global Tic Severity Scale (YGTSS), a clinician-rated instrument evaluating motor and vocal tics and their associated impairment (Leckman et al., 1989; Storch et al., 2005). Depressive symptoms were measured using the revised German version of the Children's Depression Inventory (DIKJ) (Stiensmeier-Pelster et al., 2014). Handedness was assessed with the Edinburgh Handedness Inventory (Oldfield, 1971).

4.4.3 fMRI Paradigm

We aimed to investigate network-level mechanisms of voluntary motor control using a reaction time paradigm previously employed to study movement preparation, selection, and initiation in healthy adults and neuropsychiatric conditions (Hoffstaedter et al., 2013; Michely et al., 2012; Michely et al., 2015; Michely et al., 2018). To accommodate young children, the original blocked design was modified into an event-related format with two conditions presented separately (in randomised order). In the 'Internal' condition (Fig. 1A), subjects were instructed to press either of two buttons as soon as possible following the appearance of a non-informative

target-stimulus (Sherriff). In this condition, subjects were free about the lateralisation of their movement (left or right) but were restricted concerning response timing. In the 'External' condition (see Fig. 1B), participants were instructed to press the button on the side indicated by an arrow as quickly as possible. Both conditions ended after the participants completed 25 left- and right-handed button presses respectively. Task stimuli were generated using the software package *Presentation* (Version 10.3, Neurobehavioral Systems Inc., Albany, CA), projected onto a screen at the rear of the scanner bore, and viewed during image acquisition via an individually adjusted mirror mounted on the head coil.

4.4.4 Blink-Suppression Paradigm

We assessed inhibitory control via a blink-suppression task consisting of six 36-second blocks (three "suppress" and three "release" blocks). Participants suppressed eye-blinks or blinked freely while viewing videoclips of blinking individuals, with task instructions cued by a traffic light signal. Blinks were video recorded and analysed for suppression efficacy using the Behavioural Observation Research Interactive Software (BORIS) (Friard & Gamba, 2016). The number of blinks occurring during the task was counted by two independent raters, with excellent interrater reliability (ICC = 0.93; 95% CI: 0.87–0.97; $P < 0.001$).

4.4.5 Statistical Analysis of Behavioural Data

Reaction times (RTs) and task accuracy were analysed as behavioural measures derived from the fMRI paradigm. RT was defined as the latency between stimulus onset and button press; accuracy reflected the percentage of correct responses per condition. Across all trials, RTs below 150 ms, exceeding 2000 ms and outliers beyond three standard deviations (SD) from individual averages per condition were excluded (Michely et al., 2015). Blink suppression, derived from the blink-suppression paradigm, was quantified as the difference between blink counts in suppression and release conditions, normalised as a percentage reduction.

To study the development of motor network functions, we explored the relationship between age (mean-centred) and fMRI task measures (RT, accuracy) using regression analyses, including linear, quadratic, and cubic models within the healthy sample. Group differences between TD patients and age-matched healthy controls were calculated using independent-samples t-test or, in cases of non-normality (assessed via Shapiro-Wilk tests and histogram inspection), non-parametric Mann-Whitney-U tests. This approach was chosen due to the

matched between-group design with relatively small group sizes, which limited the use of covariate-adjusted regression models. For more details, see supplementary material.

4.4.6 fMRI Data Acquisition and Analyses

Participants were trained in a mock-scanner before the scanning session to minimize movement artifacts. They received feedback on head motion while practising the fMRI paradigms in a realistic setting. Additionally, participants' heads were fixated using foam pads surrounding the head.

MRI scans were performed on a 3-Tesla Siemens MAGNETOM Prisma scanner (Siemens Healthcare, Erlangen, Germany) at Research Centre Juelich. T1-weighted structural images were acquired by a magnetisation-prepared rapid gradient echo (MP-RAGE) sequence (repetition time [T_R] = 1790 ms, echo time [T_E] = 2.53 ms, flip angle = 8°, number of slices = 176, slice thickness = 0.9 mm, interslice gap = 0.45 mm, field of view [FOV] = 256 mm, voxel size = 0.9 × 0.9 × 0.9 mm). Whole-brain T2-weighted functional images were obtained using an echoplanar imaging (EPI) multiband sequence, with blood oxygenation level-dependent (BOLD) contrast (T_R = 980 ms, T_E = 30 ms, flip angle = 70°, number of slices = 64, slice thickness = 2.0 mm, interslice gap = 0.2 mm, FOV = 207 mm, voxel size = 2.2 × 2.2 × 2.0 mm). Image pre-processing was performed using Statistical Parametric Mapping (SPM12; The Wellcome Centre for Human Neuroimaging, UCL Queen Square Institute of Neurology, London, UK [www.fil.ion.ucl.ac.uk/spm]) implemented in MATLAB (The MathWorks, Natick, USA). Pre-processing included motion correction, spatial normalisation, and smoothing with an 8 mm Gaussian kernel. Detailed pre-processing steps are described in the supplementary material. Head motion was assessed through visual inspection of motion plots generated by SPM12. Datasets with displacement exceeding one voxel (2.2 mm) or abrupt motion peaks greater than 1.1 mm were excluded, following thresholds commonly used in developmental fMRI studies (Peelen et al., 2009; Walbrin et al., 2020). Following pre-processing, all datasets were visually re-inspected to ensure pre-processing quality.

Task-related BOLD responses were modelled using the GLM framework, with contrasts capturing left- and right-handed movements (from stimulus presentation until button presses) relative to baseline. Contrast images were defined as follows: 'right-handed movements > baseline' and 'left-handed movements > baseline'. Model parameter estimates and t-statistic images were submitted to second level group analyses. Baseline task activations for these

contrasts, obtained through one-sample t-tests for patients and control subjects separately, are provided in Supplementary Tables 3–10. In healthy subjects, we examined the association between age and whole-brain activation from these contrasts using regression analysis, adding mean-centred age, mean-centred age-squared and mean-centred age cubed as covariates. Moreover, using an independent-samples t-test, we compared task-related activity from these contrasts between TD patients and healthy controls. Effects were considered significant if they exceeded a voxel-level threshold ($P< 0.001$, uncorrected), cluster-level corrected at $P_{FWE} < 0.05$.

4.4.7 Dynamic Causal Modelling (DCM)

DCM was applied to explore interhemispheric motor-network connectivity, following Michely et al., (Michely et al., 2018) who used the paradigm to examine age-related connectivity changes in healthy adults. The same regions of interest were used to assess neural interactions across developmental stages. We specified nine ROIs for the interhemispheric DCM model: 1. left PFC, 2. right PFC, 3. left PMC, 4. right PMC, 5. SMA, 6. left M1, 7. right M1, 8. left IPS, 9. right IPS. Time series were extracted from subject-specific coordinates defined in the 'External' condition. Within an 8-mm-radius sphere around the group peak coordinates, which were set as origin (see Supplementary Table 11), we located the nearest individual activation peak coordinates from each subject's first level GLM-analysis. We extracted the first eigenvariate of the individual BOLD time series. For extraction of time series, we employed a threshold of $P < 0.05$ (uncorrected). Following recommendations by Zeidman et al. (Zeidman et al., 2019) for handling cases where ROIs showed no significant voxel response at this threshold, a stepwise lowering of the threshold was conducted in steps of 0.05, until a peak was discernible. Group-level mean ROI coordinates are also reported in Supplementary Table 12.

We defined (1) the endogenous connectivity matrix (DCM-A), representing connectivity independent of task-dependent modulation; (2) external inputs to the PFC and IPS (DCM-C), assuming experimental inputs directly influencing these regions; and (3) nine models exploring alternative hypotheses about modulatory changes in interregional connectivity driven by task demands (i.e., right-handed responses, DCM-B). Random-effects Bayesian model selection (BMS) was applied to determine winning models for the developmental cohort and for the group of TD patients and age-matched controls. Winning models were established based on

posterior evidence, ensuring an optimal balance between model complexity and generalizability.

We examined the association between age (mean-centred) and coupling estimates (CE) of the winning model using regression analyses with linear, quadratic, and cubic models. Following recommendations by Dash et al., (Dash et al., 2023) we identified outliers using the interquartile range (IQR) and employed winsorising to reduce the impact of outliers in the models. Values larger than Q3 + 1.5 * IQR or smaller than Q1 – 1.5 * IQR were considered outliers. Any value above or below this cut-off was substituted with the value of that cut-off itself. To investigate differences in neural coupling between TD patients and healthy controls, CEs of the winning model were compared using independent-samples t-test and non-parametric Mann-Whitney-U test. All analyses were conducted separately for endogenous connections (DCM-A) and task-specific connectivity (DCM-B).

Explorative correlation analyses tested associations of brain network organisation and motor control. To this end, behavioural measures (RT, accuracy, working memory (WM), visuomotor coordination (VMC)) – the latter two reflecting higher-order cognitive and sensorimotor processes relevant to task performance – were related to measures of task activation (mean beta values) or CEs significantly associated with age or TD (DCM-A and DCM-B). No alpha adjustment was applied due to the exploratory nature of this analysis.

4.5 Results

4.5.1 Behavioural Task Performance

Regression analysis showed that age was significantly associated with accuracy in typically developing children and adolescents for both internally and externally cued responses. For accuracy, age displayed a positive linear association with both conditions ('External': R^2 = 0.309, B = 0.021, P < 0.001; see Fig. 1C; 'Internal': R^2 = 0.240, B = 1.401, P < 0.001; see Supplementary Fig. 1). For RTs, there was a significant cubic association between age and externally cued responses (R^2 = 0.251, B = -0.952, P < 0.001; see Fig. 1C) and a significant quadratic association with age for internally cued responses (R^2 = 0.359, B = 3.475, P < 0.001; see Supplementary Fig. 1), with RTs decreasing throughout development in both conditions.

Between-group comparisons revealed significant differences in accuracy for internal and external cues, with TD patients showing higher accuracy than age-matched controls in both

conditions. In contrast, RTs did not significantly differ between groups for either cue type. Both groups exhibited significantly longer RTs (patients: Z = -4.015, P < 0.001, r = -0.88; controls: Z = -3.385, P < 0.001, r = -0.82) and reduced accuracy (patients: Z = 2.739, P = 0.006, r = 0.60; controls: Z = 3.480, P < 0.001, r = 0.84) for externally cued responses than internally cued responses. There were no significant correlations between accuracy and RT across cue types ('External': $t_{b\ patients}$ = 0.255, P = 0.114; $t_{b\ controls}$ = 0.059, P = 0.720, and 'Internal': $t_{b\ patients}$ = -0.163, P = 0.341; $t_{b\ controls}$ = -0.107, P = 0.560).

Between-group comparisons further revealed significant differences in blink reduction, with healthy control subjects demonstrating greater ability to suppress blinks than TD patients (patients: Mdn = 69.00, IQR = 36.50; controls: Mdn = 79.00, IQR = 31.25; U = 80.000, Z = -2.417, P = 0.015, r = -0.41). No between-group differences were evident regarding WM (patients: M = 11.71, SD = 3.23; controls: M = 11.89, SD = 2.56; t(37) = -0.185, P = 0.854, Cohen's d = -0.062) or VMC (patients: Mdn = 10.00, IQR = 4.00; controls: Mdn = 10.00, IQR = 3.50; U = 167.000, Z = -0.344, P = 0.750, r = -0.056).

Table 2. Task-performance parameters in patients and matched controls

Performance parameter	Controls	TS	Statistic	p
RT (Intern) |M; SD|	417.83; 105.58	395.52; 77.35	t(36) = -.752	.457
Accuracy (Intern) |Mdn; IQR|	.95; .06	1.0; .05	Z = 2.361	.021
RT (Extern) |Mdn; IQR|	482.0; 140.9	508.73; 182.1	Z = .026	.979
Accuracy (Extern) |Mdn; IQR|	.80; .18	.92; .15	Z = 1.999	.046
Blink reduction |Mdn; IQR|	79.00; 31.25	69.00; 36.50	Z = -2.417	.015

Note. RT = Reaction time, M = Mean, SD = Standard deviation, Mdn = Median, IQR = Interquartile range.

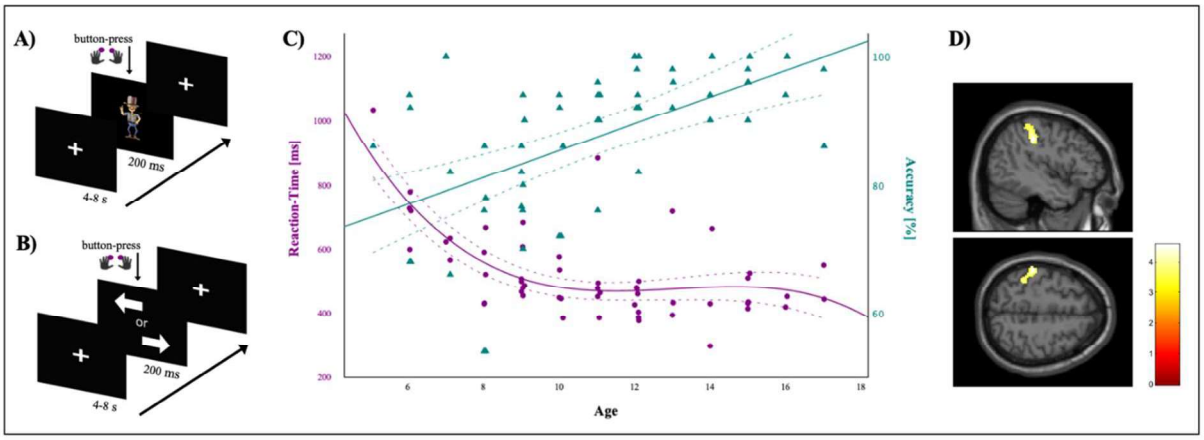

Figure 1. Experimental paradigm and typical developmental trajectories. (**A**) fMRI task condition 'Internal': Subjects were instructed to press either of two buttons as soon as possible following the appearance of a non-informative target-stimulus (Sherriff). (**B**) fMRI task condition 'External': Participants were instructed to press the button on the side indicated by an arrow as quickly as possible. (**C**) Developmental trajectory of externally cued responses in typically developing children and adolescents (N = 55). Regression analyses revealed linear age-related improvements in accuracy (teal; $R^2 = 0.309$, B = 0.021, P < 0.001) and a steep decline in reaction times during early childhood (purple; $R^2 = 0.251$, B = -0.952, P < 0.001). Reaction times are displayed in milliseconds (ms). Each data point represents one participant. Teal triangles represent individual accuracy values; purple circles represent individual reaction time values. Dashed lines indicate 95% confidence intervals for the fitted regression lines. (**D**) Linear age-related increase in BOLD activation for externally cued right-handed movements in typically developing children and adolescents (N = 43), observed in a left-sided (contralateral) cluster including primary somatosensory cortex (S1), intraparietal sulcus (IPS), inferior parietal lobule (IPL) and superior parietal lobule (SPL). Peak activation was located at MNI coordinates x = -44, y = -30, z = 40 (k = 427 voxels, t = 4.57). Activations are rendered on a canonical brain ($P_{FWE\text{-}corr.} < 0.001$). Colour bar indicates t-values.

4.5.2 Neural Activation Patterns

No significant association was observed between age and task-related neural activations for internally cued responses in typically developing children and adolescents. In contrast, for externally cued right-handed responses, a significant linear increase in task-related BOLD activation was found alongside increasing age in a cluster within the left (contralateral) parietal lobe, which included the postcentral gyrus (primary somatosensory cortex; Areas 3a, 3b, 1, 2), the intraparietal sulcus (IPS; Areas hIp1, hIP2, hIP3), the inferior parietal lobule (IPL; Areas PF, PFt) and superior parietal lobule (SPL; Area 7PC) (x, y, z = -44, -30, 40; $k_E = 427$; t = 4.57; $P_{FWE\text{-}corr.} = 0.005$; see Fig. 1D). Moreover, task activation in this cluster significantly positively correlated with task accuracy (r = 0.375, P = 0.013) and VMC (r = 0.440, P = 0.005).

Between-group comparisons revealed no significant differences in task activation related to internally cued responses. In contrast, during externally cued right-handed movements, TD patients exhibited significantly enhanced activation in a right-sided (ipsilateral) cluster, including the precentral gyrus (primary motor cortex; Areas 4a, 4p), postcentral gyrus (primary somatosensory cortex; Areas 3a, 3b, 1, 2) and the supplementary motor area (SMA; Area 6d1) (x, y, z = 36, -24, 74; $k_{E\,=}$ 845; t = 5.20; $P_{FWE\text{-}corr.} < 0.001$; see Fig. 2A and B). Additionally, beta-values derived from the peak voxel of this cluster significantly positively correlated with task accuracy (t_b = 0.381, P = 0.006; see Fig. 2C).

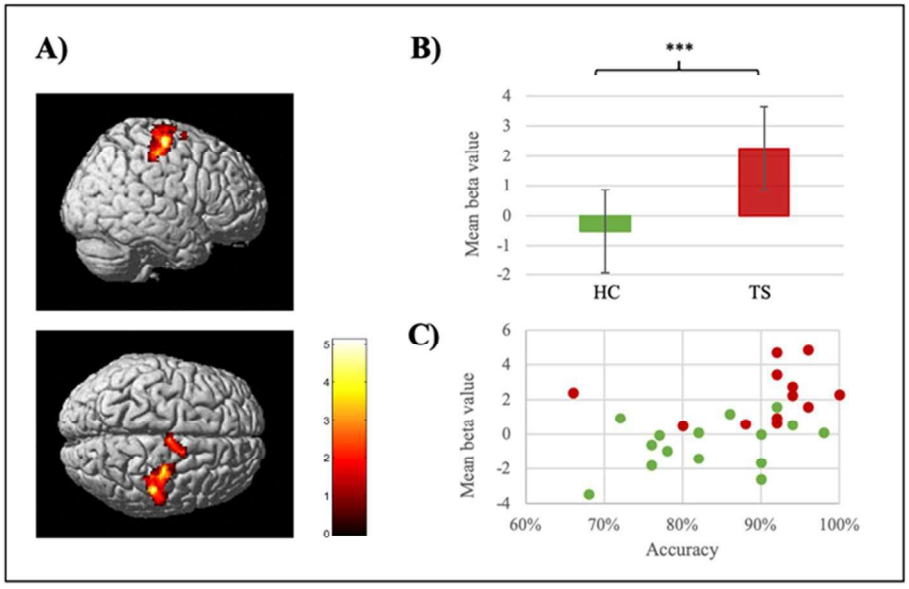

Figure 2. Neural overactivation in patients with TD. (**A**) Enhanced BOLD activation in TD patients (N = 12) compared to matched healthy controls (N = 15) during externally cued right-handed movements, observed in a right-sided (ipsilateral) cluster including the primary motor cortex (M1), primary somatosensory cortex (S1), and supplementary motor area (SMA). Activations are rendered on a canonical brain ($P_{FWE\text{-}corr.} < 0.001$). Peak activation was located at MNI coordinates x = 36, y = -24, z = 74 (k = 845 voxels, t = 5.20). Colour bar indicates t-values. (**B**) Mean beta values derived from the peak voxel of this cluster. Between-group comparison (independent-samples t-test) revealed significantly higher activation in patients (M = 2.25, SD = 1.51) than in controls (M = -0.54, SD = 1.44), t(25) = 4.894, *** P < 0.001, two-tailed. Error bars represent the standard error of the mean. (**C**) Significant positive correlation between task accuracy and mean beta values from this cluster (t_b = 0.381, P = 0.006). Each data point represents one participant. HC/blue = healthy controls, TD/yellow = patients.

4.5.3 Connectivity Analyses

Bayesian Model Selection (BMS)

According to BMS, out of all interhemispheric models tested for the group of healthy controls, Model 4 (without interhemispheric PMC-coupling; Fig. 3A) was most likely given our data. Model selection across groups (patients and matched controls) revealed Model 5 (without interhemispheric M1-coupling; Fig. 3B) as the winning model. Supplementary Figures 2 and 3 provide a complete overview of the tested model space and the corresponding evidence supporting selection of the winning models.

Endogenous Connectivity (DCM-A)

In typically developing children and adolescents, regression analysis revealed that CEs between the left PFC and the SMA followed a significant quadratic (inverted U-shaped) trajectory with age (R^2 = 0.285, B = -0.005, P = 0.007; see Fig. 3A) and were significantly positively correlated with WM (r = 0.479, P = 0.028).

Significant deviations in endogenous connectivity were found in TD patients compared to age-matched controls using independent-samples t-tests. Notably, the left IPS in TD patients exerted an excitatory influence on the left PMC (M = 0.05, SD = 0.18), whereas this connection was inhibitory in healthy controls (M = -0.11, SD = 0.13, t(18) = 2.262, P = 0.036, Cohen's d = 1.012; see Fig. 3B). No significant correlation was found between the coupling strengths of this connection and measures of task performance, WM, or VMC.

Task-dependent Connectivity (DCM-B)

For interhemispheric task-dependent connections, regression analyses revealed that in healthy subjects, the connection from the left IPS to the SMA showed a significant cubic age-related decrease, transitioning from excitatory to inhibitory influence (R^2 = 0.226, B = -0.006, P = 0.019; see Fig. 3A). Furthermore, CEs from this connection negatively correlated with WM (t_b = -0.345, P = 0.033) and VMC (t_b = -0.381, P = 0.017). Conversely, the connection from the SMA to the right M1 followed a cubic age-related shift from inhibitory to excitatory influence (R^2 = 0.247, B = 0.010, P = 0.014; see Fig. 3A). Spearman's rank correlation further indicated a positive correlation between CEs of this connection and task accuracy (r = 0.407, P = 0.049). The excitatory influence from the left PFC to the SMA followed a quadratic (U-shaped)

developmental pattern (R^2 = 0.209, B = 0.023, P = 0.025; see Fig. 3A) and was not significantly correlated with any measure of task performance, WM, or VMC.

Non-parametric between-group comparisons (Mann-Whitney-U) revealed significant differences in task-dependent connectivity between patients with TD and controls. Specifically, the interhemispheric connection between the left and right IPS was excitatory in TD (Mdn = 0.59, IQR = 2.119) but inhibitory in controls (Mdn = 0.032, IQR = 0.554; U = 81.000, Z = 2.343, P = 0.019, r = 0.52; see Fig. 3B). Again, no significant correlation was found between CEs of this connection and measures of task performance, WM, or VMC. Supplementary Tables 13–15 provide group-mean coupling strengths for all examined connections, including both endogenous (DCM-A) and task-dependent (DCM-B) connectivity.

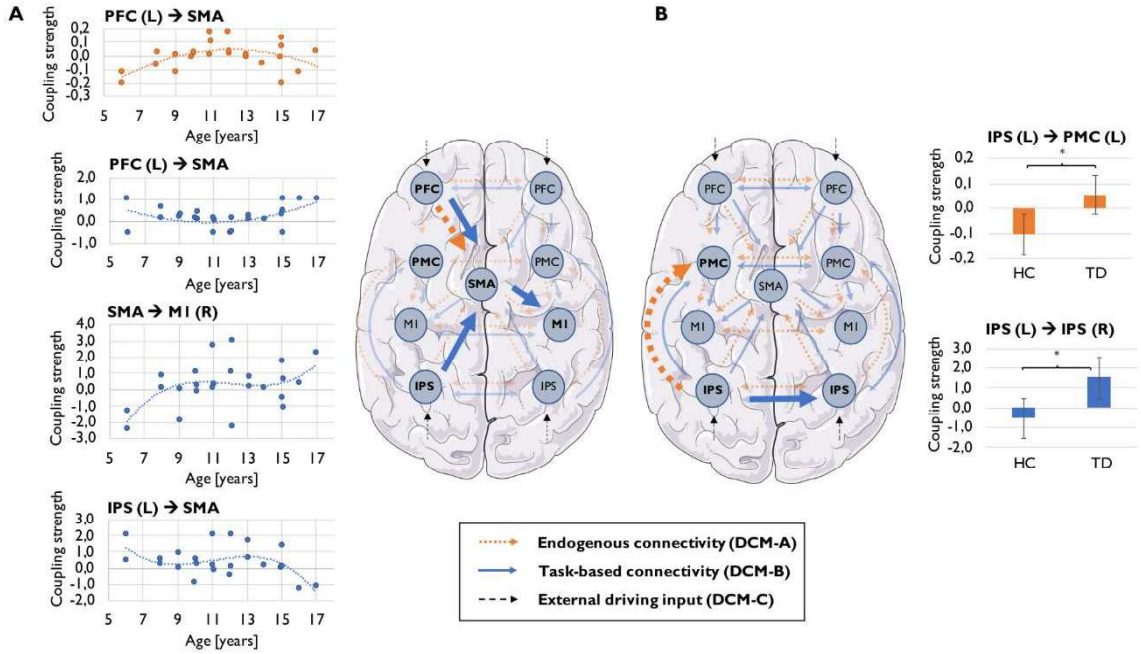

Figure 3. Motor network connectivity in patients with TD and typically developing controls. (**A**) Age-related changes in coupling strength in typically developing participants (N = 24). Each scatterplot depicts individual coupling estimates (y-axis) plotted against age (x-axis); dotted regression lines represent the best-fitting models. Regression analyses revealed a quadratic trajectory for endogenous PFC-SMA coupling (R^2 = 0.285, P = 0.007), and for task-based PFC-SMA coupling (R^2 = 0.209, P = 0.025), as well as cubic trajectories for IPS-SMA coupling (R^2 = 0.226, P = 0.019) and SMA-M1 coupling (R^2 = 0.247, P = 0.014). Each data point represents one participant. (**B**) Between-group differences in coupling estimates for endogenous (top) and task-based (bottom) connections. Patients (N = 10) showed significantly stronger excitatory connectivity from left IPS to left PMC (t(18) = 2.26, P = 0.036), and significantly enhanced excitatory task-based interhemispheric IPS-IPS coupling compared to controls (N = 10; U = 81.00, Z = 2.34, P = 0.019). Error bars represent the standard error of the mean. Asterisks denote statistically significant differences (P < 0.05, two-tailed). In both

panels, endogenous connections (DCM-A) are shown in orange, task-based connections (DCM-B) in blue, and external driving input (DCM-C) in black. Bold arrows highlight connections with significant effects. L = left; R = right; HC = healthy controls; TD = patients; IPS = intraparietal sulcus; PMC = premotor cortex; PFC = prefrontal cortex; SMA = supplementary motor area; M1 = primary motor cortex.

4.6 Discussion

This study investigated neural mechanisms underlying motor control in paediatric drug-naïve TD patients, within the framework of typical motor development. TD patients outperformed healthy controls in task accuracy, suggesting enhanced reactive motor control, but exhibited deficits in sustained inhibitory control, as evidenced by impaired blink suppression. At the neural level, ipsilateral motor overactivation and altered interhemispheric connectivity patterns reflected TD-specific adaptations rather than delayed or accelerated normative trajectories. These results highlight a complex interplay between compensatory mechanisms that enhance reactive motor control and persistent deficits in inhibitory control, offering new insights into the pathophysiology of TD.

4.6.1 Age-related Motor Development

Our developmental sample showed age-related improvements in motor performance, which were still evident in the age range between 5 and 16 years, consistent with previous research (Bucsuházy & Semela, 2017; Denckla, 1974; Hale, 1990; Haywood & Getchell, 2009; Rueda et al., 2004; Schmidgen et al., 2024). In line with earlier studies in healthy adults,(Michely et al., 2015; Michely et al., 2018) our child- and adolescent participants displayed longer RTs and reduced accuracy for directive cues compared to non-informative cues. This difference likely reflects the higher load in motor control required when participants not only had to ensure adequate timing but also choose the correct hand. In our sample, RTs declined steeply during early childhood and continued to improve more gradually into adolescence, showing a relative flattening of the curve after age ten (see Fig. 1B). Accuracy improved in a more linear fashion, approaching adult-like performance by mid-adolescence (Chevalier et al., 2014; Denckla, 1973, 1974; Largo et al., 2003; Michely et al., 2018; Niechwiej-Szwedo et al., 2020). Comparisons with previous adult samples (aged 21–35)(Michely et al., 2018) suggest that adolescents in our study (aged 13–16) still exhibited greater RT variability and overall slower average RTs. Furthermore, in the ‘Internal’ condition, slower RTs observed in our adolescent

sample – relative to previously reported young adult data –may be attributed to the increased complexity of the task stimuli used in our study (i.e., pictures of a Sherriff vs. double-sided arrows).

At the neural level, we observed an age-related linear increase in activation within a left parietal cluster, encompassing the IPL, IPS, SPL and postcentral gyrus. Similar age-related increases in parietal activation have previously been demonstrated in children and adolescents across a variety of motor- and WM tasks associated with attention, higher-order motor planning and response selection (Adleman et al., 2002; Klingberg, 2006; Klingberg et al., 2002; Neufang et al., 2008). While the parietal cortex is widely recognised for its involvement in visuospatial attention, (Gillebert et al., 2009; Numssen et al., 2021) specific regions are associated with distinct aspects of motor control, such as the storage of action representations (IPL),(Fogassi & Luppino, 2005) integration of visuospatial information into motor plans (IPS), (Grefkes et al., 2004; Hoffstaedter et al., 2013) online sensorimotor integration (SPL) (Friedrich et al., 2020) and motor learning through somatosensory feedback (postcentral gyrus) (Borich et al., 2015; Vidoni et al., 2010). In our sample, increased parietal activation was associated with enhanced task accuracy and VMC. Conversely, reduced activation in the left parietal and postcentral cortices has been linked to impaired motor performance in children with a developmental coordination disorder, emphasising these regions' significance in the development of integratory processes essential for motor refinement and coordination (Kashiwagi et al., 2009).

4.6.2 Motor Adaptations in TD

Patients with TD outperformed healthy controls regarding task accuracy, while maintaining comparable RTs. This finding suggests that the ability to control cued volitional movements may be enhanced in children and adolescents with TD and aligns with a few studies showing improved motor performance in young TD patients (Jackson et al., 2007; Jackson et al., 2011; Jung et al., 2015; Mueller et al., 2006). These improvements have been hypothesised to reflect compensatory processes driven by frequent inhibitory training through tic suppression (Eichele & Plessen, 2013; Mueller et al., 2006). However, despite enhanced performance in the RT task, patients in our sample displayed deficits in sustained inhibitory motor control, as evidenced by impaired blink suppression (see Table 2). These findings challenge the assumption that compensatory mechanisms in TD are facilitated via training-induced increases in inhibition.

Instead, these findings point to task-specific adaptations that selectively support reactive motor control. This distinction emphasises the complexity of motor control in TD, where adaptations may be tailored to specific motor demands unrelated to tic suppression per se.

4.6.3 Neural Overactivation as a Compensatory Mechanism?

Improved motor performance in patients with TD was linked to distinct changes in motor network activation patterns: for right-handed movements, patients exhibited ipsilateral overactivation of M1 and S1, which correlated positively with task accuracy. These findings align with previous research showing that children with TD recruit additional brain networks during voluntary movements compared to healthy controls (Roessner et al., 2013; Roessner et al., 2012; Zapparoli et al., 2016). While earlier studies proposed that recruitment of additional motor resources may reflect compensatory mechanisms, they lacked performance measures to relate neural activity to behaviour. Conversely, our current findings directly link altered motor network activity and enhanced reactive motor control in young TD patients. Interestingly, this compensatory pattern contrasts with earlier findings in adult TD patients, where reduced task-related activation in primary and secondary motor cortices has been linked to poorer performance, suggesting that such compensatory mechanisms may be impaired or insufficiently developed in adult TD patients (Thomalla et al., 2014).

Unlike dysfunctional overactivations seen in older adults or patients with early-onset neurodegenerative diseases (e.g., Huntington's, Alzheimer's, and PD), the ipsilateral overactivations in our TD sample appeared highly efficient, likely enhancing performance rather than merely compensating for deficits (Elman et al., 2014; Gregory et al., 2018; Loibl et al., 2011; Mattay et al., 2002; Michely et al., 2018; Riecker et al., 2006; Scheller et al., 2014; Wolf et al., 2014). In children with TD, prior studies have reported decreased activation in contralateral motor regions during voluntary movements, paired with increased frontal activations (Roessner et al., 2013; Roessner et al., 2012; Zapparoli et al., 2016). These reductions may reflect top-down inhibition of contralateral motor areas, which have been demonstrated to be hyper-excitable at rest (Orth et al., 2008; Ziemann et al., 1997) and modulated before volitional movements (Draper et al., 2014; Heise et al., 2010; Jackson et al., 2011; Jackson et al., 2013; Pépés et al., 2016). Our data did not indicate increased frontal influence or reduced engagement of contralateral motor regions. Instead, ipsilateral overactivation may represent an alternative compensatory strategy, enhancing task

performance by recruiting additional resources. Although these compensatory adaptations appear highly efficient, they seem specifically beneficial for reactive motor control. The observed deficits in sustained inhibition, such as impaired blink suppression, suggest that this adaptation may not generalise across different domains of motor control. This raises two possibilities: first, that the compensatory mechanisms enhancing reactive control may be task-specific and operate independently of inhibitory ability, or second, that these adaptations cannot efficiently counteract deficits in sustained inhibitory control. These findings emphasise the complexity of compensatory processes and highlight the importance of considering task-specific demands when evaluating TD motor adaptations. Notably, prior research suggests substantial heterogeneity within the TD population. For instance, Tajik-Parvinchi and Sandor (Tajik-Parvinchi & Sandor, 2013) reported that while some children with TD may develop adaptive mechanisms to control their tics – leading to improved voluntary control over eye movements – others exhibit reduced saccadic inhibitory control.

4.6.4 Interhemispheric Connectivity and Motor Networks in TD

Consistent with our task activation findings, effective PFC connectivity to motor regions was not significantly altered. Rather, we identified abnormal interhemispheric connectivity in patients with TD, which has previously been reported in both adult and paediatric TD and has mainly been associated with reduced interhemispheric inhibition (Baumer et al., 2010; Bruce et al., 2021; Liao et al., 2017; Neuner et al., 2010; Plessen et al., 2004).

In our sample, patients with TD displayed increased excitatory task-based connectivity from left to right IPS. Given the IPS' prominent role in integrating spatial information and coordinating attentional resources for movement planning, (Grefkes et al., 2004; Hoffstaedter et al., 2013) this may reflect altered functional integration of somatosensory information across hemispheres, which may help maintain control over motor outputs.

Within the left hemisphere, we observed significant between-group differences in endogenous connectivity from the IPS to the PMC. In healthy controls, the IPS exerted an inhibitory influence on PMC, while in TD patients, this influence was excitatory. This shift from inhibition to excitation could contribute to the hyperexcitability of contralateral motor regions commonly observed in TD patients (Orth et al., 2008; Ziemann et al., 1997). Alternatively, it may reflect stronger interactions between perceptual and motor processes, as suggested by increased perception-action binding previously documented in TD patients (Beste et al., 2016;

Kleimaker et al., 2020; Petruo et al., 2019). Despite these alterations, connectivity changes did not significantly correlate with behavioural performance, suggesting they represent broader network adaptations rather than direct compensatory mechanisms. Future research should investigate whether these patterns reflect pathological adaptive processes and their relationship to symptom severity and disease chronicity.

4.6.5 Typical Motor Development: effective connectivity changes with age

In healthy subjects, age-related increases in activation within the left parietal lobe were accompanied by changes in effective connectivity linked to task accuracy, WM and VMC. These changes prominently involved the SMA, a region critically involved in initiating and coordinating voluntary movements. The SMA is known to play a dual role in facilitating intended actions while suppressing unintended ones, positioning it as a central hub in motor planning and execution networks (Chen et al., 2010; Cote et al., 2020; Cunnington et al., 1996; Kasess et al., 2008; Nachev et al., 2008; Sumner et al., 2007). Age-related connectivity changes in SMA-associated pathways suggest that the SMA plays a critical role in supporting healthy motor development, integrating signals from other brain regions to enhance motor control over time. Age-related shifts in SMA connectivity suggest a developmental transition from reactive to proactive motor control, aligning with previous findings (Chevalier et al., 2014; Schmidgen et al., 2024). Specifically, our data showed a change in the SMA's influence on ipsilateral M1, evolving from inhibitory in younger children to excitatory in older children. This influence positively correlated with task accuracy, suggesting that excitatory SMA-M1 coupling supports more precise motor execution throughout development. Connections from the left IPS to the SMA also displayed age-related changes, following a reverse trajectory to the SMA-M1 connection. This connectivity shift, in turn, was associated with measures of WM and VMC, where inhibitory input from IPS to SMA was linked to higher performance on both Digit Span and Coding subtests. These findings suggest that the IPS plays a critical role in modulating SMA activity to balance motor output with cognitive demands.

PFC connections to the SMA exhibited distinct developmental patterns for endogenous and task-based connectivity, which followed quadratic trajectories in opposite directions, with connectivity patterns in the youngest and oldest subjects appearing comparable. Notably, endogenous PFC-SMA connectivity positively correlated with WM, highlighting the PFC's

role in supporting higher-order cognitive processes during motor performance (Klingberg, 2006; Klingberg et al., 2002; Tanji & Hoshi, 2008).

4.6.6 Developmental Trajectories in TD: deviant, delayed or accelerated?

Our findings offer a nuanced picture of developmental trajectories in TD. Behaviourally, patients outperformed age-matched controls in task accuracy while exhibiting comparable RTs, consistent with previous reports of enhanced reactive motor control and possibly indicating accelerated motor development (Jackson et al., 2007; Jackson et al., 2011; Mueller et al., 2006). However, their deficits in sustained voluntary motor control may point toward delayed motor development in this domain, which was previously suggested to improve steadily throughout middle childhood and reach mature levels by early adolescence (Fiske & Holmboe, 2019).

At the neural level, activation patterns in TD patients deviated from the age-related changes seen in healthy controls. While accuracy improvements in controls were associated with increased task-related activation in the contralateral parietal cortex, enhanced accuracy in patients was linked to pronounced activation in ipsilateral M1 and S1. Notably, ipsilateral overactivation partially mirrored the contralateral activations observed in typically developing children, as both involved the primary somatosensory cortex. This observation implies that ipsilateral overactivation serves as a compensatory mechanism, deviating from typical developmental trajectories yet enhancing reactive motor control and potentially mitigating deficits associated with TD (Debes et al., 2017; Franzkowiak et al., 2012; Heise et al., 2010; Jackson et al., 2015; Rae & Critchley, 2022; Worbe et al., 2015).

Similarly, task-related connectivity in patients with TD diverged from age-related changes in healthy controls. Interestingly, intra-, and interhemispheric connectivity alterations in TD patients involved the left IPS, a region showing age-related activation increases in typically developing children and adolescents. While this indicates increased parietal cortex engagement in TD patients, mirroring recruitment patterns in older children, other findings, e.g., increased excitatory endogenous connectivity from the IPS to the PMC, may reflect pathological rather than compensatory mechanisms. This altered connectivity could contribute to hyperexcitability of motor regions or enhanced action-perception binding, both commonly reported in TD (Beste et al., 2016; Kleimaker et al., 2020; Orth et al., 2008; Petruo et al., 2019; Ziemann et al., 1997). However, the lack of significant correlations between connectivity measures and behaviour renders a conclusive distinction of compensation and pathophysiological processes highly

challenging and modulatory approaches are needed to further explore the mechanistic role of these connectivity changes in the future.

In conclusion, early deficits in TD may drive compensatory changes that resemble typical or even accelerated development on the behavioural level. Conversely, when compensatory processes are insufficient, pathological neural dynamics may lead to behavioural deficits comparable to delayed development. At the neural level, compensatory mechanisms produce developmental trajectories distinct from typical patterns, reflecting a dynamic interplay between adaptation and pathophysiological processes (Eichele & Plessen, 2013; Nielsen et al., 2020).

4.7 Limitations

While our current study advances the understanding of typical motor development and compensatory mechanisms in TD, several limitations must be addressed: (1) Small sample sizes necessitate caution in interpreting our findings, which require replication in larger cohorts to enhance robustness and generalisability. Significant age- and TD-related activation patterns were identified, but only when using a more lenient voxel-level threshold. Our focus on right-handed responses required excluding participants with insufficient ipsilateral task activation from DCM analysis. This reduced sample size but allowed for integrating behavioural, activation and connectivity analyses, revealing significant group- and age-related effects on both endogenous and task-based motor-network connectivity. (2) While our cross-sectional design allowed for contextualisation within a developmental framework, future longitudinal studies are essential to capture the dynamic nature of developmental trajectories in TD and further investigate compensatory mechanisms, particularly about symptom remission versus persistence in adulthood. (3) Including patients with comorbid ADHD limits the attribution of findings exclusively to TD but enhances ecological validity by reflecting the clinical reality of high comorbidity rates in paediatric TD (El Malhany et al., 2015).

4.8 Conclusion

Our study highlights the dual nature of motor adaptations in children and adolescents with TD, combining a developmental and clinical approach. Enhanced accuracy in reactive motor tasks was supported by compensatory overactivation of ipsilateral motor regions and altered interhemispheric connectivity, likely reflecting efficient neural adaptations tailored to specific

task demands. However, deficits in sustained inhibition, such as impaired blink suppression, suggest that these compensatory mechanisms do not generalise across all motor domains.

In typically developing children, age-related increases in parietal activation and SMA connectivity were associated with improved motor precision, WM and VMC. These findings provide insights into the typical developmental trajectory of motor networks and the role of integrative brain regions in motor control.

In contrast, TD patients exhibited patterns of neural activation and effective connectivity that diverged from typical development, reflecting TD-specific adaptations rather than delayed or accelerated maturation. These adaptations highlight the interplay between compensation and pathophysiological processes in TD, where efficient reactive control coexists with persistent deficits in inhibitory control.

Future research should explore how these adaptations evolve with age and whether they contribute to long-term symptom management or persistence. Understanding the balance between adaptive and maladaptive processes in TD could inform targeted interventions to enhance compensatory mechanisms while mitigating pathological changes.

4.9 Data availability

The data and project-specific code supporting the findings of this study are archived in the CRC1451 data registry at https://www.crc1451.uni-koeln.de/. This includes batch scripts for standard pre-processing and model estimation pipelines, generated via the graphical user interface in SPM12 (Wellcome Centre for Human Neuroimaging, UCL Queen Square Institute of Neurology, London, UK [www.fil.ion.ucl.ac.uk/spm]), as well as an adapted batch script for Dynamic Causal Modelling, based on code available at https://www.fil.ion.ucl.ac.uk/spm/data/attention/. Access can be granted upon reasonable request via the CRC1451 registry.

4.10 Acknowledgements

The authors utilized ChatGPT (OpenAI) for language editing, particularly to optimize sentence structure, wording, and grammatical precision. The tool was employed exclusively for language refinement, and all original content was independently developed by the authors. The

final manuscript was carefully reviewed and approved to accurately represent the study's findings and conclusions.

Figure 3 was created using a template from Servier Medical Art, provided under a Creative Commons Attribution 4.0 International License (CC BY 4.0), accessible at https://smart.servier.com/category/anatomy-and-the-human-body/nervous-system/brain/. Modifications to the original template included resizing and the addition of figure elements. Full license details are available at https://creativecommons.org/licenses/by/4.0/. The same template was used in the graphical abstract. Additional illustrations in the graphical abstract were generated using a second Servier Medical art template (MRI scanner, https://smart.servier.com/smart_image/mri-imaging-equipment/), provided under the same license, and using DALL·E 3 (OpenAI) based on a text prompt provided by the authors.

We extend our gratitude to all participants and their families for the time and effort they dedicated to this study. We also thank Lara Sobolewski, Julius Ernst, Mira Kratzenstein, Larissa Kahler, Selina Cohnen, Klara Bodewig, Leonie Borowczak and Nora Osten for their support in recruiting participants and collecting data.

4.11 Funding

This work was funded by the Deutsche Forschungsgemeinschaft (DFG, German Research Foundation); Project-ID 431549029 – CRC 1451.

4.12 References

Adleman, N. E., Menon, V., Blasey, C. M., White, C. D., Warsofsky, I. S., Glover, G. H., & Reiss, A. L. (2002). A developmental fMRI study of the Stroop color-word task. *Neuroimage*, *16*(1), 61-75.

Baumer, T., Thomalla, G., Kroeger, J., Jonas, M., Gerloff, C., Hummel, F. C., Muller-Vahl, K., Schnitzler, A., Siebner, H. R., Orth, M., & Munchau, A. (2010). Interhemispheric motor networks are abnormal in patients with Gilles de la Tourette syndrome. *Mov Disord*, *25*(16), 2828-2837.

Baym, C. L., Corbett, B. A., Wright, S. B., & Bunge, S. A. (2008). Neural correlates of tic severity and cognitive control in children with Tourette syndrome. *Brain*, *131*(Pt 1), 165-179.

Beste, C., Tubing, J., Seeliger, H., Baumer, T., Brandt, V., Stock, A. K., & Munchau, A. (2016). Altered perceptual binding in Gilles de la Tourette syndrome. *Cortex*, *83*, 160-166.

Black, K. J., Black, E. R., Greene, D. J., & Schlaggar, B. L. (2016). Provisional Tic Disorder: What to tell parents when their child first starts ticcing. *F1000Res*, *5*, 696.

Borich, M. R., Brodie, S. M., Gray, W. A., Ionta, S., & Boyd, L. A. (2015). Understanding the role of the primary somatosensory cortex: Opportunities for rehabilitation. *Neuropsychologia*, *79*(Pt B), 246-255.

Bruce, A. B., Yuan, W., Gilbert, D. L., Horn, P. S., Jackson, H. S., Huddleston, D. A., & Wu, S. W. (2021). Altered frontal-mediated inhibition and white matter connectivity in pediatric chronic tic disorders. *Exp Brain Res*, *239*(3), 955-965.

Bucsuházy, K., & Semela, M. (2017). Case study: Reaction time of children according to age. *Procedia Engineering*, *187*, 408-413.

Channon, S., Drury, H., Martinos, M., Robertson, M. M., Orth, M., & Crawford, S. (2009). Tourette's syndrome (TS): inhibitory performance in adults with uncomplicated TS. *Neuropsychology*, *23*(3), 359-366.

Chen, X., Scangos, K. W., & Stuphorn, V. (2010). Supplementary motor area exerts proactive and reactive control of arm movements. *J Neurosci*, *30*(44), 14657-14675.

Chevalier, N., James, T. D., Wiebe, S. A., Nelson, J. M., & Espy, K. A. (2014). Contribution of reactive and proactive control to children's working memory performance: Insight from item recall durations in response sequence planning. *Dev Psychol*, *50*(7), 1999-2008. https://doi.org/10.1037/a0036644

Church, J. A., Wenger, K. K., Dosenbach, N. U., Miezin, F. M., Petersen, S. E., & Schlaggar, B. L. (2009). Task control signals in pediatric tourette syndrome show evidence of immature and anomalous functional activity. *Front Hum Neurosci*, *3*, 38.

Cohen, S. C., Leckman, J. F., & Bloch, M. H. (2013). Clinical assessment of Tourette syndrome and tic disorders. *Neurosci Biobehav Rev*, *37*(6), 997-1007.

Cote, S. L., Elgbeili, G., Quessy, S., & Dancause, N. (2020). Modulatory effects of the supplementary motor area on primary motor cortex outputs. *J Neurophysiol*, *123*(1), 407-419.

Cunnington, R., Bradshaw, J. L., & Iansek, R. (1996). The role of the supplementary motor area in the control of voluntary movement. *Human Movement Science*, *15*(5), 627-647.

Dash, C., Behera, A. K., Dehuri, S., & Ghosh, A. (2023). An outliers detection and elimination framework in classification task of data mining. *Decision Analytics Journal*, *6*, 100164.

Debes, N., Jeppesen, S., Raghava, J. M., Groth, C., Rostrup, E., & Skov, L. (2015). Longitudinal Magnetic Resonance Imaging (MRI) Analysis of the Developmental Changes of Tourette Syndrome Reveal Reduced Diffusion in the Cortico-Striato-Thalamo-Cortical Pathways. *J Child Neurol*, *30*(10), 1315-1326.

Debes, N., Preel, M., & Skov, L. (2017). Functional neuroimaging in Tourette syndrome: recent perspectives. *Neuroscience and Neuroeconomics*, *Volume 6*, 1-13.

Denckla, M. B. (1973). Development of speed in repetitive and successive finger-movements in normal children. *Dev Med Child Neurol*, *15*(5), 635-645.

Denckla, M. B. (1974). Development of motor co-ordination in normal children. *Dev Med Child Neurol*, *16*(6), 729-741.

Draper, A., Stephenson, M. C., Jackson, G. M., Pepes, S., Morgan, P. S., Morris, P. G., & Jackson, S. R. (2014). Increased GABA contributes to enhanced control over motor excitability in Tourette syndrome. *Curr Biol*, *24*(19), 2343-2347.

Dursun, S. M., Burke, J. G., & Reveley, M. A. (2000). Antisaccade eye movement abnormalities in Tourette syndrome: evidence for cortico-striatal network dysfunction? *J Psychopharmacol*, *14*(1), 37-39.

Eichele, H., Eichele, T., Marquardt, L., Adolfsdottir, S., Hugdahl, K., Sorensen, L., & Plessen, K. J. (2017). Development of Performance and ERPs in a Flanker Task in Children and Adolescents with Tourette Syndrome-A Follow-Up Study. *Front Neurosci*, *11*, 305.

Eichele, H., & Plessen, K. J. (2013). Neural plasticity in functional and anatomical MRI studies of children with Tourette syndrome. *Behav Neurol*, *27*(1), 33-45.

El Malhany, N., Gulisano, M., Rizzo, R., & Curatolo, P. (2015). Tourette syndrome and comorbid ADHD: causes and consequences. *Eur J Pediatr*, *174*(3), 279-288.

Elman, J. A., Oh, H., Madison, C. M., Baker, S. L., Vogel, J. W., Marks, S. M., Crowley, S., O'Neil, J. P., & Jagust, W. J. (2014). Neural compensation in older people with brain amyloid-beta deposition. *Nat Neurosci*, *17*(10), 1316-1318.

Fan, S., Cath, D. C., van der Werf, Y. D., de Wit, S., Veltman, D. J., & van den Heuvel, O. A. (2018). Trans-diagnostic comparison of response inhibition in Tourette's disorder and obsessive-compulsive disorder. *World J Biol Psychiatry*, *19*(7), 527-537.

Fiske, A., & Holmboe, K. (2019). Neural substrates of early executive function development. *Developmental Review*, *52*, 42-62.

Fogassi, L., & Luppino, G. (2005). Motor functions of the parietal lobe. *Curr Opin Neurobiol*, *15*(6), 626-631.

Franzkowiak, S., Pollok, B., Biermann-Ruben, K., Südmeyer, M., Paszek, J., Thomalla, G., Jonas, M., Orth, M., Münchau, A., & Schnitzler, A. (2012). Motor-cortical interaction in Gilles de la Tourette syndrome. *PLoS One*, *7*(1), e27850.

Friard, O., & Gamba, M. (2016). BORIS: A free, versatile open-source event-logging software for video/audio coding and live observations. *Methods in Ecology and Evolution*, *7*.

Friedrich, J., Verrel, J., Kleimaker, M., Munchau, A., Beste, C., & Baumer, T. (2020). Neurophysiological correlates of perception-action binding in the somatosensory system. *Sci Rep*, *10*(1), 14794.

Ganos, C., Kuhn, S., Kahl, U., Schunke, O., Feldheim, J., Gerloff, C., Roessner, V., Baumer, T., Thomalla, G., Haggard, P., & Munchau, A. (2014). Action inhibition in Tourette syndrome. *Mov Disord*, *29*(12), 1532-1538.

Georgiou, N., Bradshaw, J. L., Phillips, J. G., Bradshaw, J. A., & Chiu, E. (1995). The Simon effect and attention deficits in Gilles de la Tourette's syndrome and Huntington's disease. *Brain*, *118 (Pt 5)*, 1305-1318.

Gerard, E., & Peterson, B. S. (2003). Developmental processes and brain imaging studies in Tourette syndrome. *J Psychosom Res*, *55*(1), 13-22.

Gillebert, C. R., Op de Beeck, H. P., Panis, S., & Wagemans, J. (2009). Subordinate categorization enhances the neural selectivity in human object-selective cortex for fine shape differences. *J Cogn Neurosci*, *21*(6), 1054-1064.

Greene, D. J., Williams Iii, A. C., Koller, J. M., Schlaggar, B. L., Black, K. J., & The Tourette Association of America Neuroimaging, C. (2017). Brain structure in pediatric Tourette syndrome. *Mol Psychiatry*, *22*(7), 972-980.

Grefkes, C., Ritzl, A., Zilles, K., & Fink, G. R. (2004). Human medial intraparietal cortex subserves visuomotor coordinate transformation. *Neuroimage*, *23*(4), 1494-1506.

Gregory, S., Long, J. D., Klöppel, S., Razi, A., Scheller, E., Minkova, L., Johnson, E. B., Durr, A., Roos, R. A. C., Leavitt, B. R., Mills, J. A., Stout, J. C., Scahill, R. I., Tabrizi, S. J., & Rees, G. (2018). Testing a longitudinal compensation model in premanifest Huntington's disease. *Brain*, *141*(7), 2156-2166.

Hale, S. (1990). A global developmental trend in cognitive processing speed. *Child Dev*, *61*(3), 653-663.

Haywood, K., & Getchell, N. (2009). *Lifespan Motor Development*.

Heise, K. F., Steven, B., Liuzzi, G., Thomalla, G., Jonas, M., Muller-Vahl, K., Sauseng, P., Munchau, A., Gerloff, C., & Hummel, F. C. (2010). Altered modulation of intracortical excitability during movement preparation in Gilles de la Tourette syndrome. *Brain*, *133*(Pt 2), 580-590.

Hoffstaedter, F., Grefkes, C., Zilles, K., & Eickhoff, S. B. (2013). The "what" and "when" of self-initiated movements. *Cereb Cortex*, *23*(3), 520-530.

Jackson, G. M., Draper, A., Dyke, K., Pépés, S. E., & Jackson, S. R. (2015). Inhibition, Disinhibition, and the Control of Action in Tourette Syndrome. *Trends Cogn Sci*, *19*(11), 655-665.

Jackson, G. M., Mueller, S. C., Hambleton, K., & Hollis, C. P. (2007). Enhanced cognitive control in Tourette Syndrome during task uncertainty. *Exp Brain Res*, *182*(3), 357-364.

Jackson, S. R., Parkinson, A., Jung, J., Ryan, S. E., Morgan, P. S., Hollis, C., & Jackson, G. M. (2011). Compensatory neural reorganization in Tourette syndrome. *Curr Biol*, *21*(7), 580-585.

Jackson, S. R., Parkinson, A., Manfredi, V., Millon, G., Hollis, C., & Jackson, G. M. (2013). Motor excitability is reduced prior to voluntary movements in children and adolescents with Tourette syndrome. *J Neuropsychol*, *7*(1), 29-44.

Jung, J., Jackson, S. R., Nam, K., Hollis, C., & Jackson, G. M. (2015). Enhanced saccadic control in young people with Tourette syndrome despite slowed pro-saccades. *J Neuropsychol*, *9*(2), 172-183.

Jung, J., Jackson, S. R., Parkinson, A., & Jackson, G. M. (2013). Cognitive control over motor output in Tourette syndrome. *Neurosci Biobehav Rev*, *37*(6), 1016-1025.

Jurgiel, J., Miyakoshi, M., Dillon, A., Piacentini, J., Makeig, S., & Loo, S. K. (2021). Inhibitory control in children with tic disorder: aberrant fronto-parietal network activity and connectivity. *Brain Commun*, *3*(2), fcab067.

Kasess, C. H., Windischberger, C., Cunnington, R., Lanzenberger, R., Pezawas, L., & Moser, E. (2008). The suppressive influence of SMA on M1 in motor imagery revealed by fMRI and dynamic causal modeling. *Neuroimage*, *40*(2), 828-837.

Kashiwagi, M., Iwaki, S., Narumi, Y., Tamai, H., & Suzuki, S. (2009). Parietal dysfunction in developmental coordination disorder: a functional MRI study. *Neuroreport*, *20*(15), 1319-1324.

Kleimaker, M., Takacs, A., Conte, G., Onken, R., Verrel, J., Baumer, T., Munchau, A., & Beste, C. (2020). Increased perception-action binding in Tourette syndrome. *Brain*, *143*(6), 1934-1945.

Klingberg, T. (2006). Development of a superior frontal-intraparietal network for visuo-spatial working memory. *Neuropsychologia*, *44*(11), 2171-2177.

Klingberg, T., Forssberg, H., & Westerberg, H. (2002). Increased brain activity in frontal and parietal cortex underlies the development of visuospatial working memory capacity during childhood. *J Cogn Neurosci*, *14*(1), 1-10.

Knight, T., Steeves, T., Day, L., Lowerison, M., Jette, N., & Pringsheim, T. (2012). Prevalence of tic disorders: a systematic review and meta-analysis. *Pediatr Neurol*, *47*(2), 77-90.

Largo, R. H., Fischer, J. E., & Rousson, V. (2003). Neuromotor development from kindergarten age to adolescence: developmental course and variability. *Swiss Med Wkly*, *133*(13-14), 193-199.

Leckman, J. F., Riddle, M. A., Hardin, M. T., Ort, S. I., Swartz, K. L., Stevenson, J., & Cohen, D. J. (1989). The Yale Global Tic Severity Scale: Initial testing of clinician-rated scale of tic severity. *J Am Acad Child and Adolesc Psychiatry*, *28*, 556-573.

Liao, W., Yu, Y., Miao, H. H., Feng, Y. X., Ji, G. J., & Feng, J. H. (2017). Inter-hemispheric Intrinsic Connectivity as a Neuromarker for the Diagnosis of Boys with Tourette Syndrome. *Mol Neurobiol*, *54*(4), 2781-2789.

Loibl, M., Beutling, W., Kaza, E., & Lotze, M. (2011). Non-effective increase of fMRI-activation for motor performance in elder individuals. *Behav Brain Res*, *223*(2), 280-286.

Makki, M. I., Govindan, R. M., Wilson, B. J., Behen, M. E., & Chugani, H. T. (2009). Altered fronto-striato-thalamic connectivity in children with Tourette syndrome assessed with

diffusion tensor MRI and probabilistic fiber tracking. *J Child Neurol*, *24*(6), 669-678. https://doi.org/10.1177/0883073808327838

Margraf, J., Cwik, J. C., Pflug, V., & Schneider, S. (2017). Strukturierte klinische Interviews zur Erfassung psychischer Störungen über die Lebensspanne: Gütekriterien und Weiterentwicklungen der DIPS-Verfahren. *Z Klin Psychol Psychother*, *46*, 176-186.

Marsh, R., Zhu, H., Wang, Z., Skudlarski, P., & Peterson, B. S. (2007). A developmental fMRI study of self-regulatory control in Tourette's syndrome. *Am J Psychiatry*, *164*(6), 955-966.

Mattay, V. S., Fera, F., Tessitore, A., Hariri, A. R., Das, S., Callicott, J. H., & Weinberger, D. R. (2002). Neurophysiological correlates of age-related changes in human motor function. *Neurology*, *58*(4), 630-635.

Michely, J., Barbe, M. T., Hoffstaedter, F., Timmermann, L., Eickhoff, S. B., Fink, G. R., & Grefkes, C. (2012). Differential effects of dopaminergic medication on basic motor performance and executive functions in Parkinson's disease. *Neuropsychologia*, *50*(10), 2506-2514.

Michely, J., Volz, L. J., Barbe, M. T., Hoffstaedter, F., Viswanathan, S., Timmermann, L., Eickhoff, S. B., Fink, G. R., & Grefkes, C. (2015). Dopaminergic modulation of motor network dynamics in Parkinson's disease. *Brain*, *138*(Pt 3), 664-678.

Michely, J., Volz, L. J., Hoffstaedter, F., Tittgemeyer, M., Eickhoff, S. B., Fink, G. R., & Grefkes, C. (2018). Network connectivity of motor control in the ageing brain. *Neuroimage Clin*, *18*, 443-455.

Mink, J. W. (2003). The basal ganglia and involuntary movements: impaired inhibition of competing motor patterns. *Archives of neurology*, *60*(10), 1365-1368.

Mueller, S. C., Jackson, G. M., Dhalla, R., Datsopoulos, S., & Hollis, C. P. (2006). Enhanced cognitive control in young people with Tourette's syndrome. *Curr Biol*, *16*(6), 570-573.

Müller-Vahl, K. (2015). Tourette-Syndrom und andere Tic-Erkrankungen im Kindes- und Erwachsenenalter. *Klinische Neurophysiologie*, *46*(02), 109-109.

Nachev, P., Kennard, C., & Husain, M. (2008). Functional role of the supplementary and pre-supplementary motor areas. *Nat Rev Neurosci*, *9*(11), 856-869.

Neufang, S., Fink, G. R., Herpertz-Dahlmann, B., Willmes, K., & Konrad, K. (2008). Developmental changes in neural activation and psychophysiological interaction patterns of brain regions associated with interference control and time perception. *Neuroimage*, *43*(2), 399-409.

Neuner, I., Kupriyanova, Y., Stocker, T., Huang, R., Posnansky, O., Schneider, F., Tittgemeyer, M., & Shah, N. J. (2010). White-matter abnormalities in Tourette syndrome extend beyond motor pathways. *Neuroimage*, *51*(3), 1184-1193.

Niechwiej-Szwedo, E., Meier, K., Christian, L., Nouredanesh, M., Tung, J., Bryden, P., & Giaschi, D. (2020). Concurrent maturation of visuomotor skills and motion perception in typically-developing children and adolescents. *Dev Psychobiol*, *62*(3), 353-367.

Nielsen, A. N., Gratton, C., Church, J. A., Dosenbach, N. U. F., Black, K. J., Petersen, S. E., Schlaggar, B. L., & Greene, D. J. (2020). Atypical Functional Connectivity in Tourette Syndrome Differs Between Children and Adults. *Biol Psychiatry*, *87*(2), 164-173.

Numssen, O., Bzdok, D., & Hartwigsen, G. (2021). Functional specialization within the inferior parietal lobes across cognitive domains. *Elife*, *10*.

Oldfield, R. C. (1971). The assessment and analysis of handedness: The Edinburgh inventory. *Neuropsychologia*, *9*(1), 97-113.

Openneer, T. J. C., van der Meer, D., Marsman, J. C., Forde, N. J., Akkermans, S. E. A., Naaijen, J., Buitelaar, J. K., Hoekstra, P. J., & Dietrich, A. (2021). Impaired response inhibition during a stop-signal task in children with Tourette syndrome is related to ADHD symptoms: A functional magnetic resonance imaging study. *World J Biol Psychiatry*, *22*(5), 350-361.

Orth, M., Munchau, A., & Rothwell, J. C. (2008). Corticospinal system excitability at rest is associated with tic severity in tourette syndrome. *Biol Psychiatry*, *64*(3), 248-251.

Peelen, M. V., Glaser, B., Vuilleumier, P., & Eliez, S. (2009). Differential development of selectivity for faces and bodies in the fusiform gyrus. *Developmental Science 12*(6), F16-F25.

Pépés, S. E., Draper, A., Jackson, G. M., & Jackson, S. R. (2016). Effects of age on motor excitability measures from children and adolescents with Tourette syndrome. *Developmental Cognitive Neuroscience*, *19*, 78-86.

Petruo, V., Bodmer, B., Brandt, V. C., Baumung, L., Roessner, V., Münchau, A., & Beste, C. (2019). Altered perception-action binding modulates inhibitory control in Gilles de la Tourette syndrome. *J Child Psychol Psychiatry*, *60*(9), 953-962. https://doi.org/10.1111/jcpp.12938

Plessen, K. J., Bansal, R., & Peterson, B. S. (2009). Imaging evidence for anatomical disturbances and neuroplastic compensation in persons with Tourette syndrome. *J Psychosom Res*, *67*(6), 559-573.

Plessen, K. J., Wentzel-Larsen, T., Hugdahl, K., Feineigle, P., Klein, J., Staib, L. H., Leckman, J. F., Bansal, R., & Peterson, B. S. (2004). Altered interhemispheric connectivity in individuals with Tourette's disorder. *Am J Psychiatry*, *161*(11), 2028-2037.

Polyanska, L., Critchley, H. D., & Rae, C. L. (2017). Centrality of prefrontal and motor preparation cortices to Tourette Syndrome revealed by meta-analysis of task-based neuroimaging studies. *Neuroimage Clin*, *16*, 257-267.

Rae, C., & Critchley, H. (2022). Mechanistic insight into the pathophysiological basis of Tourette syndrome. In (pp. 209-244).

Rae, C. L., Parkinson, J., Betka, S., Gouldvan Praag, C. D., Bouyagoub, S., Polyanska, L., Larsson, D. E. O., Harrison, N. A., Garfinkel, S. N., & Critchley, H. D. (2020). Amplified engagement of prefrontal cortex during control of voluntary action in Tourette syndrome. *Brain Commun*, *2*(2), fcaa199.

Rawji, V., Modi, S., Latorre, A., Rocchi, L., Hockey, L., Bhatia, K., Joyce, E., Rothwell, J. C., & Jahanshahi, M. (2020). Impaired automatic but intact volitional inhibition in primary tic disorders. *Brain*, *143*(3), 906-919.

Raz, A., Zhu, H., Yu, S., Bansal, R., Wang, Z., Alexander, G. M., Royal, J., & Peterson, B. S. (2009). Neural substrates of self-regulatory control in children and adults with Tourette syndrome. *Can J Psychiatry*, *54*(9), 579-588.

Riecker, A., Groschel, K., Ackermann, H., Steinbrink, C., Witte, O., & Kastrup, A. (2006). Functional significance of age-related differences in motor activation patterns. *Neuroimage*, *32*(3), 1345-1354.

Roessner, V., Albrecht, B., Dechent, P., Baudewig, J., & Rothenberger, A. (2008). Normal response inhibition in boys with Tourette syndrome. *Behav Brain Funct*, *4*, 29.

Roessner, V., Wittfoth, M., August, J. M., Rothenberger, A., Baudewig, J., & Dechent, P. (2013). Finger tapping-related activation differences in treatment-naïve pediatric Tourette syndrome: a comparison of the preferred and nonpreferred hand. *J Child Psychol Psychiatry*, *54*(3), 273-279. https://doi.org/10.1111/j.1469-7610.2012.02584.x

Roessner, V., Wittfoth, M., Schmidt-Samoa, C., Rothenberger, A., Dechent, P., & Baudewig, J. (2012). Altered motor network recruitment during finger tapping in boys with Tourette syndrome. *Hum Brain Mapp*, *33*(3), 666-675. https://doi.org/10.1002/hbm.21240

Rueda, M. R., Fan, J., McCandliss, B. D., Halparin, J. D., Gruber, D. B., Lercari, L. P., & Posner, M. I. (2004). Development of attentional networks in childhood. *Neuropsychologia*, *42*(8), 1029-1040.

Scheller, E., Minkova, L., Leitner, M., & Kloppel, S. (2014). Attempted and successful compensation in preclinical and early manifest neurodegeneration - a review of task FMRI studies. *Front Psychiatry*, *5*, 132.

Schmidgen, J., Heinen, T., Konrad, K., & Bender, S. (2024). From preparation to post-processing: Insights into evoked and induced cortical activity during pre-cued motor reactions in children and adolescents. *Neuroimage*, *297*, 120735.

Schmidgen, J., Konrad, K., Roessner, V., & Bender, S. (2023). The external evocation and movement-related modulation of motor cortex inhibition in children and adolescents with Tourette syndrome - a TMS/EEG study. *Front Neurosci*, *17*, 1209801.

Schneider, S., Pflug, V., In-Albon, T., & Margraf, J. (2018). Kinder-DIPS Open Access: Diagnostisches Interview bei psychischen Störungen im Kindes- und Jugendalter. 3rd ed. *Mental Health Research and Treatment Center, Ruhr-University Bochum.* .

Serrien, D. J., Orth, M., Evans, A. H., Lees, A. J., & Brown, P. (2005). Motor inhibition in patients with Gilles de la Tourette syndrome: functional activation patterns as revealed by EEG coherence. *Brain*, *128*(Pt 1), 116-125.

Spencer, T., Biederman, J., Harding, M., Wilens, T., & Faraone, S. (1995). The relationship between tic disorders and Tourette's syndrome revisited. *J Am Acad Child Adolesc Psychiatry*, *34*(9), 1133-1139.

Stiensmeier-Pelster, J., Braune-Krickau, M., Schürmann, M., & Duda, K. (2014). *Depressionsinventar für Kinder und Jugendliche (DIKJ).* 3rd ed. *Hogrefe.*

Storch, E. A., Murphy, T. K., Geffken, G. R., Sajid, M., Allen, P., & Roberti, J. W. (2005). Reliability and validity of the Yale global tic severity scale. *Psychol. Assess*, *17*, 486-491.

Sumner, P., Nachev, P., Morris, P., Peters, A. M., Jackson, S. R., Kennard, C., & Husain, M. (2007). Human medial frontal cortex mediates unconscious inhibition of voluntary action. *Neuron*, *54*(5), 697-711.

Tajik-Parvinchi, D., & Sandor, P. (2013). Enhanced antisaccade abilities in children with Tourette syndrome: the gap-effect reversal. *Front Hum Neurosci*, *7:768*.

Tanji, J., & Hoshi, E. (2008). Role of the lateral prefrontal cortex in executive behavioral control. *Physiol Rev*, *88*(1), 37-57.

Thomalla, G., Jonas, M., Baumer, T., Siebner, H. R., Biermann-Ruben, K., Ganos, C., Orth, M., Hummel, F. C., Gerloff, C., Muller-Vahl, K., Schnitzler, A., & Munchau, A. (2014). Costs of control: decreased motor cortex engagement during a Go/NoGo task in Tourette's syndrome. *Brain*, *137*(Pt 1), 122-136.

Tourette Association of America. (2017). *Spectrum of Tourette syndrome and tic disorders: consensus of the scientific advisors of the Tourette Association of America*. Retrieved December 11 from https://tourette.org/spectrum-tourette-syndrome-tic-disorders-consensus-scientific-advisors-tourette-association-america/

Vidoni, E. D., Acerra, N. E., Dao, E., Meehan, S. K., & Boyd, L. A. (2010). Role of the primary somatosensory cortex in motor learning: An rTMS study. *Neurobiol Learn Mem*, *93*(4), 532-539.

Walbrin, J., Mihai, I., Landsiedel, J., & Koldewyn, K. (2020). Developmental changes in visual responses to social interactions. *Developmental Cognitive Neuroscience*, *42*, 100774.

Wechsler, D. (2017). Wechsler intelligence scale for children - fifth edition (WISC-V). Translated and edited by Petermann F. *Pearson.*

Wolf, R. C., Sambataro, F., Vasic, N., Depping, M. S., Thomann, P. A., Landwehrmeyer, G. B., Süssmuth, S. D., & Orth, M. (2014). Abnormal resting-state connectivity of motor and cognitive networks in early manifest Huntington's disease. *Psychol Med*, *44*(15), 3341-3356.

Worbe, Y., Marrakchi-Kacem, L., Lecomte, S., Valabregue, R., Poupon, F., Guevara, P., Tucholka, A., Mangin, J. F., Vidailhet, M., Lehericy, S., Hartmann, A., & Poupon, C. (2015). Altered structural connectivity of cortico-striato-pallido-thalamic networks in Gilles de la Tourette syndrome. *Brain*, *138*(Pt 2), 472-482.

Zapparoli, L., Porta, M., Gandola, M., Invernizzi, P., Colajanni, V., Servello, D., Zerbi, A., Banfi, G., & Paulesu, E. (2016). A functional magnetic resonance imaging investigation of motor control in Gilles de la Tourette syndrome during imagined and executed movements. *Eur J Neurosci*, *43*(4), 494-508. https://doi.org/10.1111/ejn.13130

Zeidman, P., Jafarian, A., Corbin, N., Seghier, M. L., Razi, A., Price, C. J., & Friston, K. J. (2019). A guide to group effective connectivity analysis, part 1: First level analysis with DCM for fMRI. *Neuroimage*, *200*, 174-190.

Ziemann, U., Paulus, W., & Rothenberger, A. (1997). Decreased motor inhibition in Tourette's disorder: evidence from transcranial magnetic stimulation. *Am J Psychiatry*, *154*(9), 1277-1284.

5 Study 4: Assessing Motor Inhibition with TMS-EEG

The external evocation and movement-related modulation of motor cortex inhibition in children and adolescents with Tourette syndrome - a TMS/EEG study

Julia Schmidgen , Theresa Heinen, Kerstin Konrad , Stephan Bender

This article has been published in *Front Neurosci*. 2023 Oct 19;17:1209801.

doi: 10.3389/fnins.2023.1209801.

This study builds on the preceding multimodal findings by employing a combined transcranial magnetic stimulation and electroencephalography (TMS-EEG) approach to directly probe cortical excitability and inhibition in children and adolescents with and without TS. Unlike the other studies in this dissertation, the data for this work were collected in an earlier, independent study with a distinct participant sample and protocol. Nevertheless, careful participant selection and experimental design ensure the comparability and relevance of these findings within the broader context of motor network development.

While both groups showed age-related maturation of inhibitory processing, characterized by progressive refinement of GABAergic mechanisms, children with TS exhibit alterations in the modulatory capacity of cortical inhibition. Integrating these TMS-EEG findings with the broader multimodal dataset advances our understanding of the neurophysiological basis of inhibitory control, providing mechanistic insights that complement the spatial and temporal perspectives offered by EEG and fMRI. The direct assessment of cortical inhibition provides critical insights into the neural mechanisms that contribute to the inhibitory control deficits observed in TS.

5.1 Contribution

I contributed substantially to the main data analysis, including reanalyzing key aspects of the dataset and conducting the statistical evaluation of the results. I was actively involved in interpreting the findings to current literature and the study's research questions. Although an initial draft existed, I extensively revised and rewrote the manuscript, integrated feedback from co-authors, and ensured the overall coherence and clarity of the final version.

frontiers | Frontiers in Neuroscience

TYPE Original Research
PUBLISHED 19 October 2023
DOI 10.3389/fnins.2023.1209801

OPEN ACCESS

EDITED BY
Paul Horn,
Cincinnati Children's Hospital Medical Center, United States

REVIEWED BY
Yosuke Morishima,
University of Bern, Switzerland
Jack Jiaqi Zhang,
Hong Kong Polytechnic University, Hong Kong SAR, China

*CORRESPONDENCE
Julia Schmidgen
julia.schmidgen@uk-koeln.de

RECEIVED 21 April 2023
ACCEPTED 26 September 2023
PUBLISHED 19 October 2023

CITATION
Schmidgen J, Konrad K, Roessner V and Bender S (2023) The external evocation and movement-related modulation of motor cortex inhibition in children and adolescents with Tourette syndrome – a TMS/EEG study. *Front. Neurosci.* 17:1209801. doi: 10.3389/fnins.2023.1209801

The external evocation and movement-related modulation of motor cortex inhibition in children and adolescents with Tourette syndrome – a TMS/EEG study

Julia Schmidgen[1]*, Kerstin Konrad[2,3], Veit Roessner[4] and Stephan Bender[1,4]

[1]Department of Child and Adolescent Psychiatry, Medical Faculty and University Hospital, University of Cologne, Cologne, Germany, [2]Child Neuropsychology Section, Department of Child and Adolescent Psychiatry, Psychosomatics and Psychotherapy, University Hospital, RWTH Aachen, Aachen, Germany, [3]JARA-BRAIN Institute II, Molecular Neuroscience and Neuroimaging, Forschungszentrum Jülich GmbH and RWTH Aachen University, Jülich, Germany, [4]Department of Child and Adolescent Psychiatry, Faculty of Medicine Carl Gustav Carus, TU, Dresden, Germany

Objective: This study tested the reactivity of motor cortex inhibition to different intensities of external stimulation by transcranial magnetic stimulation (TMS) and its internal modulation during different motor states in children and adolescents with Tourette syndrome.

Methods: TMS-evoked N100 served as an indirect measure of $GABA_B$ receptor function which is related to cortical inhibition. Combined TMS/EEG was used to analyze the TMS-evoked N100 component evoked by different stimulation intensities as well as during resting condition, movement preparation (contingent negative variation task) and movement execution. The study included 18 early adolescents with Tourette syndrome and 15 typically developing control subjects.

Results: TMS-evoked N100 showed a less steep increase with increasing TMS intensity in Tourette syndrome together with less modulation (disinhibition) over the primary motor cortex during the motor states movement preparation and movement execution. Children with Tourette syndrome showed equally high N100 amplitudes at 110% resting motor threshold (RMT) intensity during resting condition and a parallel decline of RMT and N100 amplitude with increasing age as control subjects.

Conclusion: Our study yields preliminary evidence that modulation of motor cortical inhibitory circuits, during external direct stimulation by different TMS intensities and during volitional movement preparation and execution is different in children and adolescents with Tourette syndrome compared to controls. These results suggest that a reduced resting motor cortical inhibitory "reserve" could contribute to the production of unwanted movements. Our findings are compatible with increased regulation of motor cortex excitability by perception-action binding in Tourette syndrome instead of top-down / motor regulation and need to be replicated in further studies.

KEYWORDS

Tourette syndrome, inhibition, TMS, EEG, N100, MEP

1. Introduction

Tourette syndrome (TS) is a complex neurodevelopmental childhood-onset condition characterized by the co-occurrence of multiple motor and at least one vocal tic over the period of minimum 1 year. Although the underlying mechanism of TS is currently poorly understood, evidence suggests functional impairments within the basal ganglia and several parallel cortico-striato-thalamocortical circuits. However, it remains unclear, which components within the pathways contribute to tics, which may be regarded as a surplus of actions. Some studies indicate that multiple sources within the circuits lead to a divergent input to the primary motor cortex. Motor cortical areas might be hyperexcited due to a reduced inhibitory input to the motor cortex, as shown by transcranial magnetic stimulation (TMS) studies. However, various studies showed contradictory findings regarding tic-related pathophysiological mechanisms.

Especially animal model data and magnetic resonance spectroscopy studies have indicated a major role of differences in the glutamate (excitatory) and γ-aminobutyric acid (GABA) neurotransmitter system (inhibitory) in tic pathophysiology. GABAergic neurotransmission plays a crucial role in the regulation of neuronal activity during various states of motor activation. During the resting state it ensures a constant level of neuronal activity and prevents uncontrolled generation and spreading of excitatory signals. During movement preparation and execution, regulation of GABAergic inhibition (Nowak et al., 2017) modulates the excitability of motor circuits to ensure an efficient and controllable movement execution (Dupont-Hadwen et al., 2019). Preparatory excitation of motor networks prior to a movement enables the fast transmission of neuronal signals, effective muscle activation and enhanced precision due to suppression of competing motor areas. However, excessive excitability during motor facilitation, execution, or resting state, could cause uncontrolled, premature, or inefficient movements. Regarding TS, post-mortem investigations showed a reduced number and altered distribution of inhibitory GABAergic interneurons within the sensorimotor areas of the striatum (Kalanithi et al., 2005; Kataoka et al., 2010). Multiple paired-pulse TMS studies consistently reported diminished $GABA_A$-mediated intracortical inhibition within the TS motor cortex (Gilbert et al., 2004; Orth et al., 2008; Orth and Rothwell, 2009; Heise et al., 2010). Reduced GABA-mediated motor cortical inhibition has frequently been interpreted as a core pathophysiological mechanism contributing to the generation of tics (Jackson et al., 2015).

TS usually reaches its maximum severity in early adolescence. Afterwards most TS patients experience a considerable improvement of the symptoms, characterized by a diminution of intensity and frequency of tics in late adolescence or early adulthood. Compensatory mechanisms are thought to contribute to an increased control over the motor output and concomitant over tics due to an elevated tonic inhibition. TMS-based findings have been interpreted as reduced gain within motor cortical circuits, which could represent a secondary consequence of or adaptation to TS. In this sense, deficits in inhibitory circuits in children and adolescents with TS might be compensated by reducing the gain in corticospinal excitability. Consequently, this would lead to decreased sensitivity to changes in input from other brain areas or external stimuli (Schilke et al., 2022).

Besides deficits in $GABA_A$-mediated inhibitory circuits, $GABA_B$-mediated circuits might also be deficient within the TS motor cortex. According to this notion, evidence from human TMS (Sanger et al., 2001), human pharmaco-TMS (McDonnell et al., 2006), and animal studies (Pitler and Alger, 1994; Deisz, 1999) suggest that activation of presynaptic $GABA_B$ receptors may halt release of GABA. Even though $GABA_A$-mediated motor cortical inhibition is evidently deficient in TS, the influence of $GABA_B$-mediated intracortical inhibition has been studied rarely. Previous studies have reported inconsistent results and focused mainly on long interval intracortical inhibition (LICI) as a measure of $GABA_B$-mediated inhibition at rest (Ziemann et al., 1997; Gilbert et al., 2004; Orth et al., 2008).

Combined TMS/EEG studies have highlighted the possibility of directly assessing primarily $GABA_B$-mediated motor cortical inhibition (Ilmoniemi and Kičić, 2010; Daskalakis et al., 2012). This has been verified by Premoli et al. (2014) in a pharmaco-TMS-EEG study. Their study showed that baclofen, a $GABA_B$ receptor agonist, specifically increased the TMS-evoked N100 amplitude, whereas Alprozam and Zolpidem, $GABA_A$ receptor positive agonists, exerted a diminishing of the component or no effect. There is a body of evidence showing a strong relation between the TMS-evoked N100 and LICI as a measure of $GABA_B$-mediated cortical inhibition in humans (Rogasch et al., 2013). Therefore, as in recent TMS/EEG research (Farzan et al., 2013; Rogasch et al., 2013; Premoli et al., 2014), it has been suggested that the TMS-evoked N100 is the most effective TMS measure of $GABA_B$-mediated motor cortical inhibition (Rogasch et al., 2013). Since TMS evoked N100 component amplitudes were shown to be reduced during movement execution (Nikulin et al., 2003) and preparation (Bender et al., 2005; D'Agati et al., 2014), several findings further imply that the TMS-evoked N100 is also a functional marker of motor cortical inhibition.

To our knowledge, TMS/EEG has never been used to assess cortical inhibition through the analysis of TMS-evoked N100 component in TS. More importantly, the dependence of motor cortical deficits on specific motor cortical activity states (motor states) in early adolescent TS has not yet been investigated. The present study examined how motor cortex inhibition depends on top down-modulation by other cortical and subcortical areas during distinct motor states. In addition, we examined the responsiveness and modulatory capacities of cortical inhibition to different intensities of external direct stimulation by TMS. This way, two types of modulation of motor cortex inhibition could be examined, which are both independent from modulation by sensory input similar to an "urge," though movement execution includes reafferent sensory feedback. In 18 early adolescent TS patients and 15 control subjects, we investigated motor cortical inhibitory processes associated with $GABA_B$-mediated inhibition by the analysis of the TMS-evoked N100 component using combined TMS/EEG. Participants performed three different tasks, each aimed to examine a specific motor state, i.e., rest, movement preparation (forewarned reaction time task), and movement execution. Less reactivity to external stimulation together with less

Abbreviations: ADHD, Attention deficit hyperactivity disorder; AEP, Auditory evoked potential; CNV, Contingent negative variation; CSTC, Cortico-striato-thalamocortical; EEG, Electroencephalogram; EHI, Edinburgh Handedness Inventory; GABA, γ-aminobutyric acid; LICI, Long-interval intracortical inhibition; MEP, Motor evoked potential; MSO , Maximum stimulator output; RMT, Resting motor threshold; SMA, Supplementary motor area; TS, Tourette syndrome; TEP, TMS evoked potential; TMS, Transcranial magnetic stimulation; YGTSS, Yale Global Tic Severity Scale.

movement-related modulation of motor cortex inhibition could point towards lower inhibitory capacities and differences in the modulation of motor cortical excitability in TS, so that unwanted activity in "tic generator" circuits would pass the threshold to involuntary movements more easily (Heise et al., 2010).

2. Methods

2.1. Subjects

Eighteen adolescent subjects with a current diagnosis of TS were included from the outpatient TS clinic of the Department of Child and Adolescent Psychiatry, Dresden. Patients fulfilled DSM 5 criteria for TS. The control group included 15 typically developing adolescents (control subjects). All subjects were right-handed (Oldfields Edinburgh Handedness Inventory, 1971) and of normal intelligence. Intelligence levels were assessed using a validated short version of the fourth edition of the Wechsler intelligence test (Waldmann, 2008). Groups did not differ with respect to age [$t(31) = 0.79$; $p = 0.43$], handedness [$t(31) - 0.03$; $p - 0.98$], IQ [$t(31) - -1.28$; $p - 0.21$], or gender distribution [$t(31) = 1.09$; $p = 0.28$; cf. Table 1].

Both groups were screened for psychiatric disorders using the German version of the M.I.N.I KID (Sheehan et al., 2010). Comorbid disorders, except for attention deficit hyperactivity disorder (ADHD), were excluded from the study. Comorbid ADHD, present in six subjects with TS, was assessed using a validated German ADHD questionnaire (Brühl et al., 2000), that has shown reliability as well as factorial and convergent/discriminant validity comparable to the Conners' scale (Erhart et al., 2008).

Current tic severity was assessed using the Yale global tic severity score interview (YGTSS) on the day of the testing (Leckman et al., 1989; Storch et al., 2005). Most subjects with TS were treatment naive, yet two subjects received tiapride and one subject received aripiprazole. All participants as well as their first-degree family members had no history of epilepsy or any kind of seizures. For sample characteristics, see Table 1. Informed written consent was obtained by all participants and their legal guardians in accordance with the declaration of Helsinki. The study was approved by the local ethics committee.

TABLE 1 Demographic, clinical, and TMS sample measures.

	Controls	TS
Sample size	$N = 15$	$N = 18$
Age (years; mean ± SD; range)	12.2 (2.3; 8.2–15.8)	12.8 (2.0; 10.7–17.6)
Gender (male, female)	9 m, 6 f	14 m, 4 f
EHI (mean ± SD)	77.6 (19.1)	77.8 (15.1)
IQ (mean ± SD)	116.5 (8.9)	111.6 (12.6)
YGTSS total symptom score (mean ± SD)	-	23.3 (18.2)
Comorbid ADHD	-	6 (18)
Resting motor threshold (mean ± SD)	72.9 (9.3) % MSO	74.5 (12.6) % MSO

TS = Tourette syndrome; EHI = Edinburgh Handedness Inventory; YGTSS = Yale global tic severity score; ADHD = Attention deficit hyperactivity disorder, MSO = maximum stimulator output.

2.2. Transcranial magnetic stimulation

Biphasic single pulse TMS (PowerMAG research 100; MAG & More GmbH, DE) was applied using a standard figure-of-eight coil (196 mm × 100 mm × 13.5 mm). Resting motor threshold (RMT) of the left primary motor cortex was assessed and determined using a conventional protocol (Conforto et al., 2004; Wu et al., 2012). First, participants were familiarized with the TMS sensation at low stimulation intensity of 40%. The intensity was then increased in steps of 10% of the device's maximum stimulator output (MSO) until the first motor evoked potential (MEP) was identified. MEPs were recorded from the right first dorsal interosseous (FDI) muscle.

Next, optimal target location and coil orientation was adjusted to elicit a well-formed, peak-to peak measured and reliable MEP. The left primary motor cortex was determined functionally at the site where the largest MEP was elicited. To ensure accuracy of targeting and orientation we employed navigated TMS. Neuronavigation served to control for coil displacement throughout the measurement including coil angle (to maintain stimulation constant on the functionally determined hot spot). Thus, individual head landmarks were matched with a dummy head model using Brainvoyager QX software (Version 2.3, Brain Innovation BV, NL). The optimal individual stimulation target point was then pinpointed on the standard head model. Hence, optimal coil orientation and placement was live monitored and adjusted when necessary.

Finally, the RMT was assessed by sequential 2% increments in intensity starting at intensity 20% below hot-spot determination until five out of 10 MEPs (peak-to-peak) of at least 50 μV were registered. Suprathreshold single pulse TMS was applied at 110% of participants RMT. In addition to RMT-adjusted stimulation, due to only limited correlations of TMS-evoked potentials and MEP amplitudes, an RMT-independent stimulus-intensity slope was measured by stimulation at 40, 60, and 80% MSO for all subjects. Note that this differs from the RMT-standardization in most studies. It has the advantage to avoid a masking of TEP recruitment by RMT (EMG-related) effects, as TEPs and MEPs are qualitatively different measures.

2.3. Electroencephalographic recordings

EEG activity was continuously recorded at 5 kHz sampling rate using 64 channel TMS-compatible EEG equipment (Brainamp DC, BrainProducts). The high sampling served to minimize the TMS-artifact duration. Online filtering was set at DC and 1 kHz high-cutoff. Equidistant electrode caps (Easycap GmbH) were fixed carrying 64 sintered silver/silver chloride electrodes. The size of the electrode caps was adjusted to head circumference. Recording reference was electrode "Fpz." Electrode impedance level was kept below 5 kΩ. Vertical electro-oculogram was recorded from electrodes FP1 and one electrode attached 2 cm below the left eye. Two electrodes each 1 cm lateral to the outer canthi recorded the horizontal electro-oculogram. NBS Presentation software (Version 15.0, Neurobehavioral Systems Inc.) was used to send triggers to both the EEG recording

system and the TMS device. Recorded EEG data were first processed offline using Brain Vision Analyzer (BrainProducts). As this study focused on late TEPs >50 ms latency, TMS artifacts were eliminated by means of linear interpolation of the interval 5 to 40 ms with respect to the TMS trigger (Fuggetta et al., 2006; Taylor et al., 2010). Due to long-lasting sine wave artifacts (the anti-aliasing filter turns amplifier saturation into sine wave artifacts) because of high stimulation intensities in children with higher resting motor thresholds, the interpolated period was longer than usual (Taylor et al., 2008). We assured, that later time intervals were not affected by TMS-artifacts (Bonato et al., 2006), comparing ICA-based correction to interpolated data in single subject averages. Next, data were down-sampled to 500 Hz and filtered (48 dB/Oct) using a 50 Hz notch filter, a time constant of 1 s and a high-cutoff filter of 25 Hz. Then, data were average referenced. Segments comprised 1 s duration, −500 to 500 ms with respect to the TMS pulse. A 100 ms interval, −130 to −30 ms, was used for baseline correction. Visual inspection revealed no time-locked activity between −30 and −5 ms, however, we wanted to exclude any possible effects of the filtering near the interpolation interval on the baseline. Next, ocular artifact correction (Gratton et al., 1983) was applied as implemented in Brain Vision Analyzer (BrainProducts) followed by an automatic artifact removal of the segmented data (max allowed voltage step = 50 μV/ms; max allowed differences of values in intervals = 300 μV). The results of this automatic procedure were controlled for by visual inspection by a research assistant blind to the study hypotheses. Corrected and remaining segments were averaged by subject and condition. The TEP at a latency of approximately 100 ms, i.e., the TMS evoked N100, was registered at electrode C3 since previous studies have shown N100 to peak over the stimulated primary motor cortex (Nikulin et al., 2003; Bender et al., 2005; Bruckmann et al., 2012). The TMS-evoked N100 was quantified as the area under the curve in the time interval 70–150 ms (mean amplitude * 80 ms), in order to equalize any latency differences and to consider not only the peak amplitude but also the duration of the N100 component.

2.4. Electromyographic recordings

Electromyographic activity was recorded (Brainamp ExG, BrainProducts) by electrodes placed in a belly-tendon montage at the contralateral first dorsal interosseous muscle (FDI) using silver/silver-chloride self-adhesive surface electrodes (Neuroline 700, Ambu). EMG was sampled at 5 kHz with a time constant of 10 s and a high cutoff of 1 kHz. Offline, data were downsampled to 500 Hz and high pass filtered at 20 Hz (48 dB/Oct). Segmentation and baseline correction were carried out identical to the EEG processing (see section EEG above). Next, data were averaged across subjects and conditions. MEPs were quantified as the peak-to-peak amplitude within 18–40 ms after the TMS pulse.

2.5. Experimental procedure

Participants were seated in a sound attenuated, dimly lit room, facing a 22-inch computer screen (Fujitsu B22W-7 LED, 1680 × 1050 resolution). The sequence of the three experimental tasks was counterbalanced to obtain 18 individual sequences. Each sequence was randomly assigned to one participant of each group. The counterbalancing was imperfect due to the size of our sample. This however did not exert a significant confounding influence when we tested for order effects statistically. Experimental paradigms were implemented using NBS Presentation software (Version 15.0, Neurobehavioral Systems Inc.). Subjects were seated at 0.7 m distance to the PC screen. The default computer screen showed a vertically and horizontally centered white fixation cross (font size = 36) on a dark grey background and served to minimize eye movement. To reduce head movements and the risk of neck strain due to the TMS coil weight, subjects placed their heads on a cushioned, custom-made chin rest. To minimize TMS related acoustic evoked potentials participants wore earplugs. Every task started with an instruction presented in white font on the default background, followed by five rehearsal trials to ensure task comprehension. No acoustic masking by white noise was employed (Jarczok et al., 2021; Roos et al., 2021) as this masking procedure is not well tolerated in children and TMS-evoked N100 differs largely in frequency (duration), lateralization and amplitude from an auditory N1 in the examined age range. In contrast to the analyzed TMS-evoked N100 component, developmental AEP data showed that frontocentral N1b increases in children and adolescents and that the evoked peak is less broad and shows lower amplitudes (Bender et al., 2006). We applied 20 TMS pulses for each motor state condition. Due to larger TEP amplitudes in children (Bender et al., 2005) and adolescents, fewer trials are sufficient than in adults (D'Agati et al., 2014; Jarczok et al., 2016), especially because children do not tolerate long recording times with larger numbers of trials.

2.6. Experimental conditions – 3 motor states: rest, preparation, movement execution, and reactivity to external stimulation at different intensities at rest

2.6.1. At rest (motor state 1)

Participants were instructed to rest, look at the fixation cross and neglect the occasional TMS sensation. Twenty single TMS pulses at 110% RMT were applied at an inter-trial-interval that randomly varied between 6 and 10 s. The inter-trial-interval was within the same range for all tasks (motor states 1 to 3).

2.6.2. Motor preparation (motor state 2)

The task consisted of 20 trials of a contingent negative variation (CNV) paradigm, starting with a visual warning stimulus S1 (white exclamation mark, size = 34 × 27 mm) presented for a duration of 150 ms. An imperative stimulus S2 (white outline of a right hand, size – 34 × 27 mm) was presented for 150 ms, 3.3 s following S1 onset. Participants were instructed to prepare, at occurrence of S1, and to respond as quick as possible by clicking the left mouse button with the index finger of their right hand upon presentation of S2. Trials were terminated by the button press and followed by the inter-trial-interval. The 20 TMS pulses at 110% RMT occurred 2.8 s after S1 onset, to probe advanced motor preparation.

2.6.3. Motor execution (motor state 3)

Participants were asked to trigger 20 TMS pulses with an intensity of 110% RMT in a self-paced manner by clicking the left mouse button with the index finger of their right hands. During task execution, i.e.,

10.3389/fnins.2023.1209801

20 mouse clicks, participants were instructed to look at the fixation cross of the default screen and to produce self-paced clicks without any rhythm, rapid sequences or response pattern.

2.6.4. Reactivity to external stimulation at different intensities

At rest, 20 TMS pulses were applied for 40, 60, and 80% maximum stimulator output (equal conditions as motor state 1).

2.7. Statistical analysis

All statistical analysis were performed using Statistica. Statistical significance level was determined as alpha = 0.05. Age-dependent development of RMT and N100 amplitude were compared between the two diagnostic groups in linear models. General linear models with the intersubject factor diagnostic group (TS versus control subjects), gender (male, female) as well as the repeated measurement factors modulation TYPE (internal modulation by motor state vs. external stimulation/intensity slope), each at two different INTENSITIES (internal: difference rest – motor preparation, difference rest – motor execution; external stimulation: difference 40–60% and 60–80% MSO) were calculated for N100 amplitude modulation between the conditions (N100 amplitude differences) with the linear predictors age and N100 amplitude at rest (110% MSO). The classification into "small" and "large" intensities refers to the amount of modulation, i.e., the size of the difference of TMS-evoked N100 amplitude in this condition compared to the resting condition. Raffin et al. (2020) showed that an increase in small stimulation intensities (40 to 60% RMT) had a lower effect on TEP amplitudes than the same increase in larger stimulation intensities, closer to the resting motor threshold (60 to 80% RMT). In the same line, it was shown that TMS-evoked neuronal activity increases in a sigmoid-shaped stimulus-intensity curve with a stronger modulatory effect for higher stimulation intensities around the RMT (Komssi et al., 2004). With regard to movement states, previous studies showed that the effect size of movement preparation on the TMS-evoked N100 (Bender et al., 2005) is lower than the effect size of movement execution (Nikulin et al., 2003). Though in these studies a RMT-standardization of the TMS-intensities has been performed, we believe that this fact does not qualitatively change the sigmoid recruitment curves. In order to analyze motor cortical inhibition modulation in general and to avoid multiple testing, the modulation types were included in one model. A main or interaction effect involving modulation TYPE would point towards specific effects of external and top-down modulation. Levene's test did not detect any violation of the assumption of variance homogeneity. Note that due to the non-linear slope of the input–output curve (steeper slope around the RMT 60 vs. 80% MSO than for the subthreshold intensities 40 vs. 60% MSO), the difference 60 vs. 80% MSO was larger than 40 vs. 60% MSO, though the TMS-evoked N100 rises already at lower intensities than the MEP (cortical response before EMG response). MEP and N100 amplitudes at 110% RMT were compared between the two diagnostic groups, correcting for age and gender.

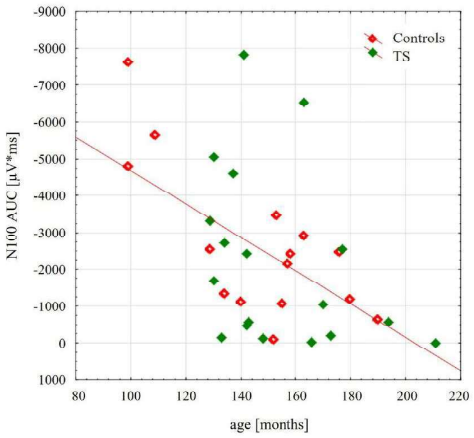

FIGURE 1
Scatterplot illustrating the age-related decrease of the TMS evoked N100 component, respectively, for control group (red) and for adolescents with tourette disorder (green). TEP-N100 amplitudes were recorded at CP6' with a stimulation intensity of 110% resting motor threshold (RMT). Note that TEP-N100 component is represented as area under the curve (AUC) due to broad N100 potentials and high variability of N100 latency shown in children and adolescents.

3. Results

3.1. Behavioral performance during motor state 2 (motor preparation)

Adolescents with TS showed comparable task performance to control subjects regarding reaction times in the motor preparation (motor state 2) task paradigm (Controls: 161 ± 36 ms; TS: 150 ± 33 ms). Due to the small number of TS subjects, comorbid ADHD did not show any covariate effects on performance.

3.2. Cortical inhibition

TMS-evoked N100 amplitude at 110% RMT stimulation intensity during the resting condition did not differ between the groups [$F(1;29) = 0.16$; $p = 0.69$]. TMS-evoked N100 amplitudes showed an age-dependent maturational decrease with increasing age through late childhood and adolescence [$F(1;29) = 13.4$; $p = 0.001$], as shown in Figure 1. Although on a descriptive level, this decrease was more pronounced for control subjects, there were no significant differences between the two groups [interaction age × diagnosis $F(1;29) = 0.45$; $p = 0.51$].

Moreover, we tested the internal modulation of N100 amplitude by movement preparation and movement execution (Table 2). Figure 2 shows the EEG response to TMS at electrode C3 averaged across control subjects and children with TS, respectively, for motor preparation as well as motor execution condition. Both conditions led to a significant reduction of TMS-evoked N100 amplitude compared to stimulation at rest [movement preparation $F(1;29) = 6.9$; $p = 0.01$; movement execution $F(1;29) = 16.9$; $p = 0.0003$], taking age and gender into consideration as covariates (main effects).

10.3389/fnins.2023.1209801

When the external and internal *modulation* of cortical inhibition (dependent variable TMS-evoked N100 amplitude *difference*) was examined (general linear model with the categorical predictors DIAGNOSIS (TS, CO), GENDER (female, male); the linear predictors AGE (months) and TMS-evoked N100 AREA UNDER THE CURVE (AUC) AT REST (110% RMT); the repeated measurement variables MODULATION TYPE (external stimulation versus internal modulation) and INTENSITY (small: stimulation difference 40 vs. 60% MSO, motor preparation, large: stimulation difference 60 vs. 80% MSO, motor execution)), subjects with TS showed less modulation than the control subjects [$F(1;28) = 4.34$; $p = 0.047$; Figure 3].

Controlling for age-dependent maturation (covariate age), this effect was similar for both types of modulation (different external stimulation intensities, internally prepared movement states) as there was no main effect of stimulation type [$F(1;28) = 1.1$; $p = 0.30$].

There was a strong effect of N100 amplitude at rest [$F(1;28) = 15.4$; $p = 0.0005$], which was stronger than simple age effects, justifying the inclusion of this covariate. There was no significant effect of comorbid ADHD [6/18 TS subjects; $F(1;27) = 0.65$; $p = 0.43$] or medication [3/18 subjects; $F(1;27) = 0.12$; $p = 0.73$], when included into the model, so these predictors did not enter the final model. In order to exclude artificial effects produced by covariates, we verified that there was still a strong trend towards the effect of diagnosis without suprathreshold TMS-evoked N100 amplitude at rest as a covariate [$F(1;29) = 3.8$; $p = 0.06$], with age now showing significant effects [$F(1;29) = 7.4$; $p = 0.01$].

TABLE 2 Responsivity of inhibitory systems to different TMS intensities and internal modulation by movement state.

	40% MSO [μV*ms]	60% MSO [μV*ms]	80% MSO [μV*ms]
Controls	−84.0 ± 73.5	−307,9 ± 311.5	−2577.6 ± 2148.8
TS	−230.7 ± 320.1	−377,1 ± 520.8	−1908.3 ± 1454.3
	At rest (110% RMT) [μV*ms]	Motor preparation [μV*ms]	Movement execution [μV*ms]
Controls	−2632.7 ± 2046.5	−1921.0 ± 1810.9	−1158.1 ± 1380.3
TS	−2211.9 ± 2399.1	−1827.4 ± 1911.2	−1267.7 ± 1750.1

Please note that the mean of the individual differences between rest and motor states movement preparation and execution is NOT equal to the difference of the group means for these movement states, when comparing this table to Figure 2. TS = Tourette syndrome; MSO = maximum stimulator output.

3.3. Cortico-spinal-excitability

Resting motor thresholds did not differ between the two groups [$F(1;29) = 0.49$; $p = 0.49$], considering covariates age and gender. There was a trend towards a decrease of RMT with increasing age in both groups [$F(1;29) = 2.9$; $p = 0.10$].

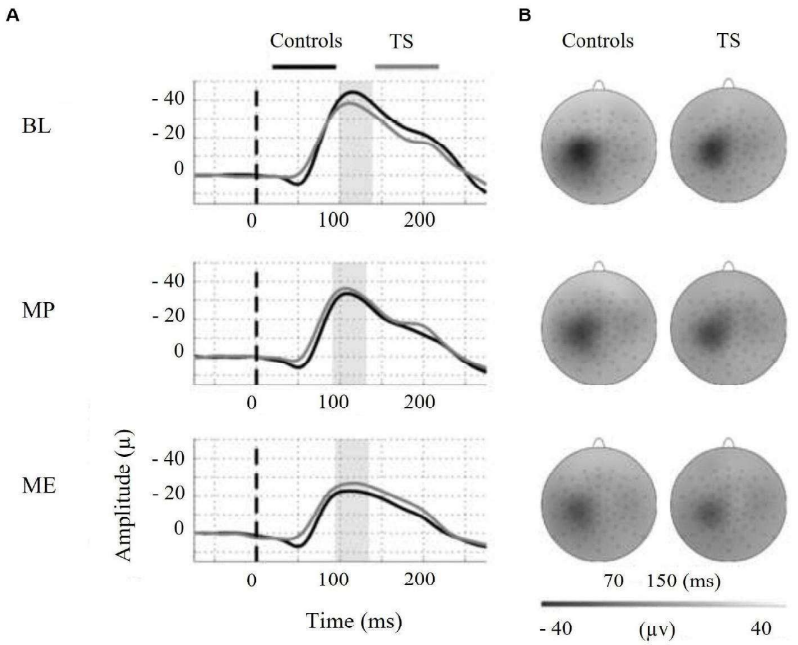

FIGURE 2
On the left-hand side, motor states are indicated as follows: BL – baseline, MP – motor preparation, ME – motor execution. **(A)** Shows the N100-TEP assessed at electrode C3. Note that voltage values at the y-axis are presented upside down. The vertical dashed line at time point zero indicates TMS, applied to the right motor cortex. The average N100-TEP amplitude latency by condition is highlighted in grey. **(B)** Shows voltage distribution around the TMS evoked N100 peak. The topographic time range selected represent the 95% confidence intervals of N100-TEP amplitudes across groups and conditions. Controls = typically developing subjects, TS = Tourette syndrome.

10.3389/fnins.2023.1209801

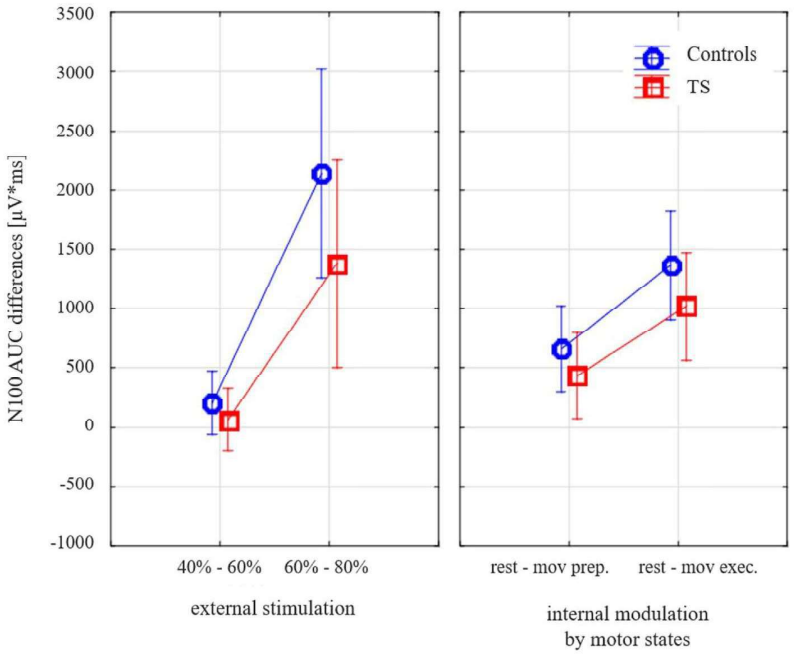

FIGURE 3
Effects of varying external stimulation intensity (increase from 40 to 60% maximum stimulator output, MSO, versus increase from 60 to 80% MSO) and internal modulation by motor state (difference resting state versus movement preparation and difference resting state versus movement execution) on the TMS-evoked N100 area under the curve (AUC) for subjects with Tourette syndrome and control subjects. Please note that all values illustrate adjusted means (after controlling for the effect of age and gender). Since the corrections for the covariates are taken into account, there are small deviations from the values in Table 2.

When MEP amplitude at 110% was tested for group differences with the covariates age and gender, there was no significant difference between the groups [$F(1;29) = 2.27$; $p = 0.14$], despite descriptively lower amplitudes in children with TS (CO 389 ± 95 µV vs. TS 210 ± 55 µV).

4. Discussion

This study investigated potential differences in motor cortical inhibition (TMS-evoked N100 amplitude) in early adolescents with TS using combined TMS/EEG. We examined the modulation of inhibitory control in different activation states of the motor cortex. TMS/EEG studies of neurodevelopmental disorders are still rare. To our knowledge, this is the first study to report TMS evoked brain potentials (TMS-evoked N100, presumably related to $GABA_B$-mediated cortical inhibition) in adolescent subjects with TS.

Our main findings are as follows: (1) TMS-evoked N100 amplitudes (cortical inhibition) at 110% RMT were comparable in early adolescent control subjects and subjects with TS; they showed no differences with respect to their cross-sectional maturational trajectory. (2) Compared to controls subjects, TS subjects showed reduced modulation of the $GABA_B$-mediated TMS-evoked N100 when stimulated at varying fixed (non RMT-adjusted) intensities at rest and during top-down modulation by different motor states (movement preparation and movement execution). In sum, inhibitory systems in primary motor cortex were less responsive in TS. Reduced disinhibition of primary motor cortex from resting state to movement execution and reduced recruitment of $GABA_B$-related inhibition in primary motor cortex to increasing intensities of external transcranial magnetic stimulation could point towards a reduced "inhibitory reserve" in the primary motor cortex (Heise et al., 2010). While the study of Heise et al. (2010) referred to a sample of 11 adult subjects with TS and short-interval intracortical inhibition (based on EMG-responses, $GABA_A$-related), our study examined an early adolescent sample and used a cortical readout (TMS-evoked N100, $GABA_B$-related). There was no main effect or interaction involving modulation TYPE. Thus, we obtained no hint in our data towards specific deficits in the two modulation TYPEs, however, we cannot exclude that such specific effect could be found in future studies in larger samples. Our conclusions refer to the capacity of modulation of motor cortex inhibition in general and not to either modulation type separately. Note that this concept of reduced modulation of inhibition in the motor cortex is different from higher cognitive control-related processes and inhibition of responses in a Go/NoGo task (such as reflected by a frontal N2 event-related potential component).

4.1. Motor cortical inhibition in subjects with TS

Impaired or altered inhibitory control has been proposed in many studies as a major cause of TS (Stern et al., 2008). However, there are also studies that did not find a deficient inhibitory performance

(Ganos et al., 2014) or even an increased inhibitory control (Jackson et al., 2011).

Consistent with previous studies, we replicated the maturation related decline in $GABA_B$-mediated TMS-evoked N100 amplitudes with increasing age (Bender et al., 2005; Bruckmann et al., 2012; D'Agati et al., 2014; Määttä et al., 2019). Moreover, our data showed that TMS-evoked N100 amplitudes decreases during motor preparation and execution, providing further evidence that TMS-evoked N100 represents motor cortical inhibitory processes. It has been shown that the TMS evoked N100 component as well as the TMS based long-interval intracortical inhibition (LICI) represent $GABA_B$-receptor mediated neurotransmission (Farzan et al., 2013; Rogasch et al., 2013; Premoli et al., 2014). Therefore, the TMS-evoked N100 has been proposed to represent cortical mechanisms associated with $GABA_B$-mediated motor cortical inhibition (Rogasch et al., 2013). Singer et al. (2001) showed that baclofen, a $GABA_B$-agonist, did not lead to a reduction of tic symptoms in TS subjects. Our finding of normal TMS-evoked N100 amplitudes at 110% RMT could contribute to the notion that $GABA_B$-mediated cortical inhibition in early adolescent TS might not be generally altered in TS motor cortex.

Compared to control subjects, TS subjects showed no significantly different resting motor thresholds as shown in other studies (Ziemann et al., 1997; Moll et al., 1999, 2001; Orth et al., 2005; Heise et al., 2010). However, when TMS was applied at progressive suprathreshold intensities, MEP recruitment curves were shallower in subjects with TS (Orth et al., 2008). The reported descriptively lower MEP amplitude at 110% would be in line with a shallower I/O curve. For most subjects, 40 and 60% MSO were subthreshold stimulation intensities, so no MEP changes corresponding to the TMS-evoked N100 could be obtained. Furthermore, motor cortex excitability was shown to be reduced in TS when examined at suprathreshold intensity during movement preparation (Heise et al., 2010; Draper et al., 2015) as well as movement execution (Jackson et al., 2013).

Concise, our data showed a reduced modulational effects of motor cortical inhibition in early adolescent subjects with TS for both motor states (movement execution more strongly than movement preparation) and increasing external stimulation, leading to a shallower stimulus-intensity slope of the TMS-evoked N100 component. These findings corroborate to the notion that the responsivity and recruitment of synaptic inhibition is deficient to both top-down modulation and external stimulation in early adolescent TS whereas axonal excitability is normal (Orth et al., 2005). Differences of control subjects and TS subjects may arise due to differences in balancing between motor cortical excitatory and inhibitory processes. Orth et al. (2005) found a reduced inhibitory interaction between sensory input and motor output in TS. They assumed that sensory input could lead to a reduction of motor cortical output in order to prevent involuntary movements. Therefore, a reduced disinhibition during distinct motor states and in response to external stimulation could represent a mechanism to reduce the triggering of tic movements. Differences of cortical inhibition might arise due to a divergent input from multiple sites within the cortico-basal ganglia-thalamocortical circuit to the primary motor cortex. A recent hypothesis classifies tics rather as a surplus of action due to an abnormally strong perception-action binding (Beste and Münchau, 2018). Our finding that modulation of motor cortex inhibition by top-down control and by external stimulation was reduced in TS, would be well compatible with increased perception-action binding, i.e., a control of motor cortex excitability by other sources than within the motor system. A reduced top-down modulation of motor cortex excitability could be seen as contributing to this strong perception-action binding due to relatively stronger bottom-up than top-down control. However, the similar effect of varying movement related brain states and stimulation intensity rather points towards a reduced motor inhibitory reserve to any kind of modulation within the motor system. In any case, our findings are well compatible with increased perception-action binding and point towards a specific contribution of the developing motor system.

So far, mechanisms underlying altered top-down modulation of motor cortical inhibition in TS have not been well understood, likely because both, short- and long-range cortical patterns of cortical connectivity may be involved. Various motor cortical excitability measures in TS lead to the assumption that all motor cortical circuits may show a reduced gain (for reviews, see Orth, 2009; Orth and Münchau, 2013). Many recent studies have focused specifically on the role of the supplementary motor area (SMA) with regard to TS pathophysiology and showed the following: First, the SMA shows increased activity immediately before the onset of a tic (Bohlhalter et al., 2006). Second, functional connectivity between SMA and motor cortex is increased in TS subjects compared to control subjects (Franzkowiak et al., 2012). Third, inhibitory repetitive TMS applied to the SMA caused a decrease in tic frequency (Mantovani et al., 2006; Kwon et al., 2011; Le et al., 2013). Fourth, using magnetic resonance spectroscopy, Draper et al. (2014) recently showed that GABA concentration related to SMA was increased in TS subjects compared to controls. Moreover, GABA concentration within the SMA was inversely associated with motor cortex excitability. The altered modulation of the TMS evoked N100 component during internal modulation by movement states could be caused by "upstream" modifications in the SMA. However, we also observed an altered modulation of the TMS-evoked N100 when the primary motor cortex was stimulated at rest with different intensities. This suggests either a deficit directly within the primary motor cortex or a tonic effect of SMA inputs or other circuits (e.g., including the basal ganglia) on the primary motor cortex at rest. From our data, we cannot infer which other cortical or subcortical areas may be involved in reduced efficiency of motor cortical inhibition in TS or which subcortical or cortical areas may act as "tic generators," creating unintended motor system excitation and triggering of tic movements.

Even though our TS sample did not exhibit a uniform operationalization of motor states regarding movement preparation and initiation in comparison to previous studies, the most striking distinction appears to be the lower age range of the investigated TS sample. Many TS subjects gain control over their tics during adolescence and experience symptom relief reaching adulthood. It is presumed, that compensatory changes in brain structure and function of adolescent TS subjects lead to an elevated tonic inhibition which in turn improve the control over motor output (Plessen et al., 2004; Serrien et al., 2005; Mueller et al., 2006; Jackson et al., 2011; Jung et al., 2013). However, in our study, we investigated a reduced responsiveness of the motor cortex rather than a generally increased cortical inhibition. The age of the investigated TS sample could play a major role regarding reported differences in TS related mechanisms. Since TS shows an age-related development reaching the maximum severity of symptoms in early adolescence (Bloch and Leckman, 2009), compensatory mechanisms may adapt to developmental changes of underlying deficits. It is conceivable that a reduced motor cortical output as a response to external input is no longer sufficient to control

involuntary movements effectively and may need to be replaced or extended by an overall elevated tonic inhibition.

4.2. Limitations

It should be noted that some confounding influences may not be completely ruled out regarding the TMS-evoked N100 component, such as the sound produced upon TMS pulse emission. Although all participants wore earplugs to minimize sensory confounds, it has been shown that auditory evoked potentials (AEP) are nonetheless at least partially superimposed upon the TMS-evoked N100 amplitude (Ter Braack et al., 2015). Besides AEPs, also SSEPs can have an influence on TEPs. However, previous studies investigated that early SSEP components occur with a latency of around 20 ms following the pulse (Verroust et al., 1990). Pokorny et al. (2022) showed, that late SSEP components are most prominent over contralateral somatosensory areas, in contrast to the analyzed N100 potential (ipsilaterally to the stimulation). In this context, it has to be considered that most patients with TS experience sensory hypersensitivity to internal and external stimuli, due to altered central processing of perceptual information, including auditory stimuli (Kleimaker et al., 2020). Therefore, it cannot be ruled out, that AEPs and SSEPs had a divergent influence on the TMS evoked N100 component of the analyzed groups. However, the analysis of broad TMS-evoked N100 areas under the curve should have minimized possible AEP and SSEP influences. Moreover, children show a reduced auditory N100 component projecting from the auditory cortex to central areas (Bender et al., 2005). No ICA components with characteristic AEP topography could be detected, confounding our data. AEPs show a lower amplitude, less duration and less lateralized potentials than the TMS-evoked N100 component reported here.

5. Conclusion

Single-pulse TMS was used to assess alterations in motor cortical excitability during resting condition, movement preparation and movement execution in young adolescents with TS. Our data showed a reduced cortical responsiveness of TS subjects to external stimulation by TMS and a reduced modulational effects of movement related brain states on motor cortical inhibition, compared to control subjects. These results provide preliminary evidence of altered modulation of motor cortical inhibition related to $GABA_B$-mediated inhibitory processes and show evidence for a reduced efficiency of the primary motor cortical inhibition (reduced "inhibitory reserve") in TS.

Data availability statement

The datasets presented in this article are not readily available because participants have not consented to the transfer of data. Requests to access the datasets should be directed to julia.schmidgen@uk-koeln.de.

Ethics statement

The studies involving humans were approved by Ethics Committee at the TU Dresden. The studies were conducted in accordance with the local legislation and institutional requirements. Written informed consent for participation in this study was provided by the participants' legal guardians/next of kin.

Author contributions

JS contributed to the main data analysis, to interpretation of the results and to manuscript writing. SB contributed to both the conception and design of the study, provided supervision for data analysis, and edited the manuscript. KK and VR contributed to manuscript revision. All authors contributed to the article and approved the submitted version.

Funding

This work was funded by the Deutsche Forschungsgemeinschaft (DFG, German Research Foundation) – Project-ID 431549029–SFB 1451.

Acknowledgments

We would like to thank Gabriel Dippel for his help with data acquisition, data evaluation, and the writing of earlier versions of this manuscript.

Conflict of interest

KK was employed by Forschungszentrum Jülich GmbH.

The remaining authors declare that the research was conducted in the absence of any commercial or financial relationships that could be construed as a potential conflict of interest.

Publisher's note

All claims expressed in this article are solely those of the authors and do not necessarily represent those of their affiliated organizations, or those of the publisher, the editors and the reviewers. Any product that may be evaluated in this article, or claim that may be made by its manufacturer, is not guaranteed or endorsed by the publisher.

References

Bender, S., Basseler, K., Sebastian, I., Resch, F., Kammer, T., Oelkers-Ax, R., et al. (2005). Electroencephalographic response to transcranial magnetic stimulation in children: evidence for giant inhibitory potentials. *Ann. Neurol.* 58, 58–67. doi: 10.1002/ana.20521

Bender, S., Oelkers-Ax, R., Resch, F., and Weisbrod, M. (2006). Frontal lobe involvement in the processing of meaningful auditory stimuli develops during childhood and adolescence. *NeuroImage* 33, 759–773. doi: 10.1016/j.neuroimage.2006.07.003

Beste, C., and Münchau, A. (2018). Tics and Tourette syndrome—surplus of actions rather than disorder?. *Movement Disorders*, 33, 238–242.

Bloch, M. H., and Leckman, J. F. (2009). Clinical course of Tourette syndrome. *J. Psychosom. Res.* 67, 497–501. doi: 10.1016/j.jpsychores.2009.09.002

Bohlhalter, S., Goldfine, A., Matteson, S., Garraux, G., Hanakawa, T., Kansaku, K., et al. (2006). Neural correlates of tic generation in Tourette syndrome: an event-related functional MRI study. *Brain* 129, 2029–2037. doi: 10.1093/brain/awl050

Bonato, C., Miniussi, C., and Rossini, P. M. (2006). Transcranial magnetic stimulation and cortical evoked potentials: a TMS/EEG co-registration study. *Clin. Neurophysiol.* 117, 1699–1707. doi: 10.1016/j.clinph.2006.05.006

Bruckmann, S., Hauk, D., Roessner, V., Resch, F., Freitag, C. M., Kammer, T., et al. (2012). Cortical inhibition in attention deficit hyperactivity disorder: new insights from the electroencephalographic response to transcranial magnetic stimulation. *Brain* 135, 2215–2230. doi: 10.1093/brain/aws071

Brühl, B., Döpfner, M., and Lehmkuhl, G. (2000). Der Fremdbeurteilungsbogen für hyperkinetische Störungen (FBB-HKS)–Prävalenz hyperkinetischer Störungen im Elternurteil und psychometrische Kriterien. *Kindheit und Entwicklung* 9, 116–126.

Conforto, A. B., Z'Graggen, W. J., Kohl, A. S., Rösler, K. M., and Kaelin-Lang, A. (2004). Impact of coil position and electrophysiological monitoring on determination of motor thresholds to transcranial magnetic stimulation. *Clin. Neurophysiol.* 115, 812–819. doi: 10.1016/j.clinph.2003.11.010

D'Agati, E., Hoegl, T., Dippel, G., Curatolo, P., Bender, S., Kratz, O., et al. (2014). Motor cortical inhibition in ADHD: modulation of the transcranial magnetic stimulation-evoked N100 in a response control task. *J. Neural Transm.* 121, 315–325. doi: 10.1007/s00702-013-1097-7

Daskalakis, Z. J., Farzan, F., Radhu, N., and Fitzgerald, P. B. (2012). Combined transcranial magnetic stimulation and electroencephalography: its past, present and future. *Brain Res.* 1463, 93–107. doi: 10.1016/j.brainres.2012.04.045

Deisz, R. A. (1999). GABAB receptor-mediated effects in human and rat neocortical neurones in vitro. *Neuropharmacology* 38, 1755–1766. doi: 10.1016/S0028-3908(99)00136-7

Draper, A., Jude, L., Jackson, G. M., and Jackson, S. R. (2015). Motor excitability during movement preparation in Tourette syndrome. *J. Neuropsychol.* 9, 33–44. doi: 10.1111/jnp.12033

Draper, A., Stephenson, M. C., Jackson, G. M., Pépés, S., Morgan, P. S., Morris, P. G., et al. (2014). Increased GABA contributes to enhanced control over motor excitability in Tourette syndrome. *Curr. Biol.* 24, 2343–2347. doi: 10.1016/j.cub.2014.08.038

Dupont-Hadwen, J., Bestmann, S., and Stagg, C. J. (2019). Motor training modulates intracortical inhibitory dynamics in motor cortex during movement preparation. *Brain Stimul.* 12, 300–308. doi: 10.1016/j.brs.2018.11.002

Erhart, M., Döpfner, M., and Ravens-Sieberer, U.Bella Study Group (2008). Psychometric properties of two ADHD questionnaires: comparing the Conners' scale and the FBB-HKS in the general population of German children and adolescents–results of the BELLA study. *Eur. Child Adolesc. Psychiatry* 17, 106–115. doi: 10.1007/s00787-008-1012-1

Farzan, F., Barr, M. S., Hoppenbrouwers, S. S., Fitzgerald, P. B., Chen, R., Pascual-Leone, A., et al. (2013). The EEG correlates of the TMS-induced EMG silent period in humans. *NeuroImage* 83, 120–134. doi: 10.1016/j.neuroimage.2013.06.059

Franzkowiak, S., Pollok, B., Biermann-Ruben, K., Südmeyer, M., Paszek, J., Thomalla, G., et al. (2012). Motor-cortical interaction in Gilles de la Tourette syndrome. *PLoS One* 7:e27850. doi: 10.1371/journal.pone.0027850

Fuggetta, G., Pavone, E. F., Walsh, V., Kiss, M., and Eimer, M. (2006). Cortico-cortical interactions in spatial attention: a combined ERP/TMS study. *J. Neurophysiol.* 95, 3277–3280. doi: 10.1152/jn.01273.2005

Ganos, C., Kühn, S., Kahl, U., Schunke, O., Feldheim, J., Gerloff, C., et al. (2014). Action inhibition in Tourette syndrome. *Mov. Disord.* 29, 1532–1538. doi: 10.1002/mds.25944

Gilbert, D. L., Bansal, A. S., Sethuraman, G., Sallee, F. R., Zhang, J., Lipps, T., et al. (2004). Association of cortical disinhibition with tic, ADHD, and OCD severity in Tourette syndrome. *Movement Disord.* 19, 416–425. doi: 10.1002/mds.20044

Gratton, G., Coles, M. G., and Donchin, E. (1983). A new method for off-line removal of ocular artifact. *Electroencephalogr. Clin. Neurophysiol.* 55, 468–484. doi: 10.1016/0013-4694(83)90135-9

Heise, K. F., Steven, B., Liuzzi, G., Thomalla, G., Jonas, M., Müller-Vahl, K., et al. (2010). Altered modulation of intracortical excitability during movement preparation in Gilles de la Tourette syndrome. *Brain* 133, 580–590. doi: 10.1093/brain/awp299

Ilmoniemi, R. J., and Kičić, D. (2010). Methodology for combined TMS and EEG. *Brain Topogr.* 22, 233–248. doi: 10.1007/s10548-009-0123-4

Jackson, G. M., Draper, A., Dyke, K., Pépés, S. E., and Jackson, S. R. (2015). Inhibition, disinhibition, and the control of action in Tourette syndrome. *Trends Cogn. Sci.* 19, 655–665. doi: 10.1016/j.tics.2015.08.006

Jackson, S. R., Parkinson, A., Jung, J., Ryan, S. E., Morgan, P. S., Hollis, C., et al. (2011). Compensatory neural reorganization in Tourette syndrome. *Curr. Biol.* 21, 580–585. doi: 10.1016/j.cub.2011.02.047

Jackson, S. R., Parkinson, A., Manfredi, V., Millon, G., Hollis, C., and Jackson, G. M. (2013). Motor excitability is reduced prior to voluntary movements in children and adolescents with Tourette syndrome. *J. Neuropsychol.* 7, 29–44. doi: 10.1111/j.1748-6653.2012.02033.x

Jarczok, T. A., Fritsch, M., Kröger, A., Schneider, A. L., Althen, H., Siniatchkin, M., et al. (2016). Maturation of interhemispheric signal propagation in autism spectrum disorder and typically developing controls: a TMS-EEG study. *J. Neural Transm.* 123, 925–935. doi: 10.1007/s00702-016-1550-5

Jarczok, T. A., Roebruck, F., Pokorny, L., Biermann, L., Roessner, V., Klein, C., et al. (2021). Single-pulse TMS to the temporo-occipital and dorsolateral prefrontal cortex evokes lateralized long latency EEG responses at the stimulation site. *Front. Neurosci.* 15:616667. doi: 10.3389/fnins.2021.616667

Jung, J., Jackson, S. R., Parkinson, A., and Jackson, G. M. (2013). Cognitive control over motor output in Tourette syndrome. *Neurosci. Biobehav. Rev.* 37, 1016–1025. doi: 10.1016/j.neubiorev.2012.08.009

Kalanithi, P. S., Zheng, W., Kataoka, Y., DiFiglia, M., Grantz, H., Saper, C. B., et al. (2005). Altered parvalbumin-positive neuron distribution in basal ganglia of individuals with Tourette syndrome. *Proc. Natl. Acad. Sci.* 102, 13307–13312. doi: 10.1073/pnas.0502624102

Kataoka, Y., Kalanithi, P. S., Grantz, H., Schwartz, M. L., Saper, C., Leckman, J. F., et al. (2010). Decreased number of parvalbumin and cholinergic interneurons in the striatum of individuals with Tourette syndrome. *J. Comp. Neurol.* 518, 277–291. doi: 10.1002/cne.22206

Kleimaker, A., Kleimaker, M., Bäumer, T., Beste, C., and Münchau, A. (2020). Gilles de la Tourette syndrome—a disorder of action-perception integration. *Front. Neurol.* 11:597898. doi: 10.3389/fneur.2020.597898

Komssi, S., Kähkönen, S., and Ilmoniemi, R. J. (2004). The effect of stimulus intensity on brain responses evoked by transcranial magnetic stimulation. *Hum. Brain Mapp.* 21, 154–164. doi: 10.1002/hbm.10159

Kwon, H. J., Lim, W. S., Lim, M. H., Lee, S. J., Hyun, J. K., Chae, J. H., et al. (2011). 1-Hz low frequency repetitive transcranial magnetic stimulation in children with Tourette's syndrome. *Neurosci. Lett.* 492, 1–4. doi: 10.1016/j.neulet.2011.01.007

Leckman, J. F., Riddle, M. A., Hardin, M. T., Ort, S. I., Swartz, K. L., Stevenson, J. O. H. N., et al. (1989). The Yale global tic severity scale: initial testing of a clinician-rated scale of tic severity. *J. Am. Acad. Child Adolesc. Psychiatry* 28, 566–573. doi: 10.1097/00004583-198907000-00015

Le, K., Liu, L., Sun, M., Hu, L., and Xiao, N. (2013). Transcranial magnetic stimulation at 1 Hertz improves clinical symptoms in children with Tourette syndrome for at least 6 months. *J. Clin. Neurosci.* 20, 257–262. doi: 10.1016/j.jocn.2012.01.049

Määttä, S., Säisänen, L., Kallioniemi, E., Lakka, T. A., Lintu, N., Haapala, E. A., et al. (2019). Maturation changes the excitability and effective connectivity of the frontal lobe: a developmental TMS–EEG study. *Hum. Brain Mapp.* 40, 2320–2335. doi: 10.1002/hbm.24525

Mantovani, A., Lisanby, S. H., Pieraccini, F., Ulivelli, M., Castrogiovanni, P., and Rossi, S. (2006). Repetitive transcranial magnetic stimulation (rTMS) in the treatment of obsessive–compulsive disorder (OCD) and Tourette's syndrome (TS). *Int. J. Neuropsychopharmacol.* 9, 95–100. doi: 10.1017/S1461145705005729

McDonnell, M. N., Orekhov, Y., and Ziemann, U. (2006). The role of GABAB receptors in intracortical inhibition in the human motor cortex. *Exp. Brain Res.* 173, 86–93. doi: 10.1007/s00221-006-0365-2

Moll, G. H., Heinrich, H., Trott, G. E., Wirth, S., Bock, N., and Rothenberger, A. (2001). Children with comorbid attention-deficit-hyperactivity disorder and tic disorder: Evidence for additive inhibitory deficits within the motor system. *Annals Neurol.* 49, 393–396.

Moll, G. H., Wischer, S., Heinrich, H., Tergau, F., Paulus, W., and Rothenberger, A. (1999). Deficient motor control in children with tic disorder: evidence from transcranial magnetic stimulation. *Neurosci. Lett.* 272, 37–40. doi: 10.1016/S0304-3940(99)00575-3

Mueller, S. C., Jackson, G. M., Dhalla, R., Datsopoulos, S., and Hollis, C. P. (2006). Enhanced cognitive control in young people with Tourette's syndrome. *Curr. Biol.* 16, 570–573. doi: 10.1016/j.cub.2006.01.064

Nikulin, V. V., Kičić, D., Kähkönen, S., and Ilmoniemi, R. J. (2003). Modulation of electroencephalographic responses to transcranial magnetic stimulation: evidence for changes in cortical excitability related to movement. *Eur. J. Neurosci.* 18, 1206–1212. doi: 10.1046/j.1460-9568.2003.02858.x

Nowak, M., Hinson, E., Van Ede, F., Pogosyan, A., Guerra, A., Quinn, A., et al. (2017). Driving human motor cortical oscillations leads to behaviorally relevant changes in local GABAA inhibition: a tACS-TMS study. *J. Neurosci.* 37, 4481–4492. doi: 10.1523/JNEUROSCI.0098-17.2017

Oldfield, R. C. (1971). The assessment and analysis of handedness: the Edinburgh inventory. *Neuropsychologia* 9, 97–113.

Orth, M. (2009). Transcranial magnetic stimulation in Gilles de la Tourette syndrome. *Journal of psychosomatic research*, 67, 591–598.

Orth, M., Amann, B., Robertson, M. M., and Rothwell, J. C. (2005). Excitability of motor cortex inhibitory circuits in Tourette syndrome before and after single dose nicotine. *Brain* 128, 1292–1300. doi: 10.1093/brain/awh473

Orth, M., and Münchau, A. (2013). Transcranial magnetic stimulation studies of sensorimotor networks in Tourette syndrome. *Behav. Neurol.* 27, 57–64. doi: 10.1155/2013/349137

Orth, M., Münchau, A., and Rothwell, J. C. (2008). Corticospinal system excitability at rest is associated with tic severity in Tourette syndrome. *Biol. Psychiatry* 64, 248–251. doi: 10.1016/j.biopsych.2007.12.009

Orth, M., and Rothwell, J. C. (2009). Motor cortex excitability and comorbidity in Gilles de la Tourette syndrome. *J. Neurol. Neurosurg. Psychiatry* 80, 29–34. doi: 10.1136/jnnp.2008.149484

Pitler, T. A., and Alger, B. E. (1994). Differences between presynaptic and postsynaptic GABAB mechanisms in rat hippocampal pyramidal cells. *J. Neurophysiol.* 72, 2317–2327. doi: 10.1152/jn.1994.72.5.2317

Plessen, K. J., Wentzel-Larsen, T., Hugdahl, K., Feineigle, P., Klein, J., Staib, L. H., et al. (2004). Altered interhemispheric connectivity in individuals with Tourette's disorder. *Am. J. Psychiatr.* 161, 2028–2037. doi: 10.1176/appi.ajp.161.11.2028

Pokorny, L., Jarczok, T. A., and Bender, S. (2022). Topography and lateralization of long-latency trigeminal somatosensory evoked potentials. *Clin. Neurophysiol.* 135, 37–50. doi: 10.1016/j.clinph.2021.11.073

Premoli, I., Rivolta, D., Espenhahn, S., Castellanos, N., Belardinelli, P., Ziemann, U., et al. (2014). Characterization of GABAB-receptor mediated neurotransmission in the human cortex by paired-pulse TMS–EEG. *NeuroImage* 103, 152–162. doi: 10.1016/j.neuroimage.2014.09.028

Raffin, E., Harquel, S., Passera, B., Chauvin, A., Bougerol, T., and David, O. (2020). Probing regional cortical excitability via input–output properties using transcranial magnetic stimulation and electroencephalography coupling. *Finter* 41, 2741–2761. doi: 10.1002/hbm.24975

Rogasch, N. C., Daskalakis, Z. J., and Fitzgerald, P. B. (2013). Mechanisms underlying long-interval cortical inhibition in the human motor cortex: a TMS-EEG study. *J. Neurophysiol.* 109, 89–98. doi: 10.1152/jn.00762.2012

Roos, D., Biermann, L., Jarczok, T. A., and Bender, S. (2021). Local differences in cortical excitability–a systematic mapping study of the TMS-evoked N100 component. *Front. Neurosci.* 15:623692. doi: 10.3389/fnins.2021.623692

Sanger, T. D., Garg, R. R., and Chen, R. (2001). Interactions between two different inhibitory systems in the human motor cortex. *J. Physiol.* 530, 307–317. doi: 10.1111/j.1469-7793.2001.0307l.x

Schilke, E. D., Tremolizzo, L., Appollonio, I., and Ferrarese, C. (2022). Tics: neurological disorders determined by a deficit in sensorimotor gating processes. *Neurol. Sci.* 43, 5839–5850. doi: 10.1007/s10072-022-06235-0

Serrien, D. J., Orth, M., Evans, A. H., Lees, A. J., and Brown, P. (2005). Motor inhibition in patients with Gilles de la Tourette syndrome: functional activation patterns as revealed by EEG coherence. *Brain* 128, 116–125. doi: 10.1093/brain/awh318

Sheehan, D. V., Sheehan, K. H., Shytle, R. D., Janavs, J., Bannon, Y., Rogers, J. E., et al. (2010). Reliability and validity of the mini international neuropsychiatric interview for children and adolescents (MINI-KID). *J. Clin. Psychiatry* 71, 313–326. doi: 10.4088/JCP.09m05305whi

Singer, H. S., Wendlandt, J., Krieger, M., and Giuliano, J. (2001). Baclofen treatment in Tourette syndrome: a double-blind, placebo-controlled, crossover trial. *Neurology* 56, 599–604. doi: 10.1212/WNL.56.5.599

Stern, E. R., Blair, C., and Peterson, B. S. (2008). Inhibitory deficits in Tourette's syndrome. *Dev. Psychobiol.* 50, 9–18. doi: 10.1002/dev.20266

Storch, E. A., Murphy, T. K., Geffken, G. R., Sajid, M., Allen, P., Roberti, J. W., et al. (2005). Reliability and validity of the Yale global tic severity scale. *Psychol. Assess.* 17, 486–491. doi: 10.1037/1040-3590.17.4.486

Taylor, P. C., Walsh, V., and Eimer, M. (2008). Combining TMS and EEG to study cognitive function and cortico–cortico interactions. *Behav. Brain Res.* 191, 141–147. doi: 10.1016/j.bbr.2008.03.033

Taylor, P. C., Walsh, V., and Eimer, M. (2010). The neural signature of phosphene perception. *Hum. Brain Mapp.* 31, 1408–1417. doi: 10.1002/hbm.20941

Ter Braack, E. M., de Vos, C. C., and van Putten, M. J. (2015). Masking the auditory evoked potential in TMS–EEG: a comparison of various methods. *Brain Topogr.* 28, 520–528. doi: 10.1007/s10548-013-0312-z

Verroust, J., Blinowska, A., Vilfrit, R., Couperie, D., Malapert, D., and Perrier, M. (1990). Somatosensory evoked potentials from median nerve; normative data. *Electromyogr. Clin. Neurophysiol.* 30, 35–39.

Waldmann, H. C. (2008). German WISC-IV short forms: a scenario-based evaluation of statistical properties. *Diagnostica* 54, 202–210. doi: 10.1026/0012-1924.54.4.202

Wu, S. W., Gilbert, D. L., Shahana, N., Huddleston, D. A., and Mostofsky, S. H. (2012). Transcranial magnetic stimulation measures in attention-deficit/hyperactivity disorder. *Pediatr. Neurol.* 47, 177–185. doi: 10.1016/j.pediatrneurol.2012.06.003

Ziemann, U., Paulus, W., and Rothenberger, A. (1997). Decreased motor inhibition in Tourette's disorder: evidence from transcranial magnetic stimulation. *Am. J. Psychiatry* 154, 1277–1284.

6 Discussion

The main aim of this work was to investigate the neural mechanisms of motor control underlying healthy brain development and to reveal deviations observed in TS. To provide a comprehensive perspective on maturational trajectories, this dissertation integrates four manuscripts, each examining different aspects of motor control. The combination of behavioral data with multimodal neuroimaging (EEG and fMRI), as well as the integration of TMS-EEG, enables a detailed understanding of developmental restructuring processes. The following discussion integrates the key findings from these studies to identify overarching patterns, address methodological strengths and limitations, and outline directions for future research.

6.1 Summary of Main Findings across Manuscripts

The first publication focused on healthy motor network maturation. The study provides detailed evidence of developmental changes in attention allocation, motor preparation, and movement evaluation in healthy children aged 5 to 16, using high-density EEG and a directional CNV task paradigm. Behaviorally, younger children showed higher error rates and slower reaction times. The most pronounced changes in motor control were observed in children aged 5 to 8 years, following a curvilinear pattern. At the neural level, this developmental progress was reflected in increasingly more efficient recruitment of the SMA during processes related to attention allocation and movement preparation. Younger children showed increased engagement in posterior visual areas, suggesting a stimulus-driven orienting strategy, while older participants exhibited a shift toward anterior top-down attention networks. These changes support a developmental transition from reactive to proactive motor control. Additionally, mu-rhythm activity indicated a transition from ipsilateral inhibition in younger children to contralateral motor preactivation in adolescents, reflecting the maturation of hemispheric specialization.

Building on the EEG analysis of typical development, the second study investigated functional connectivity patterns in children with TS compared to age and gender-matched controls. Despite comparable behavioral performance between groups, the EEG analyses revealed pronounced deviations in TS at the network level. Following the informative S1 warning-cue of the CNV paradigm, children with TS showed widespread reductions in theta-band connectivity strength and significantly decreased network efficiency across all investigated brain regions (frontal, central, parietal, and occipital regions). These deviations may indicate

difficulties in sensorimotor integration and attentional resource allocation, but could although reflect compensatory mechanisms to prevent premature motor output. During the processing of the imperative cue S2, connectivity patterns remained altered in TS, with increased coupling observed in SMA and premotor areas. However, connectivity strength was no longer reduced, and network efficiency did not differ significantly from controls, indicating a compensatory network reorganization during late motor preparation and execution. This pattern may account for the intact motor performance observed in TS, despite preceding disruptions in connectivity during early preparatory phases.

The third study extended the analysis with fMRI-based DCM to probe effective connectivity patterns in both healthy children and adolescents and those with TS. In healthy development, improved accuracy and faster reaction times were accompanied by stronger SMA-M1 coupling and increased inhibitory influence from the intraparietal sulcus (IPS) to SMA, suggesting a developmentally refined top-down control over motor output. In contrast, children with TS exhibited, besides normal or even enhanced motor task performance, increased task-related activation in ipsilateral M1 and S1, and abnormal interhemispheric connectivity, such as increased excitatory influence from left to right IPS. These findings point to an altered integration of sensory and spatial information across hemispheres, potentially compensating for deficits in inhibitory control. A shift from an inhibitory to an excitatory influence of the IPS on the PMC in TS, as opposed to healthy motor control, may contribute to hyperexcitability in contralateral motor regions. Results indicated that TS patients may achieve normal motor performance by recruiting additional, reactive control mechanisms.

The fourth study combines TMS and EEG to directly compare dynamic motor cortex inhibition in healthy development and TS-related deviations. In both groups, developmental changes were characterized by a significant age-related reduction in N100 amplitudes during rest, reflecting the typical maturation of cortical inhibitory circuits and improved inhibitory control. Moreover, the study provides evidence for altered modulation of motor cortical inhibition in children and adolescents with TS, rather than a general reduction in inhibitory capacity. While baseline N100 amplitudes at rest were comparable between groups, individuals with TS showed a reduced modulation of N100 amplitudes in response to both rising TMS intensity and varying motor states (movement preparation and execution). These results indicate that TS involves not a global deficit in inhibition, but a reduced capacity to dynamically regulate cortical inhibition.

6.2 Integration and Interpretation

6.2.1 Healthy Development of Motor Control

Across all studies, behavioral improvements, characterized by reduced reaction times and improved accuracy, were accompanied by increasingly refined motor-related brain activation and connectivity patterns. The findings reinforce and extend previous work showing that motor performance and underlying neural activation mature well into adolescence (Constantinidis & Luna, 2019; Schulte et al., 2020). Both neuroimaging studies highlighted the crucial involvement of the SMA in maturational processes. While EEG data indicated an increased and earlier regulatory influence of the SMA on preparatory processes of motor control, fMRI data revealed pronounced connectivity changes, specifically a shift in SMA influence on ipsilateral M1 from inhibitory to excitatory, reflecting maturation of top-down motor regulation. Notably, this shift in SMA-M1 connectivity correlated with task accuracy, directly linking these neural changes to improvements in motor control. Furthermore, an increased inhibitory influence of the IPS on the SMA was also associated with higher task accuracy, reflecting the integration of cognitive and motor demands (Chen et al., 2010; Nachev et al., 2008; P. Nachev et al., 2007).

Maturational changes in SMA integration were accompanied by a shift toward increased contralateral motor excitation and reduced ipsilateral recruitment. While fMRI revealed an age-related increase in left parietal activity (IPL, IPS, SPL, postcentral gyrus), regions central to attention, sensorimotor integration, and motor planning (Adleman et al., 2002; Grefkes et al., 2004; Hoffstaedter et al., 2013), EEG data showed a reduction in posterior-temporal and occipital activity during processes related to early orienting responses. These results seem to be contradictory, however likely reflect differences in task-specific demands and motor control processes. The fMRI task involved direct sensorimotor integration, requiring participants to respond immediately to arrow cues. This task engages parietal regions critical for visuomotor transformation (Andersen & Buneo, 2002; Culham & Valyear, 2006; Gogtay et al., 2004), and the observed increase in left parietal activity with age suggests enhanced efficiency and maturation of these sensorimotor pathways (Casey et al., 2005; Scherf et al., 2006). In contrast, the EEG task emphasized anticipatory processes, with participants preparing for an upcoming response following a warning stimulus in a CNV paradigm. Importantly, the analyzed iCNV time window primarily captures preparatory attentional and cognitive control mechanisms, rather than processes of sensorimotor integration (Bender et al., 2004; Nagai et al., 2004;

Röhricht et al., 2018). The observed reduction in posterior activity with age likely indicates a developmental refinement of attentional allocation, as older participants may rely less on visual and associative regions during the preparatory phase (Casey et al., 2005; Konrad & Eickhoff, 2010; Turoman et al., 2021). Thus, these findings highlight that developmental changes in neural activity are closely modulated by the distinct cognitive and motor demands of each context.

TMS-EEG data provided additional insight into the maturation of intracortical inhibitory mechanisms. Specifically, when TMS was applied over M1, I observed an age-related decrease in the amplitude of the TMS-evoked N100 component. The N100 is widely considered a marker of $GABA_B$-mediated inhibitory processes in the cortex (X. Du et al., 2018; Harrington & Hammond-Tooke, 2015; Premoli et al., 2014). This developmental reduction in N100 amplitude suggests a refinement of inhibitory and excitatory circuits within M1 as children mature into adolescence. Such changes likely reflect increased neural efficiency and a shift toward more precise, context-dependent modulation of motor cortical excitability, supporting the observed improvements in motor control and coordination.

The analyses showed that basic sensorimotor networks are present in early childhood, however, their organization evolves from local, random connectivity toward more globally efficient and integrated patterns through adolescence (Berchicci et al., 2015; Fair et al., 2007; Supekar et al., 2009). Recent studies extended the developmental framework by integrating the role of motor skill training and cognitive development during critical periods (Chen et al., 2024; Veldman et al., 2019). These findings expand our results by suggesting that both natural maturation and extended motor experiences contribute to the refinement of neural circuits supporting motor control. Motor network development is not a linear process, but a dynamic reorganization of neural systems driven by both intrinsic maturation and experience-dependent plasticity. This reorganization is accompanied by a fundamental age-related shift from predominantly reactive motor control in early childhood to increasingly proactive, anticipatory control in older subjects, reflecting the increasing integration of cognitive and motor processes (Chevalier et al., 2014; Killikelly & Szucs, 2013). Together, these multimodal findings provide a comprehensive framework for understanding how the maturation of both large-scale networks and local inhibitory mechanisms supports the development of efficient, flexible motor control throughout childhood and adolescence.

6.2.2 TS-related Deviations in Motor Control

When comparing these healthy developmental trajectories with TS-related findings, the data provide pronounced evidence that widespread and multi-level deviations in motor network organization and function characterize the disorder. The analyses revealed that children and adolescents with TS show alterations that extend the classical cortico-striatal-thalamo-cortical (CSTC) loop, involving broader sensorimotor and associative networks. Behaviorally, children and adolescents with TS showed comparable or even improved performance in motor reaction tasks, but exhibited deficits in blink suppression, highlighting specific deficits in inhibitory control.

At the neural level, EEG analyses revealed reduced theta-band connectivity and decreased network efficiency following informative warning cues. The findings indicated impaired sensorimotor integration and constrained flexibility in neural networks. This reduced variability in network function was paralleled by findings from TMS/EEG studies, which revealed reduced modulatory capacity of M1 inhibition during motor preparation and execution. Notably, as children with TS did not exhibit an increased error rate due to premature button presses following the warning cue, the observed reduction in theta connectivity may reflect a compensatory mechanism aimed at weakening perception-action binding, thereby preventing involuntary motor outputs. Recent studies have identified increased perception-action binding ("hyper-binding") to play a crucial role in TS (Friedrich et al., 2021; M. Kleimaker et al., 2020; Petruo et al., 2019). This increased binding of stimulus and response-related features results in a reduced ability to modulate motor output, especially in situations requiring behavioral flexibility. fMRI data further support this interpretation, revealing a shift from inhibitory to excitatory influence of the IPS on the PMC. This pattern contrasts with the typical inhibitory influence from IPS to premotor areas observed in healthy children and may reflect a hyperactive sensorimotor system that causes the described increased binding of perception and action.

Following the imperative stimulus (S2), when motor execution was necessary, EEG data revealed a reorganization of network coupling, particularly increased connectivity in SMA and premotor areas. Despite these changes, network efficiency and motor performance remained intact, possibly reflecting effective compensatory adaptations. fMRI-based effective connectivity findings added important spatial and directional context to the EEG results. The data showed an altered interhemispheric connectivity, particularly increased excitatory

influence from the left to the right IPS. Furthermore, subjects with TS revealed overactivation of M1 and S1, which correlated with task accuracy, suggesting recruitment of additional brain networks to support motor performance. The recruitment of additional brain regions during voluntary movements has been previously reported in other studies (Roessner et al., 2013; Roessner et al., 2012; Zapparoli et al., 2016), however, the results directly link ipsilateral M1/S1 overactivation to improved reactive motor performance. These adaptations appeared specific to reactive control mechanisms and did not reflect broader inhibitory deficits. Moreover, the finding that network efficiency improves during late stages of motor preparation and execution suggests that temporal specificity is crucial: deficits may be more prominent during anticipatory processes and stimulus processing, while reactive mechanisms may be intact or even enhanced in TS. Although these compensatory adaptations may support preserved motor performance in simple tasks, they could also contribute to motor network hyperexcitability, impaired sensorimotor integration, and abnormal perception-action binding (Beste et al., 2016; A. Kleimaker et al., 2020; Petruo et al., 2019).

While our findings, as well as other studies (Jackson et al., 2015; Jung et al., 2013; Mueller et al., 2006) demonstrate that children and adolescents with TS can maintain or even enhance task accuracy in voluntary motor control through compensatory recruitment of additional sensorimotor resources; this compensation has clear limits. Specifically, TS participants continued to show deficits in sustained motor inhibition (Yaniv et al., 2017), as evidenced in the third study by poorer performance in blink suppression tasks. This suggests that while compensatory mechanisms can support certain aspects of motor function, they do not fully extend to all inhibitory processes. The reduced flexibility in dynamically regulating inhibition, as revealed by TMS/EEG, may therefore particularly impact tasks that require sustained or proactive inhibitory control.

Taken the results together, tic-related deviations seem to underly disrupted or delayed maturation of long-range, top-down control networks that impair the ability to proactively prepare and inhibit motor responses. However, as a compensatory mechanism, the motor system adapts by recruiting additional or alternative neural resources during movement preparation and execution, which leads to normal or even improved motor performance. In summary, the multimodal findings highlight that network immaturity and compensatory reorganization are key characteristics of tic-related neural deviations. By integrating data across multiple modalities, I was able to differentiate between reduced adaptive regulatory

mechanisms, such as inflexible inhibitory control, and compensatory adaptations, including the recruitment of alternative neural pathways. TS is not a simple disorder of delayed development, but a dynamic, complex, and context-dependent network reorganization. Compensatory adaptations can enhance performance in specific domains but may coexist with persistent deficits and broader network alterations. This integrated perspective provides a framework for understanding the heterogeneity of motor control in TS and highlights potential targets for individualized intervention.

Although EEG and fMRI-derived measures, such as CNV components, oscillatory dynamics, TEPs, or connectivity patterns, were able to precisely identify developmental and disorder-related differences, the potential usability as clinical biomarkers remains limited. Given the complex and dynamic pathophysiology of TS, these measures should be interpreted cautiously, require further validation before clinical application, and might be better considered as a complementary tool rather than a stand-alone diagnostic marker. However, these data may contribute to a broader multimodal biomarker framework when integrated with other clinical and neurobiological measures (Saha et al., 2025; Woo et al., 2017). To move toward clinical applicability, future research will require larger, longitudinal datasets, replication across cohorts, and enhanced integration with behavioral data to capture the complex characteristics of TS and other disorders (Cortese et al., 2023; Ewen et al., 2019; Uddin et al., 2017). With further validation, multimodal data could help to identify clinical subtypes, predict individual developmental trajectories, and estimate intervention outcomes.

6.3 Methodological Strengths

This cumulative dissertation combines several methodological strengths that enhance the robustness and interpretability of the discussed findings. Except for TMS/EEG findings, analyses were based on a shared, well-characterized cohort of children and adolescents, including both typically developing individuals and participants with TS. This consistency across studies increased the comparability of the reported results.

A key strength lies in the multimodal approach (Barch & Carter, 2016), integrating high-temporal-resolution EEG, TMS-evoked EEG measures, and high-spatial-resolution fMRI. This combination enabled complementary insights: EEG allowed for the precise temporal tracking of motor preparation and cognitive control processes (e.g., CNV, oscillatory activity, and

connectivity dynamics), while TMS-EEG enabled the direct assessment of cortical excitability and inhibitory function. In parallel, fMRI provided spatially detailed insights into motor network connectivity and its developmental changes. By integrating these methods, I enabled a more comprehensive understanding of the neurophysiological mechanisms underlying motor control than any single modality alone could provide. The use of advanced connectivity analyses, such as sensor-space graph theoretical measures in EEG and effective connectivity modeling in fMRI (DCM), reflects a further methodological strength (Bassett & Sporns, 2017; Friston et al., 2003; Rubinov & Sporns, 2010; Stam & Reijneveld, 2007). These analyses moved beyond traditional activation-based approaches and allowed for an investigation of network-level dynamics and directional interactions between brain regions. This was particularly important for understanding sensorimotor integration and the mechanisms of compensation in TS.

In addition, the age range and inclusion of young children starting at age five allowed the investigation of childhood developmental changes, a period often underrepresented in neuroimaging studies, due to methodological and practical challenges (Gilmore et al., 2018). This enabled the identification of non-linear developmental patterns (Casey et al., 2005; Johnson, 2011). Moreover, including younger children enhances the sensitivity to detect critical periods of increased neuroplasticity, when interventions or environmental factors may have the highest impact on brain reorganization processes.

6.4 Limitations and Methodological Considerations

While each study in this work addressed its specific methodological limitations, it is important to consider general and shared constraints to place the findings in a broader context and to guide future research.

One major limitation across the studies is the cross-sectional design, which restricts the ability to draw conclusions about individual developmental trajectories or to capture intra-individual changes over time. A longitudinal approach would have been particularly valuable for examining how motor control and brain connectivity evolve within the same individuals and how these changes relate to symptom persistence or remission in children with TS. A longitudinal design offers several advantages: (1) reduces the influence of inter-individual variability and between-subject noise, (2) enables precise analysis of individual developmental

trajectories, (3) links neural changes to behavioral or symptomatic progression, (4) enables the identification of neural predictors of future behavioral outcomes or symptom development and a more reliable identification of biomarkers.

Another primary limitation involves the sample size, particularly for the analysis of TS-related neural and behavioral deviations. Small sample sizes limit statistical power and the generalizability of the findings. Power failure can lead to a reduced probability that a statistically significant finding corresponds to true neuronal effects and significantly reduce reproducibility (Button et al., 2013). The analysis of TS-specific deviations was constrained by (1) the exclusion of subjects with comorbid ADHD to isolate disorder-specific effects in the second study and (b) fMRI-DCM requirements for right-handed responses and ipsilateral activation, which led to the exclusion of several participants in the third study. While this step improved the interpretability of the connectivity modeling, it reduced the final sample available for advanced analyses.

From a methodological perspective, EEG provided high temporal resolution, making it well-suited for investigating fast neural processes. However, its limited spatial resolution remains an important limitation. While the application of source reconstruction methods in the EEG studies enhanced spatio-temporal resolution (Burle et al., 2015), integrating individual MRI-based source models could have refined spatial precision even further (Michel et al., 2004). However, I chose not to implement this approach, as not all participants were able to complete fMRI sessions, which would have further reduced the sample size.

Finally, the inclusion of participants with comorbid ADHD in the TS group in the TMS-EEG and MRI-based analyses introduces potential confounding effects, as it is not possible to precisely break down the specific contributions of each condition to the observed neural and behavioral patterns. Nevertheless, this approach reflects the clinical characteristics of TS, which frequently show multiple comorbidities (Hirschtritt et al., 2015). While the integration of comorbid ADHD introduces additional variability in the data, it significantly increases the clinical relevance of the findings.

In sum, while these limitations do not undermine the main findings of this work, they highlight important areas for improvement in future studies, particularly the integration of longitudinal study designs, recruitment of larger samples, and control for confounding variables.

6.5 Future Directions

Building on the presented findings, future studies should address the methodological constraints: (1) a longitudinal study design to disentangle whether observed neural patterns reflect transient, developmental delays, persistent alterations, or compensatory adaptations, particularly concerning symptom persistence or remission, (2) integrating individual structural MRI data into EEG analysis for more accurate source localization and spatial precisicion, (3) include larger samples to improve statistical power.

Importantly, some of the methodological challenges outlined above are already being addressed in ongoing analyses using the same dataset. I am currently combining EEG with individual MRI-based source localization in the resting state, allowing for more spatially precise investigation of functional connectivity in both TS and typically developing children. These analyses include phase synchronization and EEG microstate analysis, offering deeper insights into temporal dynamics and functional organization of neuronal networks.

Building on this work, a new follow-up study has been initiated for the next funding period, with several conceptual and methodological advancements. (1) A third clinical group with ADHD has been included to allow for a more precise differentiation between TS- and ADHD-specific effects. (2) We also integrated fNIRS with EEG recordings to improve spatial resolution while preserving temporal accuracy. (3) Lastly, we introduced a hyperscanning paradigm in which children and their parents perform cooperation and competition tasks simultaneously, allowing us to investigate the effects of social interactions.

While the ongoing projects already address key limitations of the current work, further conceptual improvement could increase clinical relevance. A shift towards individual-level predictions rather than group comparisons could be highly beneficial. Machine learning algorithms, such as classifiers or regression models, could identify subject-specific neurodevelopmental characteristics that predict behavioral outcomes or treatment response. In addition, upcoming research should increase the focus on processes besides motor control. Given that TS often co-occurs with attentional and emotional regulation difficulties, it is essential to examine interactions between motor, cognitive, and affective networks across development. Further research into compensatory mechanisms may clarify whether these adaptations represent long-term benefits or impairments.

Finally, these findings can support the development of targeted interventions. Behavioral training and non-invasive neuromodulation techniques (e.g., neurofeedback, TMS) could be applied during crucial developmental phases, identified as sensitive to network reorganization. Such approaches may not only refine our understanding of developmental neuroplasticity but also offer possibilities for individualized, mechanism-based treatment strategies and outcome predictions.

7 Reference

Adleman, N. E., Menon, V., Blasey, C. M., White, C. D., Warsofsky, I. S., Glover, G. H., & Reiss, A. L. (2002). A developmental fMRI study of the Stroop color-word task. *Neuroimage*, 16(1), 61-75.

Amzica, F., & Lopes da Silva, F. H. (2017). 20C2Cellular Substrates of Brain Rhythms. In D. L. Schomer, F. H. Lopes da Silva, D. L. Schomer, & F. H. Lopes da Silva (Eds.), *Niedermeyer's Electroencephalography: Basic Principles, Clinical Applications, and Related Fields* (pp. 0). Oxford University Press. https://doi.org/10.1093/med/9780190228484.003.0002

Andersen, R. A., & Buneo, C. A. (2002). Intentional maps in posterior parietal cortex. *Annual review of neuroscience*, *25*(1), 189-220.

Aydore, S., Pantazis, D., & Leahy, R. M. (2013). A note on the phase locking value and its properties. *Neuroimage*, *74*, 231-244. https://doi.org/10.1016/j.neuroimage.2013.02.008

Baillet, S. (2022). Forward and inverse problems of MEG/EEG. In *Encyclopedia of computational neuroscience* (pp. 1464-1471). Springer.

Barch, D. M., & Carter, C. S. (2016). Functional and Structural Brain Connectivity in Psychopathology. *Biological Psychiatry: Cognitive Neuroscience and Neuroimaging*, *1*(3), 196-198. https://doi.org/https://doi.org/10.1016/j.bpsc.2016.03.006

Bassett, D. S., & Sporns, O. (2017). Network neuroscience. *Nature Neuroscience*, *20*(3), 353-364. https://doi.org/10.1038/nn.4502

Bender, S., Resch, F., Weisbrod, M., & Oelkers-Ax, R. (2004). Specific task anticipation versus unspecific orienting reaction during early contingent negative variation. *Clinical Neurophysiology*, *115*(8), 1836-1845.

Bender, S., Weisbrod, M., Bornfleth, H., Resch, F., & Oelkers-Ax, R. (2005). How do children prepare to react? Imaging maturation of motor preparation and stimulus anticipation by late contingent negative variation. *Neuroimage*, *27*(4), 737-752. https://doi.org/10.1016/j.neuroimage.2005.05.020

Bender, S., Weisbrod, M., Just, U., Pfuller, U., Parzer, P., Resch, F., & Oelkers-Ax, R. (2002). Lack of age-dependent development of the contingent negative variation (CNV) in migraine children? *Cephalalgia*, *22*(2), 132-136. https://doi.org/10.1046/j.1468-2982.2002.00334.x

Berchicci, M., Pontifex, M., Drollette, E., Pesce, C., Hillman, C., & Di Russo, F. (2015). From cognitive motor preparation to visual processing: The benefits of childhood fitness to brain health. *Neuroscience*, *298*, 211-219.

Beste, C., Tübing, J., Seeliger, H., Bäumer, T., Brandt, V., Stock, A.-K., & Münchau, A. (2016). Altered perceptual binding in Gilles de la Tourette syndrome. *Cortex*, *83*, 160-166.

Bhattacharjee, S., Kashyap, R., Abualait, T., Annabel Chen, S.-H., Yoo, W.-K., & Bashir, S. (2021). The role of primary motor cortex: more than movement execution. *Journal of motor behavior*, *53*(2), 258-274.

Biane, J. S., Scanziani, M., Tuszynski, M. H., & Conner, J. M. (2015). Motor cortex maturation is associated with reductions in recurrent connectivity among functional subpopulations

and increases in intrinsic excitability. *J Neurosci*, *35*(11), 4719-4728. https://doi.org/10.1523/jneurosci.2792-14.2015

Bloch, M. H., & Leckman, J. F. (2009). Clinical course of Tourette syndrome. *Journal of psychosomatic research*, *67*(6), 497-501.

Bloch, M. H., Peterson, B. S., Scahill, L., Otka, J., Katsovich, L., Zhang, H., & Leckman, J. F. (2006). Adulthood outcome of tic and obsessive-compulsive symptom severity in children with Tourette syndrome. *Archives of pediatrics & adolescent medicine*, *160*(1), 65-69.

Bloom, M. S., Orthmann-Murphy, J., & Grinspan, J. B. (2022). Motor learning and physical exercise in adaptive myelination and remyelination. *ASN neuro*, *14*, 17590914221097510.

Bostan, A. C., & Strick, P. L. (2010). The Cerebellum and Basal Ganglia are Interconnected. *Neuropsychology Review*, *20*(3), 261-270. https://doi.org/10.1007/s11065-010-9143-9

Böttcher, A., Wilken, S., Adelhöfer, N., Raab, M., Hoffmann, S., & Beste, C. (2023). A dissociable functional relevance of theta-and beta-band activities during complex sensorimotor integration. *Cerebral Cortex*, *33*(14), 9154-9164.

Brass, M., & Von Cramon, D. Y. (2002). The role of the frontal cortex in task preparation. *Cerebral Cortex*, *12*(9), 908-914.

Bruckmann, S., Hauk, D., Roessner, V., Resch, F., Freitag, C. M., Kammer, T., Ziemann, U., Rothenberger, A., Weisbrod, M., & Bender, S. (2012). Cortical inhibition in attention deficit hyperactivity disorder: new insights from the electroencephalographic response to transcranial magnetic stimulation. *Brain*, *135*(7), 2215-2230.

Bullmore, E., & Sporns, O. (2009). Complex brain networks: graph theoretical analysis of structural and functional systems. *Nature reviews neuroscience*, *10*(3), 186-198.

Bunge, S. A., Dudukovic, N. M., Thomason, M. E., Vaidya, C. J., & Gabrieli, J. D. (2002). Immature frontal lobe contributions to cognitive control in children: evidence from fMRI. *Neuron*, *33*(2), 301-311.

Burle, B., Spieser, L., Roger, C., Casini, L., Hasbroucq, T., & Vidal, F. (2015). Spatial and temporal resolutions of EEG: Is it really black and white? A scalp current density view. *Int J Psychophysiol*, *97*(3), 210-220. https://doi.org/10.1016/j.ijpsycho.2015.05.004

Buse, J., Schoenefeld, K., Münchau, A., & Roessner, V. (2013). Neuromodulation in Tourette syndrome: dopamine and beyond. *Neuroscience & Biobehavioral Reviews*, *37*(6), 1069-1084.

Button, K. S., Ioannidis, J. P., Mokrysz, C., Nosek, B. A., Flint, J., Robinson, E. S., & Munafò, M. R. (2013). Power failure: why small sample size undermines the reliability of neuroscience. *Nat Rev Neurosci*, *14*(5), 365-376. https://doi.org/10.1038/nrn3475

Caligiore, D., Pezzulo, G., Baldassarre, G., Bostan, A. C., Strick, P. L., Doya, K., Helmich, R. C., Dirkx, M., Houk, J., & Jörntell, H. (2017). Consensus paper: towards a systems-level view of cerebellar function: the interplay between cerebellum, basal ganglia, and cortex. *The Cerebellum*, *16*, 203-229.

Casey, B. J., Tottenham, N., Liston, C., & Durston, S. (2005). Imaging the developing brain: what have we learned about cognitive development? *Trends in cognitive sciences*, *9*(3), 104-110. https://doi.org/10.1016/j.tics.2005.01.011

Chen, D., Zhao, G., Fu, J., Shun, S., Su, L., He, Z., Chen, R., Jiang, T., Hu, X., Li, Y., & Shen, F. (2024). Effects of structured and unstructured interventions on fundamental motor skills in preschool children: a meta-analysis [Systematic Review]. *Frontiers in Public Health*, *Volume 12 - 2024*. https://doi.org/10.3389/fpubh.2024.1345566

Chen, X., Scangos, K. W., & Stuphorn, V. (2010). Supplementary motor area exerts proactive and reactive control of arm movements. *Journal of Neuroscience*, *30*(44), 14657-14675.

Chevalier, N., James, T. D., Wiebe, S. A., Nelson, J. M., & Espy, K. A. (2014). Contribution of reactive and proactive control to children's working memory performance: Insight from item recall durations in response sequence planning. *Dev Psychol*, *50*(7), 1999-2008. https://doi.org/10.1037/a0036644

Clarke, R. A., Lee, S., & Eapen, V. (2012). Pathogenetic model for Tourette syndrome delineates overlap with related neurodevelopmental disorders including Autism. *Translational Psychiatry*, *2*(9), e158-e158.

Constantinidis, C., & Luna, B. (2019). Neural substrates of inhibitory control maturation in adolescence. *Trends in neurosciences*, *42*(9), 604-616.

Cope, L. M., Hardee, J. E., Martz, M. E., Zucker, R. A., Nichols, T. E., & Heitzeg, M. M. (2020). Developmental maturation of inhibitory control circuitry in a high-risk sample: A longitudinal fMRI study. *Dev Cogn Neurosci*, *43*, 100781. https://doi.org/10.1016/j.dcn.2020.100781

Cortese, S., Solmi, M., Michelini, G., Bellato, A., Blanner, C., Canozzi, A., Eudave, L., Farhat, L. C., Højlund, M., & Köhler-Forsberg, O. (2023). Candidate diagnostic biomarkers for neurodevelopmental disorders in children and adolescents: a systematic review. *World Psychiatry*, *22*(1), 129-149.

Cruikshank, L. C., Singhal, A., Hueppelsheuser, M., & Caplan, J. B. (2012). Theta oscillations reflect a putative neural mechanism for human sensorimotor integration. *Journal of neurophysiology*, *107*(1), 65-77.

Culham, J. C., & Valyear, K. F. (2006). Human parietal cortex in action. *Current Opinion in Neurobiology*, *16*(2), 205-212. https://doi.org/https://doi.org/10.1016/j.conb.2006.03.005

Dattola, S., Morabito, F. C., Mammone, N., & La Foresta, F. (2020). Findings about loreta applied to high-density eeg—a review. *Electronics*, *9*(4), 660.

de la Peña, M. J., Gil-Robles, S., de Vega, V. M., Aracil, C., Acevedo, A., & Rodríguez, M. R. (2020). A practical approach to imaging of the supplementary motor area and its subcortical connections. *Current neurology and neuroscience reports*, *20*, 1-10.

Diedrichsen, J., & Kornysheva, K. (2015). Motor skill learning between selection and execution. *Trends in cognitive sciences*, *19*(4), 227-233.

Du, X., Rowland, L. M., Summerfelt, A., Wijtenburg, A., Chiappelli, J., Wisner, K., Kochunov, P., Choa, F.-S., & Hong, L. E. (2018). TMS evoked N100 reflects local GABA and glutamate balance. *Brain stimulation*, *11*(5), 1071-1079.

Du, X., Rowland, L. M., Summerfelt, A., Wijtenburg, A., Chiappelli, J., Wisner, K., Kochunov, P., Choa, F. S., & Hong, L. E. (2018). TMS evoked N100 reflects local GABA and glutamate balance. *Brain Stimul*, *11*(5), 1071-1079. https://doi.org/10.1016/j.brs.2018.05.002

Ebbesen, C. L., Insanally, M. N., Kopec, C. D., Murakami, M., Saiki, A., & Erlich, J. C. (2018). More than just a "motor": recent surprises from the frontal cortex. *Journal of Neuroscience*, *38*(44), 9402-9413.

Erenberg, G., Cruse, R. P., & David Rothner, A. (1987). The natural history of Tourette syndrome: A follow-up study. *Annals of Neurology: Official Journal of the American Neurological Association and the Child Neurology Society*, *22*(3), 383-385.

Ewen, J. B., Sweeney, J. A., & Potter, W. Z. (2019). Conceptual, regulatory and strategic imperatives in the early days of EEG-based biomarker validation for neurodevelopmental disabilities. *Frontiers in integrative neuroscience*, *13*, 45.

Fair, D. A., Dosenbach, N. U., Church, J. A., Cohen, A. L., Brahmbhatt, S., Miezin, F. M., Barch, D. M., Raichle, M. E., Petersen, S. E., & Schlaggar, B. L. (2007). Development of distinct control networks through segregation and integration. *Proceedings of the National Academy of Sciences*, *104*(33), 13507-13512.

Faust, T. E., Gunner, G., & Schafer, D. P. (2021). Mechanisms governing activity-dependent synaptic pruning in the developing mammalian CNS. *Nature reviews neuroscience*, *22*(11), 657-673.

Finisguerra, A., Borgatti, R., & Urgesi, C. (2019). Non-invasive brain stimulation for the rehabilitation of children and adolescents with neurodevelopmental disorders: a systematic review. *Frontiers in Psychology*, *10*, 135.

Fornito, A., & Harrison, B. J. (2012). Brain connectivity and mental illness. In (Vol. 3, pp. 72): Frontiers Research Foundation.

Franzkowiak, S., Pollok, B., Biermann-Ruben, K., Südmeyer, M., Paszek, J., Thomalla, G., Jonas, M., Orth, M., Münchau, A., & Schnitzler, A. (2012). Motor-cortical interaction in Gilles de la Tourette syndrome. *PLoS One*, *7*(1), e27850.

Friedrich, J., Spaleck, H., Schappert, R., Kleimaker, M., Verrel, J., Bäumer, T., Beste, C., & Münchau, A. (2021). Somatosensory perception–action binding in Tourette syndrome. *Scientific reports*, *11*(1), 13388. https://doi.org/10.1038/s41598-021-92761-4

Friston, K. J. (2011). Functional and effective connectivity: a review. *Brain connectivity*, *1*(1), 13-36.

Friston, K. J., Harrison, L., & Penny, W. (2003). Dynamic causal modelling. *Neuroimage*, *19*(4), 1273-1302.

Gehring, W. J., & Coles, M. G. (1994). Readiness potential. *Neurology*, *44*(11), 2212-2212-b.

Gilmore, J. H., Knickmeyer, R. C., & Gao, W. (2018). Imaging structural and functional brain development in early childhood. *Nature reviews neuroscience*, *19*(3), 123-137. https://doi.org/10.1038/nrn.2018.1

Gogtay, N., Giedd, J. N., Lusk, L., Hayashi, K. M., Greenstein, D., Vaituzis, A. C., Nugent, T. F., Herman, D. H., Clasen, L. S., Toga, A. W., Rapoport, J. L., & Thompson, P. M. (2004). Dynamic mapping of human cortical development during childhood through early adulthood. *Proceedings of the National Academy of Sciences*, *101*(21), 8174-8179. https://doi.org/doi:10.1073/pnas.0402680101

Goldberg, G. (1985). Supplementary motor area structure and function: review and hypotheses. *Behavioral and brain sciences*, *8*(4), 567-588.

Gomez, C. M., Marco, J., & Grau, C. (2003). Preparatory visuo-motor cortical network of the contingent negative variation estimated by current density. *Neuroimage*, *20*(1), 216-224. https://doi.org/10.1016/s1053-8119(03)00295-7

Greene, D. J., Williams Iii, A. C., Koller, J. M., Schlaggar, B. L., Black, K. J., & and The Tourette Association of America Neuroimaging, C. (2017). Brain structure in pediatric Tourette syndrome. *Molecular Psychiatry*, *22*(7), 972-980. https://doi.org/10.1038/mp.2016.194

Grefkes, C., Ritzl, A., Zilles, K., & Fink, G. R. (2004). Human medial intraparietal cortex subserves visuomotor coordinate transformation. *Neuroimage*, *23*(4), 1494-1506.

Groenewegen, H. J. (2003). The basal ganglia and motor control. *Neural plasticity*, *10*(1-2), 107-120.

Hall, M. D., Gipson, K. S., Gipson, S. Y.-M. T., Colvin, M. K., Nguyen, S. T., & Greenberg, E. (2025). Disrupted Cortico-Striato-Thalamo-Cortical Circuitry and Sleep Disturbances in Obsessive-Compulsive Spectrum, Chronic Tic, and Attention-Deficit/Hyperactivity Disorders. *Harvard Review of Psychiatry*, *33*(3), 114-126.

Hallett, M. (2007). Transcranial Magnetic Stimulation: A Primer. *Neuron*, *55*(2), 187-199. https://doi.org/10.1016/j.neuron.2007.06.026

Hampson, M., Tokoglu, F., King, R. A., Constable, R. T., & Leckman, J. F. (2009). Brain areas coactivating with motor cortex during chronic motor tics and intentional movements. *Biological psychiatry*, *65*(7), 594-599.

Hao, L., Peng, S., Zhou, Y., Chen, X., Qiu, J., Luo, W., Zhuang, L., Xu, J., Wang, Y., & Su, H. (2024). Neural specialization with generalizable representations underlies children's cognitive development of attention. *American Psychologist*.

Hari, R., & Salmelin, R. (1997). Human cortical oscillations: a neuromagnetic view through the skull. *Trends in neurosciences*, *20*(1), 44-49. https://doi.org/10.1016/S0166-2236(96)10065-5

Harrington, A., & Hammond-Tooke, G. D. (2015). Theta burst stimulation of the cerebellum modifies the TMS-evoked N100 potential, a marker of GABA inhibition. *PLoS One*, *10*(11), e0141284.

Hartwigsen, G., & Volz, L. J. (2021). Probing rapid network reorganization of motor and language functions via neuromodulation and neuroimaging. *Neuroimage*, *224*, 117449.

Hatsopoulos, N. G., & Suminski, A. J. (2011). Sensing with the motor cortex. *Neuron*, *72*(3), 477-487. https://doi.org/10.1016/j.neuron.2011.10.020

Hirschtritt, M. E., Lee, P. C., Pauls, D. L., Dion, Y., Grados, M. A., Illmann, C., King, R. A., Sandor, P., McMahon, W. M., Lyon, G. J., Cath, D. C., Kurlan, R., Robertson, M. M., Osiecki, L., Scharf, J. M., & Mathews, C. A. (2015). Lifetime prevalence, age of risk, and genetic relationships of comorbid psychiatric disorders in Tourette syndrome. *JAMA Psychiatry*, *72*(4), 325-333. https://doi.org/10.1001/jamapsychiatry.2014.2650

Hoffstaedter, F., Grefkes, C., Zilles, K., & Eickhoff, S. B. (2013). The "what" and "when" of self-initiated movements. *Cerebral Cortex*, *23*(3), 520-530.

Iacoboni, M. (2006). Visuo-motor integration and control in the human posterior parietal cortex: evidence from TMS and fMRI. *Neuropsychologia*, *44*(13), 2691-2699.

Ilmoniemi, R. J., & Kičić, D. (2010). Methodology for combined TMS and EEG. *Brain Topography*, *22*, 233-248.

Ismail, L. E., & Karwowski, W. (2020). A graph theory-based modeling of functional brain connectivity based on EEG: a systematic review in the context of neuroergonomics. *Ieee Access*, *8*, 155103-155135.

Jackson, G. M., Draper, A., Dyke, K., Pépés, S. E., & Jackson, S. R. (2015). Inhibition, disinhibition, and the control of action in Tourette syndrome. *Trends in cognitive sciences*, *19*(11), 655-665.

Jafari, F., Abbasi, P., Rahmati, M., Hodhodi, T., & Kazeminia, M. (2022). Systematic review and meta-analysis of Tourette syndrome prevalence; 1986 to 2022. *Pediatric neurology*, *137*, 6-16.

Jannati, A., Ryan, M. A., Kaye, H. L., Tsuboyama, M., & Rotenberg, A. (2022). Biomarkers obtained by transcranial magnetic stimulation in neurodevelopmental disorders. *Journal of Clinical Neurophysiology*, *39*(2), 135-148.

Jenson, D., Bowers, A. L., Hudock, D., & Saltuklaroglu, T. (2020). The Application of EEG Mu Rhythm Measures to Neurophysiological Research in Stuttering [Original Research]. *Frontiers in human neuroscience*, *Volume 13 - 2019*. https://doi.org/10.3389/fnhum.2019.00458

Johnson, K. A., Worbe, Y., Foote, K. D., Butson, C. R., Gunduz, A., & Okun, M. S. (2023). Tourette syndrome: clinical features, pathophysiology, and treatment. *The Lancet Neurology*, *22*(2), 147-158.

Johnson, M. H. (2011). Interactive Specialization: A domain-general framework for human functional brain development? *Developmental cognitive neuroscience*, *1*(1), 7-21. https://doi.org/https://doi.org/10.1016/j.dcn.2010.07.003

Jonkman, L. M. (2006). The development of preparation, conflict monitoring and inhibition from early childhood to young adulthood: a Go/Nogo ERP study. *Brain Res*, *1097*(1), 181-193. https://doi.org/10.1016/j.brainres.2006.04.064

Jung, J., Jackson, S. R., Parkinson, A., & Jackson, G. M. (2013). Cognitive control over motor output in Tourette syndrome. *Neuroscience & Biobehavioral Reviews*, *37*(6), 1016-1025.

Kaarre, O., Äikiä, M., Kallioniemi, E., Könönen, M., Kekkonen, V., Heikkinen, N., Kivimäki, P., Tolmunen, T., Määttä, S., & Laukkanen, E. (2018). Association of the N100 TMS-evoked potential with attentional processes: A motor cortex TMS–EEG study. *Brain and cognition*, *122*, 9-16.

Kanaan, A. S., Gerasch, S., García-García, I., Lampe, L., Pampel, A., Anwander, A., Near, J., Möller, H. E., & Müller-Vahl, K. (2017). Pathological glutamatergic neurotransmission in Gilles de la Tourette syndrome. *Brain*, *140*(1), 218-234.

Kandel, E. R., Schwartz, J. H., Jessell, T. M., Siegelbaum, S., Hudspeth, A. J., & Mack, S. (2000). *Principles of neural science* (Vol. 4). McGraw-hill New York.

Killikelly, C., & Szucs, D. (2013). Delayed development of proactive response preparation in adolescents: ERP and EMG evidence. *Dev Cogn Neurosci*, *3*, 33-43. https://doi.org/10.1016/j.dcn.2012.08.002

Kirschstein, T., & Köhling, R. (2009). What is the Source of the EEG? *Clinical EEG and Neuroscience*, *40*(3), 146-149. https://doi.org/10.1177/155005940904000305

Kleimaker, A., Kleimaker, M., Bäumer, T., Beste, C., & Münchau, A. (2020). Gilles de la Tourette syndrome—A disorder of action-perception integration. *Frontiers in Neurology*, *11*, 597898.

Kleimaker, M., Takacs, A., Conte, G., Onken, R., Verrel, J., Bäumer, T., Münchau, A., & Beste, C. (2020). Increased perception-action binding in Tourette syndrome. *Brain*, *143*(6), 1934-1945.

Knudsen, L., Guo, F., Sharoh, D., Huang, J., Blicher, J. U., Lund, T. E., Zhou, Y., Zhang, P., & Yang, Y. (2025). The laminar pattern of proprioceptive activation in human primary motor cortex. *Cerebral Cortex*, *35*(4). https://doi.org/10.1093/cercor/bhaf076

Kobayashi, M., & Pascual-Leone, A. (2003). Transcranial magnetic stimulation in neurology. *The Lancet Neurology*, *2*(3), 145-156.

Kononowicz, T. W., & Penney, T. B. (2016). The contingent negative variation (CNV): Timing isn't everything. *Current Opinion in Behavioral Sciences*, *8*, 231-237.

Konrad, K., & Eickhoff, S. B. (2010). Is the ADHD brain wired differently? A review on structural and functional connectivity in attention deficit hyperactivity disorder. *Human brain mapping*, *31*(6), 904-916.

Krämer, U. M., Solbakk, A.-K., Funderud, I., Løvstad, M., Endestad, T., & Knight, R. T. (2013). The role of the lateral prefrontal cortex in inhibitory motor control. *Cortex*, *49*(3), 837-849.

Krigolson, O. E., & Holroyd, C. B. (2007). Predictive information and error processing: The role of medial-frontal cortex during motor control. *Psychophysiology*, *44*(4), 586-595.

Kwon, H. J., Lim, W. S., Lim, M. H., Lee, S. J., Hyun, J. K., Chae, J.-H., & Paik, K. C. (2011). 1-Hz low frequency repetitive transcranial magnetic stimulation in children with Tourette's syndrome. *Neuroscience letters*, *492*(1), 1-4.

Le, K., Liu, L., Sun, M., Hu, L., & Xiao, N. (2013). Transcranial magnetic stimulation at 1 Hertz improves clinical symptoms in children with Tourette syndrome for at least 6 months. *Journal of Clinical Neuroscience*, *20*(2), 257-262.

Leckman, J. F., Cohen, D. J., Goetz, C. G., & Jankovic, J. (2001). Tourette syndrome: pieces of the puzzle. *Advances in neurology*, *85*, 369-390.

Leckman, J. F., Zhang, H., Vitale, A., Lahnin, F., Lynch, K., Bondi, C., Kim, Y. S., & Peterson, B. S. (1998). Course of tic severity in Tourette syndrome: the first two decades. *Pediatrics*, *102*(1 Pt 1), 14-19. https://doi.org/10.1542/peds.102.1.14

Lefaucheur, J.-P. (2019). Transcranial magnetic stimulation. *Handbook of clinical neurology*, *160*, 559-580.

Li, C.-L., Deng, Y.-J., He, Y.-H., Zhai, H.-C., & Jia, F.-C. (2019). The development of brain functional connectivity networks revealed by resting-state functional magnetic resonance imaging. *Neural regeneration research*, *14*(8), 1419-1429.

Lim, L., Howells, H., Radua, J., & Rubia, K. (2020). Aberrant structural connectivity in childhood maltreatment: a meta-analysis. *Neuroscience & Biobehavioral Reviews*, *116*, 406-414.

Liu, H., Schimpf, P. H., Dong, G., Gao, X., Yang, F., & Gao, S. (2005). Standardized shrinking LORETA-FOCUSS (SSLOFO): a new algorithm for spatio-temporal EEG source reconstruction. *IEEE Trans Biomed Eng*, *52*(10), 1681-1691. https://doi.org/10.1109/TBME.2005.855720

López-Vicente, M., Agcaoglu, O., Pérez-Crespo, L., Estévez-López, F., Heredia-Genestar, J. M., Mulder, R. H., Flournoy, J. C., van Duijvenvoorde, A. C. K., Güroğlu, B., White, T., Calhoun, V., Tiemeier, H., & Muetzel, R. L. (2021). Developmental Changes in Dynamic Functional Connectivity From Childhood Into Adolescence [Original Research]. *Frontiers in Systems Neuroscience*, *Volume 15 - 2021*. https://doi.org/10.3389/fnsys.2021.724805

Ludolph, A. G., Roessner, V., Münchau, A., & Müller-Vahl, K. (2012). Tourette syndrome and other tic disorders in childhood, adolescence and adulthood. *Deutsches Ärzteblatt International*, *109*(48), 821.

Määttä, S., Könönen, M., Kallioniemi, E., Lakka, T., Lintu, N., Lindi, V., Ferreri, F., Ponzo, D., & Säisänen, L. (2017). Development of cortical motor circuits between childhood and adulthood: A navigated TMS-HdEEG study. *Human brain mapping*, *38*(5), 2599-2615.

Mahone, E. M., Puts, N. A., Edden, R. A., Ryan, M., & Singer, H. S. (2018). GABA and glutamate in children with Tourette syndrome: A 1H MR spectroscopy study at 7 T. *Psychiatry Research: Neuroimaging*, *273*, 46-53.

Maia, T. V., & Conceição, V. A. (2018). Dopaminergic disturbances in Tourette syndrome: an integrative account. *Biological psychiatry*, *84*(5), 332-344.

Mall, V., Linder, M., Herpers, M., Schelle, A., Mendez-Mendez, J., Korinthenberg, R., Schumacher, M., & Spreer, J. (2005). Recruitment of the sensorimotor cortex--a developmental FMRI study. *Neuropediatrics*, *36*(6), 373-379. https://doi.org/10.1055/s-2005-873077

Mantovani, A., Leckman, J. F., Grantz, H., King, R. A., Sporn, A. L., & Lisanby, S. H. (2007). Repetitive transcranial magnetic stimulation of the supplementary motor area in the treatment of Tourette syndrome: report of two cases. *Clinical neurophysiology: official journal of the International Federation of Clinical Neurophysiology*, *118*(10), 2314-2315.

Marreiros, A. C., Stephan, K. E., & Friston, K. J. (2010). Dynamic causal modeling. *Scholarpedia*, *5*(7), 9568.

Michel, C. M., & Brunet, D. (2019). EEG source imaging: a practical review of the analysis steps. *Frontiers in Neurology*, *10*, 325.

Michel, C. M., Murray, M. M., Lantz, G., Gonzalez, S., Spinelli, L., & Grave de Peralta, R. (2004). EEG source imaging. *Clinical Neurophysiology*, *115*(10), 2195-2222. https://doi.org/https://doi.org/10.1016/j.clinph.2004.06.001

Middleton, F. A., & Strick, P. L. (2000). Basal ganglia and cerebellar loops: motor and cognitive circuits. *Brain research reviews*, *31*(2-3), 236-250.

Mitiureva, D., Bobrov, P., Rebreikina, A., & Sysoeva, O. (2023). An inclusive paradigm to study mu-rhythm properties. *International journal of psychophysiology*, *190*, 42-55.

Mueller, S. C., Jackson, G. M., Dhalla, R., Datsopoulos, S., & Hollis, C. P. (2006). Enhanced cognitive control in young people with Tourette's syndrome. *Curr Biol*, *16*(6), 570-573. https://doi.org/10.1016/j.cub.2006.01.064

Munakata, Y., & Michaelson, L. E. (2021). Executive functions in social context: Implications for conceptualizing, measuring, and supporting developmental trajectories. *Annual Review of Developmental Psychology*, *3*(1), 139-163.

Nachev, P., Kennard, C., & Husain, M. (2008). Functional role of the supplementary and pre-supplementary motor areas. *Nature reviews neuroscience*, *9*(11), 856-869.

Nachev, P., Wydell, H., O'Neill, K., Husain, M., & Kennard, C. (2007). The role of the pre-supplementary motor area in the control of action. *Neuroimage*, *36 Suppl 2*(3-3), T155-163. https://doi.org/10.1016/j.neuroimage.2007.03.034

Nachev, P., Wydell, H., O'neill, K., Husain, M., & Kennard, C. (2007). The role of the pre-supplementary motor area in the control of action. *Neuroimage*, *36*, T155-T163.

Nagai, Y., Critchley, H. D., Featherstone, E., Fenwick, P. B., Trimble, M. R., & Dolan, R. J. (2004). Brain activity relating to the contingent negative variation: an fMRI investigation. *Neuroimage*, *21*(4), 1232-1241. https://doi.org/10.1016/j.neuroimage.2003.10.036

Niedermeyer, E., & da Silva, F. L. (2005). *Electroencephalography: basic principles, clinical applications, and related fields*. Lippincott Williams & Wilkins.

Noda, Y., Zomorrodi, R., Cash, R. F., Barr, M. S., Farzan, F., Rajji, T. K., Chen, R., Daskalakis, Z. J., & Blumberger, D. M. (2017). Characterization of the influence of age on GABAA and glutamatergic mediated functions in the dorsolateral prefrontal cortex using paired-pulse TMS-EEG. *Aging (Albany NY)*, *9*(2), 556.

Oberman, L. M., & Benussi, A. (2024). Transcranial magnetic stimulation across the lifespan: impact of developmental and degenerative processes. *Biological psychiatry*, *95*(6), 581-591.

Ogawa, S., Lee, T.-M., Kay, A. R., & Tank, D. W. (1990). Brain magnetic resonance imaging with contrast dependent on blood oxygenation. *Proceedings of the National Academy of Sciences*, *87*(24), 9868-9872.

Ohbayashi, M. (2021). The roles of the cortical motor areas in sequential movements. *Frontiers in Behavioral Neuroscience*, *15*, 640659.

Palminteri, S., Lebreton, M., Worbe, Y., Hartmann, A., Lehéricy, S., Vidailhet, M., Grabli, D., & Pessiglione, M. (2011). Dopamine-dependent reinforcement of motor skill learning: evidence from Gilles de la Tourette syndrome. *Brain*, *134*(8), 2287-2301.

Pangelinan, M. M., Hatfield, B. D., & Clark, J. E. (2013). Differences in movement-related cortical activation patterns underlying motor performance in children with and without developmental coordination disorder. *J Neurophysiol*, *109*(12), 3041-3050. https://doi.org/10.1152/jn.00532.2012

Pascual-Marqui, R. D., Michel, C. M., & Lehmann, D. (1994). Low resolution electromagnetic tomography: a new method for localizing electrical activity in the brain. *International journal of psychophysiology*, *18*(1), 49-65.

Pennartz, C. M., Oude Lohuis, M. N., & Olcese, U. (2023). How 'visual'is the visual cortex? The interactions between the visual cortex and other sensory, motivational and motor

systems as enabling factors for visual perception. *Philosophical Transactions of the Royal Society B*, *378*(1886), 20220336.

Peters, S. K., Dunlop, K., & Downar, J. (2016). Cortico-striatal-thalamic loop circuits of the salience network: a central pathway in psychiatric disease and treatment. *Frontiers in Systems Neuroscience*, *10*, 104.

Peterson, B., Riddle, M. A., Cohen, D. J., Katz, L. D., Smith, J. C., Hardin, M. T., & Leckman, J. F. (1993). Reduced basal ganglia volumes in Tourette's syndrome using three-dimensional reconstruction techniques from magnetic resonance images. *Neurology*, *43*(5), 941-949. https://doi.org/10.1212/wnl.43.5.941

Peterson, B. S., Thomas, P., Kane, M. J., Scahill, L., Zhang, H., Bronen, R., King, R. A., Leckman, J. F., & Staib, L. (2003). Basal Ganglia volumes in patients with Gilles de la Tourette syndrome. *Arch Gen Psychiatry*, *60*(4), 415-424. https://doi.org/10.1001/archpsyc.60.4.415

Petruo, V., Bodmer, B., Brandt, V. C., Baumung, L., Roessner, V., Münchau, A., & Beste, C. (2019). Altered perception-action binding modulates inhibitory control in Gilles de la Tourette syndrome. *Journal of Child Psychology and Psychiatry*, *60*(9), 953-962.

Pfurtscheller, G., & Lopes da Silva, F. H. (1999). Event-related EEG/MEG synchronization and desynchronization: basic principles. *Clin Neurophysiol*, *110*(11), 1842-1857. https://doi.org/10.1016/s1388-2457(99)00141-8

Pfurtscheller, G., Woertz, M., Supp, G., & Da Silva, F. L. (2003). Early onset of post-movement beta electroencephalogram synchronization in the supplementary motor area during self-paced finger movement in man. *Neuroscience letters*, *339*(2), 111-114.

Pineda, J. A. (2005). The functional significance of mu rhythms: translating “seeing” and “hearing” into “doing”. *Brain research reviews*, *50*(1), 57-68.

Pollmann, A., Sasso, R., Bates, K., & Fuhrmann, D. (2024). Making Connections: Neurodevelopmental Changes in Brain Connectivity After Adverse Experiences in Early Adolescence. *The Journal of Neuroscience*, *44*(8), e0991232023. https://doi.org/10.1523/jneurosci.0991-23.2023

Premoli, I., Castellanos, N., Rivolta, D., Belardinelli, P., Bajo, R., Zipser, C., Espenhahn, S., Heidegger, T., Müller-Dahlhaus, F., & Ziemann, U. (2014). TMS-EEG Signatures of GABAergic Neurotransmission in the Human Cortex. *The Journal of Neuroscience*, *34*(16), 5603-5612. https://doi.org/10.1523/jneurosci.5089-13.2014

Rae, C., Raykov, P., Ambridge, E., Colling, L., van Praag, C. G., Bouyagoub, S., Polanski, L., Larsson, D., & Critchley, H. (2022). Elevated representational similarity of voluntary action and inhibition in Tourette syndrome.

Ramamoorthi, K., & Lin, Y. (2011). The contribution of GABAergic dysfunction to neurodevelopmental disorders. *Trends in molecular medicine*, *17*(8), 452-462.

Rizzolatti, G., Luppino, G., & Matelli, M. (1998). The organization of the cortical motor system: new concepts. *Electroencephalography and clinical neurophysiology*, *106*(4), 283-296. https://doi.org/https://doi.org/10.1016/S0013-4694(98)00022-4

Robertson, M. M. (2000). Tourette syndrome, associated conditions and the complexities of treatment. *Brain*, *123*(3), 425-462.

Roessner, V., Wittfoth, M., August, J. M., Rothenberger, A., Baudewig, J., & Dechent, P. (2013). Finger tapping-related activation differences in treatment-naïve pediatric Tourette syndrome: a comparison of the preferred and nonpreferred hand. *J Child Psychol Psychiatry*, *54*(3), 273-279. https://doi.org/10.1111/j.1469-7610.2012.02584.x

Roessner, V., Wittfoth, M., Schmidt-Samoa, C., Rothenberger, A., Dechent, P., & Baudewig, J. (2012). Altered motor network recruitment during finger tapping in boys with Tourette syndrome. *Hum Brain Mapp*, *33*(3), 666-675. https://doi.org/10.1002/hbm.21240

Rohrbaugh, J. W., Syndulko, K., & Lindsley, D. B. (1976). Brain wave components of the contingent negative variation in humans. *Science*, *191*(4231), 1055-1057. https://doi.org/10.1126/science.1251217

Röhricht, J., Jo, H.-G., Wittmann, M., & Schmidt, S. (2018). Exploring the maximum duration of the contingent negative variation. *International journal of psychophysiology*, *128*, 52-61.

Rubia, K., Smith, A. B., Taylor, E., & Brammer, M. (2007). Linear age-correlated functional development of right inferior fronto-striato-cerebellar networks during response inhibition and anterior cingulate during error-related processes. *Human brain mapping*, *28*(11), 1163-1177.

Rubinov, M., & Sporns, O. (2010). Complex network measures of brain connectivity: Uses and interpretations. *Neuroimage*, *52*(3), 1059-1069. https://doi.org/https://doi.org/10.1016/j.neuroimage.2009.10.003

Saetia, S., Rosas, F., Ogata, Y., Yoshimura, N., & Koike, Y. (2020). Comparison of resting-state functional and effective connectivity between default mode network and memory encoding related areas. *Journal of Neuroscience and Neurological Disorders*, *4*(1), 029-037.

Saha, S., Corben, L. A., Selvadurai, L. P., Harding, I. H., & Georgiou-Karistianis, N. (2025). Predictive machine learning and multimodal data to develop highly sensitive, composite biomarkers of disease progression in Friedreich ataxia. *Scientific reports*, *15*(1), 17629. https://doi.org/10.1038/s41598-025-01047-6

Scherf, K. S., Sweeney, J. A., & Luna, B. (2006). Brain Basis of Developmental Change in Visuospatial Working Memory. *Journal of Cognitive Neuroscience*, *18*(7), 1045-1058. https://doi.org/10.1162/jocn.2006.18.7.1045

Schmidt, B. T., Ghuman, A. S., & Huppert, T. J. (2014). Whole brain functional connectivity using phase locking measures of resting state magnetoencephalography. *Frontiers in Neuroscience*, *8*, 141.

Schulte, T., Hong, J.-Y., Sullivan, E. V., Pfefferbaum, A., Baker, F. C., Chu, W., Prouty, D., Kwon, D., Meloy, M. J., & Brumback, T. (2020). Effects of age, sex, and puberty on neural efficiency of cognitive and motor control in adolescents. *Brain imaging and behavior*, *14*, 1089-1107.

Schurger, A., Pak, J., & Roskies, A. L. (2021). What is the readiness potential? *Trends in cognitive sciences*, *25*(7), 558-570.

Segalowitz, S. J., Santesso, D. L., & Jetha, M. K. (2010). Electrophysiological changes during adolescence: a review. *Brain and cognition*, *72*(1), 86-100.

Shi, P., & Feng, X. (2022). Motor skills and cognitive benefits in children and adolescents: Relationship, mechanism and perspectives. *Frontiers in Psychology*, *13*, 1017825.

Singer, H. S., Butler, I. J., Tune, L. E., Seifert Jr, W. E., & Coyle, J. T. (1982). Dopaminergic dysfunction in Tourette syndrome. *Annals of Neurology: Official Journal of the American Neurological Association and the Child Neurology Society*, *12*(4), 361-366.

Singer, H. S., Morris, C., & Grados, M. (2010). Glutamatergic modulatory therapy for Tourette syndrome. *Medical hypotheses*, *74*(5), 862-867.

Singer, H. S., Reiss, A. L., Brown, J. E., Aylward, E. H., Shih, B., Chee, E., Harris, E. L., Reader, M. J., Chase, G. A., Bryan, R. N., & Denckla, M. B. (1993). Volumetric MRI changes in basal ganglia of children with Tourette's syndrome. *Neurology*, *43*(5), 950-950. https://doi.org/doi:10.1212/WNL.43.5.950

Smith, S. M. (2004). Overview of fMRI analysis. *The British Journal of Radiology*, *77*(suppl_2), S167-S175.

Song, J., Davey, C., Poulsen, C., Luu, P., Turovets, S., Anderson, E., Li, K., & Tucker, D. (2015). EEG source localization: Sensor density and head surface coverage. *Journal of neuroscience methods*, *256*, 9-21.

Sowell, E. R., Kan, E., Yoshii, J., Thompson, P. M., Bansal, R., Xu, D., Toga, A. W., & Peterson, B. S. (2008). Thinning of sensorimotor cortices in children with Tourette syndrome. *Nature Neuroscience*, *11*(6), 637-639. https://doi.org/10.1038/nn.2121

Sowell, E. R., Thompson, P. M., & Toga, A. W. (2004). Mapping changes in the human cortex throughout the span of life. *The Neuroscientist*, *10*(4), 372-392.

Stam, C. J., & Reijneveld, J. C. (2007). Graph theoretical analysis of complex networks in the brain. *Nonlinear Biomedical Physics*, *1*(1), 3. https://doi.org/10.1186/1753-4631-1-3

Supekar, K., Musen, M., & Menon, V. (2009). Development of large-scale functional brain networks in children. *PLoS biology*, *7*(7), e1000157.

Sur, S., & Sinha, V. K. (2009). Event-related potential: An overview. *Industrial psychiatry journal*, *18*(1), 70-73.

Talairach, P. J. (1988). Co-planar stereotaxic atlas of the human brain. *(No Title)*.

Tamnes, C. K., Østby, Y., Walhovd, K. B., Westlye, L. T., Due-Tønnessen, P., & Fjell, A. M. (2010). Intellectual abilities and white matter microstructure in development: a diffusion tensor imaging study. *Human brain mapping*, *31*(10), 1609-1625.

Tan, E., Troller-Renfree, S. V., Morales, S., Buzzell, G. A., McSweeney, M., Antúnez, M., & Fox, N. A. (2024). Theta activity and cognitive functioning: Integrating evidence from resting-state and task-related developmental electroencephalography (EEG) research. *Dev Cogn Neurosci*, *67*, 101404. https://doi.org/10.1016/j.dcn.2024.101404

Tübing, J., Gigla, B., Brandt, V. C., Verrel, J., Weissbach, A., Beste, C., Münchau, A., & Bäumer, T. (2018). Associative plasticity in supplementary motor area-motor cortex pathways in Tourette syndrome. *Scientific reports*, *8*(1), 11984.

Tudor, M., Tudor, L., & Tudor, K. I. (2005). [Hans Berger (1873-1941)--the history of electroencephalography]. *Acta Med Croatica*, *59*(4), 307-313. (Hans Berger (1873-1941)--povijest elektroencefalografije.)

Turesky, T. K., Olulade, O. A., Luetje, M. M., & Eden, G. F. (2018). An fMRI study of finger tapping in children and adults. *Hum Brain Mapp*, *39*(8), 3203-3215. https://doi.org/10.1002/hbm.24070

Turoman, N., Tivadar, R. I., Retsa, C., Maillard, A. M., Scerif, G., & Matusz, P. J. (2021). The development of attentional control mechanisms in multisensory environments. *Developmental cognitive neuroscience*, *48*, 100930. https://doi.org/https://doi.org/10.1016/j.dcn.2021.100930

Uddin, L. Q., Dajani, D. R., Voorhies, W., Bednarz, H., & Kana, R. K. (2017). Progress and roadblocks in the search for brain-based biomarkers of autism and attention-deficit/hyperactivity disorder. *Translational Psychiatry*, *7*(8), e1218-e1218. https://doi.org/10.1038/tp.2017.164

Urgen, B. A., Plank, M., Ishiguro, H., Poizner, H., & Saygin, A. P. (2013). EEG theta and Mu oscillations during perception of human and robot actions [Original Research]. *Frontiers in Neurorobotics*, *Volume 7 - 2013*. https://doi.org/10.3389/fnbot.2013.00019

Valizadeh, A., & Madadi Asl, M. (2023). Synaptic plasticity during brain development: Implications for therapeutic reorganization of neural circuits. In (pp. 14-24). https://doi.org/10.1016/B978-0-12-818872-9.00128-X

van Duijvenvoorde, A. C. K., Whitmore, L. B., Westhoff, B., & Mills, K. L. (2022). A methodological perspective on learning in the developing brain. *npj Science of Learning*, *7*(1), 12. https://doi.org/10.1038/s41539-022-00127-w

Van Rijn, H., Kononowicz, T. W., Meck, W. H., Ng, K. K., & Penney, T. B. (2011). Contingent negative variation and its relation to time estimation: a theoretical evaluation [Perspective]. *Frontiers in integrative neuroscience*, *Volume 5 - 2011*. https://doi.org/10.3389/fnint.2011.00091

Veldman, S. L., Santos, R., Jones, R. A., Sousa-Sá, E., & Okely, A. D. (2019). Associations between gross motor skills and cognitive development in toddlers. *Early human development*, *132*, 39-44.

Virameteekul, S., & Bhidayasiri, R. (2022). We Move or Are We Moved? Unpicking the Origins of Voluntary Movements to Better Understand Semivoluntary Movements. *Frontiers in Neurology*, *13*. https://doi.org/10.3389/fneur.2022.834217

Volpe, J. J., Kinney, H. C., Jensen, F. E., & Rosenberg, P. A. (2011). The developing oligodendrocyte: key cellular target in brain injury in the premature infant. *International Journal of Developmental Neuroscience*, *29*(4), 423-440.

Wakim, K. M., Foxe, J. J., & Molholm, S. (2023). Cued motor processing in autism and typical development: A high-density electrical mapping study of response-locked neural activity in children and adolescents. *European Journal of Neuroscience*, *58*(3), 2766-2786.

Walter, W. G., Cooper, R., Aldridge, V. J., McCallum, W. C., & Winter, A. L. (1964). Contingent Negative Variation : An Electric Sign of Sensori-Motor Association and Expectancy in the Human Brain. *Nature*, *203*(4943), 380-384. https://doi.org/10.1038/203380a0

Wang, G., Worrell, G., Yang, L., Wilke, C., & He, B. (2011). Interictal spike analysis of high-density EEG in patients with partial epilepsy. *Clinical Neurophysiology*, *122*(6), 1098-1105.

Weerts, T. C., & Lang, P. J. (1973). The effects of eye fixation and stimulus and response location on the contingent negative variation (CNV). *Biol Psychol*, *1*(1), 1-19. https://doi.org/10.1016/0301-0511(73)90010-0

Wen, W., Minohara, R., Hamasaki, S., Maeda, T., An, Q., Tamura, Y., Yamakawa, H., Yamashita, A., & Asama, H. (2018). The readiness potential reflects the reliability of action consequence. *Scientific reports*, *8*(1), 11865.

Wendelken, C., Ferrer, E., Ghetti, S., Bailey, S. K., Cutting, L., & Bunge, S. A. (2017). Frontoparietal structural connectivity in childhood predicts development of functional connectivity and reasoning ability: A large-scale longitudinal investigation. *Journal of Neuroscience*, *37*(35), 8549-8558.

Woo, C.-W., Chang, L. J., Lindquist, M. A., & Wager, T. D. (2017). Building better biomarkers: brain models in translational neuroimaging. *Nature Neuroscience*, *20*(3), 365-377.

Woods, D. W., Piacentini, J., Himle, M. B., & Chang, S. (2005). Premonitory Urge for Tics Scale (PUTS): initial psychometric results and examination of the premonitory urge phenomenon in youths with Tic disorders. *Journal of Developmental & Behavioral Pediatrics*, *26*(6), 397-403.

Wu, S. W., Maloney, T., Gilbert, D. L., Dixon, S. G., Horn, P. S., Huddleston, D. A., Eaton, K., & Vannest, J. (2014). Functional MRI-navigated repetitive transcranial magnetic stimulation over supplementary motor area in chronic tic disorders. *Brain stimulation*, *7*(2), 212-218.

Yan, Y., Liu, G., Cai, H., Wu, E. Q., Cai, J., Cheok, A. D., Liu, N., Li, T., & Fan, Z. (2024). A review of graph theory-based diagnosis of neurological disorders based on EEG and MRI. *Neurocomputing*, 128098.

Yang, Y., Zhou, J., Yang, H., Wang, A., Tian, Y., & Luo, R. (2025). Structural and functional alterations in the brain gray matter among Tourette syndrome patients: a multimodal meta-analysis of fMRI and VBM studies. *J Neurol*, *272*(2), 133. https://doi.org/10.1007/s00415-024-12852-w

Yaniv, A., Benaroya-Milshtein, N., Steinberg, T., Ruhrrman, D., Apter, A., & Lavidor, M. (2017). Specific executive control impairments in Tourette syndrome: The role of response inhibition. *Research in developmental disabilities*, *61*, 1-10.

Zapparoli, L., Porta, M., Gandola, M., Invernizzi, P., Colajanni, V., Servello, D., Zerbi, A., Banfi, G., & Paulesu, E. (2016). A functional magnetic resonance imaging investigation of motor control in Gilles de la Tourette syndrome during imagined and executed movements. *Eur J Neurosci*, *43*(4), 494-508. https://doi.org/10.1111/ejn.13130

9 Acknowledgements

First and foremost, I would like to thank Professor Stephan Bender for the opportunity to complete my PhD within his research group and for the trust he placed in me to carry out our project within the Collaborative Research Center. I am deeply grateful for his continuous support, valuable expertise, and constructive guidance throughout the course of my doctoral studies. I am very happy to continue being part of the group and look forward to the next chapter of our collaboration.

I would also like to extend my thanks to Professor Martin Nawrot, who has been an really helpful member of my TAC throughout this journey. His support and insightful input, especially his thoughtful ideas on the potential of my data, which helped broaden my analytical perspective, have been very valuable. Without his encouragement, I wouldn't have made it into my highly preferred biological graduate school, and I likely wouldn't be pursuing this PhD today. In this context, I would also like to sincerely acknowledge Professor Ansgar Büschge for his support throughout this process. For that, I am truly grateful.

I am very grateful for our project team, especially Professor Kerstin Konrad, who built this project with us from the ground up, always supported us whenever we faced challenges, and made a significant contribution to the improvement of my work. Another important thanks goes to Theresa for all the time we spent together on our project, for the countless measurements during long weekends, for sharing laughs and frustrations over endless data, and for many hours of problem-solving and brainstorming.

A special thanks also goes to Felix, who supported me with my analyses, came up with new ideas for my data and improved methods, and was always there whenever MATLAB decided not to cooperate.

I would like to sincerely thank the CRC1451 and its IRTG graduate school. I am very grateful to have been able to carry out this project as part of this large network. A special shout-out goes to Claudia, our coordinator, who kept everything running smoothly and was always there whenever we needed support. I'm also really thankful to all my fellow PhD students - sharing retreats, conferences, symposia, and endless rounds of peer reviews.

I also want to extend a heartfelt thanks to my family and friends for their tireless support and help throughout this journey. I'd like to give a very special thanks to my little sister Eva, who came to work with me countless times and convinced all her friends to participate in my study.

At this point, I want to express my deepest thanks to my partner Simeon for his unwavering support, his patience, his belief in me, and his constant encouragement throughout this journey.

Note. AI-based tools were used to assist with language editing and improving the readability of the manuscript.

10 Supplementary material

10.1 Study 1: From preparation to post-processing: Insights into evoked and induced cortical activity during pre-cued motor reactions in children and adolescents

Table 1. Mean ERP amplitude values [µV] ± standard deviation for each CNV component. Significances ($p \leq 0.17$) or trends towards significance ($p < .33$) are indicated for the respective values.

Evoked activity of CNV Component	*Age Group*	*SMA [µV]*	*M1 right [µV]*	*M1 left [µV]*
iCNV right response condition	5- to 8-year-old	0.28 ± 2.33	-0.44 ± 2.9	-0.11 ± 2.37
	9- to 12-year-old	-3.87 ± 2.89 *t*(-5.52); $p < .001$	-0.66 ± 2.08	-1.73 ± 2.44 *t*(-2.93); $p = .01$
	13- to 16-year-old	-2.98 ± 2.32 *t*(-4.99); $p < .001$	0.4 ± 1.11	-0.42 ± 1.86
iCNV left response condition	5- to 8-year-old	0.04 ± 3.24	-0.8 ± 3.05	-1.15 ± 1.38 *t*(-2.88); $p = .02$
	9- to 12-year-old	-3.45 ± 3.29 *t*(-4.33); $p < .001$	0.02 ± 2.34	-1.11 ± 2.77
	13- to 16-year-old	-2.58 ± 1.75 *t*(-5.73); $p < .001$	-0.21 ± 1.5	0.06 ± 2.11
lCNV right response condition	5- to 8-year-old	-0.4 ± 3.21	-0.6 ± 2.83	-0.59 ± 1.59
	9- to 12-year-old	-3.66 ± 2.66 *t*(-5.67); $p < .001$	-2.49 ± 2.07 *t*(-4.96); $p < .001$	-0.17 ± 2.08
	13- to 16-year-old	-3.3 ± 2.13 *t*(-6); $p < .001$	-1.23 ± 1.37 *t*(-3.48); $p = .004$	-0.31 ± 2.16
lCNV left response condition	5- to 8-year-old	-1.32 ± 3.61	-0.4 ± 4.35	-1.7 ± 1.87 *t*(-3.15); $p = .009$
	9- to 12-year-old	-3.52 ± 3.62 *t*(-4.02); $p < .001$	-1.05 ± 1.52 *t*(-2.84); $p = .01$	-1.31 ± 1.91 *t*(-2.84); $p = .01$
	13- to 16-year-old	-2.74 ± 1.53 *t*(-6.96); $p < .001$	-1.74 ± 1.49 *t*(-4.54); $p < .001$	-1.66 ± 1.87 *t*(-3.43); $p = .004$

PINV right response condition	5- to 8-year-old	-0.25 ± 2.94	-1.32 ± 4.29	-4.13 ± 3.01 *t*(-4.75); *p* < .001
	9- to 12-year-old	-2.73 ± 3.04 *t*(-3.7); *p* = .002	-1.57 ± 3.16 *t*(-2.05); *p* = .057	-2.53 ± 3.23 *t*(-3.23); *p* = .005
	13- to 16-year-old	-3 ± 2.18 *t*(-5.35); *p* < .001	0.15 ± 1.97	-1.49 ± 1.1 *t*(-5.26); *p* < .001
PINV left response condition	5- to 8-year-old	-1.48 ± 3.14	-2.79 ± 4.32 *t*(-2.23); *p* = .05	-3.02 ± 2.95 *t*(-3.54); *p* = .005
	9- to 12-year-old	-3.15 ± 3.66 *t*(-3.55); *p* = .003	-2.7 ± 2.08 *t*(-5.35); *p* < .001	-1.21 ± 3.66
	13- to 16-year-old	-2.49 ± 1.65 *t*(-5.86); *p* < .001	-1.24 ± 1.86 *t*(-2.58); *p* = .02	-0.56 ± 1.81

Table 2 Mean ERP latency values [ms] ± standard deviation for each CNV component.

Latencies of evoked activity of CNV Component	*Age Group*	*SMA [ms]*	*M1 right [ms]*	*M1 left [ms]*
iCNV right response condition	5- to 8-year-old	1116 ± 115	951 ± 155	1010 ± 230
	9- to 12-year-old	1057 ± 177	965 ± 223	1160 ± 192
	13- to 16-year-old	982 ± 161	1075 ± 183	1112 ± 163
iCNV left response condition	5- to 8-year-old	1136 ± 73	1091 ± 263	1108 ± 137
	9- to 12-year-old	1132 ± 182	1155 ± 215	1064 ± 149
	13- to 16-year-old	941 ± 294	1072 ± 205	998 ± 171
PINV right response condition	5- to 8-year-old	1102 ± 203	918 ± 276	1023 ± 112
	9- to 12-year-old	990 ± 265	868 ± 252	1103 ± 185
	13- to 16-year-old	942 ± 189	1169 ± 159	1097 ± 174
PINV left response condition	5- to 8-year-old	1040 ± 161	1019 ± 193	1020 ± 195
	9- to 12-year-old	898 ± 210	957 ± 209	1029 ± 138
	13- to 16-year-old	912 ± 246	1054 ± 242	1094 ± 219

Table 3 Mean LRP amplitude values [µV] ± standard deviation of alpha-ERD for each CNV component. Significances ($p < 0.5$) are indicated for the respective values.

Alpha-ERD LRP of CNV Component	*Age Group*	*M1left/ M1right [µV]*
iCNV right response condition	5- to 8-year-old	-12.73 ± 14 *t*(-3.14); *p* = .009
	9- to 12-year-old	-9.79 ± 10.64 *t*(-3.8); *p* = .002
	13- to 16-year-old	-5.83 ± 8.67 *t*(-3.77); *p* = .002
lCNV right response condition	5- to 8-year-old	-24.43 ± 27.97 *t*(-3.82); *p* = .003
	9- to 12-year-old	-27.22 ± 33.05 *t*(-3.4); *p* = .004
	13- to 16-year-old	-23.25 ± 20.22 *t*(-4.45); *p* < .001
PINV right response condition	5- to 8-year-old	-9.4 ± 12.19 *t*(-6.67); *p* = .02
	9- to 12-year-old	-2.69 ± 9.75
	13- to 16-year-old	-5.83 ± 8.67 *t*(-2.6); *p* = .02

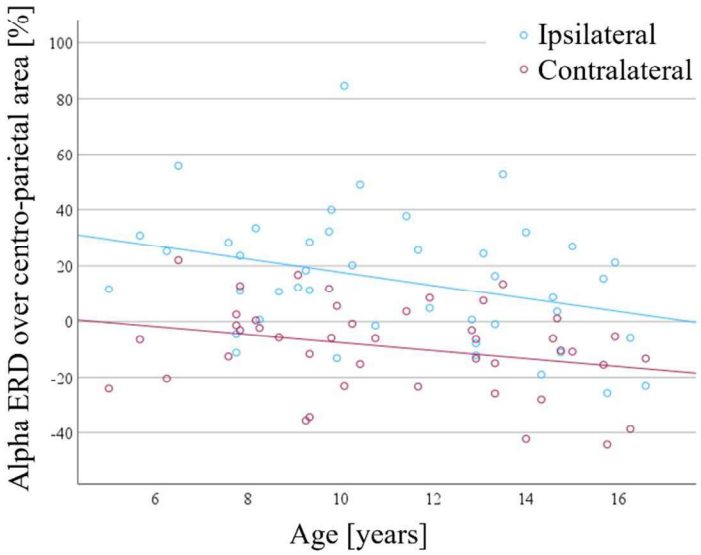

Figure 1. Scatterplot of alpha power changes over centro-parietal scalp areas. Data points represent mean values of alpha ERD (%) for both response conditions and each subject, respectively for the ipsilateral (blue dots) and contralateral hemisphere (red dots). The associated colored lines show the fitting of a linear regression with an age-related decrease of ERS over ipsilateral motor areas and an age-related increase of ERD over contralateral motor areas.

10.2 Study 2: Altered Network Connectivity and Global Efficiency in Tourette Syndrome: Insights into Sensorimotor Integration

Table 1 Significant connectivity differences between groups during S1 processing. Please note that rPLV differences were not FDR-corrected due to the large number of regions and tests, making correction impractical.

Typ	Area	Time window	Mdn [IQR] TS	Mdn [IQR] CO	U	*p* - value	r
Within Area	M1	-2900 to -2800	0.128 [0.189]	0.238 [0.159]	124	.041	.31
	POR	-3000 to -2900	0.144 [0.318]	0.438 [0.372]	112	.018	.28
	POR	-2900 to -2800	0.182 [0.299]	0.510 [0.302]	81	.001	.2
	POR	-2800 to -2700	0.030 [0.129]	0.159 [0.154]	92	.004	.23
Between Area	DLPFC – SMA/PMA	-3100 to -3000	0.081 [0.123]	0.162 [0.169]	117	.026	.29
	DLPFC – SMA/PMA	-3000 to -2900	0.126 [0.147]	0.251 [0.101]	124	.041	.31
	DLPFC – M1	-3200 to -3100	0.046 [0.032]	0.070 [0.073]	127	.049	.32
	DLPFC – M1	-3100 to -3000	0.102 [0.147]	0.218 [0.160]	101	.008	.25

	DLPFC – M1	-3000 to -2900	0.133 [0.180]	0.242 [0.214]	110	.016	.28
	DLPFC – M1	-2900 to -2800	0.153 [0.190]	0.257 [0.207]	109	.015	.27
	DLPFC – S1	-3200 to -3100	0.002 [0.110]	0.072 [0.128]	115	.022	.29
	DLPFC – S1	-3100 to -3000	0.040 [0.179]	0.167 [0.149]	100	.007	.25
	DLPFC – S1	-2900 to -2800	0.139 [0.201]	0.234 [0.207]	126	.047	.32
	DLPFC – S1	-2800 to -2700	0.151 [0.155]	0.346 [0.194]	78	.001	.2
	DLPFC – POR	-3000 to -2900	0.349 [0.285]	0.467 [0.220]	123	.039	.31
	DLPFC - POR	-2900 to -2800	0.237 [0.230]	0.392 [0.303]	99	.007	.25
	DLPFC - POR	-2800 to -2700	0.154 [0.117]	0.289 [0.305]	117	.026	.29
	SMA/PMA – S1	-2900 to -2800	0.137 [0.230]	0.302 [0.198]	101	.008	.25
	SMA/PMA - PPC	-3000 to -2900	0.300 [0.203]	0.388 [0.178]	108	.013	.27
	SMA/PMA - PPC	-2900 to -2800	0.183 [0.219]	0.301 [0.181]	114	.02	.29

	SMA/PMA - PPC	-2800 to -2700	0.305 [0.212]	0.369 [0.180]	109	.014	.28
	SMA/PMA - POR	-3000 to -2900	0.335 [0.333]	0.637 [0.438]	117	.027	.29
	SMA/PMA - POR	-2900 to -2800	0.301 [0.282]	0.510 [0.241]	101	.008	.25
	SMA/PMA - POR	-2800 to -2700	0.220 [0.153]	0.319 [0.180]	126	.047	.32
	M1 – PPC	-3000 to -2900	0.333 [0.237]	0.481 [0.260]	121	.034	.3
	M1 – PPC	-2800 to -2700	0.181 [0.127]	0.296 [0.166]	115	.022	.29
	M1 – POR	-3000 to -2900	0.347 [0.174]	0.632 [0.300]	86	.002	.22
	M1 – POR	-2900 to -2800	0.376 [0.220]	0.492 [0.292]	114	.021	.29
	M1 – POR	-2800 to -2700	0.209 [0.137]	0.316 [0.182]	92	.003	.23
	S1 – POR	-3100 to -3000	0.462 [0.279]	0.768 [0.587]	125	.044	.31
	S1 – POR	-3000 to -2900	0.274 [0.300]	0.571 [0.390]	118	.028	.3
	S1 – POR	-2800 to -2700	0.274 [0.347]	0.437 [0.343]	121	.034	.31

	PPC –POR	-3000 to -2900	0.294 [0.317]	0.660 [0.406]	118	.028	.29

Note. DLPFC = **d**orsolateral prefrontal cortex; SMA/PMA = supplementary motor area/premotor area; M1 = primary motor cortex; S1 = primary somatosensory cortex; PPC = posterior parietal cortex; POR = parieto-occipital region.

Table 2 Significant connectivity differences between groups during S2 processing. Please note that rPLV differences were not FDR-corrected due to the large number of regions and tests, making correction impractical.

Typ	Area	Time window	Mdn [IQR] TS	Mdn [IQR] CO	U	*p* - value	r
Within	DLPFC	400 to 500	0.078 [0.171]	0.183 [0.164]	117	.026	.29
	SMA/PMA	200 to 300	0.165 [0.220]	0.099 [0.173]	123	.041	.31
	SMA/PMA	300 to 400	0.275 [0.186]	0.186 [0.224]	125	.044	.31
	POR	200 to 300	0.374 [0.316]	0.618 [0.583]	125	.044	.31
Between	DLPFC – M1	400 to 500	0.253 [0.165]	0.341 [0.144]	118	.028	.3
	DLPFC – S1	0 to 100	0.080 [0.095]	0.139 [0.165]	125	.044	.31
	DLPFC – S1	300 to 400	0.166 [0.194]	0.331 [0.201]	111	.017	.28

	DLPFC – S1	400 to 500	0.161 [0.226]	0.398 [0.293]	97	.006	.24
	DLPFC - PPC	400 to 500	0.184 [0.164]	0.378 [0.219]	108	.013	.27
	SMA/PMA - PPC	400 to 500	0.203 [0.203]	0.351 [0.194]	119	.029	.3
	S1 – POR	200 to 300	0.483 [0.390]	0.706 [0.523]	115	.022	.29

Note. DLPFC = **d**orsolateral prefrontal cortex; SMA/PMA = supplementary motor area/premotor area; M1 = primary motor cortex; S1 = primary somatosensory cortex; PPC = posterior parietal cortex; POR = parieto-occipital region.

10.3 Study 3: Motor Network Organisation in Healthy Development and Chronic Tic Disorders

Table 1. Sample sizes per paradigm and analysis type

Sample size	**Healthy control subjects (HC)**		**Patients and matched controls (TD; HC)**	
	Internal	**External**	**Internal**	**External**
Behavioural	N = 52	N = 55	N = 21;17	N = 21; 20
fMRI	N = 45	N = 43	N = 14; 15	N = 12; 15
DCM	-	N = 24	-	N = 10; 10

Table 2. Age distribution of healthy control subjects across analysis samples (External condition)

Age group (Years)	**Behavioural (N = 55)**	**fMRI (N = 43)**	**DCM (N = 24)**
5-8	N = 13	N = 6	N = 4
9-11	N = 19	N = 15	N = 8
12-14	N = 14	N = 13	N = 6
15-17	N = 9	N = 9	N = 6

Statistical analysis of behavioural data

Across all trials, RTs below 150 ms, exceeding 2000 ms and outliers beyond three standard deviations (SD) from individual averages per condition were excluded.[1] Per condition, we determined participants' average individual RTs to evaluate psychomotor speed. We calculated the percentage of correct responses (i.e., the proportion of correct responses relative to the total number of stimuli presented) to indicate task accuracy. For non-informative cues, error responses were defined as misses or false alarms. For the 'External' condition, misses, false alarms, and inaccurate responses (button presses on the side opposite to the one indicated by the arrow) were defined as error responses. When subjects pressed more than one button following the stimulus presentation, only the initial response was considered. To

quantify blink reduction, we calculated the mean number of blinks across suppression and release blocks. Difference scores were derived by subtracting the mean number of blinks over the suppression blocks from the mean number of blinks over the release blocks. The absolute percentage of blink reduction across blocks was calculated by dividing the difference score by the mean number of blinks across the release blocks. To study the development of motor network functions, we explored the relationship between age (mean-centred) and task measures (RT, accuracy) using regression analyses, including linear, quadratic, and cubic models within the healthy sample. For clinical comparisons, group differences between TD patients and age-matched healthy controls were calculated using independent-samples t-test or non-parametric Mann-Whitney-U tests depending on data distribution.

Figure 1. Developmental trajectories of behavioural performance in the 'Internal' task-condition

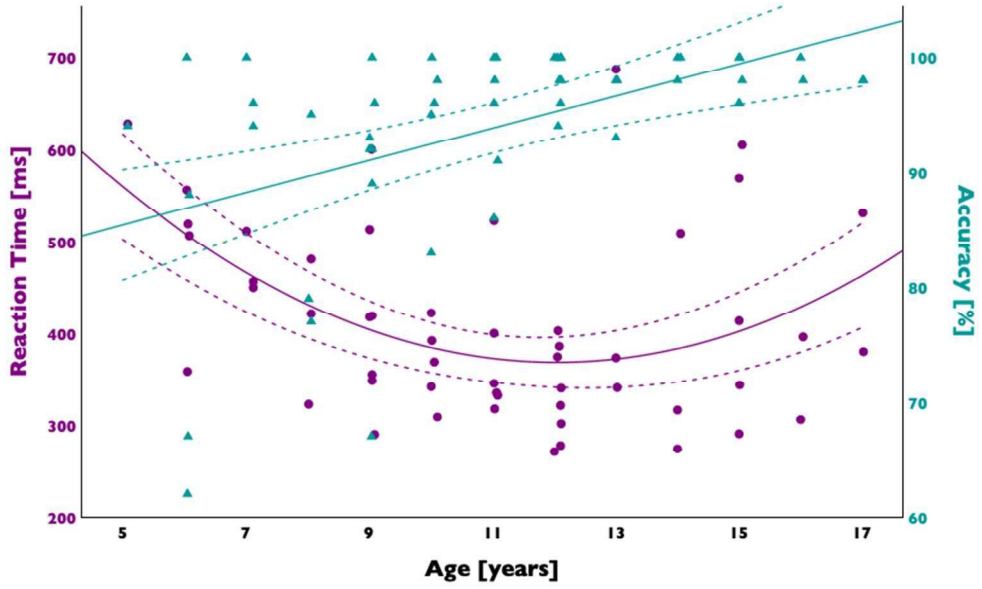

Developmental trajectory of internally cued responses in typically developing children and adolescents (N = 52). Regression analyses revealed linear age-related improvements in accuracy (teal; $R^2 = 0.240$, B = 1.401, $P < 0.001$) and a steep decline in reaction times during early childhood (purple; $R^2 = 0.359$, B = 3.475, $P < 0.001$). Reaction times are displayed in milliseconds (ms). Each data point represents one participant. Teal triangles represent individual accuracy values; purple circles represent individual reaction time values. Dashed lines indicate 95% confidence intervals for the fitted regression lines.

fMRI data acquisition and analyses

To minimize movement artifacts, participants were trained in a mock-scanner before the scanning session, receiving feedback on head-motion while practicing the fMRI paradigms in a realistic setting.

Additionally, participants' heads were fixated using foam pads surrounding the head. MRI scans were performed on a 3 Tesla Siemens MAGNETOM Prisma scanner (Siemens Healthcare, Erlangen, Germany). T1-weighted structural images were acquired by a magnetization-prepared rapid gradient echo (MP-RAGE) sequence (repetition time [T_R] = 1790 ms, echo time [T_E] = 2.53 ms, flip angle = 8°, number of slices = 176, slice thickness = 0.9 mm, interslice gap = 0.45 mm, field of view [FOV] = 256 mm, voxel size = 0.9 × 0.9 × 0.9 mm). Whole-brain T2-weighted functional images were obtained using an echoplanar imaging (EPI) multiband sequence, with blood oxygenation level-dependent (BOLD) contrast (T_R = 980 ms, T_E = 30 ms, flip angle = 70°, number of slices = 64, slice thickness = 2.0 mm, interslice gap = 0.2 mm, FOV = 207 mm, voxel size = 2.2 × 2.2 × 2.0 mm). Slices were acquired in transversal orientation in an interleaved order. Image pre-processing was performed using Statistical Parametric Mapping (SPM12; The Wellcome Centre for Human Neuroimaging, UCL Queen Square Institute of Neurology, London, UK [www.fil.ion.ucl.ac.uk/spm]) implemented in MATLAB (The MathWorks, Natick, USA). Pre-processing included slice timing about the middle slice, SPM12 standard realignment and unwarping to account for motion, co-registration to the mean EPI image, normalization to Montreal Neurological Institute (MNI) stereotactic space using unified segmentation based on the SPM tissue probability map for six tissue classes, and spatial smoothing with 8 mm full width at half-maximum isotropic Gaussian kernel, to reduce noise. Task-related blood oxygen level-dependent (BOLD) responses were modelled using the GLM framework, with contrasts capturing left- and right-handed movements (from the time of stimulus presentation until button presses) relative to baseline. Contrast images were produced as follows: 'right-handed movements > resting baseline' and 'left-handed movements > resting baseline'. Model parameter estimates and t-statistic images were submitted to group-level analysis. Separate one-sample t-tests were conducted for healthy control subjects and TD patients to explore whole-brain task-related activations for these contrasts. For the healthy control group, effects were considered significant at a family-wise error (FWE) corrected voxel-level threshold of cluster-level $P_{FWE} < 0.05$. For the TD patient group, effects were considered significant at an uncorrected voxel-level threshold of $P < 0.001$, with a cluster-level $P_{FWE} < 0.05$. Furthermore, in healthy subjects, we examined the association between age and whole-brain activation from this contrast using regression analysis, adding mean-centred age, mean-centred age-squared and mean-centred age cubed as covariates. Additionally, we used independent-samples t-test to compare task-related activity from these contrasts between TD patients and healthy controls. For these analyses, effects were considered significant if they exceeded an uncorrected ($P < 0.001$) voxel-level threshold of cluster-level $P_{FWE} < 0.05$. Cluster and local maxima labels were derived from the updated version of the AAL atlas 3 (AAL 3)[2,3] and further explored using the SPM Anatomy Toolbox, which assigns activations to the most likely cytoarchitectonic area by means of a maximum probability map.[4,5,6]

Table 3. Task activations healthy control subjects 'Internal': Left > Baseline

(P < 0.05 FWE)

Local Maxima (Side)		**x**	**y**	**z**	**Voxel**	**T-value**	**$P_{FWE-corr.}$**
Fusiform gyrus	(L)						
Cerebellum_6	(L)	-36	-68	-18	11356	10.28	< 0.001
Cerebellum_Crus (L)							
Postcentral gyrus	(R)						
Precentral gyrus	(R)	48	-18	58	7158	9.76	< 0.001
Middle frontal gyrus (R)							
Cuneus (R)							
Superior occipital gyrus	(R)	16	-104	10	517	8.87	< 0.001
Calcarine sulcus (R)							
Rolandic operculum	(L)						
Insula	(L)	-44	0	10	792	8.70	< 0.001
Frontal inferior operculum (L)							
Cerebellum_8	(R)						
Cerebellum_7b	(R)	30	-58	-48	218	6.28	< 0.001
Cerebellum_Crus1							
Heschl's gyrus	(L)						
Insula	(L)	-36	-20	8	24	6.03	0.007
Rolandic operculum (L)							
Precuneus	(L)						
Mid cingulate cortex (L)		-8	-46	60	20	5.87	0.008
Paracentral lobule (L)							

Precentral gyrus (R) Frontal inferior operculum (R) Inferior frontal gyrus (R)		60	10	30	18	5.64	0.009
Superior occipital gyrus (L) Cuneus (L) Calcarine sulcus (L)		-6	-100	20	6	5.63	0.018
Superior parietal gyrus (R) Postcentral gyrus (R) Precuneus (R)		16	-54	74	16	5.57	0.011
Insula (R) Putamen (R) Heschl's gyrus (R)		36	-18	6	22	5.48	0.007
Precentral gyrus (L) Postcentral gyrus (L) Superior frontal gyrus (L)		-40	-10	62	18	5.46	0.009
Precuneus (R) Superior parietal gyrus (R) Precuneus (L)		8	-76	52	25	5.45	0.006
Precuneus (L) Superior occipital gyrus (L) Superior parietal gyrus (L)		-12	-66	36	16	5.44	0.011
Calcarine sulcus (L) Lingual gyrus (L) Cerebellum_Crus1 (L)		-8	-90	-14	6	5.26	0.022

Per cluster, the table shows 3 local maxima > 8.0 mm apart

Table 4. Task activations healthy controls 'Internal': Right > Baseline

(P < 0.05 FWE)

Local Maxima (Side)	**x**	**y**	**z**	**Voxel**	**T-value**	**$P_{FWE-corr.}$**
Precentral gyrus (L) Postcentral gyrus (L) Superior frontal gyrus (L)	-36	-22	62	19106	12.08	< 0.001
Supplementary motor area (L) Mid cingulate gyrus (L) Supplementary motor area (R)	-6	-6	56	1165	8.20	< 0.001
Supramarginal gyrus (R) Superior temporal gyrus (R) Rolandic operculum (R)	64	-38	26	458	7.28	< 0.001
Insula (R) Frontal inferior operculum (R) Rolandic operculum (R)	44	12	-2	276	7.16	< 0.001
Middle temporal gyrus (R) Superior temporal gyrus (R) Hippocampus (R)	48	-26	-8	15	5.73	0.009
Middle occipital gyrus (L) Calcarine sulcus (L) Superior occipital gyrus (L)	-10	-104	0	8	6.03	0.018
Frontal inferior operculum (R) Inferior frontal gyrus (R) Precentral gyrus (R)	42	8	22	6	5.58	0.020

Frontal inferior operculum (R)							
Rolandic operculum (R)		54	10	12	5	5.46	0.022
Precentral gyrus (R)							
Cerebellum_Crus2	(L)						
Cerebellum_7b	(L)	-34	-68	-44	5	5.40	0.022
Cerebellum_8 (L)							

Per cluster, the table shows 3 local maxima > 8.0 mm apart

Table 5. Task activations healthy controls 'External': Left > Baseline (P < 0.05 FWE)

Local Maxima (Side)		**x**	**y**	**z**	**Voxel**	**T-value**	**$P_{FWE-corr.}$**
Precentral gyrus	(R)						
Postcentral gyrus	(R)	48	-18	62	34156	10.38	< 0.001
Middle frontal gyrus (R)							
Insula	(L)						
Rolandic operculum	(L)	-38	-4	18	885	9.37	< 0.001
Precentral gyrus (L)							
Cerebellum_8 (R)							
Cerebellum_9	(R)	28	-50	-46	73	7.11	< 0.001
Cerbellum_10 (R)							
Thalamus_PuM(R)							
Thalamus_PuL	(R)	20	-28	12	22	6.78	0.004
Hippocampus (R)							
Middle temporal gyrus	(L)						
Superior temporal gyrus	(L)	-64	-48	12	84	6.32	< 0.001
Inferior temporal gyrus (L)							

Superior frontal gyrus (L) Middle frontal gyrus (L) Inferior frontal gyrus (L)		-30	48	40	19	6.13	0.005
Mid cingulate gyrus (R) Posterior cingulate gyrus (R) Posterior cingulate gyrus (L)		8	-38	32	9	6.04	0.012
Precentral gyrus (L) Superior frontal gyrus (L) Middle frontal gyrus (L)		-38	-6	64	36	6.03	0.001
Paracentral lobule (R) Precuneus (R) Mid cingulate cortex (R)		18	-42	50	7	5.67	0.015
Paracentral lobule (R) Precuneus (R) Postcentral gyrus (R)		8	-38	58	14	5.65	0.008

Per cluster, the table shows 3 local maxima > 8.0 mm apart

Table 6. Task activations healthy controls 'External': Right > Baseline

(P < 0.05 FWE)

Local Maxima (Side)		**x**	**y**	**z**	**Voxel**	**T-value**	**$P_{FWE-corr.}$**
Precentral gyrus (L) Postcentral gyrus (L) Superior parietal gyrus (L)		-38	-30	70	32183	12.30	< 0.001

Inferior frontal gyrus (R) Precentral gyrus (R) Inferior frontal gyrus (R)		64	12	22	1419	8.87	< 0.001
Cerebellum_8 (L) Cerebellum_7b (L) Cerbellum_Crus2 (L)		-36	-58	-48	83	7.03	< 0.001
Superior parietal gyrus (L) Precuneus (R) Postcentral gyrus (R)		14	-52	62	263	6.98	0.004
Middle frontal gyrus (R) Superior frontal gyrus (R) Inferior frontal gyrus (R)		36	50	36	189	6.74	< 0.001
Cerebellum_Crus2 (L) Cerebellum_7b (L) Cerebellum_8 (L)		-14	-76	-40	43	6.35	0.001
Middle frontal gyrus (L) Superior frontal gyrus (L) Inferior frontal gyrus (L)		-32	48	38	48	6.02	0.001
Supplementary motor area (R) Superior frontal gyrus (R) Supplementary motor area (L)		12	6	74	6	5.85	0.016
Precuneus (L) Superior parietal gyrus (L) Precuneus (R)		-6	-66	48	33	5.85	0.001

Insula	(L)						
Inferior frontal gyrus	(L)	-28	32	10	5	5.69	0.019
Middle frontal gyrus (L)							
Supramarginal gyrus	(R)						
Inferior parietal gyrus	(R)	32	-42	44	9	5.67	0.012
Postcentral gyrus (R)							

Per cluster, the table shows 3 local maxima > 8.0 mm apart

Table 7. Task activations patients 'Internal': Left > Baseline (P < 0.001 unc.)

Local Maxima (Side)	**x**	**y**	**z**	**Voxel**	**T-value**	**$P_{FWE\text{-}corr.}$**
Precentral gyrus (R)						
Postcentral gyrus (R)	34	-20	58	664	5.85	0.004
Superior frontal gyrus (L)						

Per cluster, the table shows 3 local maxima > 8.0 mm apart

Table 8. Task activations patients 'Internal': Right > Baseline (P < 0.001 unc.)

Local Maxima (Side)	**x**	**y**	**z**	**Voxel**	**T-value**	**$P_{FWE\text{-}corr.}$**
Inferior occipital gyrus (R)						
Middle occipital gyrus (R)	46	-84	-8	5989	14.78	< 0.001
Inferior temporal gyrus (R)						
Precentral gyrus (L)						
Superior frontal gyrus (L)	-40	-12	70	8915	12.13	< 0.001
Postcentral gyrus (L)						
Middle frontal gyrus (L)	-36	50	20	932	8.34	< 0.001

Superior frontal gyrus (L) Inferior frontal gyrus (L)						
Cuneus (R) Superior occipital gyrus (R) Cuneus (L)	12	-94	24	401	7.48	0.005
Postcentral gyrus (R) Supramarginal gyrus (R) Precentral gyrus (R)	64	-18	50	946	7.21	< 0.001
Postcentral gyrus (R) Superior parietal gyrus (R) Inferior parietal gyrus (R)	34	-42	62	328	6.20	0.012
Supramarginal gyrus (R) Postcentral gyrus (R) Rolandic operculum (R)	46	-22	28	350	5.35	0.009

Per cluster, the table shows 3 local maxima > 8.0 mm apart

Table 9. Task activations patients 'External': Left > Baseline (P < 0.001 unc.)

Local Maxima (Side)	**x**	**y**	**z**	**Voxel**	**T-value**	**$P_{FWE\text{-}corr.}$**
Vermis_6 Vermis_4_5 Vermis_8	-2	-58	-24	226	7.04	0.036
Cerebellum_9 (L) Cerebellum_8 (L) Vermis_9	-10	-60	-44	227	6.71	0.035

Per cluster, the table shows 3 local maxima > 8.0 mm apart.

Table 10. Task activations patients 'External': Right > Baseline (P < 0.001 unc.)

Local Maxima (Side)		**x**	**y**	**z**	**Voxel**	**T-value**	**$P_{FWE-corr.}$**
Precuneus	(L)						
Precuneus	(R)	-6	-62	58	27637	11.40	< 0.001
Superior parietal gyrus (L)							
Postcentral gyrus	(R)						
Supramarginal gyrus	(R)	42	-28	38	1843	9.21	< 0.001
Precentral gyrus (R)							
Medial orbitofrontal cortex (R)							
Medial orbitofrontal cortex (L)		4	60	-12	183	7.21	0.041
Rectus (R)							
Anterior cingulate cortex	(L)						
Anterior cingulate cortex	(L)	-8	38	18	244	6.80	0.012
Superior frontal gyrus (L)							
Rolandic operculum	(R)						
Heschl's gyrus	(R)	68	0	8	298	6.71	0.005
Superior temporal gyrus (R)							

Per cluster, the table shows 3 local maxima > 8.0 mm apart.

Dynamic Causal Modelling (DCM)

DCM is a Bayesian framework incorporated into SPM12, designed to deduce hidden neuronal states based on measurements of brain activation. It can be applied to identify connectivity strengths among neuronal groups, to investigate how these connections change over time and how they are modulated depending on the context.[7]

DCM was applied to explore interhemispheric motor-network connectivity, following Michely et al.,[8] who used the paradigm to examine age-related connectivity changes in healthy adults. The same regions of interest were used to assess neural interactions across developmental stages. We specified nine ROIs

for the interhemispheric DCM model: 1. left PFC, 2. right PFC, 3. left PMC, 4. right PMC, 5. SMA, 6. left M1, 7. right M1, 8. left IPS, 9. right IPS (see Fig. 2). Time series were extracted from subject-specific coordinates defined in the 'External' condition. Within an 8-mm-radius sphere around the group peak coordinates, which were set as origin (see Table 10), we located the nearest individual activation peak coordinates from each subject's first level GLM-analysis (see Table 11 and Table 12 for group mean coordinates). We extracted the first eigenvariate of the individual BOLD time series. For extraction of time series, we employed a threshold of $P < 0.05$ (uncorrected). Following recommendations by Zeidman et al.,[9] for handling cases where ROIs showed no significant voxel response at this threshold, a stepwise lowering of the threshold was conducted in steps of 0.05, until a peak was discernible.

Figure 2. Model space for the Bayesian model selection procedure

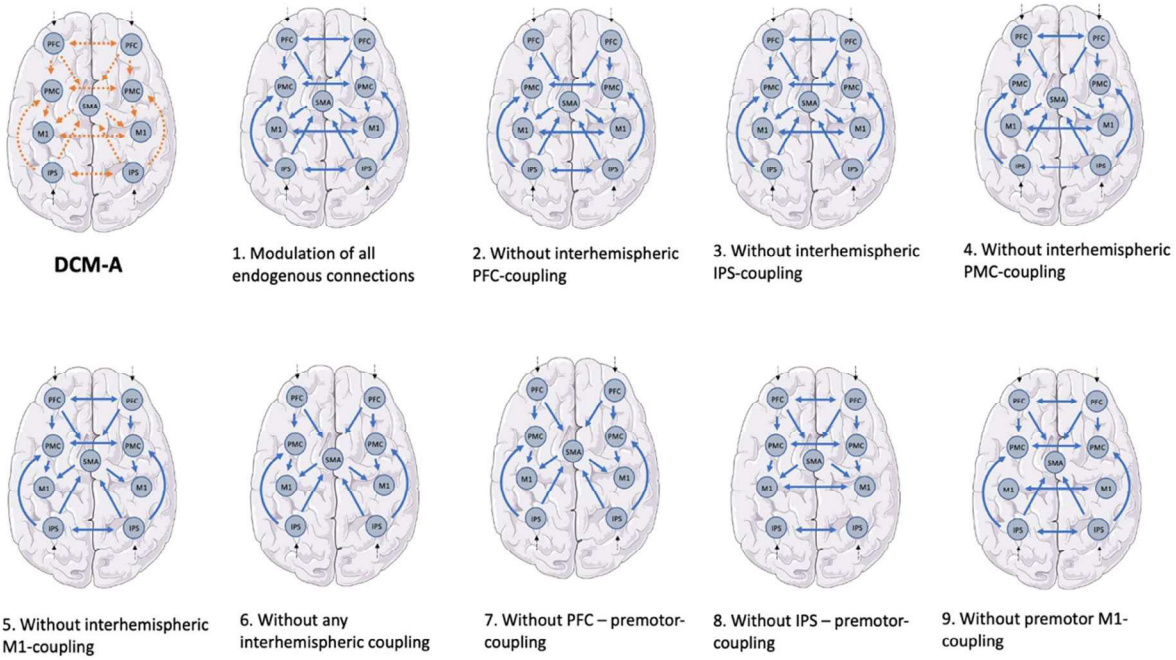

Each panel illustrates a distinct model tested using Bayesian model selection (BMS). The endogenous connectivity matrix is displayed in orange (top-left, DCM-A), while task-based connectivity matrices (DCM-B) are shown in blue across Models 1-9. Each model is labelled according to the connections excluded (e.g., Model 2: without interhemispheric PFC-PFC coupling). Arrows indicate directional connections between predefined regions of interest. PFC = prefrontal cortex; IPS = intraparietal sulcus; PMC = premotor cortex; M1 = primary motor cortex; SMA = supplementary motor area.

Figure 3. Model evidence for the selection of winning models

Healthy controls **TD patients + matched controls**

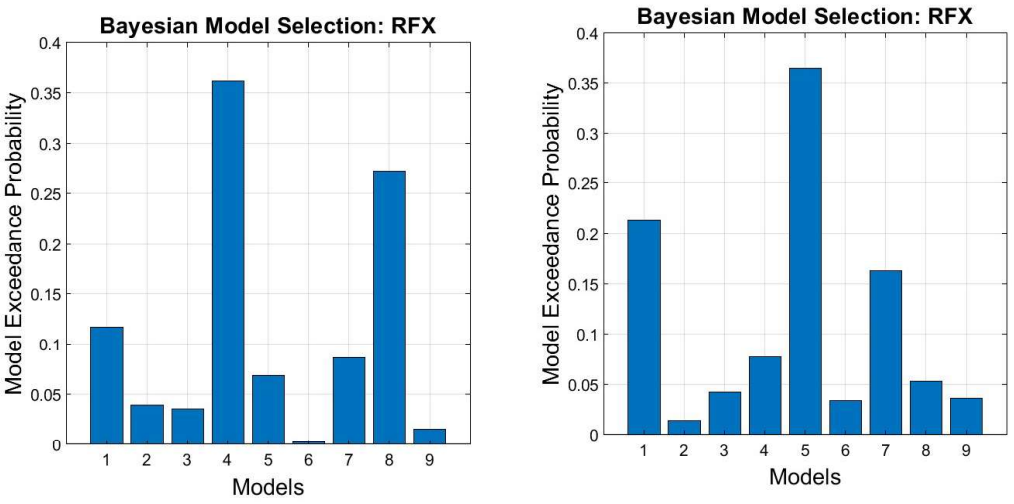

Left: Winning model for the group of healthy control subjects (N = 24) identified via Bayesian model selection (Model 4; without interhemispheric PMC coupling). **Right:** Winning model for TD patients and matched control subjects (N = 20; Model 5; without interhemispheric M1 coupling). Exceedance probabilities are shown as bar graphs. RFX = random-effects analysis; PMC = premotor cortex; M1 = primary motor cortex.

Table 11. Group peak coordinates used as origin for ROI extraction

Region	x-coordinate	y-coordinate	z-coordinate
PFC (L)	-32	48	38
PFC (R)	36	54	32
SMA	-4	-4	72
PMC (L)	-32	-18	72
PMC (R)	12	4	74
M1 (L)	-36	-28	60

M1 (R)	38	-24	72
IPS (L)	-36	-46	54
IPS (R)	54	-32	44

L = left; R = right; PFC = prefrontal cortex; SMA = supplementary motor area; PMC = premotor cortex; M1 = primary motor cortex; IPS = intraparietal sulcus.

Table 12. ROI coordinates (group mean)

Region	**Healthy control subjects**			**Patients and matched controls**		
	x- coordinate	**y-coordinate**	**z-coordinate**	**x-coordinate**	**y-coordinate**	**z-coordinate**
PFC (L)	-31.9 (± 3.1)	47.5 (± 3.0)	38.0 (± 3.3)	-32.6 (± 2.6)	47.7 (± 2.8)	38.3 (± 3.2)
PFC (R)	35.0 (± 2.0)	53.5 (± 2.8)	32.2 (± 2.3)	36.4 (± 2.3)	53.6 (± 3.1)	31.7 (± 2.1)
SMA	-3.7 (± 1.8)	-4.3 (± 2.2)	58.2 (± 2.5)	-4.2 (± 1.8)	-4.1 (± 1.3)	58.9 (± 2.6)
PMC (L)	-32.1 (± 1.6)	-18.3 (± 0.7)	71.6 (± 1.4)	-32.2 (± 1.4)	-18.0 (± 1.3)	71.6 (± 1.3)
PMC (R)	11.3 (± 3.2)	3.6 (± 2.8)	73.0 (± 3.4)	11.4 (± 3.0)	3.8 (± 2.8)	72.5 (± 2.8)
M1 (L)	-36.4 (± 1.2)	-27.9 (± 1.9)	60.8 (± 1.8)	-36.5 (± 1.4)	-28.2 (± 1.7)	60.2 (± 1.6)
M1 (R)	32.5 (± 3.1)	-23.8 (± 3.9)	70.9 (± 2.3)	37.7 (± 2.4)	-23.5 (± 3.5)	70.9 (± 2.4)
IPS (L)	-35.6 (± 2.0)	-45.2 (± 3.6)	54.8 (± 2.5)	-35.4 (± 2.4)	-45.8 (± 3.0)	54.9 (± 2.5)
IPS (R)	54.2 (± 2.4)	-31.7 (± 3.4)	43.7 (± 3.0)	54.1 (± 2.8)	-30.8 (± 2.4)	43.5 (± 2.3)

Standard deviation in parentheses; L = left; R = right; PFC = prefrontal cortex; SMA = supplementary motor area; PMC = premotor cortex; M1 = primary motor cortex; IPS = intraparietal sulcus.

Table 13. Coupling strengths of healthy control subjects (group mean)

Coupling Parameters	**Endogenous connections (DCM-A)**		**Task-based connections (DCM-B)**	
	Mean	**SEM**	**Mean**	**SEM**
PFC (L) – PFC (R)	0.199	0.041	0.143	0.249
PFC (L) – PMC (L)	- 0.438	0.019	0.428	1.282
PFC (L) – SMA	- 0.006	0.020	0.165	0.104
PFC (R) – PFC (L)	0.072	0.020	0.315	0.204
PFC (R) – PMC (R)	0.095	0.037	0.315	0.204
PFC (R) – SMA	0.033	0.021	0.083	0.095
PMC (L) – PMC (R)	0.079	0.034		
PMC (L) – M1(L)	0.022	0.022	0.502	0.083
PMC (R) – PMC (L)	0.125	0.041		
PMC (R) – M1 (R)	0.061	0.026	0.132	0.253
SMA – M1 (L)	0.038	0.021	0.308	0.209
SMA – M1 (R)	0.112	0.045	0.206	0.287
M1 (L) – M1 (R)	0.273	0.029	0.356	0.215
M1 (R) – M1 (L)	0.106	0.035	0.816	0.240
IPS (L) – PMC (L)	- 0.078	0.044	0.425	0.374

IPS (L) - SMA	0.009	0.025	0.353	0.187
IPS (L) IPS (R)	- 0.017	0.055	- 0.334	0.347
IPS (R) – PMC (R)	0.038	0.046	0.070	0.239
IPS (R) – SMA	0.061	0.035	0.282	0.159
IPS (R) – IPS (L)	- 0.057	0.075	- 0.051	0.350

SEM = Standard error of the mean L = left; R = right; PFC = prefrontal cortex; SMA = supplementary motor area; PMC = premotor cortex; M1 = primary motor cortex; IPS = intraparietal sulcus.

Table 14. Coupling strengths of patients and matched control subjects (group mean endogenous connections)

Coupling Parameters	**TD Patients**		**Matched control subjects**	
	Mean	**SEM**	**Mean**	**SEM**
PFC (L) – PFC (R)	0.015	0.052	0.002	0.043
PFC (L) – PMC (L)	- 0.015	0.041	- 0.049	0.033
PFC (L) – SMA	0.001	0.015	- 0.002	0.033
PFC (R) – PFC (L)	0.050	0.057	0.020	0.107
PFC (R) – PMC (R)	0.008	0.039	- 0.002	0.055
PFC (R) – SMA	0.001	0.021	- 0.043	0.067
PMC (L) – PMC (R)	0.032	0.045	0.019	0.076
PMC (L) – M1(L)	0.070	0.067	0.001	0.045

PMC (R) – PMC (L)	0.089	0.085	- 0.006	0.035
PMC (R) – M1 (R)	0.025	0.068	0.102	0.056
SMA – M1 (L)	0.053	0.056	0.051	0.052
SMA – M1 (R)	0.179	0.083	0.122	0.047
M1 (L) – M1 (R)	0.070	0.034	0.042	0.128
M1 (R) – M1 (L)	0.170	0.089	0.060	0.025
IPS (L) – PMC (L)	- 0.106	0.042	0.053	0.056
IPS (L) - SMA	- 0.040	0.063	0.070	0.066
IPS (L) IPS (R)	- 0.098	0.146	0.160	0.096
IPS (R) – PMC (R)	0.041	0.072	- 0.024	0.662
IPS (R) – SMA	0.034	0.058	- 0.071	0.567
IPS (R) – IPS (L)	- 0.114	0.085	0.084	0.084

SEM = Standard error of the mean; L = left; R = right; PFC = prefrontal cortex; SMA = supplementary motor area; PMC = premotor cortex; M1 = primary motor cortex; IPS = intraparietal sulcus.

Table 15. Coupling strengths of patients and matched control subjects (group mean task-based connections)

Coupling Parameters	**TD Patients**		**Matched control subjects**	
	Mean	**SEM**	**Mean**	**SEM**
PFC (L) – PFC (R)	- 0.239	0.428	0.585	0.585

PFC (L) – PMC (L)	0.022	0.119	0.199	0.235
PFC (L) – SMA	0.066	0.138	0.570	0.285
PFC (R) – PFC (L)	0.320	0.172	0.330	0.282
PFC (R) – PMC (R)	0.297	0.238	0.167	0.231
PFC (R) – SMA	0.433	0.320	0.290	0.173
PMC (L) – PMC (R)	- 0.195	0.401	0.925	0.594
PMC (L) – M1(L)	0.574	0.309	0.990	0.512
PMC (R) – PMC (L)	- 0.186	0.415	- 0.047	0.988
PMC (R) – M1 (R)	0.529	0.271	0.124	0.268
SMA – M1 (L)	0.143	0.335	0.517	0.162
SMA – M1 (R)	0.154	0.361	0.128	0.312
M1 (L) – M1 (R)				
M1 (R) – M1 (L)				
IPS (L) – PMC (L)	0.218	0.320	0.419	0.450
IPS (L) - SMA	0.160	0.238	0.209	0.184
IPS (L) IPS (R)	- 0.537	0.647	1.538	0.763
IPS (R) – PMC (R)	0.127	0.337	0.019	0.513
IPS (R) – SMA	0.448	0.375	0.777	0.424

IPS (R) – IPS (L)	- 0.363	0.404	0.450	0.672

SEM = Standard error of the mean; L = left; R = right; PFC = prefrontal cortex; SMA = supplementary motor area; PMC = premotor cortex; M1 = primary motor cortex; IPS = intraparietal sulcus.

References supplementary material Study 3

1. Michely J, Volz LJ, Barbe MT, et al. Dopaminergic modulation of motor network dynamics in Parkinson's disease. *Brain*. Mar 2015;138(Pt 3): 664-678. https://doi.org/10.1093/brain/awu381

2. Rolls ET, Huang, C-C, Lin C.P, Feng J, Joliot, M. Automated anatomical labelling atlas 3. *Neuroimage*. 2020/02/01/2020;206:116189. https://doi.org/https://doi.org/10.1016/j.neuroimage.2019.116189

3. Tzourio-Mazoyer N, Landeau B, Papathanassiou D, et al. Automated Anatomical Labeling of Activations in SPM Using a Macroscopic Anatomical Parcellation of the MNI MRI Single Subject Brain. *Neuroimage*. 2002/01/01/2002;15(1), 273-289. https://doi.org/https://doi.org/10.1006/nimg.2001.0978

4. Eickhoff SB, Heim S, Zilles K, Amunts K. Testing anatomically specified hypotheses in functional imaging using cytoarchitectonic maps. *Neuroimage*. Aug 15 2006; 32(2):570-582. https://doi.org/10.1016/j.neuroimage.2006.04.204

5. Eickhoff SB, Paus T, Caspers S, et al. Assignment of functional activations to probabilistic cytoarchitectonic areas revisited. *Neuroimage*. Jul 1 2007;36(3):511-521. https://doi.org/10.1016/j.neuroimage.2007.03.060

6. Eickhoff SB, Stephan KE, Mohlberg H, et al. A new SPM toolbox for combining probabilistic cytoarchitectonic maps and functional imaging data. *Neuroimage*. May 2005;25(4):1325-1335. https://doi.org/10.1016/j.neuroimage.2004.12.034

7. Stephan KE, Penny WD, Daunizeau J, Moran RJ, Friston KJ. Bayesian model selection for group studies. *Neuroimage*. Jul 15 2009;46(4):1004-1017. https://doi.org/10.1016/j.neuroimage.2009.03.025

8. Michely J, Volz LJ, Hoffstaedter F, et al. Network connectivity of motor control in the ageing brain. *Neuroimage Clin*. 2018;18, 443-455. https://doi.org/10.1016/j.nicl.2018.02.001

9. Zeidman P, Jafarian A, Corbin, N, et al. A guide to group effective connectivity analysis, part 1: First level analysis with DCM for fMRI. *Neuroimage*. Oct 15 2019;200, 174-190. https://doi.org/10.1016/j.neuroimage.2019.06.031